ZooKeys 793: 1–14 (2018)
doi: 10.3897/zookeys.793.28977
http://zookeys.pensoft.net

RESEARCH ARTICLE

A peer-reviewed open-access journal
ZooKeys
Launched to accelerate biodiversity research

Complete mitochondrial genome of *Echinophyllia aspera* (Scleractinia, Lobophylliidae): Mitogenome characterization and phylogenetic positioning

Wentao Niu[1], Shuangen Yu[1], Peng Tian[1], Jiaguang Xiao[1]

1 *Laboratory of Marine Biology and Ecology, Third Institute of Oceanography, State Oceanic Administration, Xiamen, China*

Corresponding author: *Wentao Niu* (wentaoniu@tio.org.cn)

Academic editor: *B.W. Hoeksema* | Received 9 August 2018 | Accepted 20 September 2018 | Published 29 October 2018

http://zoobank.org/8CAEC589-89C7-4D1D-BD69-1DB2416E2371

Citation: Niu W, Yu S, Tian P, Xiao J (2018) Complete mitochondrial genome of *Echinophyllia aspera* (Scleractinia, Lobophylliidae): Mitogenome characterization and phylogenetic positioning. ZooKeys 793: 1–14. https://doi.org/10.3897/zookeys.793.28977

Abstract

Lack of mitochondrial genome data of Scleractinia is hampering progress across genetic, systematic, phylogenetic, and evolutionary studies concerning this taxon. Therefore, in this study, the complete mitogenome sequence of the stony coral *Echinophyllia aspera* (Ellis & Solander, 1786), has been decoded for the first time by next generation sequencing and genome assembly. The assembled mitogenome is 17,697 bp in length, containing 13 protein coding genes (PCGs), two transfer RNAs and two ribosomal RNAs. It has the same gene content and gene arrangement as in other Scleractinia. All genes are encoded on the same strand. Most of the PCGs use ATG as the start codon except for ND2, which uses ATT as the start codon. The A+T content of the mitochondrial genome is 65.92% (25.35% A, 40.57% T, 20.65% G, and 13.43% for C). Bayesian and maximum likelihood phylogenetic analysis have been performed using PCGs, and the result shows that *E. aspera* clustered closely with *Sclerophyllia maxima* (Sheppard & Salm, 1988), both of which belong to Lobophylliidae, when compared with species belonging to Merulinidae and other scleractinian taxa used as outgroups. The complete mitogenome of *E. aspera* provides essential and important DNA molecular data for further phylogenetic and evolutionary analyses of corals.

Keywords

Daya Bay, gene order, next-generation sequence, phylogeny

Introduction

Reef-building coral species of the order Scleractinia play an important role in shallow tropical seas by providing an environmental base for the ecosystem (Fukami et al. 2000). These coral species have been traditionally described using morphological character traits of skeletons as demonstrated in various taxonomic revisions published in the last century (Dinesen 1980; Hoeksema 1989; Wallace 1999). Traditional morphology-based systematics does not reflect all the evolutionary relationships of Scleractinia, which therefore forms a problematic group for taxonomy. Environment-induced phenotypic variation, morphological plasticity, evolutionary convergence of skeletal characters, intraspecific variation caused by different genotypes, and genetic mixing via introgression cause intraspecific and interspecific variability to overlap (Todd 2008; Combosch and Vollmer 2015; Richards and Hobbs 2015). Molecular data have therefore become increasingly important in recent years to overcome the limitations of morphological analyses among scleractinians (e.g. Benzoni et al. 2011, 2012a, 2014; Gittenberger et al. 2011; Huang et al. 2011, 2014a, 2014b; Budd et al. 2012; Arrigoni et al. 2014a, 2017; Kitano et al. 2014; Schmidt-Roach et al. 2014; Terraneo et al. 2016a, 2017). In particular, the family Lobophylliidae has received much attention recently with regard to its phylogeny (Arrigoni et al. 2014b, 2015, 2016a, 2016b, 2018; Huang et al. 2016).

The unique characters of mitochondrial genome DNA (mitogenome), which include small size, fast evolutionary rate, simple structure, maternal inheritance, and high informational content, suggest that the constituting loci could be powerful markers for resolving ancient phylogenetic relationships (Boore 1999; Sun et al. 2003; Geng et al. 2016). This has also been applied for a number of scleractinian taxa (e.g. Fukami and Knowlton 2005; Flot and Tillier 2007; Wang et al. 2013; Arrigoni et al. 2016c; Capel et al. 2016; Niu et al. 2016; Terraneo et al. 2016b, 2016c). In recent years, next-generation sequencing (NGS), combined with bioinformatic annotation, is becoming increasingly common for recovering animal mitogenome sequences and allows a rapid amplification-free sequencing (Jex et al. 2010). However, the complete mitochondrial genomes of stony corals that we can find in NCBI (National Center for Biotechnology Information) are less than 80 species.

Echinophyllia aspera (Ellis & Solander, 1786), commonly known as the chalice coral, is a stony coral species with large polyps in the scleractinian family Lobophylliidae. It is native to the western and central Indo-Pacific (Veron 2000). In this study, we sequenced the complete mitogenome sequence of *E. aspera* for the first time using NGS and analyzed its structure. It is the second lobophylliid species to be examined for its mitogenome after *Sclerophyllia maxima* (Sheppard & Salm, 1988) (Arrigoni et al. 2015, 2016c). Furthermore, we conducted phylogenetic analyses based on the mitochondrial sequence data of this species and 10 other scleractinians with the purpose of investigating the phylogenetic position of *E. aspera*. The mitogenome information reported in this article will facilitate further investigations of evolutionary and phylogenetic relationships of stony corals.

Materials and methods

Sample collection and DNA extraction

Samples (voucher no. DYW15) of *Echinophyllia aspera* (Figure 1) were collected from Daya Bay in Guangdong, China. Specimens were identified based on skeletal morphology after detailed observation of corallite features using a dissecting microscope. The number of septa, the number of denticles, the calice, and the dimension were analyzed with reference to taxonomic descriptions (Veron 2000; Arrigoni et al. 2016b). Total genomic DNA was extracted using the DNeasy tissue Kit (Qiagen China, Shanghai) and kept at 4°C for subsequent use.

Genome sequencing and analyses

We used next generation sequencing to perform low-coverage whole-genome sequencing according to the protocol (Niu et al. 2016). PCR products were subjected to agarose gel, Nanodrop 2000 (Thermo Scientific, USA) and Qubit 2.0 Fluorometer (Life technologies, USA) to confirm its purity and concentration. A total of 2μg double strand DNA (dsDNA) passed the quality control steps were sheared to ~550bp by M220 focused-ultrasonicator (Covaris, Woburn, MA, USA). Fragmented DNA was tested for size distribution by using the Agilent Bioanalyzer 2100 (Agilent Technologies, Santa Clara, CA, USA) and library for Miseq was generated by TruSeq DNA PCR-free LT sample preparation kit (Illumina, San Diego, CA, USA) according to manufacturer's instructions. Final library concentration was determined by real-time quantitative PCR with Illumina adapter-specific primers provided by KAPA library quantification kit (KAPA Biosystems, Wilmington, MA, USA). About 0.05% raw reads (3,017 out of 6,340,606) were *de novo* assembled by using commercial software (Geneious V9, Auckland, New Zealand) to produce a single, circular form of complete mitogenome with about an average 38 × coverage.

Mitogenome annotation and analyses

The assembled consensus sequence was further annotated and analyzed. Preliminary annotation using DOGMA (Wyman et al. 2004) and MITOS (Bernt et al. 2013) webserver provided overall information on mitogenome. Protein-coding genes and rRNA genes were annotated by alignments of homologous genes of other reported mitogenome of Scleractinia. Blast searches in the National Center for Biotechnology Information also helped to identify and annotate the PCGs and rRNA genes. Transfer RNA genes were identified by comparing the results predicted by ARWEN based on cloverleaf secondary structure information (Laslett and Canback 2008). Nucleotide frequencies and codon usage were determined by MEGA7 software (Kumar et al. 2016).

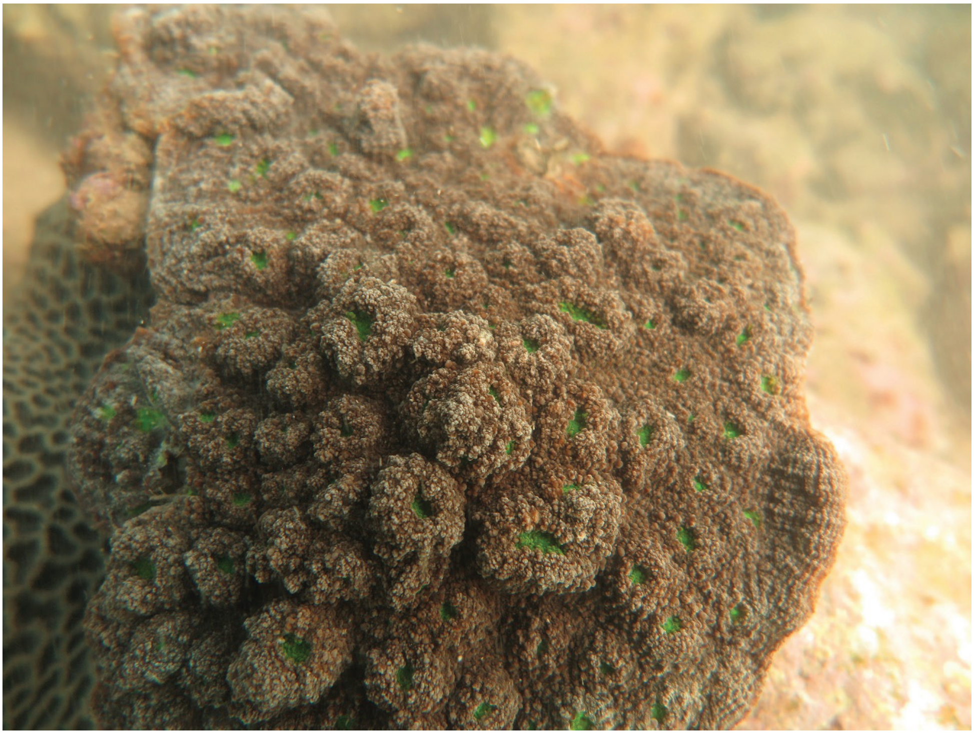

Figure 1. Example of *Echinophyllia aspera* used in the present study.

Phylogenetic analyses

To validate the phylogenetic position of *E. aspera* within the Scleractinia, the complete mitogenome sequences of an additional ten representative scleractinian species (Table 1) were incorporated together with the presently obtained *E. aspera* mitogenome sequence for phylogenetic analysis. The phylogenetic trees were built using two approaches including maximum-likelihood (ML) analysis by PAUP* 4.0 (Swofford 2002) and a partitioned Bayesian inference (BI) analysis by Mrbayes 3.12 (Huelsenbeck and Ronquist 2001) based on 13 PCGs binding sequence. The substitution model selection was conducted by a comparison of Akaike Information Criterion (AIC) scores with jModelTest 2 (Darriba et al. 2012). The GTR+I+G model was chosen as the best-fitting model for ML analyses and the node reliability was estimated after 1000 bootstrap replicates. For the Bayesian procedure, four Markov chains were run for 1,000,000 generations by sampling the trees every 1000 generations. After the first 2500 trees (25%) were discarded as burn-in, the 50% majority rule consensus tree and the Bayesian posterior probabilities (BPP) were estimated using the remaining 7500 sampled trees. *Madrepora oculata* Linnaeus, 1758, belonging to Oculinidae was used as outgroup for tree rooting.

Table 1. Representative Scleractinia species included in this study for comparison.

Species	Family	Distribution	Length (bp)	GenBank accession number
Echinophyllia aspera	Lobophylliidae	Indo-Pacific	17,697	MG792550
Sclerophyllia maxima	Lobophylliidae	Indo-Pacific	18,168	FO904931
Platygyra carnosa	Merulinidae	Indo-Pacific	16,463	NC_020049
Favites abdita	Merulinidae	Indo-Pacific	17,825	NC_035879
Favites pentagona	Merulinidae	Indo-Pacific	18,006	NC_034916
Orbicella faveolata	Merulinidae	West Atlantic	16,138	AP008978
Orbicella franksi	Merulinidae	West Atlantic	16,138	AP008975
Orbicella annularis	Merulinidae	West Atlantic	16,138	AP008974
Mussa angulosa	Mussidae	West Atlantic	17,245	NC_008163
Colpophyllia natans	Mussidae	West Atlantic	16,906	NC_008162
Madrepora oculata	Oculinidae	West Atlantic	15,841	NC_018364

Results and discussion

Mitochondrial genome organization

The complete mitogenome of *E. aspera* was 17,697 bp in size (GenBank accession number: MG792550) including unique 13 protein-coding genes (PCGs), two transfer RNA genes (tRNA-Met, tRNA-Trp) and two ribosomal RNA genes (Figure 2, Table 2). Its overall base composition was 25.35% for A, 13.43% for C, 20.65% for G and 40.57% for T, and showed a high A+T content with mean overall value of 65.92% (Figure 3, Table 3). All PCGs, tRNA and rRNA genes were encoded on H-strand. The base C was at the lowest level in different regions of the mitogenome (Figure 3). The mitochondrial genome of *E. aspera* provided no peculiar structure; its gene identity, number and order were identical to most of the scleractinian coral mitogenomes already published (Wang et al. 2013).

Protein-coding genes

The PCGs was 11,576 bp in size, and its base composition was 21.6% for A, 13.4% for C, 20.5% for G and 44.5% for T. The ND5 had a 10,136 bp intron insertion, and COI had a 1,075bp intron insertion. According to Lin et al. (2014), the ND5 intron of *E. aspera* was the canonical scleractinian organization (Type SII), ten proteincoding genes and rns are contained in the ND5 intron. According to Fukami et al. (2007), the group I intron in COI of *E. aspera* was the canonical Type 2, with one deletion of T at position 77. All of the PCGs used ATG as the start codon except for ND2, which used ATT as the start codon. Five of the 13 PCGs were inferred to terminate with TAG (ND1, ND4, ND5, COI and COIII), 8 PCGs with TAA (Cyt *b*, ATP6, ND2, ND4L, ND3, ND6, COII and ATP8). Among 13 PCGs, the longest one was ND5 gene (1,815 bp),

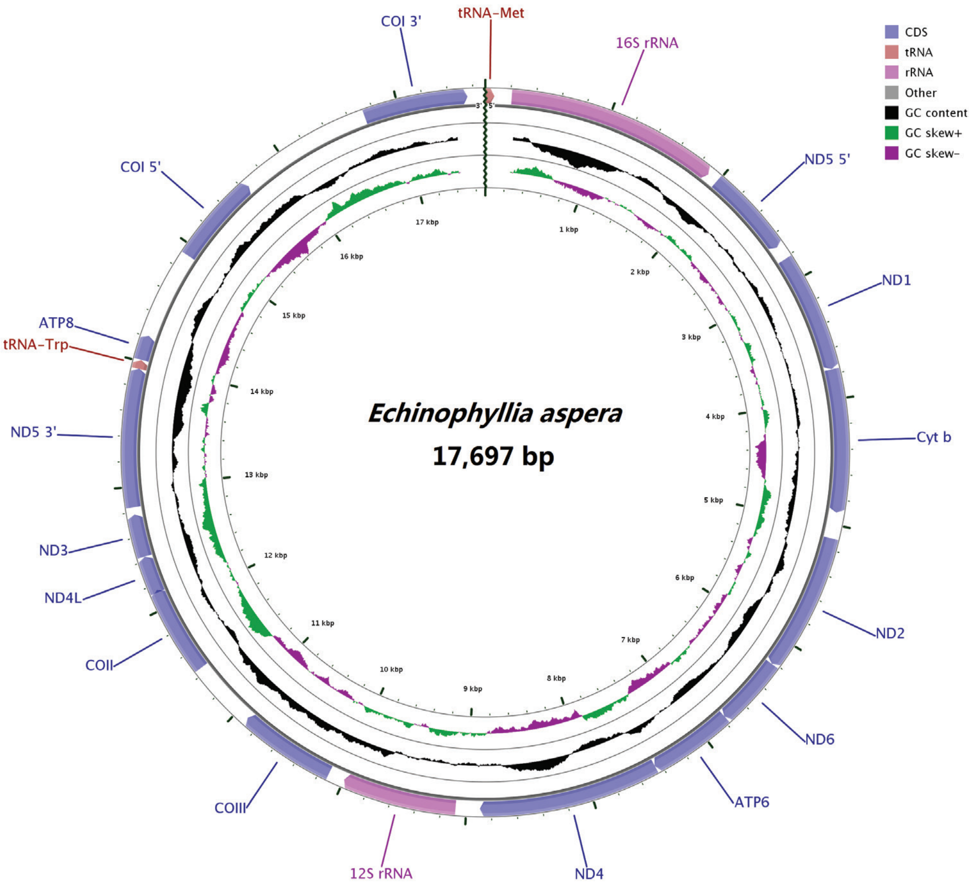

Figure 2. The mitochondrial genome of *Echinophyllia aspera*. Gene order and positions are shown; all the genes are encoded on H-strand. COI, COII, COIII refer to the cytochrome oxidase subunits, Cyt *b* refers to cytochrome b, ND1-ND6 refer to NADH dehydrogenase components.

whereas the shortest was ATP8 gene (198 bp). There were 1 bp overlapping nucleotides between ND6 and ATP6, 1 bp overlapping nucleotides between ATP6 and ND4, 2 bp overlapping nucleotides between tRNA-Trp and ND5 5’, 19 bp overlapping nucleotides between ND4L and COII, and the number of non-coding nucleotides between different genes varied from 1 to 1075 bp (Table 2). Nucleotide asymmetric research can be measured through the AT-skew and GC-skew method, the calculation formula was: AT skew = (A-T)/(A+T), GC skew = (G-C)/(G+C). According to the results (Figure 4), the PCGs showed stronger AT-skew and GC-skew, the absolute value of AT-skew was greater than GC-skew. Among 3858 codons for 20 amino acids, codons use frequency was higher in L, F, V, I and G, accounted for 53.2% of all amino acids. Nonpolar amino acid (G, A, V, L, I, M, F, Y, W) accounted for 66.2% which was the maximum, followed by polar amino acid (S, P, T, C, N, Q) accounted for 20.2%, the polarity charged amino acids (K, H, R, D, E) accounted for 13.6% which was minimum (Figure 5).

Table 2. Organization of the mitochondrial genome of *Echinophyllia aspera*.

Gene	Position		Length (bp)	Anticodon	Codon		Intergenic nucleotides*	Strand
	From	To			Start	Stop		
tRNA^{Met}	1	72	72	UAC			140	H
16S rRNA	210	1905	1696				137	H
ND5 5’	1991	2701	711		ATG		85	H
ND1	2813	3760	948		ATG	TAG	111	H
Cyt *b*	3763	4902	1140		ATG	TAA	2	H
ND2	5111	6214	1104		ATT	TAA	208	H
ND6	6216	6776	561		ATG	TAA	1	H
ATP6	6776	7453	678		ATG	TAA	-1	H
ND4	7453	8892	1440		ATG	TAG	-1	H
12S rRNA	9085	9996	912				192	H
COIII	10127	10906	780		ATG	TAG	130	H
COII	11448	12155	708		ATG	TAA	541	H
ND4L	12137	12436	300		ATG	TAA	-19	H
ND3	12439	12780	342		ATG	TAA	2	H
ND5 3’	12838	13941	1104			TAG	57	H
tRNA^{Trp}	13940	14010	71	ACU			-2	H
ATP8	14014	14211	198		ATG	TAA	3	H
COI 5’	14920	15650	731		ATG		708	H
COI 3’	16726	17556	831			TAG	1075	H

Notes: * Data are number of nucleotides between the given gene and its previous gene, negative numbers indicate overlapping nucleotides.

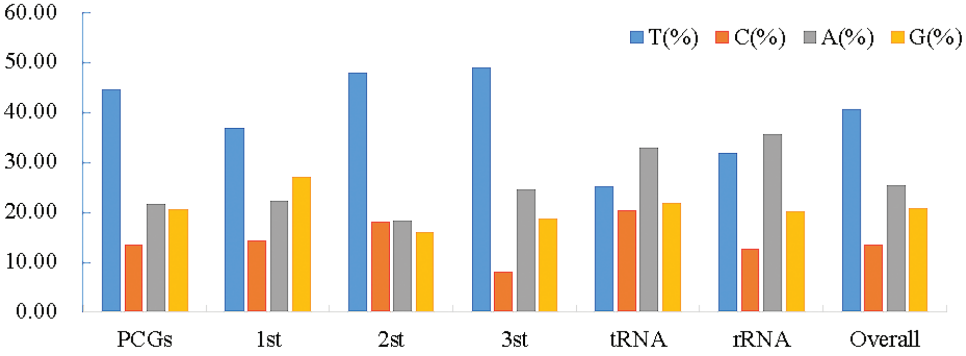

Figure 3. Codon usage bias in different regions of mitochondrial genome of *Echinophyllia aspera*.

Ribosomal and transfer RNA genes

The genes encoding the small and large ribosomal RNA subunits (12S rRNA and 16S rRNA) were identified in *E. aspera*, which were 912 bp and 1,696 bp in length, respectively. The total ribosomal RNA was 2,608 bp in size, and its base composition was 35.43% for A, 12.65% for C, 20.17% for G and 31.75% for T. The two transfer RNAs were 72 bp for tRNA-Met and 71 bp for tRNA-Trp in length respectively. They

Table 3. Nucleotide composition in different regions of mitochondrial genome of *Echinophyllia aspera*.

Gene/Region	T(%)	C(%)	A(%)	G(%)	A+T(%)	Size (bp)
ND5	46.12	12.51	21.60	19.78	67.72	1815
ND1	43.88	13.50	20.57	22.05	64.45	948
Cyt *b*	46.05	13.51	20.88	19.56	66.93	1140
ND2	46.74	13.04	20.29	19.93	67.03	1104
ND6	47.06	13.19	20.86	18.89	67.92	561
ATP6	46.46	14.01	20.65	18.88	67.11	678
ND4	44.65	14.24	20.00	21.11	64.65	1440
COIII	41.40	15.60	20.60	22.30	62.00	780
COII	39.41	12.57	25.71	22.32	65.12	708
ND4L	43.67	10.67	27.33	18.33	71.00	300
ND3	49.71	9.06	18.71	22.51	68.42	342
ATP8	43.43	10.60	33.33	12.63	76.76	198
COI	41.42	14.53	22.60	21.45	64.02	1562
PCGs	44.50	13.40	21.60	20.50	66.10	11576
1st	36.70	14.20	22.10	27.00	58.80	3859
2st	47.90	18.00	18.20	15.90	66.10	3859
3st	48.90	8.00	24.50	18.60	73.40	3858
tRNA	25.17	20.28	32.87	21.68	58.04	143
rRNA	31.75	12.65	35.43	20.17	67.18	2608
Overall	40.57	13.43	25.35	20.65	65.92	17697

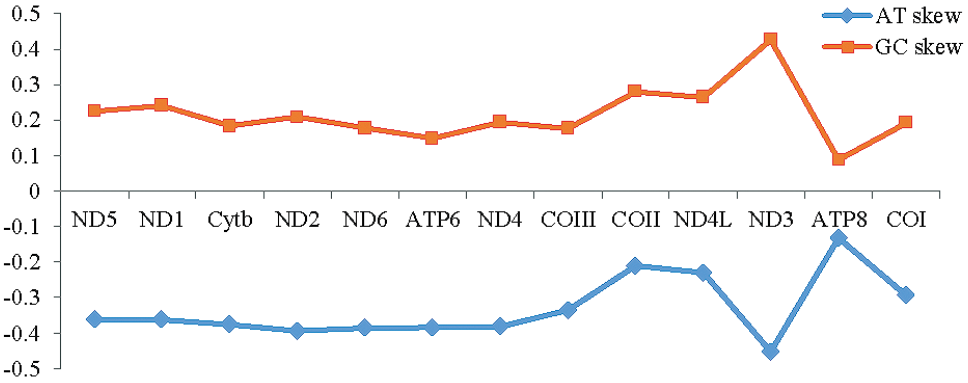

Figure 4. The PCGs' AT-skew and GC-skew of mitochondrial genome of *Echinophyllia aspera*.

can be folded into the typical cloverleaf structure, the typical cloverleaf structure contained amino acid accept stem, TψC stem, anticodon stem, and DHU stem (Figure 6).

Phylogenetic analyses

ML and BI analyses were performed with the concatenated PCG nucleotide data. The topological relationships of two phylogenetic analyses remained consistent, and all analyses provided high support values for all internodes (Figure 7). The phylogenetic tree

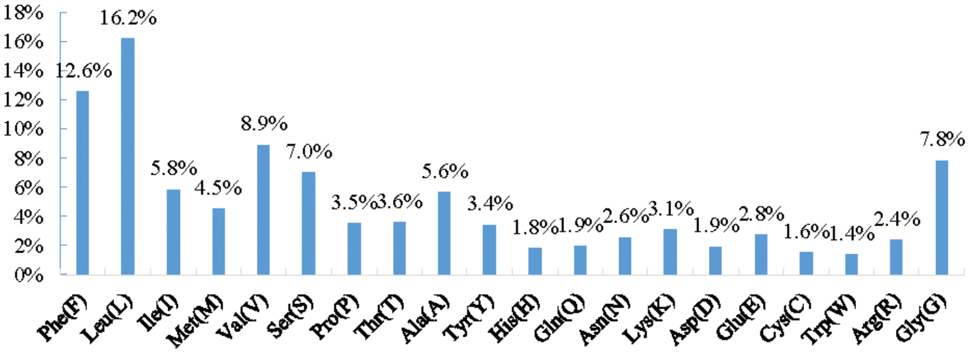

Figure 5. The PCG-codons use frequency of mitochondrial genome of *Echinophyllia aspera*.

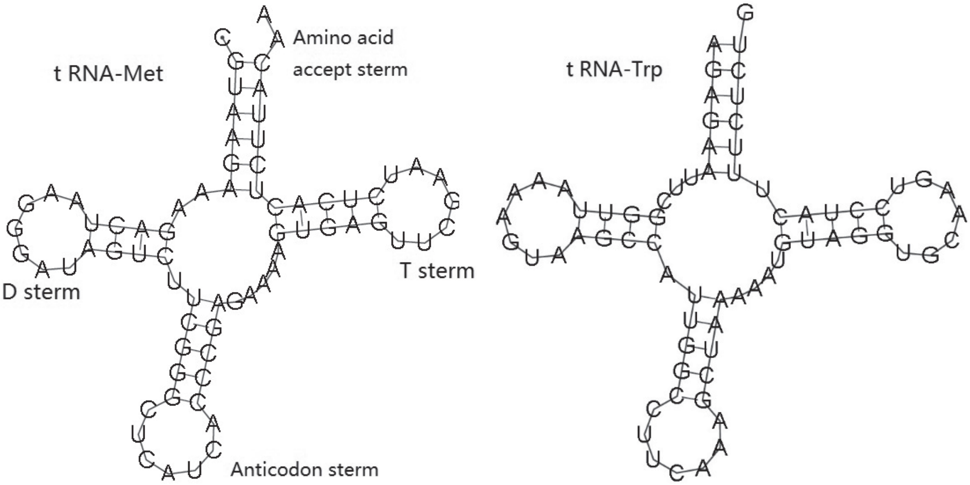

Figure 6. Putative secondary structures of two tRNA of *Echinophyllia aspera*.

showed that *E. aspera* clustered most closely with *Sclerophyllia maxima*, which also belongs to Lobophylliidae, but previously was classified as an *Acanthastrea* species (Arrigoni et al. 2015, 2016c). Both species were sister group to Merulinidae, recovering similar relationships with previous studies (Fukami et al. 2008; Kitahara et al. 2010). Indeed, molecular analyses such as the present one, together with traditional studies of micromorphology and microstructure, can help improve modern classification criteria within Scleractinia (Benzoni et al. 2012b; Kitahara et al. 2012, 2016; Budd and Bosellini 2015).

Conclusion

Limited data are available on the mitogenomes of Lobophylliidae, so the mitochondrial genome of *Echinophyllia aspera* was completed using NGS in the present study. The mitogenome of *E. aspera* was found to be 17,697 bp in length and showed a similar

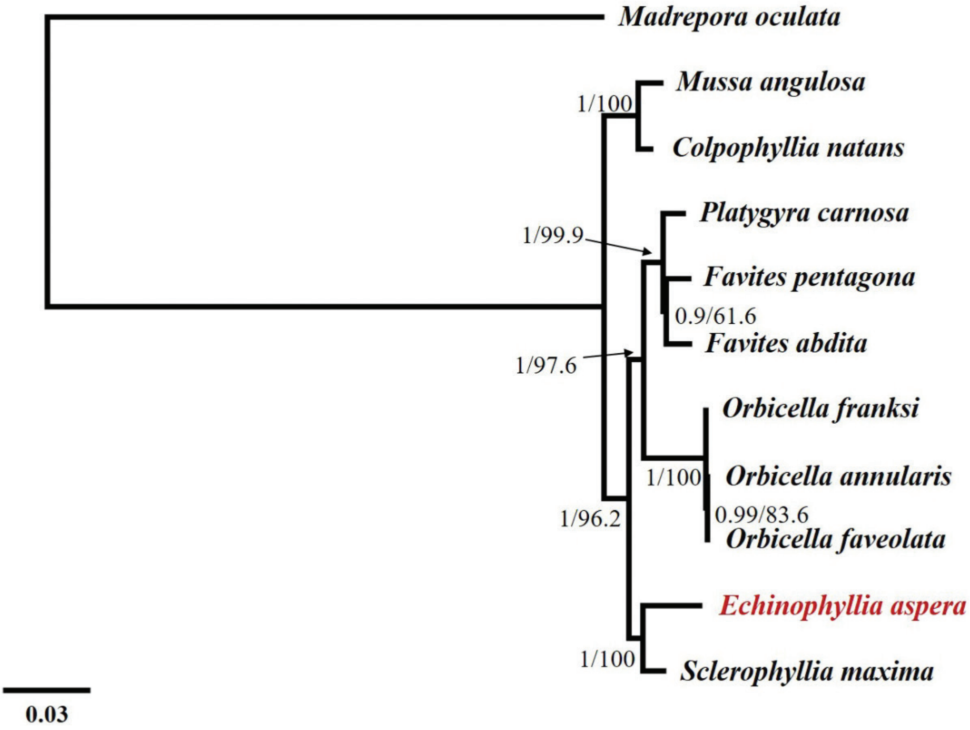

Figure 7. Inferred phylogenetic relationships based on the concatenated nucleotide sequences of 13 mitochondrial protein-coding genes using Bayesian inference (BI) and maximum likelihood (ML). Numbers on branches are Bayesian posterior probabilities and bootstrap percentages.

composition in size, low GC content and gene order to mitogenomes already available in Scleractinia. In conclusion, the complete mitogenome of *E. aspera* sequenced and analysed in this study provides essential and important DNA molecular data for further phylogenetic and evolutionary analyses for scleractinian phylogeny.

Acknowledgements

This work was supported by the National Key Research and Development Plan under grant No. 2017YFA0604902 and the National Natural Science Foundation of China under grant No.41406161.

References

Arrigoni R, Kitano YF, Stolarski J, Hoeksema BW, Fukami H, Stefani F, Galli P, Montano S, Castoldi E, Benzoni F (2014a) A phylogeny reconstruction of the Dendrophylliidae (Cnidaria, Scleractinia) based on molecular and micromorphological criteria, and its ecological implications. Zoologica Scripta 43: 661–688. https://doi.org/10.1111/zsc.12072

Arrigoni R, Terraneo TI, Galli P, Benzoni F (2014b) Lobophylliidae (Cnidaria, Scleractinia) reshuffled: Pervasive non-monophyly at genus level. Molecular Phylogenetics and Evolution 73: 60–64. https://doi.org/10.1016/j.ympev.2014.01.010

Arrigoni R, Berumen ML, Terraneo TI, Caragnano A, Bouwmeester J, Benzoni F (2015) Forgotten in the taxonomic literature: resurrection of the scleractinian coral genus *Sclerophyllia* (Scleractinia, Lobophylliidae) from the Arabian Peninsula and its phylogenetic relationships. Systematics and Biodiversity 13: 140–163. https://doi.org/10.1080/14772000.2014.978915

Arrigoni R, Benzoni F, Huang DW, Fukami H, Chen CA, Berumen ML, Hoogenboom M, Thomson DP, Hoeksema BW, Budd AF, Zayasu Y, Terraneo TI, Kitano YF, Baird AH (2016a) When forms meet genes: revision of the scleractinian genera *Micromussa* and *Homophyllia* (Lobophylliidae) with a description of two new species and one new genus. Contributions to Zoology 85: 387–422.

Arrigoni R, Berumen ML, Chen CA, Terraneo TI, Baird AH, Payri C, Benzoni F (2016b) Species delimitation in the reef coral genera *Echinophyllia* and *Oxypora* (Scleractinia, Lobophylliidae) with a description of two new species. Molecular Phylogenetics and Evolution 105: 146–159. https://doi.org/10.1016/j.ympev.2016.08.023

Arrigoni R, Vacherie B, Benzoni F, Barbe V (2016c) The complete mitochondrial genome of *Acanthastrea maxima* (Cnidaria, Scleractinia, Lobophylliidae). Mitochondrial DNA Part A 27: 927–928. https://doi.org/10.3109/19401736.2014.926489

Arrigoni R, Berumen ML, Huang DW, Terraneo TI, Benzoni F (2017) *Cyphastrea* (Cnidaria: Scleractinia: Merulinidae) in the Red Sea: phylogeny and a new reef coral species. Invertebrate Systematics 31: 141–156. https://doi.org/10.1071/IS16035

Arrigoni R, Berumen ML, Stolarski J, Terraneo TI, Benzoni F (2018) Uncovering hidden coral diversity: a new cryptic lobophylliid scleractinian from the Indian Ocean. Cladistics. https://doi.org/10.1111/cla.12346

Benzoni F, Arrigoni R, Stefani F, Pichon M (2011) Phylogeny of the coral genus *Plesiastrea* (Cnidaria, Scleractinia). Contributions to Zoology 80: 231–249.

Benzoni F, Arrigoni R, Stefani F, Reijnen BT, Montano S, Hoeksema BW (2012a) Phylogenetic position and taxonomy of *Cycloseris explanulata* and *C. wellsi* (Scleractinia: Fungiidae): lost mushroom corals find their way home. Contributions to Zoology 81: 125–146.

Benzoni F, Arrigoni R, Stefani F, Stolarski J (2012b) Systematics of the coral genus *Craterastrea* (Cnidaria, Anthozoa, Scleractinia) and description of a new family through combined morphological and molecular analyses. Systematic Biodiversity 10: 417–433. https://doi.org/10.1080/14772000.2012.744369

Benzoni F, Arrigoni R, Waheed Z, Stefani F, Hoeksema BW (2014) Phylogenetic relationships and revision of the genus *Blastomussa* (Cnidaria: Anthozoa: Scleractinia) with description of a new species. Raffles Bulletin of Zoology 62: 358–378.

Bernt M, Donath A, Juhling F, Externbrink F, Florentz C, Fritzsch G, Putz J, Middendorf M, Stadler PF (2013) MITOS: improved de novo metazoan mitochondrial genome annotation. Molecular Phylogenetics and Evolution 69: 313–319. https://doi.org/10.1016/j.ympev.2012.08.023

Boore JL (1999) Animal mitochondrial genomes. Nucleic Acids Research 27: 1767–1780. https://doi.org/10.1093/nar/27.8.1767

Budd AF, Fukami H, Smith ND, Knowlton N (2012) Taxonomic classification of the reef coral family Mussidae (Cnidaria: Anthozoa: Scleractinia). Zoological Journal of the Linnean Society 166: 465–529. https://doi.org/10.1111/j.1096-3642.2012.00855.x

Budd AF, Bosellini FR (2015) Revision of Oligocene Mediterranean meandroid corals in the scleractinian families Mussidae, Merulinidae and Lobophylliidae. Journal of Systematic Palaeontology 14: 771–798. https://doi.org/10.1080/14772019.2015.1102171

Capel KCC, Migotto AE, Zilberberg C, Lin MF, Forsman Z, Miller DJ, Kitahara MV (2016) Complete mitochondrial genome sequences of Atlantic representatives of the invasive Pacific coral species *Tubastraea coccinea* and *T. tagusensis* (Scleractinia, Dendrophylliidae): Implications for species identification. Gene 590: 270–277. https://doi.org/10.1016/j.gene.2016.05.034

Combosch DJ, Vollmer SV (2015) Trans-Pacific RAD-Seq population genomics confirms introgressive hybridization in Eastern Pacific *Pocillopora* corals. Molecular Phylogenetics and Evolution 88: 154–162. https://doi.org/10.1016/j.ympev.2015.03.022

Darriba D, Taboada GL, Doallo R, Posada D (2012) jModelTest 2: more models, new heuristics and parallel computing. Nature Methods 9: 772. https://doi.org/10.1038/nmeth.2109

Dinesen ZD (1980) A revision of the coral genus *Leptoseris* (Scleractinia: Fungina: Agariciidae). Memoirs of the Queensland Museum 20: 182–235.

Ellis J, Solander D (1786) The Natural History of many curious and uncommon Zoophytes, collected from various parts of the Globe. Systematically arranged and described by the late Daniel Solander. Benjamin White & Son, London.

Flot JF, Tillier S (2007) The mitochondrial genome of Pocillopora (Cnidaria: Scleractinia) contains two variable regions: the putative D-loop and a novel ORF of unknown function. Gene 401: 80–87. https://doi.org/10.1016/j.gene.2007.07.006

Fukami H, Knowlton N (2005) Analysis of complete mitochondrial DNA sequences of three members of the *Montastraea annularis* coral species complex (Cnidaria, Anthozoa, Scleractinia). Coral Reefs 24: 410–417. https://doi.org/10.1007/s00338-005-0023-3

Fukami H, Omori M, Hatta M (2000) Phylogenetic relationships in the coral family Acroporidae, reassessed by inference from mitochondrial genes. Zoological Science 17: 689–696. https://doi.org/10.2108/zsj.17.689

Fukami H, Chen CA, Chiou CY, Knowlton N (2007) Novel group I introns encoding a putative homing endonuclease in the mitochondrial cox1 gene of Scleractinian corals. Journal of Molecular Evolution 64: 591–600. https://doi.org/10.1007/s00239-006-0279-4

Fukami H, Chen CA, Budd AF, Collins A, Wallace C, Chuang YY, Chen C, Dai CF, Iwao K, Sheppard C, Knowlton N (2008) Mitochondrial and nuclear genes suggest that stony corals are monophyletic but most families of stony corals are not (Order Scleractinia, Class Anthozoa, Phylum Cnidaria). PLoS ONE 3: e3222. https://doi.org/10.1371/journal.pone.0003222

Geng X, Cheng R, Xiang T, Deng B, Wang Y, Deng D, Zhang H (2016) The complete mitochondrial genome of the Chinese *Daphnia pulex* (Cladocera, Daphniidae). Zookeys 27: 47–60.

Gittenberger A, Reijnen BT, Hoeksema BW (2011) A molecularly based phylogeny reconstruction of mushroom corals (Scleractinia: Fungiidae) with taxonomic consequences and evolutionary implications for life history traits. Contributions to Zoology 80: 107–132.

Hoeksema BW (1989) Taxonomy, phylogeny and biogeography of mushroom corals (Scleractinia: Fungiidae). Zoologische Verhandelingen 254: 1–295.

Huang DW, Licuanan WY, Baird AH, Fukami H (2011) Cleaning up the 'Bigmessidae': Molecular phylogeny of scleractinian corals from Faviidae, Merulinidae, Pectiniidae and Trachyphylliidae. BMC Evolutionary Biology 11: 37. https://doi.org/10.1186/1471-2148-11-37

Huang DW, Benzoni F, Arrigoni R, Baird AH, Berumen ML, Bouwmeester J, Chou LM, Fukami H, Licuanan WY, Lovell ER, Meier R, Todd PA, Budd AF(2014a) Towards a phylogenetic classification of reef corals: the Indo-Pacific genera *Merulina*, *Goniastrea* and *Scapophyllia* (Scleractinia, Merulinidae). Zoologica Scripta 43: 531–548. https://doi.org/10.1111/zsc.12061

Huang DW, Benzoni F, Fukami H, Knowlton N, Smith ND, Budd AF (2014b) Taxonomic classification of the reef coral families Merulinidae, Montastraeidae, and Diploastraeidae (Cnidaria: Anthozoa: Scleractinia). Zoological Journal of the Linnean Society 171: 277–355. https://doi.org/10.1111/zoj.12140

Huang DW, Arrigoni R, Benzoni F, Fukani H, Knowlton N, Smith ND, Stolarski J, Chou LM, Budd AF (2016) Taxonomic classification of the reef coral family Lobophylliidae (Cnidaria: Anthozoa: Scleractinia). Zoological Journal of the Linnean Society 178: 436–481. https://doi.org/10.1111/zoj.12391

Huelsenbeck JP, Ronquist F (2001) MRBAYES: Bayesian inference of phylogenetic trees. Bioinformatics 17: 754–755. https://doi.org/10.1093/bioinformatics/17.8.754

Jex AR, Hall RS, Littlewood DT, Gasser RB (2010) An integrated pipeline for next-generation sequencing and annotation of mitochondrial genomes. Nucleic Acids Research 38: 522–533. https://doi.org/10.1093/nar/gkp883

Kitahara MV, Cairns SD, Stolarski J, Blair D, Miller DJ (2010) A comprehensive phylogenetic analysis of the Scleractinia (Cnidaria, Anthozoa) based on mitochondrial CO1 sequence data. PLoS ONE 5: e11490. https://doi.org/10.1371/journal.pone.0011490

Kitahara MV, Stolarski J, Cairns SD, Benzoni F, Stake JL, Miller DJ (2012) The first modern solitary Agariciidae (Anthozoa, Scleractinia) revealed by molecular and microstructural analysis. Invertebrate Systematics 26: 303–315. https://doi.org/10.1071/IS11053

Kitahara MV, Fukami H, Benzoni F, Huang DW (2016) The new systematics of Scleractinia: integrating molecular and morphological evidence. In: Goffredo S, Dubinsky Z. (Eds) The Cnidaria, Past, Present and Future: The World of Medusa and Her Sisters. Springer Netherlands, Dordrecht, 41–59. https://doi.org/10.1007/978-3-319-31305-4_4

Kitano YF, Benzoni F, Arrigoni R, Shirayama Y, Wallace CC, Fukami H (2014) A phylogeny of the family Poritidae (Cnidaria, Scleractinia) based on molecular and morphological analyses. PLoS ONE 9: e98406. https://doi.org/10.1371/journal.pone.0098406

Kumar S, Stecher G, Tamura K (2016) MEGA7: molecular evolutionary genetics analysis version 7.0 for bigger datasets. Molecular Biology and Evolution 33: 1870–1874. https://doi.org/10.1093/molbev/msw054

Laslett D, Canback B (2008) ARWEN: a program to detect tRNA genes in metazoan mitochondrial nucleotide sequences. Bioinformatics 24: 172–175. https://doi.org/10.1093/bioinformatics/btm573

Lin MF, Kitahara MV, Luo HW, Tracey D, Geller J, Fukami H, Miller DJ, Chen CA (2014) Mitochondrial genome rearrangements in the Scleractinia/Corallimorpharia complex: Implications for coral phylogeny. Genome Biology and Evolution 6: 1086–1095. https://doi.org/10.1093/gbe/evu084

Linnaeus C (1758) Systema Naturae per regna tria naturae, secundum classes, ordines, genera, species, cum characteribus, differentiis, synonymis, locis. Editio decima, reformata. Holmiae, Laurentius Salvius.

Niu WT, Lin RC, Shi XF, Chen CH, Shen KN, Hsiao CD (2016) Next-generation sequencing yields the complete mitogenome of massive coral, *Porites lutea* (Cnidaria: Poritidae). Mitochondrial DNA Part B 1: 8–9. https://doi.org/10.1080/23802359.2015.1137795

Richards ZT, Hobbs JPA (2015) Hybridisation on coral reefs and the conservation of evolutionary novelty. Current Zoology 61: 132–145. https://doi.org/10.1093/czoolo/61.1.132

Schmidt-Roach S, Miller KJ, Lundgren P, Andreakis N (2014) With eyes wide open: a revision of species within and closely related to the *Pocillopora damicornis* species complex (Scleractinia; Pocilloporidae) using morphology and genetics. Zoological Journal of the Linnean Society 170: 1–33. https://doi.org/10.1111/zoj.12092

Sheppard CRC, Salm RV (1988) Reef and coral communities of Oman, with a description of a new coral species (Order Scleractinia, genus *Acanthastrea*). Journal of Natural History 22: 263–279. https://doi.org/10.1080/00222938800770201

Sun HY, Zhou KY, Song DX (2003) Mitochondrial genome and phylogenetic reconstruction of arthropods. Zoological Research 24: 467–479.

Swofford DL (2002) PAUP* 4.0: Phylogenetic analysis using parsimony. Sinauer Associates, Inc., Sunderland, MA.

Terraneo TI, Benzoni F, Arrigoni R, Berumen ML (2016a) Species delimitation in the coral genus *Goniopora* (Scleractinia, Poritidae) from the Saudi Arabian Red Sea. Molecular Phylogenetics and Evolution 102: 278–294. https://doi.org/10.1016/j.ympev.2016.06.003

Terraneo TI, Arrigoni R, Benzoni F, Forsman ZH, Berumen ML (2016b) Using ezRAD to reconstruct the complete mitochondrial genome of *Porites fontanesii* (Cnidaria: Scleractinia). Mitochondrial DNA Part B 3: 173–174. https://doi.org/10.1080/23802359.2018.1437805

Terraneo TI, Arrigoni R, Benzoni F, Forsman ZH, Berumen ML (2016c) The complete mitochondrial genome of *Porites harrisoni* (Cnidaria: Scleractinia) obtained using next-generation sequencing. Mitochondrial DNA Part B 3: 286–287. https://doi.org/10.1080/23802359.2018.1443852

Terraneo TI, Arrigoni R, Benzoni F, Tietbohl MB, Berumen ML (2017) Exploring the genetic diversity of shallow-water Agariciidae (Cnidaria: Anthozoa) from the Saudi Arabian Red Sea. Marine Biodiversity 47: 1065–1078. https://doi.org/10.1007/s12526-017-0722-3

Todd PA (2008) Morphological plasticity in scleractinian corals. Biological Reviews of the Cambridge Philosophical Society 83: 315–337. https://doi.org/10.1111/j.1469-185X.2008.00045.x

Veron JEN (2000) Corals of the World. Australian Institute of Marine Science, Townsville.

Wyman SK, Jansen RK, Boore JL (2004) Automatic annotation of organellar genomes with DOGMA. Bioinformatics 20: 3252–3255. https://doi.org/10.1093/bioinformatics/bth352

Wallace CC (1999) Staghorn corals of the world: a revision of the coral genus *Acropora*. CSIRO Publishing, Collingwood.

Wang M, Sun J, Li J, Qiu JW (2013) Complete mitochondrial genome of the brain coral *Platygyra carnosus*. Mitochondrial DNA 24: 194–195. https://doi.org/10.3109/19401736.2012.744981

ZooKeys 793: 15–28 (2018)
doi: 10.3897/zookeys.793.29221
http://zookeys.pensoft.net

RESEARCH ARTICLE

A peer-reviewed open-access journal
ZooKeys
Launched to accelerate biodiversity research

The first record of the anopsobiid genus *Shikokuobius* Shinohara, 1982 in continental Asia, with the description of a new species from the Altais, southwestern Siberia, Russia (Chilopoda, Lithobiomorpha, Anopsobiidae)

Gyulli Sh. Farzalieva[1], Pavel S. Nefediev[2,3]

1 *Department of Invertebrate Zoology and Aquatic Ecology, Perm State University, Bukireva 15, Perm 614990, Russia* **2** *Department of Ecology, Biochemistry and Biotechnology, Altai State University, Lenina 61, Barnaul 656049, Russia* **3** *Biological Institute, Tomsk State University, Biological Institute, Lenina 36, Tomsk 634050, Russia*

Corresponding author: *Pavel S. Nefediev* (p.nefediev@mail.ru)

Academic editor: *M. Zapparoli* | Received 21 August 2018 | Accepted 18 September 2018 | Published 29 October 2018

http://zoobank.org/41B189DD-5038-4FA5-9F64-CD76168B2EAA

Citation: Farzalieva GSh, Nefediev PS (2018) The first record of the anopsobiid genus *Shikokuobius* Shinohara, 1982 in continental Asia, with the description of a new species from the Altais, southwestern Siberia, Russia (Chilopoda, Lithobiomorpha, Anopsobiidae). ZooKeys 793: 15–28. https://doi.org/10.3897/zookeys.793.29221

Abstract

A new lithobiomorph species, *Shikokuobius altaicus* **sp. n.**, is described from the Altai Mountains in southwestern Siberia, Russia. This is the first record of the genus *Shikokuobius* Shinohara, 1982 in continental Asia, all previous reports being from Japan. The distribution of *Shikokuobius* is mapped.

Keywords

Centipede, taxonomy, new species, Altai Mountains, Siberia, Russia

Introduction

The family Anopsobiidae Verhoeff, 1907 is currently known to be represented in the Northern Hemisphere by one small and eight monotypic genera: *Yobius* Chamberlin, 1945 (Utah, USA), *Hedinobius* Verhoeff, 1934 (Tien Shan, western China), *Rhodobius* Silvestri, 1932 (Europe), *Anopsobiella* Attems, 1938 (Vietnam), *Shikokuobius* Shinohara, 1982 (Japan), *Ghilaroviella* Zalesskaja, 1975 (Tajikistan), *Dzhungaria* Farzalieva, Zalesskaja et Edgecombe, 2004 (eastern Kazakhstan), *Speleopsobius* Shear, 2018 (southern Idaho, USA), as well as *Buethobius* Chamberlin, 1911, with 5 species from the USA (Silvestri 1909, Attems 1938, Zalesskaja 1975, Shinohara 1982, Farzalieva et al. 2004, Zapparoli and Edgecombe 2011, Shear 2018).

A collection of lithobiomorph centipedes from the Republic of Altai, Russia, deposited in the Zoological Museum of the Lomonosov Moscow State University, has yielded a single male of a new anopsobiid species of *Shikokuobius*. Four additional specimens of that new species have also been freshly collected from the Altai Province, Russia.

Shikokuobius altaicus sp. n. is very similar to *S. japonicus* (Murakami, 1967) from Japan (Sakuragi, Honshu; Nakameguro and Shirogane; the DNA voucher specimen of Edgecombe and Giribet (2003, 2004), Shizen-Kyoiku-en, Meguro-ku, all in Tokyo). The present paper describes the new species and refines the distribution of the genus *Shikokuobius*.

Material and methods

The material used in the present study was collected by S.I. Golovatch (Moscow, Russia) in the environs of Lake Teletskoye, Republic of Altai and by T.M. Krugova (Barnaul, Russia) with her team of volunteers in the Tigirek State Nature Reserve, Altai Province. Both sites are located in the Russian Altais, southwestern Siberia, Russia. Most of the material is currently deposited in the collection of the Zoological Museum of the Lomonosov Moscow State University, Moscow, Russia (ZMUM), partly also shared with the collection of the Perm State University, Perm, Russia (PSU).

The total body length was measured from the fore margin of the cephalic plate to the posterior end of the postpedal tergite. Leg length was measured excluding the length of the claw. Lengths are given as the minimum and maximum values. All measurements are given in millimeters (mm).

The mouthparts, legs and body segments of the new species were cleared in 10% KOH and mounted in permanent slides in sandarac medium (Krasheninnikov 2011) for examination. The specimens were examined and measured using a Meiji EMZ-5 stereo microscope, and stacks of colour images were manually generated using an Olympus OMD EM-10 digital camera with a Panasonic Lumix H-H025 25 mm f/1.7 lens mounted on a Zeiss microscope. Digital images were prepared using Photoshop CS6 image stacking software. The drawings were executed using a Zeiss microscope and a Zeiss drawing tube. The distribution map was composed using QGIS 3.0.

The terminology of the external anatomy follows Bonato et al. (2010).

The following abbreviations are used in the text:

T, TT	tergite, tergites;	P	prefemur;
C, CC	coxa, coxae;	F	femur.
t	trochanter;		

Results

Taxonomy

***Shikokuobius altaicus* sp. n.**
http://zoobank.org/34A98474-0F2E-41D8-9E7A-A1E84EE30F4C
Figs 1–43, 45

Type material. Holotype ♂ (ZMUM, Rc 7867): Russia, southwestern Siberia, Altai Province, Krasnoshchiokovo District, near Tigirek village, buffer zone of the Tigirek State Nature Reserve, foot of W slope of Mt. Kozyr, 51°09'26.54"N, 83°00'01.59"E, thicket of *Padus avium*, *Lonicera tatarica* and *Viburnum opulus*, 600 m a.s.l., soil sample (30–40 cm deep), 29–30.08.2016, leg. T.M. Krugova, L.Yu. Gruntova, V.V. Zelensky, K.V. Smirnova, A.E. Pupkova, M.N. Terioshkina and R.V. Scherbakova.

Paratypes. 1 ♂ (ZMUM, Rc 7868), 1 ♀ (ZMUM, Rc 7869), together with holotype, soil samples (30–40 cm deep and 0–10 cm deep, respectively); 1 ♀ (PSU-612), Russia, southwestern Siberia, Altai Province, Krasnoshchiokovo District, near Tigirek village, Tigirek State Nature Reserve, Khankhara Site, right bank of Khankhara River, upper part of N slope, 51°11'35.36"N, 82°58'48.26"E, *Larix sibirica* forest with *Betula pendula*, 920 m a.s.l., soil sample (20–30 cm deep), 19.08.2016, leg. T.M. Krugova, L.Yu. Gruntova, V.V. Zelensky, K.V. Smirnova, A.E. Pupkova, M.N. Terioshkina and R.V. Scherbakova.

Non-type material. 1 ♂ (PSU-536), [Russia, southwestern Siberia, Republic of Altai, Turochak District], near Lake Teletskoye, environs of Artybash village [51.814745N, 87.278742E, ca 450 m a.s.l.], *Betula pendula*, *Abies sibirica* and *Pinus sibirica* forest, litter, 4–13.07.1982, leg. S.I. Golovatch.

Name. The specific epithet refers to Altai, the *locus typicus*.

Diagnosis. A *Shikokuobius* species with the body 4–6 mm long, the antennae composed of 15–17 antennomeres, commonly 15; coxosternal teeth large, separated from each other by distances less than width at the base of a tooth; P, F and T of 15 leg relatively short and thick, 15 C with a prominent, acute, mesodistal process; the number of coxal pores varying from 1 to 2 on 12–15 CC (formula 1,1,1,1 in the male and 1,1,1,2 in the female); 15 t and 15 P with bifurcate ventral spines (seldom on legs 13 and 14); at least each leg 15 with a bifurcate spine at the distodorsal end of P; 1–10 tibiae with a distal spinose projection (Figs 7–8, 24); 1–12 tarsi clearly unipartite, claws of 1–14 legs with two accessory spines, claw of legs 15 with a single accessory spine; 1st female gonopodal segment with 2+2 coniform spurs and eight long setae, 2nd with four setae, 3rd with a single seta on the external face; terminal claw simple; male gonopod with four segments including terminal filament.

Distribution (Fig. 46). Altai Province and Republic of Altai, southwestern Siberia, Russia.

Description. Holotype ♂. Body ca 4.0 mm long, ca 0.4 mm wide (in 70% alcohol); colour yellow. Tergites: almost smooth, with relatively long and sparse setae, as in Figs 32–33; T 15 indistinct; posterior margin of TT 1, 3, 5, 8, 10, 12 and 14

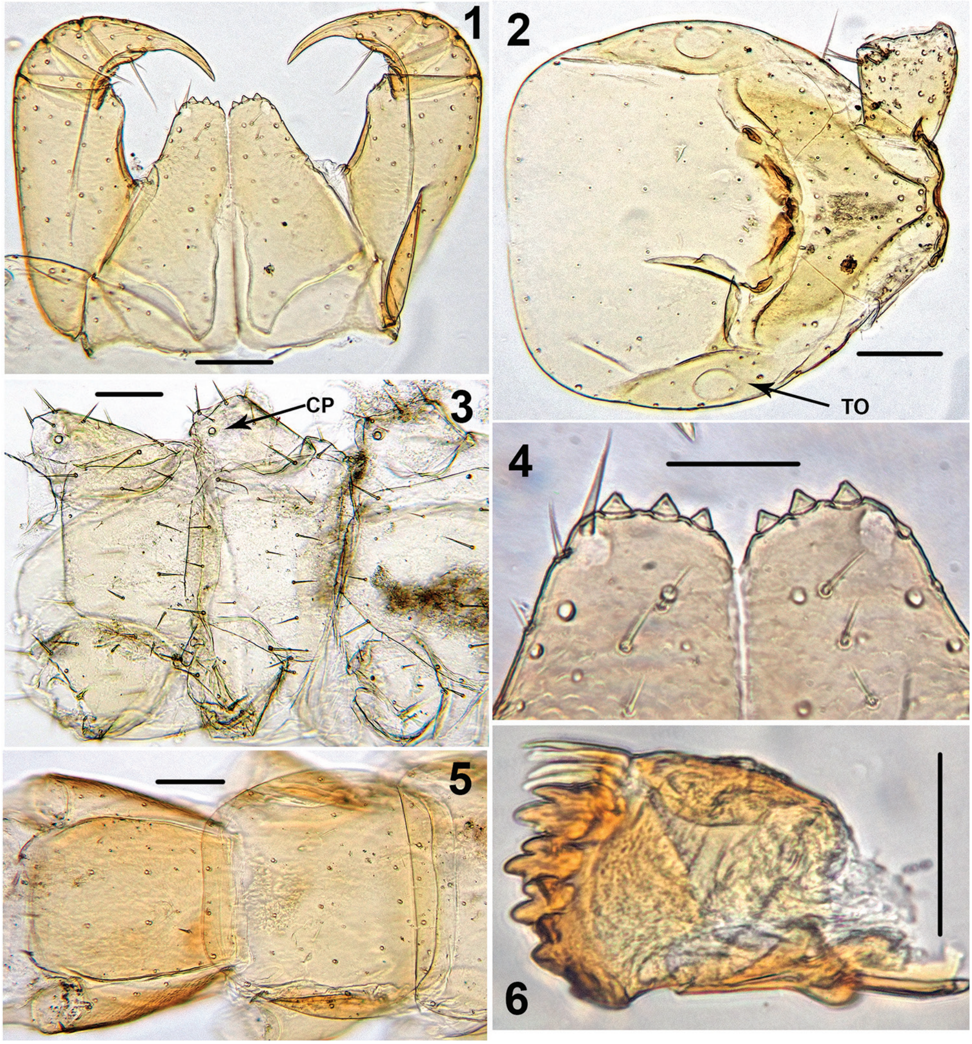

Figures 1–6. *Shikokuobius altaicus* sp. n., male paratype (**1, 3, 6**) and female paratype (**2, 4, 5**). **1** forcipulae, ventral view **2** head, ventral view **3** 12–14 sternites and coxae, ventral view **4** dental margin of forcipular coxosternite **5** 13–16 tergites, dorsal view **6** mandibula, ventrolateral view. Abbreviations: **TO** Tömösváry's organ, **CO** coxal pore. Scale bars: 0.1 mm (**1–5**), 0.05 mm (**6**).

slightly sinuate; TT 2, 4, 6 7 9 11 and 13 almost straight; intermediate T slightly elongated, as in Fig. 5. Cephalic plate: width/length ratio 0.8 (width 0.4 mm, length 0.5 mm). Antennae short, reaching the middle of T3, composed of 15+15 short moniliform articles (Fig. 13). Ocelli absent; Tömösváry's organ very large, oval (Fig. 2). The sides of the labrum with poorly-expressed fringes of bristles; a pair of setae projecting across the labral midpiece present (Figs 14–15). Gnathal edge of mandible with 4 pairs of well-developed teeth and 3–4 rather thick aciculae (Fig. 6). First maxillae: edge with 5–6 plumose bristles and simple setae as well (Figs 28, 36). Sec-

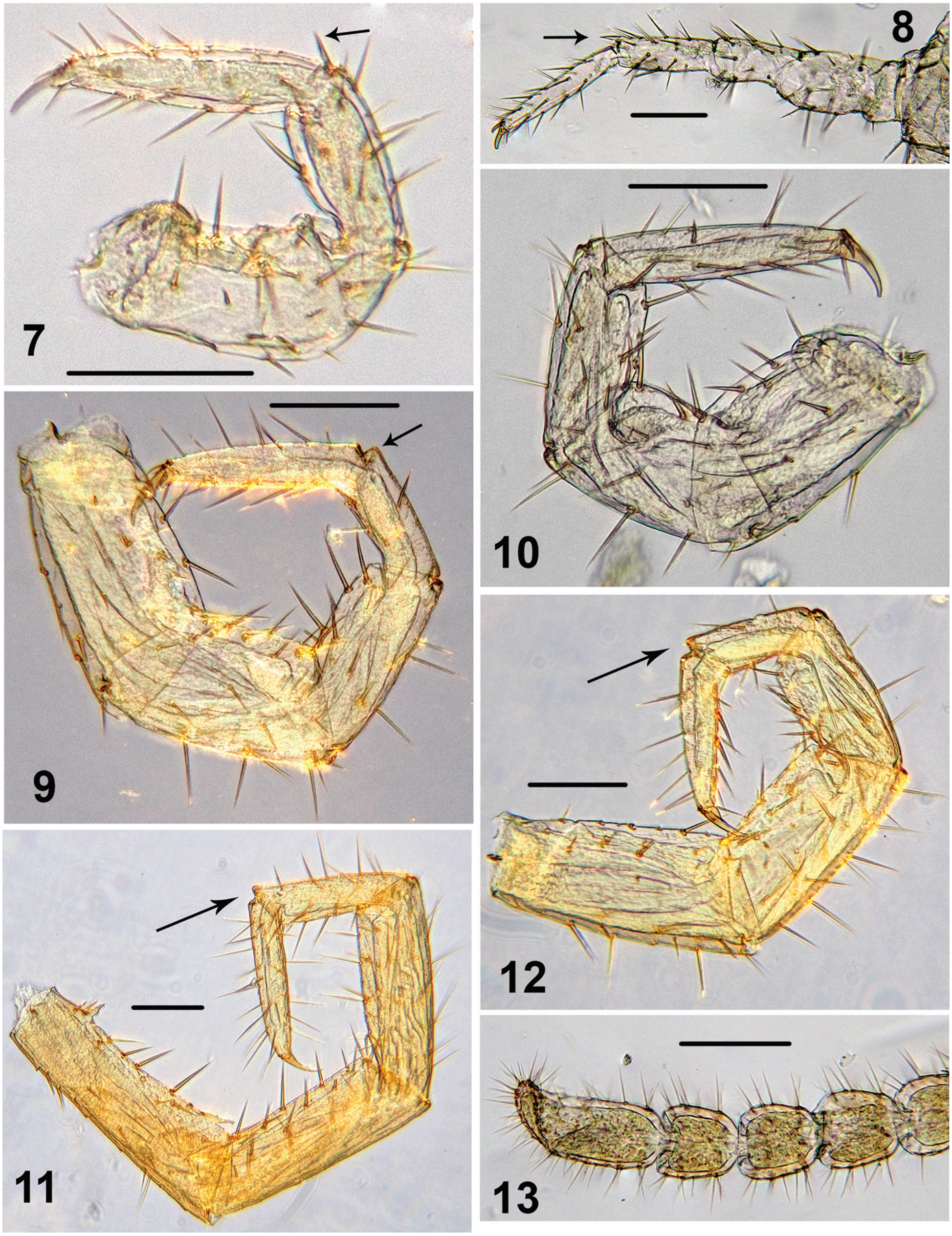

Figures 7–13. *Shikokuobius altaicus* sp. n., male paratype, lateral views. **7** leg 1 **8** leg 3 **9** leg 14 **10** leg 12 **11** leg 15 **12** leg 13 **13** 5 terminal antennomeres. Scale bars: 0.1 mm (**7, 9–13**), 0.5 mm (**8**).

ond maxillary telopodite with simple and plumose bristles on the tip (two plumose bristles on the left and right parts, respectively) (Fig. 20). Forcipulae: dental margin of coxosternite almost straight, with 3+3 teeth and long setiform porodonts, teeth

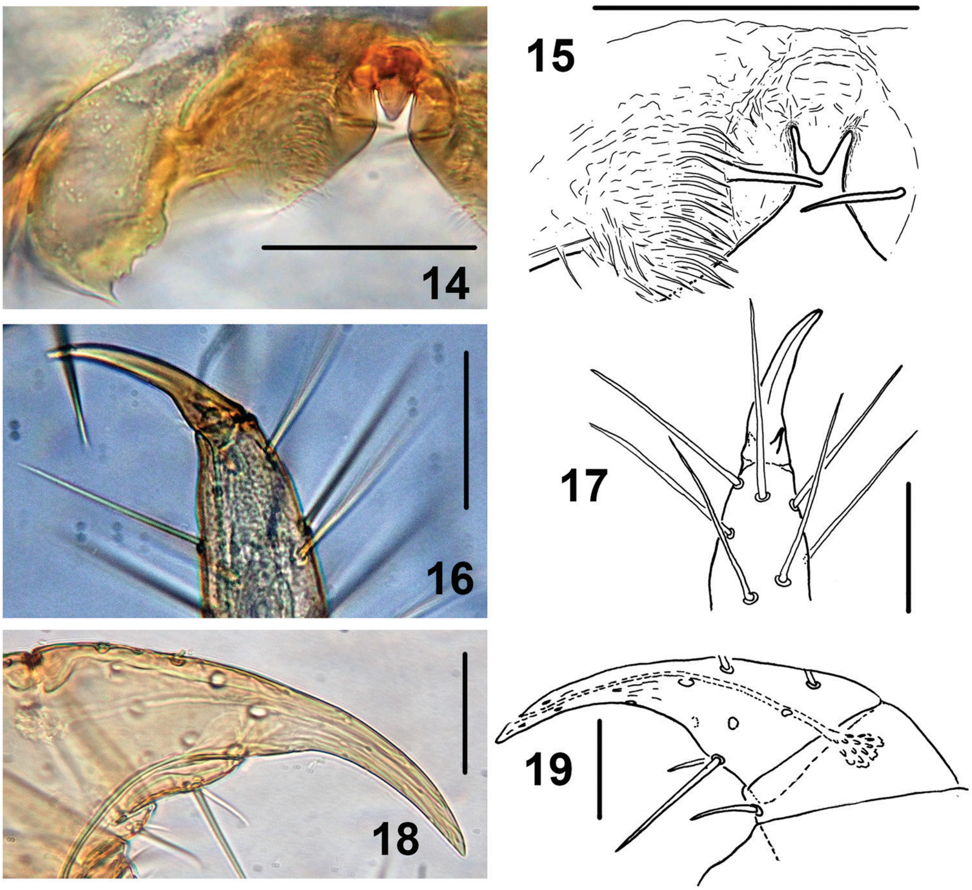

Figures 14–19. *Shikokuobius altaicus* sp. n., male paratype (**14–17**) and female paratypes (**18, 19**). **14, 15** labrum, ventral views **16, 17** apical claw of leg 15, ventrolateral views **18, 19** apical part of forcipular telopodite, ventral views. Scale bar: 0.05 mm.

relatively large, separated from each other by distances less than width at the base of a tooth, median diastema V-shaped; shoulders of coxosternite strongly sloping, as in Figs 1, 4; claw as in Figs 18–19.

Tarsal articulation of legs 1–12 indistinct, tarsi distinctly longer than tibiae. 1–10 tibiae with a distal spinose projection, as in Figs 7–8, 24. 1–14 legs with two accessory spines. 14 and 15 legs not incrassate, with long setae (Figs 11–12). 15 leg: P, F and T relatively short and thick (Fig. 11); C ventrally with a long process (Fig. 26); t and P ventrally with bifurcate spines (Figs 11, 21–22); tarsus 2 with a small distodorsal projection (Fig. 11, shown by arrow). 14–13 legs with the same, but less strongly expressed distodorsal projections. Accessory spines on 15 leg small, poorly-developed (Figs 16–17). At least 13–15 legs dorsally with trace of a broken spine or process (Figs 9, 11–12). A single coxal pore on each of 12–15 legs small and rounded (Fig. 3). Gonopods 4-segmented including terminal filament; 1st segment with three, 2nd segment with four long setae on the external face (Fig. 25).

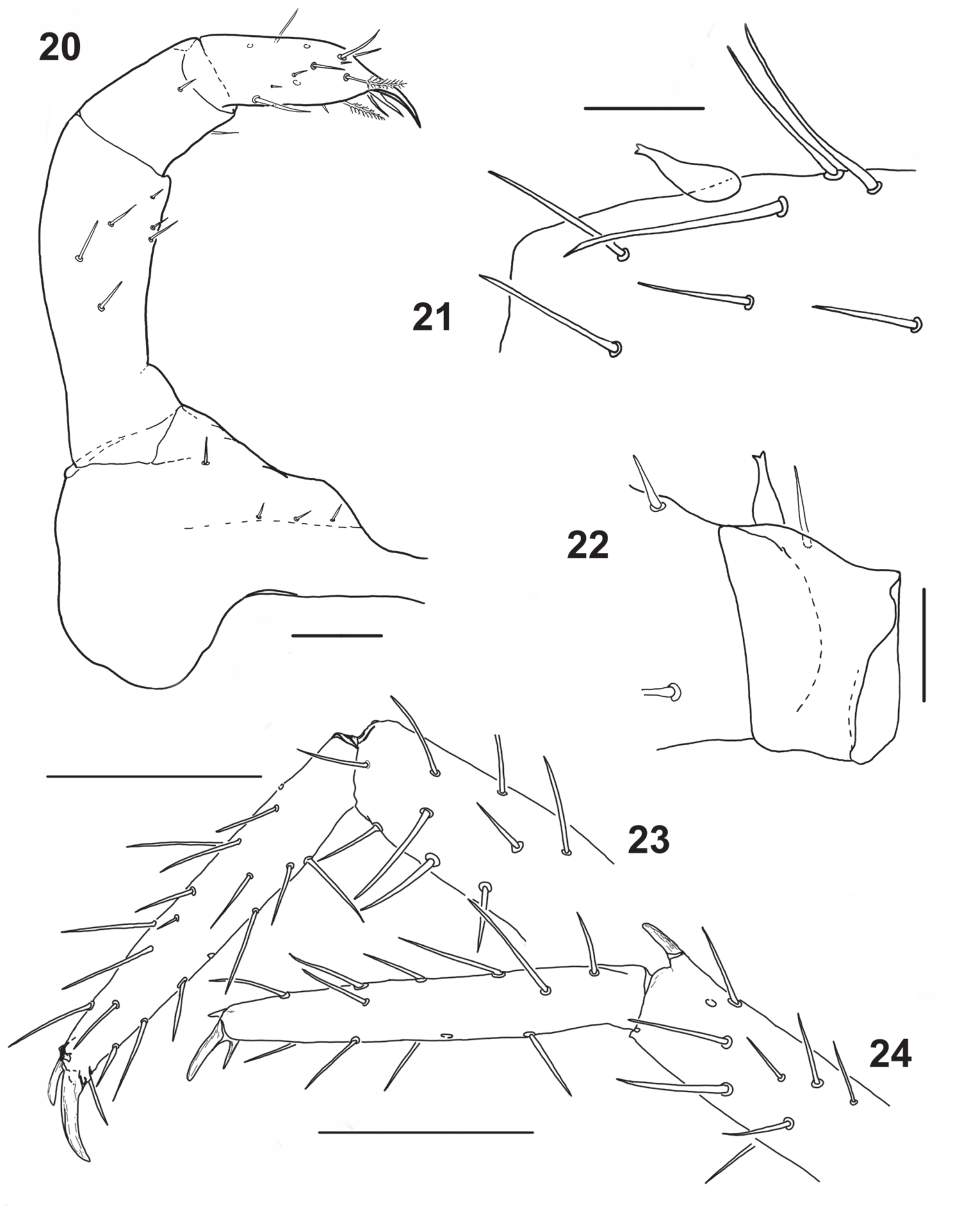

Figures 20–24. *Shikokuobius altaicus* sp. n., male holotype (**20–22**) and male paratype (**23, 24**). **20** left part of second maxilla, ventral view **21** ventral spine on prefemur 15, lateral view **22** ventral spine on trochanter 15, lateral view **23** leg 11, lateral view **24** leg 10, lateral view. Scale bars: 0.05 mm (**20–22**), 0.1 mm (**23, 24**).

Paratype ♂. Length 4.0 mm, width 0.4 mm. All other characters as in holotype, but coxal process on leg 15 broken off on both legs.

Non-type material ♂. Length 4.9 mm, width 0.5 mm. All other characters as in holotype (Figs 39–40, 42), but antennae with 17+17 articles, first maxillae with at

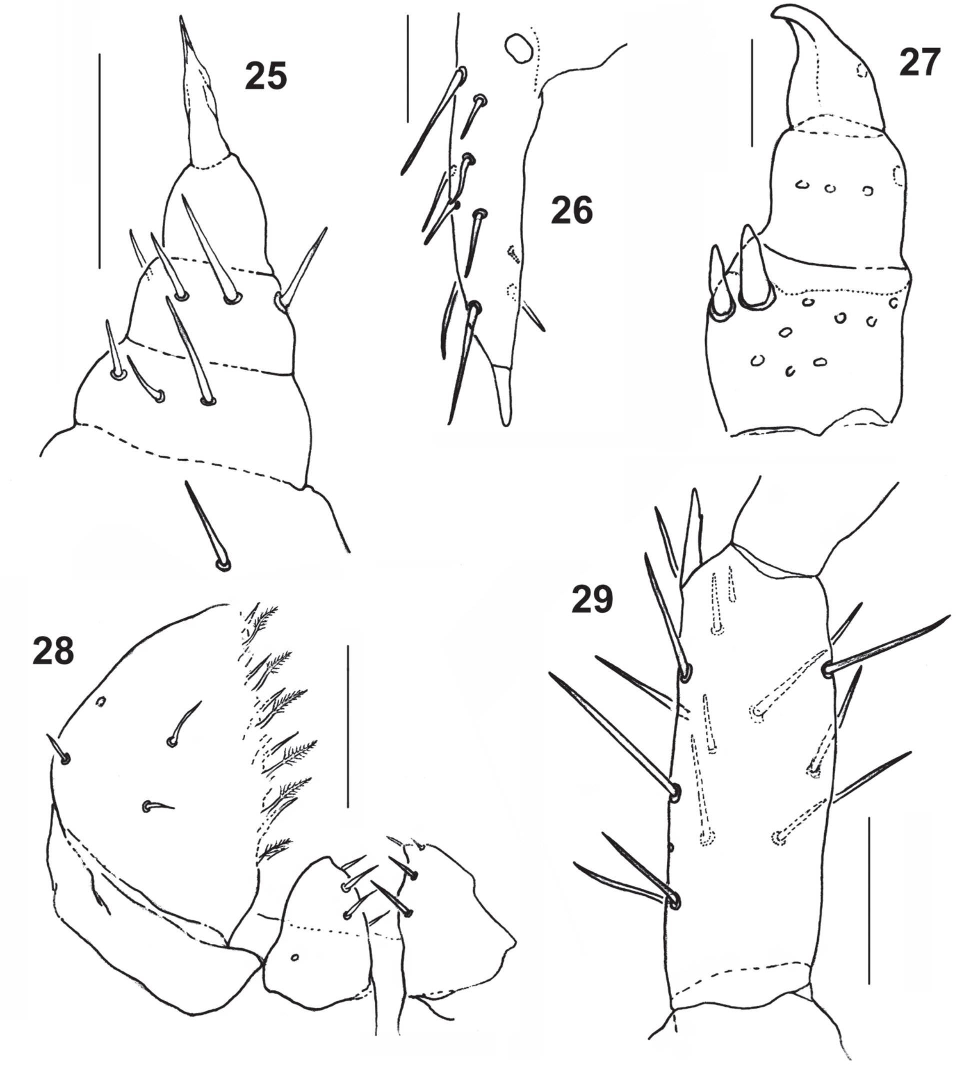

Figures 25–29. *Shikokuobius altaicus* sp. n., male holotype (**25, 26, 28, 29**) and female paratype (**27**). **25** left gonopod, ventral view **26** left mesodistal process on 15 coxa, ventral view **27** left gonopod, ventral view **28** left part of first maxilla **29** distodorsal process on tibia 3, lateral view. Scale bar: 0.05 mm.

least six plumose bristles (Fig. 37); second maxillae with four plumose bristles; 14 C ventrally with a tiny denticle, as in Fig. 38; 15 P with a bifurcate spine at distodorsal end (Figs 41, 43); 15 leg with a single well-developed accessory spine; 3rd gonopodal segment with two long setae on the external face.

Paratype ♀♀. All characters as in ♂♂. The number of antennomeres in females unknown: one ♀ with antennae completely broken off, while another ♀ with damaged antennae, having 12+7 antennal articles. Coxal pores as in holotype, formula 1,1,1,2 (Figs 34–35). The number of accessory spines unknown: both females had no 15 leg-pairs.

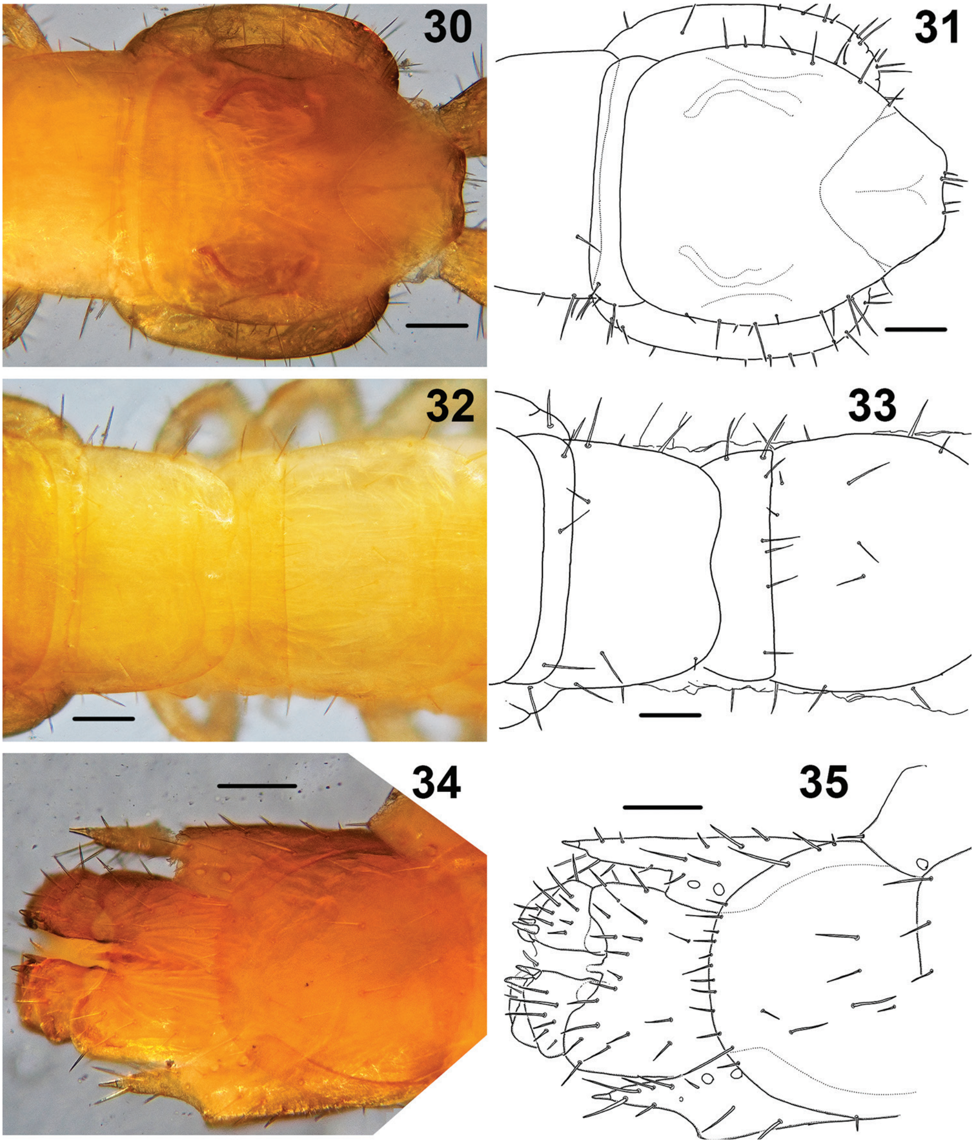

Figures 30–35. *Shikokuobius altaicus* sp. n., female paratype. **30, 31** front body part, dorsal view **32, 33** forcipular and 1–3 leg-bearing segments, dorsal view **34, 35** rear body part, ventral view. Scale bar: 0.1 mm.

Gonopods without setae on internal face, with 2+2 conical spurs and simple claw (Fig. 27). All segments of gonopods with long setae (broken off as in Fig. 27): 1st segment with eight setae, 2nd with four ones, while 3rd with a single seta on the external face of gonopod.

Habitats. The new species was collected in the lowland Altais in small-leaved and mixed taiga forests at 450 to 920 m a.s.l. (Fig. 45), mainly in soil samples, frequently in deep layers down to 40 cm.

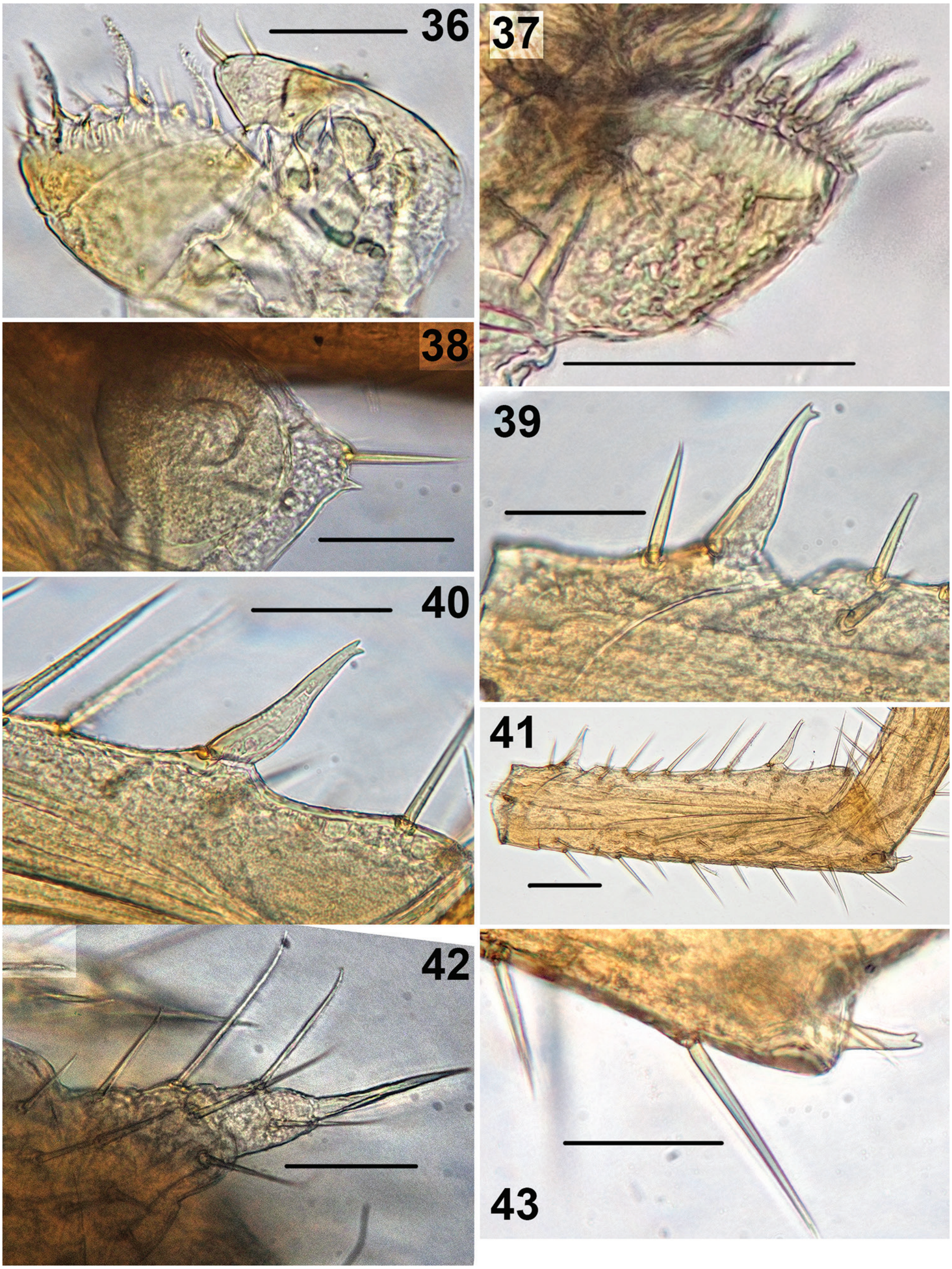

Figures 36–43. *Shikokuobius altaicus* sp. n., male paratype (**36**) and not-type male (**37–43**). **36** left part of first maxilla, ventral view **37** right part of first maxilla, ventral view **38** distal part of coxa 15, ventral view **39** spine on trochanter 15, lateral view **40** spine on prefemur 15, lateral view **41** trochanter and prefemur 15, lateral view **42** right gonopod, ventral view **43** distodorsal spine on prefemur 15, lateral view. Scale bars: 0.05 mm (**36–40, 42, 43**), 0.1 mm (**41**).

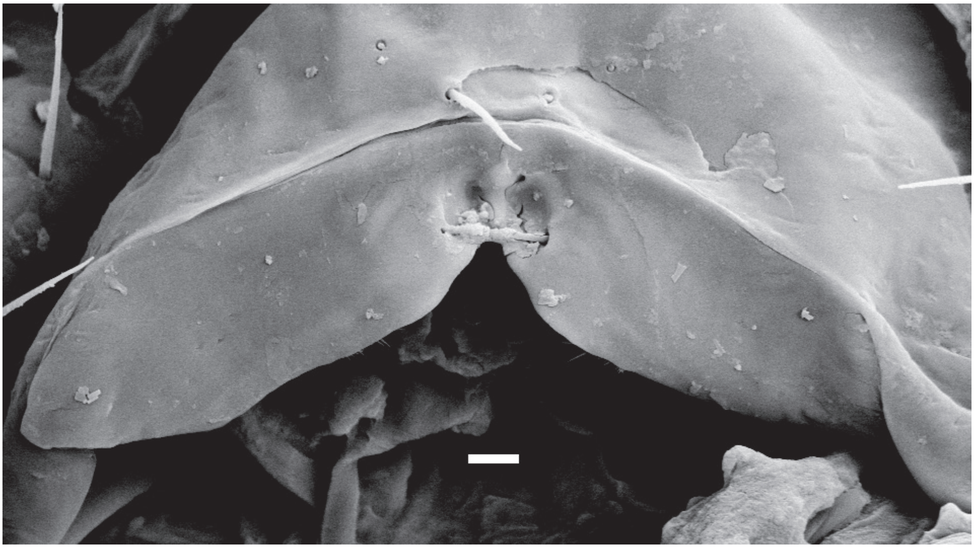

Figure 44. *Shikokuobius japonicus* (Murakami, 1967), DNA voucher specimen of Edgecombe and Giribet (2003, 2004), labrum, ventral view. Scale bar: 0.01 mm (courtesy of G.D. Edgecombe).

Figure 45. Habitat of *Shikokuobius altaicus* sp. n. (♀, PSU-612) in the Tigirek State Nature Reserve (courtesy of T.M. Krugova).

Table 1. The main differences between *S. japonicus* (Murakami, 1967) and *S. altaicus* sp. n.

	***S. japonicus* (Murakami, 1967)**		***S. altaicus* sp. n.**
	***sensu* Murakami 1967**	***sensu* Shinohara 1982**	
front body part	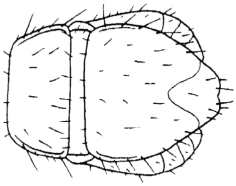	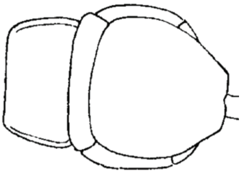	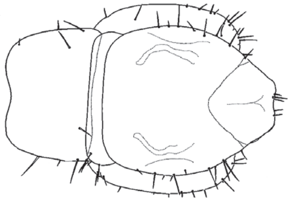
	cephalic plate equal in width and length; posterior margin of T1 straight		cephalic plate slightly elongate, width/length ratio 0.8; posterior margin of T1 slightly sinuate
number of antennomeres	18	up to 18	15*
labrum	 sides are smooth; pair of setae projecting across the labral midpiece absent**	no data	 sides with poorly-expressed fringes of bristles; pair of setae projecting across the labral midpiece present
forcipular coxosternite	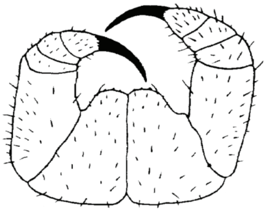	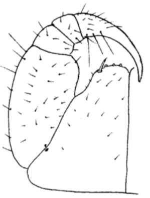	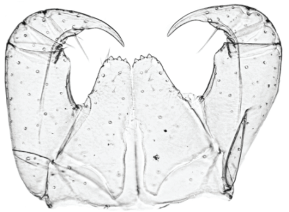
	approximately broad, width/length ratio 1.6–1.8:1		narrower, width/length ratio 1.2–1.3:1
dental margin of forcipulae coxosternite	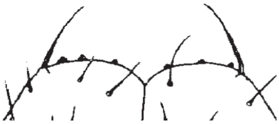	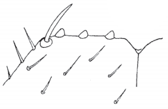	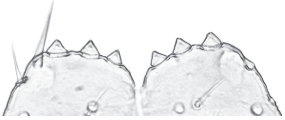
	teeth very small, separated from each other by distances more than width at the base of a tooth		teeth relatively large, separated from each other by distances less than width at the base of a tooth
leg 15	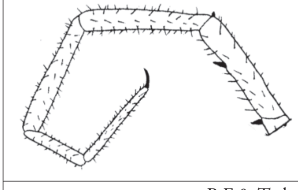	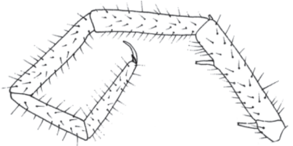	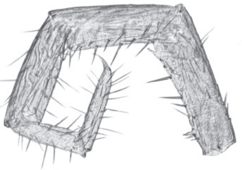
	P, F & T elongate and thin		P, F & T shorter and thicker

* antennae in a single male (non-type material) with 17+17 articles

** the apparent absence of a pair of setae projecting across the labral midpiece is likely due to them not being noticed by the author of the original description, but sensu G.D. Edgecombe (previously unpublished SEM image of the DNA voucher specimen of Edgecombe and Giribet (2003, 2004) as in Fig. 44), this pair of setae present.

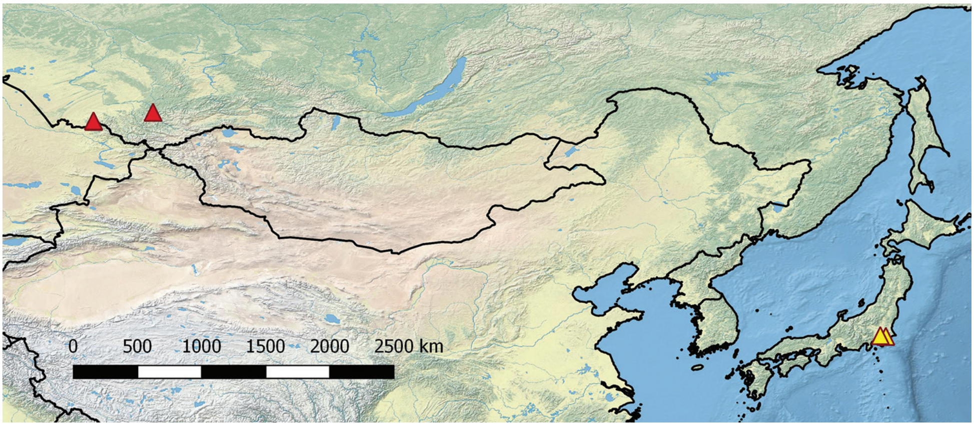

Figure 46. Distribution of *Shikokuobius* species: *altaicus* sp. n. (red triangle) and *japonicus* (Murakami, 1967) (yellow triangle).

Remarks. The new species belongs to the genus *Shikokuobius* Shinohara, 1982 that shows the following synapomorphies: antenna with up to 18 articles, 3+3 coxosternal teeth; spiracles on leg-bearing segments 3, 5, 8, 10, 12 and 14; coxal pores on 12–15 legs; 15 C with a prominent, acute, mesodistal process; 15 t and 15 P with spines, ventrally bifurcated at their tips; at least 15 P with a bifurcate spine at distodorsal end (as some specimens with spines apparently broken off, so these are not visible).

S. altaicus sp. n. is similar to *S. japonicus* (Murakami, 1967), so far the single species in the genus *Shikokuobius*, with the above characters. The main differences between them are given in Table 1. Besides this, the new species differs from *S. japonicus* by: (1) a small distodorsal process on tarsus 2 of legs 13–15 (absent from *S. japonicus*); (2) the number of coxal pores (1,1,1,1(2) in *S. altaicus* sp. n. vs. 2(1),2,2,2 sensu Murakami 1967 and 2,2,2,2(3) sensu Shinohara 1982 in *S. japonicus*).

Finally, *S. altaicus* sp. n. is also rather similar to *Ghilaroviella valiachmedovi* Zalesskaja, 1975, from the Tajikistan in showing the same body length, simple and plumose bristles on the second maxillae; the number of antennomeres, 1–2 coxal pores, 2+2 spurs and a simple ♀ gonopodal claw. However, *S. altaicus* sp. n. is well-distinguished from the latter species by: (1) 3+3 coxosternal teeth (vs. 2+2 in *G. valiachmedovi*); (2) coxal process well-developed only on leg 15 (vs. on legs 14 and 15 in *G. valiachmedovi*) and (3) the absence of small warts at the base of the ♀ gonopodal claw (vs. 2 small warts in *G. valiachmedovi*).

Acknowledgments

The authors wish to thank S.I. Golovatch (Moscow, Russia) for kindly editing the English of an advanced draft. Special gratitude goes to S.L. Esyunin (Perm, Russia) for his constant guidance, encouragement and support of the first co-author. We are also very much obliged to A.A. Schileyko (Moscow, Russia) for the provision some of material from ZMUM and to T.M. Krugova (Barnaul, Russia) and her team of volunteers who collected fresh specimens of the new species and donated us their material for study. Special thanks are also addressed to reviewers, G.D. Edgecombe (London, UK) and M. Zapparoli (Viterbo, Italy), for very valuable comments and an SEM image. We are also grateful to I.H. Tuf (Olomouc, Czechia) who kindly shared some of old literature and corrected the draft.

References

Attems C (1938) Die von Dr. C. Dawydoff in Französisch Indochina gesammelten Myriopoden. Mémoires du Muséum d'Histoire Naturelle (Paris) NS 6(2): 187–353.

Bonato L, Edgecombe GD, Lewis JGE, Minelli A, Pereira LA, Shelley RM, Zapparoli M (2010) A common terminology for the external anatomy of centipedes (Chilopoda). ZooKeys 69: 17–51. https://doi.org/10.3897/zookeys.69.737

Edgecombe GD, Giribet G (2003) Relationships of Henicopidae (Chilopoda: Lithobiomorpha): New molecular data, classification and biogeography. African Invertebrates 44: 13–38.

Edgecombe GD, Giribet G (2004) Molecular phylogeny of Australasian anopsobiine centipedes (Chilopoda: Lithobiomorpha). Invertebrate Systematics 18: 235–49. https://doi.org/10.1071/IS03033

Farzalieva GSh, Zalesskaja NT, Edgecombe GD (2004) A new genus and species of lithobiomorph centipede (Chilopoda: Lithobiomorpha: Anopsobiidae) from eastern Kazakhstan. Arthropoda Selecta 13(4): 219–224.

Krasheninnikov AB (2011) Mounting technique of entomological preparations in sandarac medium. Eurasian entomological journal 10(3): 278–279.

Murakami Y (1967) Postembryonic development of the common Myriapoda of Japan XXIV. A new species of the family Henicopidae. Zoological Magazine, Tokyo, 76: 7–12.

Shear WA (2018) The centipede family Anopsobiidae new to North America, with the description of a new genus and species and notes on the Henicopidae of North America and the Anopsobiidae of the Northern Hemisphere (Chilopoda, Lithobiomorpha). Zootaxa 4422(2): 259–283. https://doi.org/10.11646/zootaxa.4422.2.6

Shinohara K (1982) A new genus of centipede of the subfamily Anopsobiinae (Henicopidae, Chilopoda). Proceedings of the Japanese Society for Systematic Zoology 24: 41–46.

Silvestri F (1909) Descrizioni preliminari di vari artropodi specialmente d'America. Rendiconti della R. Accademia dei Lincei. Classe di Scienze Fisiche Matematiche e Naturali 18: 267–271.

Zalesskaja NT (1975) [New genera and species of Chilopoda (Lithobiomorpha) from Central Asia and Far East]. Zoologicheskii Zhurnal 54(9): 1316–1325. [in Russian]

Zapparoli M, Edgecombe GD (2011) Order Lithobiomorpha. In: Minelli A (Ed.) Treatise on Zoology – Anatomy, Taxonomy, Biology – The Myriapoda, Volume 1. Brill, Leiden – Boston, 371–389.

ZooKeys 793: 29–51 (2018)
doi: 10.3897/zookeys.793.25005
http://zookeys.pensoft.net

RESEARCH ARTICLE

A peer-reviewed open-access journal
ZooKeys
Launched to accelerate biodiversity research

Bryocyclops asetus sp. n. and the presence of *Bryocyclops muscicola* (Menzel, 1926) from Thailand (Crustacea, Copepoda, Cyclopoida, Cyclopidae)

Santi Watiroyram[1]

1 *Division of Biology, Faculty of Science, Nakhon Phanom University, Nakhon Phanom 48000, Thailand*

Corresponding author: *Santi Watiroyram* (santi.watiroyram@npu.ac.th)

Academic editor: *D. Defaye* | Received 13 March 2018 | Accepted 19 September 2018 | Published 29 October 2018

http://zoobank.org/21DC524C-5894-4C0C-86BB-2D8E5810C2FE

Citation: Watiroyram S (2018) *Bryocyclops asetus* sp. n. and the presence of *Bryocyclops muscicola* (Menzel, 1926) from Thailand (Crustacea, Copepoda, Cyclopoida, Cyclopidae). ZooKeys 793: 29–51. https://doi.org/10.3897/zookeys.793.25005

Abstract

The description of *Bryocyclops asetus* **sp. n.** and the record of *B. muscicola* (Menzel, 1926) from Thailand are presented. The new species is most similar to *B. maewaensis* Watiroyram, Brancelj & Sanoamuang, 2012, the cave-dwelling species described from northern and western Thailand. They share morphological characteristics, such as the free margin of the anal operculum which is ovated and serrate, the same setae and the spines formulae on P1–P4 Exp-2 (setae: 5.5.5.4; spines: 3.3.3.3) and Enp-2 of P1–P2, P4 (setae formula 3.4.3) in both sexes. The new species is easily distinguished from *B. maewaensis* due to typical divergent caudal rami, the absence of coxal seta on P1, and the absence of blunt-tipped setae on P2–P3 Exp-2. A dichotomous key to the species of *Bryocyclops* group I *sensu* Lindberg (1953) is proposed.

Keywords

Caves, copepods, freshwater, redescription of *Bryocyclops muscicola*, new species, taxonomy

Introduction

The genus *Bryocyclops* Kiefer, 1927 is the most abundant genus of Cyclopidae Rafinesque, 1815 from Thailand and it is widely distributed in Southeast Asia. At present, six species have been reported from Thailand: *B. maewaensis* Watiroyram, Brancelj & Sanoamuang, 2012; *B. maholarnensis* Watiroyram, Brancelj & Sanoamuang, 2015;

B. muscicoloides Watiroyram, 2018; *B. trangensis* Watiroyram, 2018; *B. muscicola* (Menzel, 1926) and *B. asetus* sp. n. (Figure 1). All species have so far been found in caves and are presumed to be endemic to Thailand, except *B. muscicola*, which frequently has been found in both subterranean and non-subterranean habitats (Jocque et al. 2013; present study). *Bryocyclops asetus* sp. n. belongs to group I *sensu* Lindberg (1953) because it shares the armature of the first to the fourth swimming legs. Group I is the most diverse group of the genus, consisting of *B. anninae* (Menzel, 1926) from Guam, Hawaii, Vanuatu, and Indonesia (Java, Sumatra); *B. ankaratranus* Kiefer, 1955 and *B. mandrakanus* Kiefer, 1955 from Madagascar; *B. apertus* Kiefer, 1935, *B. difficilis* Kiefer, 1935, and *B. elachistus* Kiefer, 1935 from Kenya; *B. chappuisi* Kiefer, 1928 from Indonesia (Java); *B. phyllopus* Kiefer, 1935 from Congo, Ethiopia, Kenya; and *B. maewaensis* and *B. asetus* sp. n. from Thailand (Dussart and Defaye 2006; Watiroyram et al. 2012). *Bryocyclops absalomi* Por, 1981 from Israel which has not been assigned into a species group by Por (1981) and Dussart and Defaye (2006), could be part of another species of group I (except the P1 coxa lacking inner seta). However, most group I members, even other *Bryocyclops* members, have been inadequately described by authors who usually focus on the anal operculum and selected legs. Indeed, the fine details (i.e. microcharacters) on the body ornamentation (cephalothorax scar, posterior margins, pores or grooves) and the structure of swimming legs (transformed setae and spines, and spiniform processes, especially the fourth leg and the male's third leg) are often considered to be important characters in the most recently described species. These characteristics are useful for determining closely related species and degrees of leg modifications (Reid 1999; Fiers and van Damme 2017; Watiroyram 2018). The new species, *B. asetus* and the new record of *B. muscicola* from Thailand are presented and their morphological and physical adaptations briefly discussed. An updated key to species of *Bryocyclops* group I *sensu* Lindberg (1953) is also provided.

Materials and methods

Water samples were collected using plankton and hand nets (60 µm) and preserved in 70% ethanol. Adult animals were sorted and dissected under an Olympus SZ51 stereomicroscope in a mixture of glycerol and 70% ethanol (ratio ~ 1:10 v/v) and pure glycerol. Dissected specimens were mounted in pure glycerol and sealed with nail polish. All appendages and body ornamentation were examined under an Olympus compound microscope (CX31) at 1000× magnification. Drawings were made with a drawing tube (an Olympus U-Da) mounted on a compound microscope. The final versions of the drawings were made using the CORELDRAW® 12.0 graphic program. Specimens for scanning electron microscopy (SEM) were dehydrated in an ethanol series (70%, 80%, 90%, 95%, 100%, and 100% absolute ethanol) for 15 min each concentration. Specimens were dried in a critical point dryer using liquid carbon dioxide as exchange medium. Dried specimens were mounted on stubs using adhesive

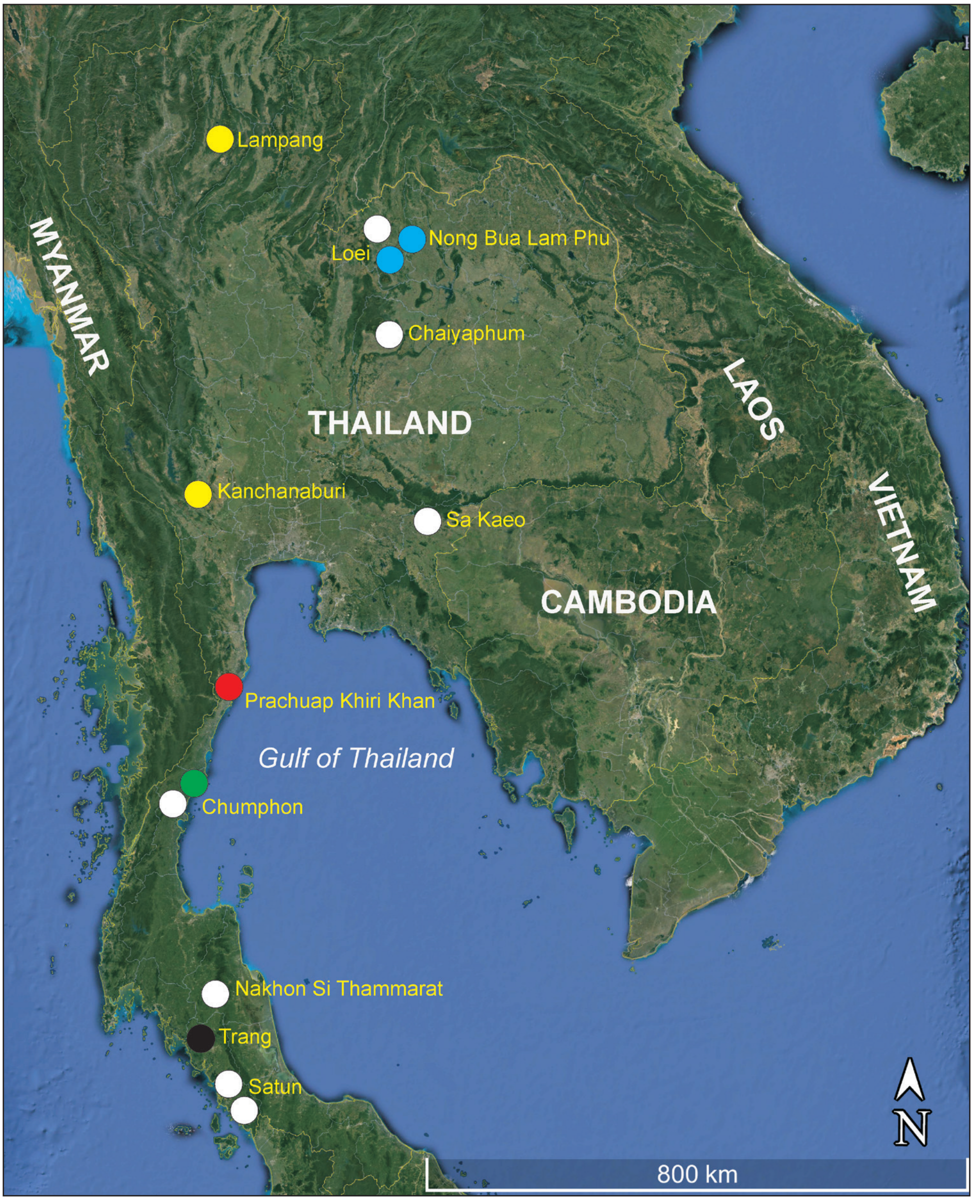

Figure 1. The geographical distribution of the genus *Bryocyclops* Kiefer, 1927 in Thailand. The coloured circles (O) indicate approximate location of species: yellow, *B. maewaensis* from Lampang and Kanchanaburi Provinces; white, *B. muscicola* from Loei, Chaiyaphum, Sa Kaeo, Chumphon, Nakhon Si Thammarat, and Satun Provinces; blue, *B. maholarnensis* from Loei and Nong Bua Lam Phu Provinces; red, *B. asetus* sp. n. from Prachuap Khiri Khan Province; green, *B. muscicoloides* from Chumphon Province; black, *B. trangensis* from Trang Province.

tape under stereomicroscope. Specimens were coated with gold in a sputter-coater. The SEM photographs were made using a scanning electron microscope (LEO 1450 VP).

The following abbreviations are used throughout the text and figures:

A	aesthetasc;	**P1–P6**	swimming legs 1–6;
Enp	endopod;	**S**	seta/setae;
Exp	exopod;	**Sp**	spine/spines
Exp/Enp-n	exopodal segment n/endopodal segment n;		

The appendage terminology follows Huys and Boxshall (1991). Specimens were deposited at the Natural History Museum, London, United Kingdom (**NHMUK**) and at the Nakhon Phanom University, Faculty of Science, Thailand (**NPU**).

Taxonomic section

Order Cyclopoida Rafinesque, 1815
Family Cyclopidae Rafinesque, 1815
Genus *Bryocyclops* Kiefer, 1927

Bryocyclops asetus sp. n.

http://zoobank.org/FAA0B3EA-9B61-44E1-8836-309C3C7524BD
Figs 2–8

Type locality. A rimstone pool in Sai Cave, Khao Daeng Subdistrict, Kui Buri District, Prachuap Khiri Khan Province, western Thailand; 12°10'46"N; 100°00'26"E, altitude: 107 m above sea level.

Material examined. Holotype: one adult male, NHMUK 2018.1043, dissected and mounted on one slide; allotype: one adult female, NHMUK 2018.1044, dissected and mounted in one slide; paratypes: one ovigerous female, two adult females and three adult males, NHMUK 2018.1045-1050, preserved in 70% ethanol in 1.5 ml microtube and three adult females and three adult males, NPU 2018–003, preserved in 70% ethanol in 1.5 ml microtube; all specimens collected on 1 December 2016 by author.

Differential diagnosis. Anal operculum ovate and serrate. P1–P4 with acute projections on distal margin of intercoxal sclerite; no inner coxal seta. Basis of P1 with inner spine. P1–P4 with two-segmented Exp and Enp. Setal and spine formula of P1–P4 Exp-2 as follows: 5.5.5.4; 3.3.3.3; with no blunt-tipped setae; P1–P4 Enp-2 as 3.4.5.3 and 1.1.1.1. Male P3 Enp-2 with six elements, including one transformed spine and seta: transformed spine with acute tip; slightly swollen in medians part, armed with strong spinules; transformed seta bare, strong.

Description of adult female. Preserved specimens colourless. Nauplius eye and refractile points on integument absent. Body length (Figs 2A, 3A) (n = 5) measured from

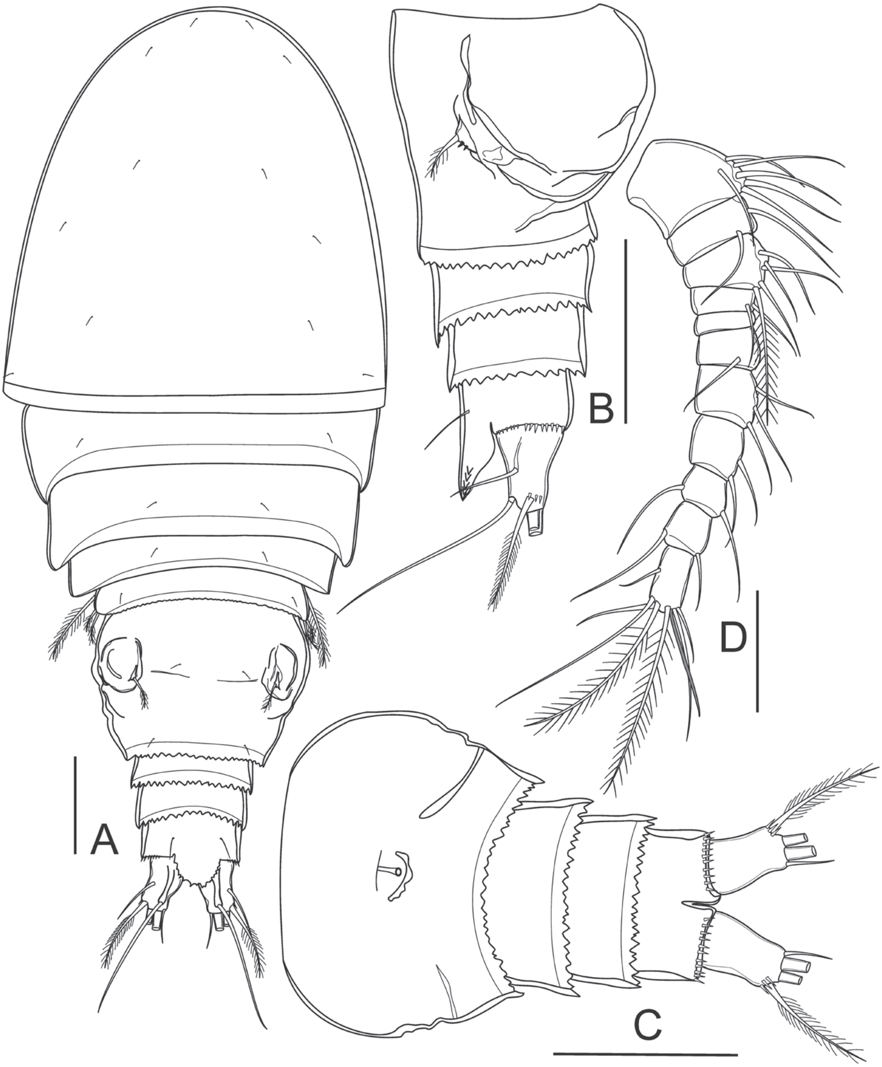

Figure 2. *Bryocyclops asetus* sp. n., female: **A** habitus, dorsal view **B** urosome (without pediger V), lateral view **C** urosome (without pediger V), ventral view **D** antennule. Scale bar: 50 μm.

anterior margin of rostrum to posterior margin of caudal rami 398–415 μm (mean 406 μm, n = 5); greatest width at distal part of cephalothorax 156–169 μm (mean 164 μm, n = 5); body length/width ratio 2.5. Cephalothorax completely fused to pediger I, without dorsal scar. Prosome length 245–248 μm (mean 246 μm, n = 5), urosome length 165–169 μm (mean 167 μm, n = 5); prosome/urosome length ratio 1.5. Prosomites with posterior dorsal margins smooth; urosomites serrated; pediger V finely serrated, and genital double-somite and two later urosomites coarsely serrated, both dorsally and ventrally (Fig. 3B, D). Genital double-somite (Figs 2A–C, 3F) symmetrical; length 73–76 μm (mean 75 μm, n = 5), width 98–100 μm (mean 99 μm, n = 5); 1.3 times wider than broad. Pair of sclerotized

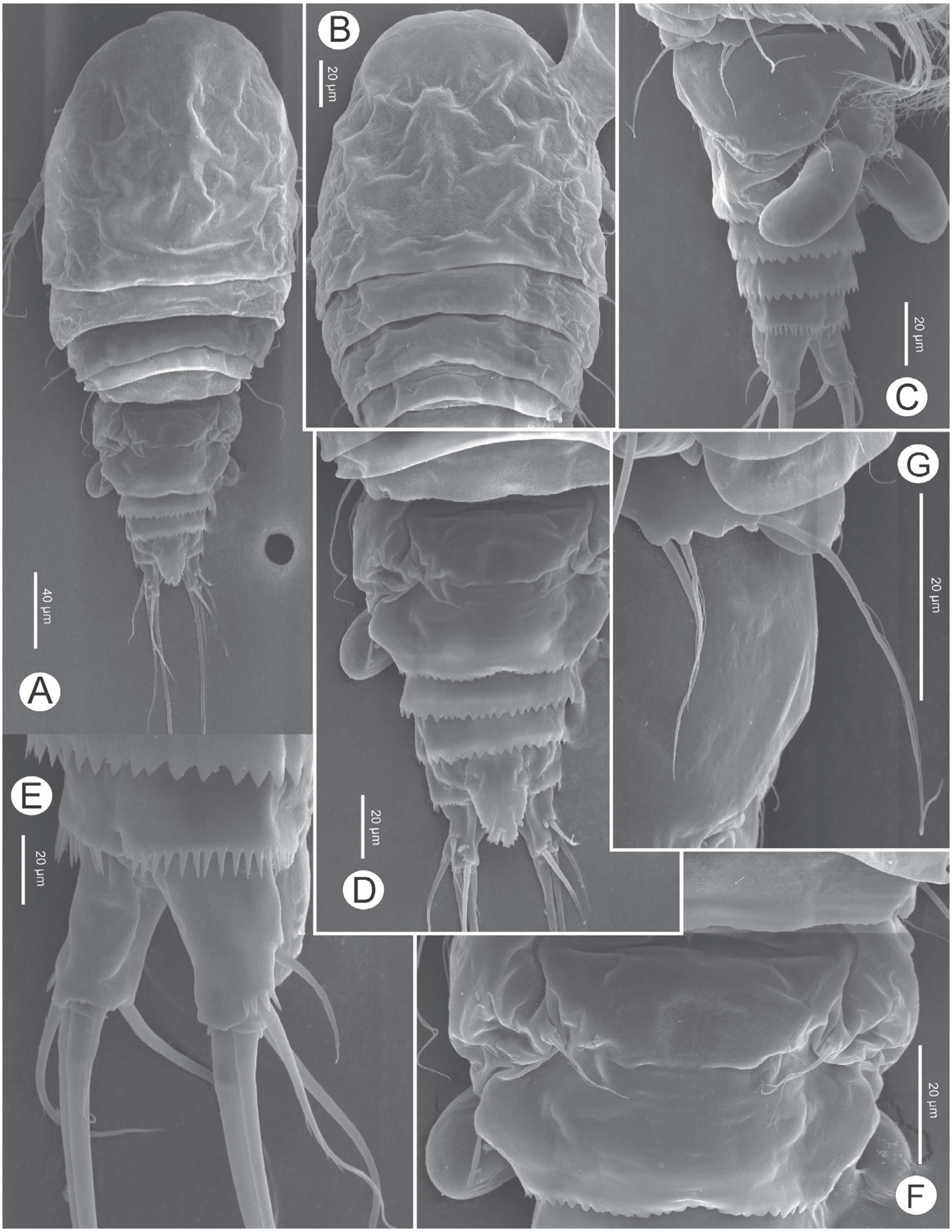

Figure 3. *Bryocyclops asetus* sp. n., SEM photographs of female: **A** habitus, dorsal view **B** prosome, dorsal view **C** urosome (genital double-somite with spermatophore), ventrolateral view **D** urosome, dorsal view **E** caudal ramus, ventrolateral view **F** genital double-somite, dorsal view **G** P5.

structures dorsolaterally, remnant of ancestral segment both dorsally and ventrolaterally; copulatory pore situated midventrally. Anal somite (Figs 2A–C, 3D–E) with strong spinules along entire posterior margin; pair of long sensilla above base of anal operculum. Anal operculum ovate, coarsely serrated, extending over three-fourths of caudal ramus length.

Caudal rami (Figs 2A–C, 3D–E) divergent, slightly tapering on distal half, 1.5 times as long as wide. Each ramus with six setae (seta II–VII): anterolateral (II) seta bare, slightly shorter than ramus; posterolateral (III) seta pinnate, 1.3 times as long as ramus, with strong spinules near venterolateral insertion; outer terminal (IV) and inner terminal (V) setae longest, pinnate, with fracture plane; terminal accessory (VI) seta shortest, bare, 0.5 times as long as ramus; dorsal (VII) seta located on distal margin of dorsal keel, bare, 2.2 times as long as ramus, with articulate insertion.

Antennule (Figure 2D) 11-segmented do not reach posterior margin of cephalothorax. Armature formula: 1(6S), 2(2S), 3(5S), 4(2S), 5(0), 6(1S), 7(3S), 8(2S), 9(2S), 10(2S), 11(7S+1A).

Antenna (Figure 4A) uniramous, consisting of coxobasis, and three-segmented Enp. Coxobasis with one smooth seta on distal inner corner. Enp-1–3 with 1, 5, and 7 setae respectively; with row of spinules on outer margin.

Mandible (Figure 4B) with six strongly chitinized teeth; dorsal seta on gnathobase. Palp reduced to single seta.

Maxillule (Figure 4C) with four strongly chitinized teeth on precoxal arthrite; inner margin with four bare setae and one plumose seta. Palp two-segmented: proximal segment with distal plumose seta; two bare setae distally; one bare seta dorsally; distal segment with three bare setae.

Maxilla (Figure 4D) with precoxal endite with two pinnate setae. Coxa with two endites: proximal endite with one bare seta; distal endite with one pinnate, and one bare setae. Basis with two strong claw-like expansions, bare seta close to its base. Two-segmented Enp, Enp-1 with unipinnate seta; Enp-2 with one unipinnate seta, two bare setae.

Maxilliped (Figure 4E) syncoxal endite with two strong spiniform setae, and row of spinules on anterior surface. Basis with spiniform seta, two rows of spinules on anterior surface. Two-segmented Enp; Enp-1 with one pinnate seta; Enp-2 with two bare setae.

P1–P4 (Fig. 5A–D) biramous, with two-segmented Exp and Enp. Intercoxal sclerites with no ornamentation, with acute projections on distal margin. P1 with group of tiny spinules at insertion of inner spine. All setae on P1–P4 Exp-2 with normal tips. P1–P4 Enp-1 with spiniform process on outer distal corner. Outer seta and inner proximal seta on P1 Enp-2 as long as spine, shorter than inner distal seta. Outer seta and inner proximal seta on P2 Enp-2 as long as spine, shorter than two inner distal setae. Proximal inner seta on P3 Enp-2 as long as spine, shorter than the rest of segment; outer seta slightly longer than spine, followed by two inner medial setae and apical seta. Apical seta on P4 Enp-2 longest, 2.5 times as long as spine, followed by inner and outer seta. Spine and setal formula of P1–P4 as follows (seta in Arabic numerals, spine in Roman numerals for outer-inner or outer-apical-inner seta/spine):

	Coxa	Basis	Exp		Enp	
			1	2	1	2
P1	0-0	1-I	I-0	III-2-3	0-1	1-I-2
P2	0-0	1-0	I-0	III-2-3	0-1	1-I+1-2
P3	0-0	1-0	I-0	III-2-3	0-1	1-I+1-3
P4	0-0	1-0	I-0	III-2-2	0-1	1-I+1-1

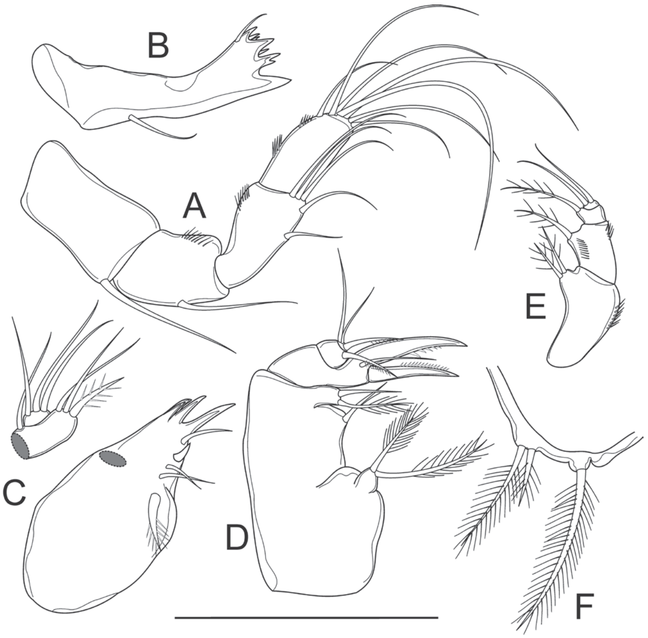

Figure 4. *Bryocyclops asetus* sp. n., female: **A** antenna **B** mandible **C** maxillule **D** maxilla **E** maxilliped **F** P5. Scale bar: 50 µm.

P5 (Figs 3G, 4F) fused to pediger, represented by three pinnate setae on small prominence: dorsal seta longer than two ventral setae; outer seta longer than inner one.

P6 (Figs 2A–B, 3F) situated laterodorsally next to heavily sclerotized structure on genital double-somite: with one short pinnate seta dorsally; two tiny spinules next to it ventrally element on small plate.

Adult females with pair of egg sacs (Figure 12A), each with two eggs, with a mean diameter of 64 µm (n = 8).

Description of adult male. Body length (Figs 6A, 7A) measured from anterior margin of rostrum to posterior margin of caudal rami 369–373 µm (mean 371 µm, n = 5); smaller than female. General segmentation and ornamentation (Figs 6A–C, 7A–C) similar to female, with five-segmented urosome. Anal operculum (Figure 7C) more finely serrated than in female. Antennae, mouthparts, P1–P2, P3 Exp-2, and P5 (Figs 7G, 8A–C) similar to those of female, except P2 Enp-2 with longer inner medial seta.

Antennule (Figs 6D, 7F) 16-segmented, geniculate. Armature formula as follows: 1(7S+2A), 2(3S), 3(1S), 4(2S+1A), 5(2S), 6(1S), 7(2S), 8(1A), 9(1S), 10(2S), 11(1Sp), 12(0), 13(2S+1A+1Sp), 14(1S), 15(3S), 16(7S+1A).

P3 (Figure 8C) intercoxal sclerite with acute projections on distal margin. Enp-1 with inner pinnate seta. Enp-2 with outer pinnate seta; transformed apical spine with hook-like tip, thin pinnate seta; inner strong bare seta, two inner pinnate setae. Transformed apical spine with several spinules at 2/3 length of it; less-produced medial portion; with short, acute tip.

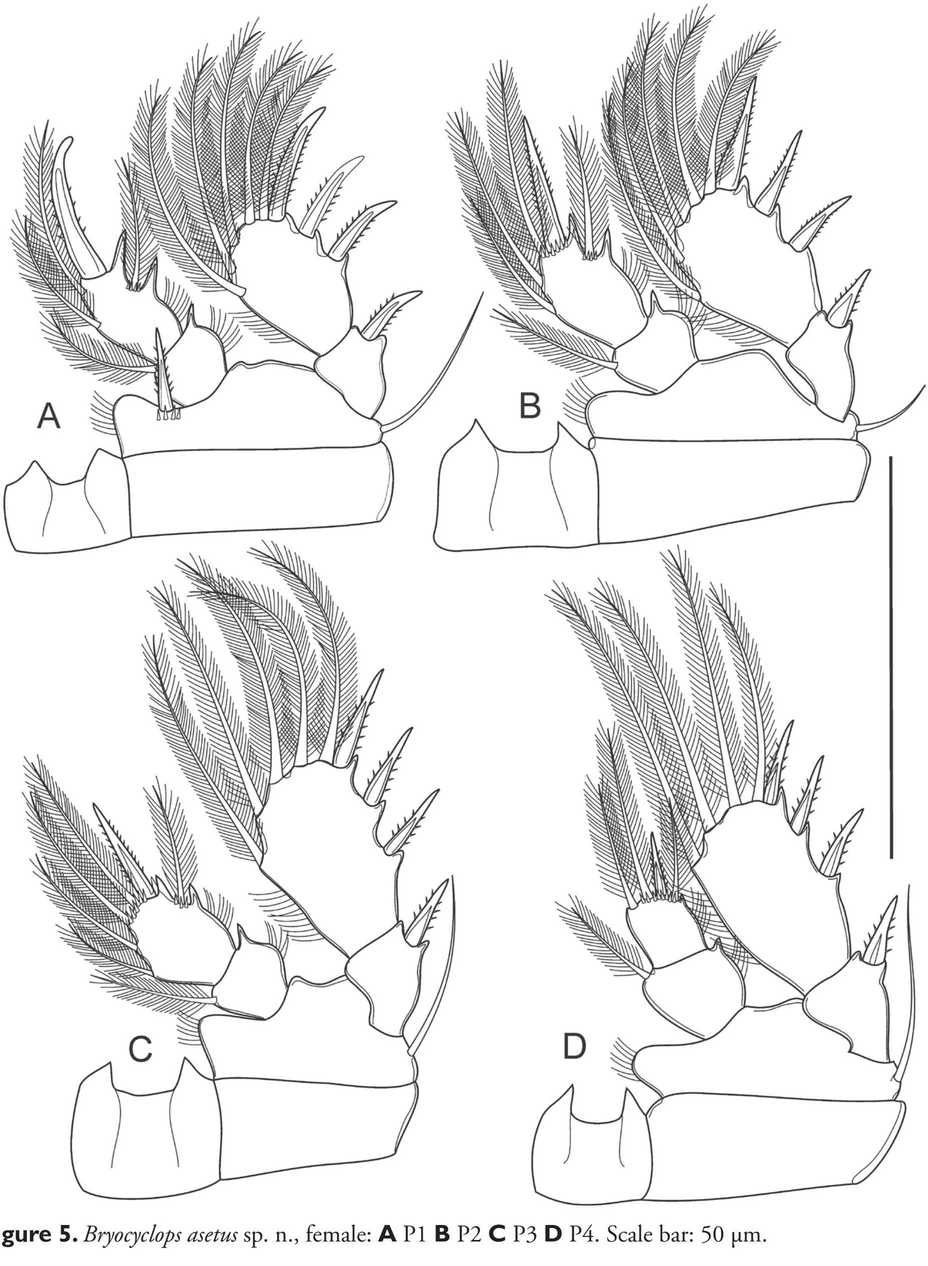

Figure 5. *Bryocyclops asetus* sp. n., female: **A** P1 **B** P2 **C** P3 **D** P4. Scale bar: 50 μm.

P4 (Figure 8D) intercoxal sclerite with acute projections on distal margin. Coxa without inner seta. Basis and Exp-1 with outer seta and spine, respectively. Exp-2 with three outer spines and two pinnate apical and inner setae. Enp-1 with inner pinnate seta and spiniform process on inner and outer distal margins. Enp-2 with apical spine and three long pinnate setae: apical and inner setae equal in length, 3.0 times as long as spine; outer seta 1.5 times longer than spine.

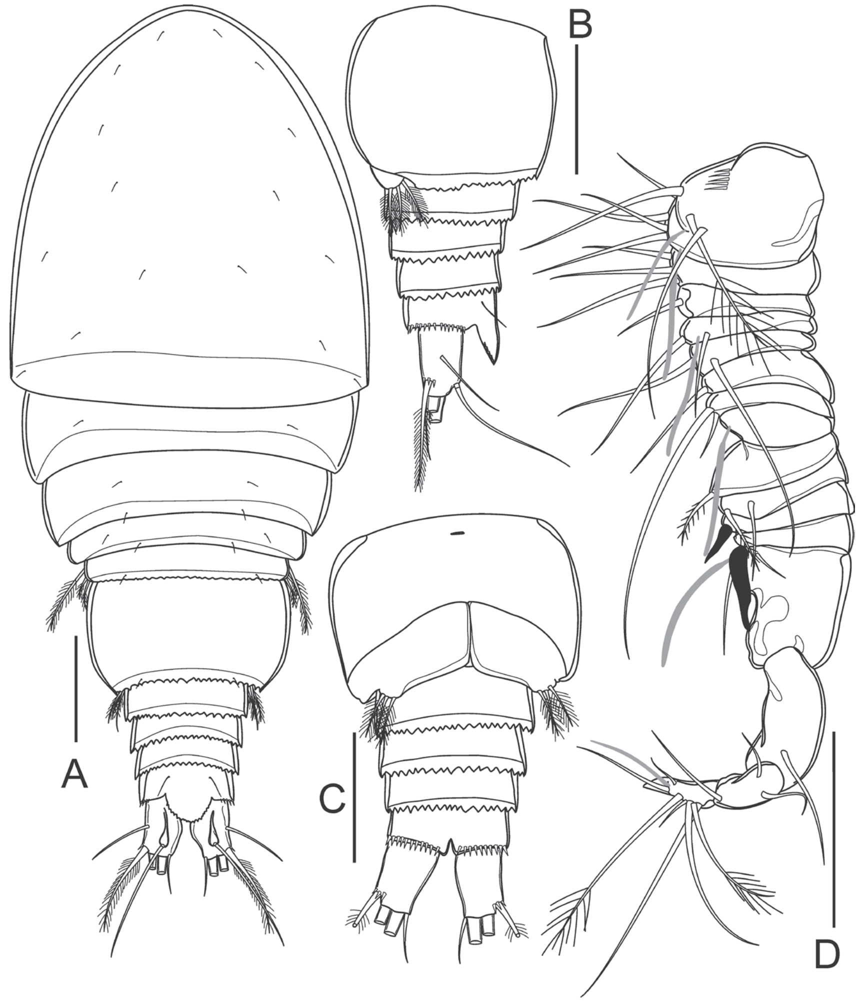

Figure 6. *Bryocyclops asetus* sp. n., male: **A** habitus, dorsal view **B** urosome (without pediger V), lateral view **C** urosome (without pediger V), ventral view **D** antennule. Scale bar: 50 µm.

P6 (Figs 6B, C, 7D) reduced to simple plate, represented by three subequal pinnate setae.

Variability. Two out of five examined females have round rather than acute distal margins on intercoxal sclerite of P1.

Etymology. The specific name *asetus* refers to the one of the primary characteristic that discriminates the new species from other species of group I *sensu* Lindberg (1953) by the first swimming leg without an inner coxal seta.

Geographical distribution. This species is currently known only from Sai Cave, Khao Daeng Subdistrict, Kui Buri District, Prachuap Khiri Khan Province, Thailand.

Remarks. The new species is most similar to *B. maewaensis*, found in caves in northern and western Thailand. They share the same morphological characteristics,

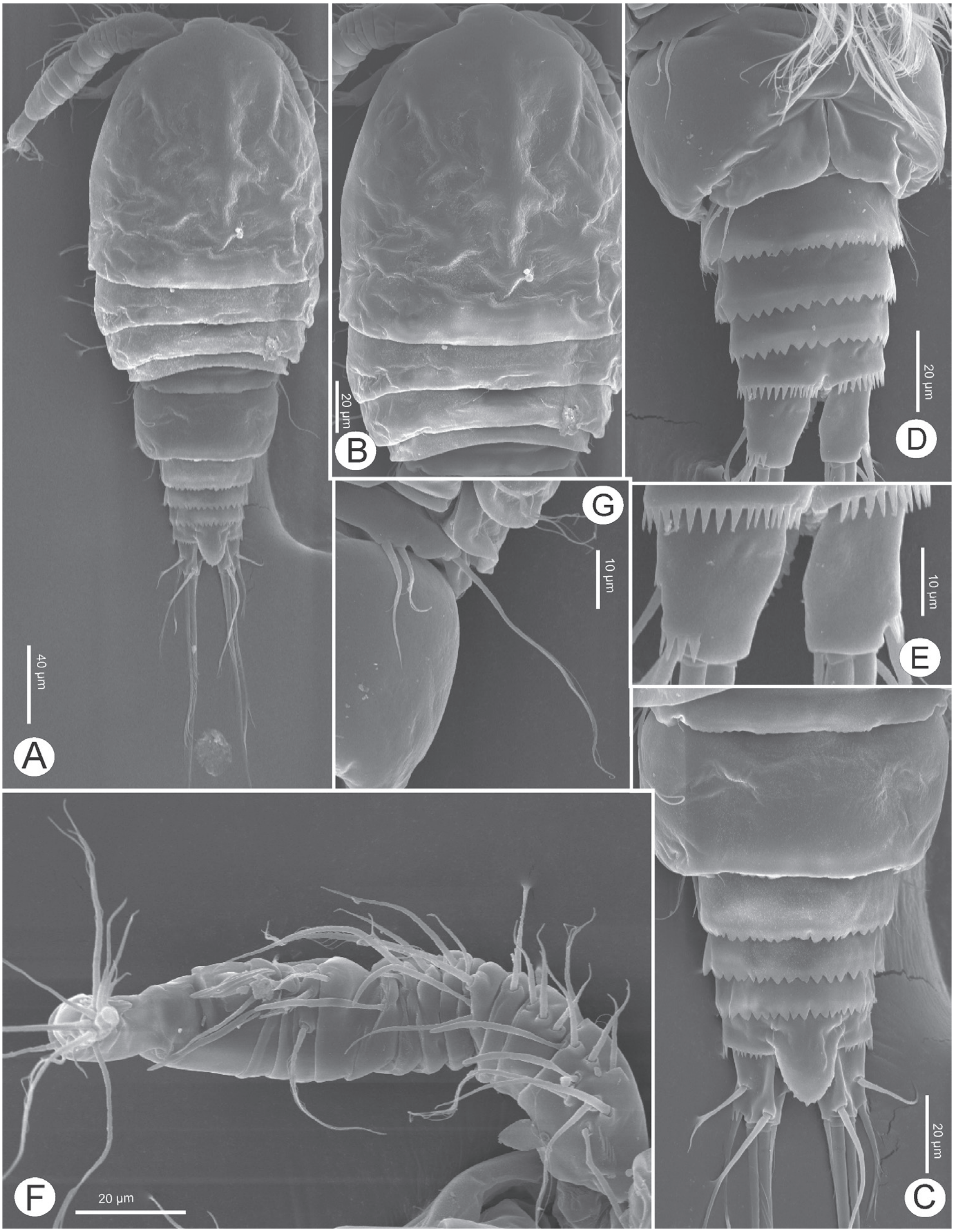

Figure 7. *Bryocyclops asetus* sp. n., SEM photographs of male: **A** habitus, dorsal view **B** prosome, dorsal view **C** urosome, dorsal view **D** urosome, ventral view **E** caudal ramus, ventral view **F** antennule.

such as the free margin of anal operculum ovate and serrate, the same setae and spines formula on P1–P4 Exp-2 (setae: 5.5.5.4; spines: 3.3.3.3) and the same setae formula on P1–P4 Enp-2 (3.4.5.3) in both sexes, except the male P3 Enp-2 of *B. asetus* sp. n. which has five instead of four setae. The new species is clearly differentiated from

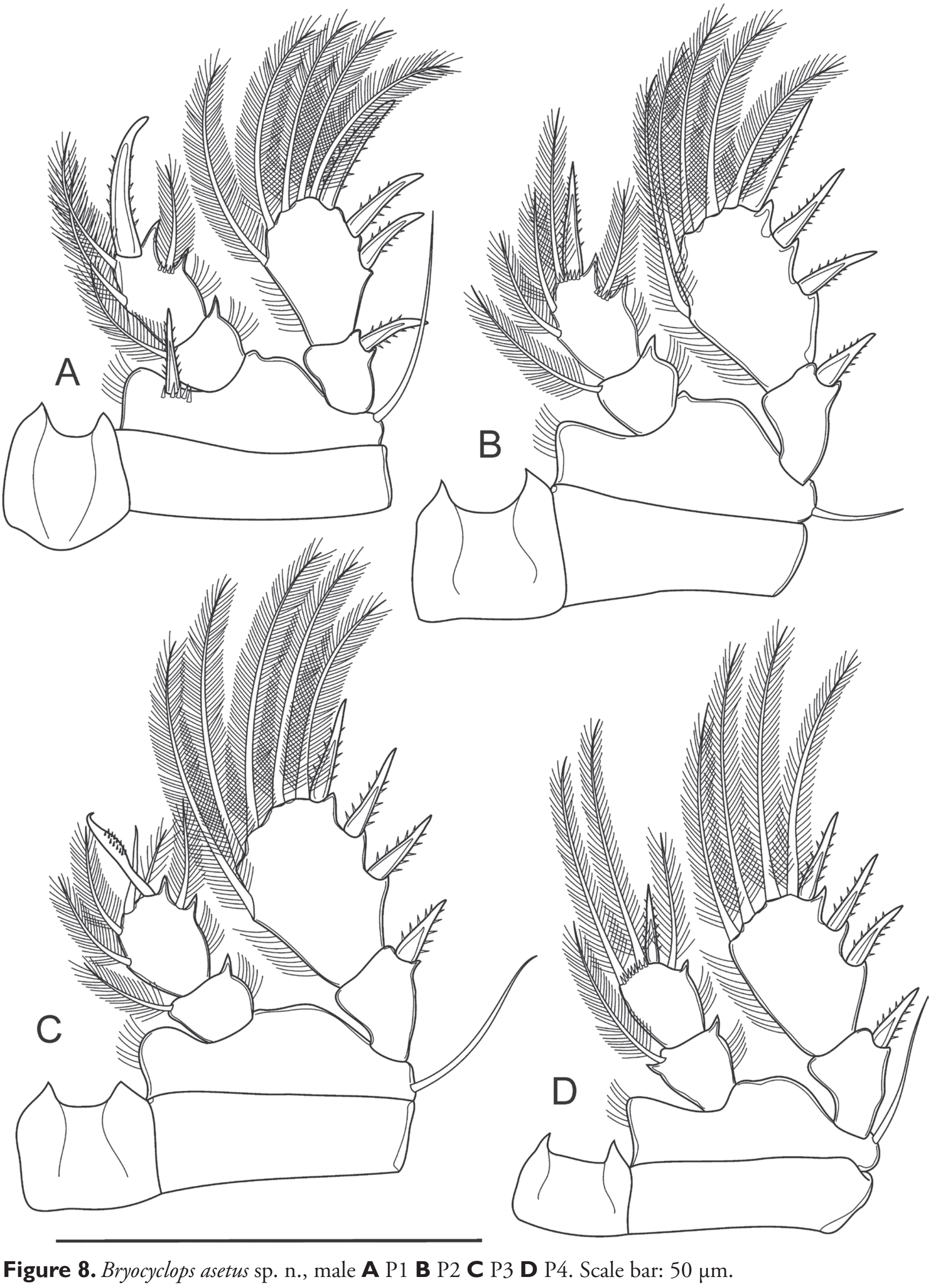

Figure 8. *Bryocyclops asetus* sp. n., male **A** P1 **B** P2 **C** P3 **D** P4. Scale bar: 50 µm.

B. maewaensis by its typical divergent caudal rami, the absence of a coxal seta on P1 and the absence of blunt-tipped setae on P2–P3 Exp-2. Female P4 Enp-1 of *B. asetus* sp. n. is larger than Enp-2 and has no spiniform process on the inner distal margin, which is present in *B. maewaensis*. Female P4 Enp-2 of the new species has three long slender setae which are longer than the apical spine on the same segment, but *B. maewaensis* has robust and short setae that are approximately as long as spine. Male P3 Enp-2 of the new species has a different transformed spine compared to *B. maewaensis*: the expansion is less expressed and is armed with strong spinules in the new species, but *B. maewaensis* has a well-expressed expansion and no ornamented surface.

Bryocyclops muscicola **(Menzel, 1926)**

Figs 9–11

Material examined. One dissected adult female and male mounted separately on one slide from each (seven) caves: Pha Pu Cave (NPU 2018–004-005), Na-Or Subdistrict, Muang District, Loei Province, 17°33'21"N; 101°43'39"E, altitude: 247 m, collected on 18 August 2014; Chang Phueak Cave (NPU 2018–006-007), Banna Subdistrict, Muang District, Chumphon Province, 10°26'46"N; 99°02'06"E, altitude: 104 m, collected on 10 August 2015; Mae Nang Songsi Cave (NPU 2018–008-009), Hin Tok Subdistrict, Ron Phibun District, Nakhon Si Thammarat Province, 08°14'45"N; 99°52'01"E, altitude: 45 m collected on 23 October 2015; Khao Tiphon Cave (NPU 2018–010-011), Thung Wa Subdistrict, Thung Wa District, Satun Province, 07°05'10"N; 99°47'53"E, altitude: 46 m collected on 24 October 2015; Khao Jean Cave (NPU 2018–012-013), Khlong Khut Subdistrict, Muang District, Satun Province, 06°38'32"N; 100°05'77"E, altitude: 38 m collected on 25 October 2015; Kaew Cave (NPU 2018–014-015), Laem Thong Subdistrict, Phakdi Chumphon District, Chaiyaphum Province, 15°58'27"N; 101°24'36"E, altitude: 394 m, collected on 19 September 2016; Khao Maka Cave (NPU 2018–016-017), Sala Lamduan Subdistrict, Muang District, Sa Kaeo Province, 13°47'10"N; 101°56'51"E, altitude: 121 m, collected on 5 November 2017. Four adult males and four adult females from Chang Phueak Cave mounted on one stub for SEM analysis (NPU 2018–018). All specimens collected by author.

Description of adult female. Body length (n = 5) excluding caudal setae, 481–491 µm (mean 486 µm), width 154–156 µm (mean 155 µm), body length/width ratio approximately 3.0 (Figs 9A, 11A). Prosome length 290–293 µm (mean 292 µm), urosome length 208–213 µm (mean 210 µm); prosome/urosome length ratio 1.4. Body surface with refractile points from cephalothorax to genital double-somite. Cephalothorax with dorsally incorporated scar, pair of dorsolateral body pits. Prosomites with smooth posterior dorsal margins; pedigers I-IV with serrated lines above posterior margins; pedigers I and II with dorsolateral body pits. Urosomites with dorsally serrated posterior margins; finely serrated on pediger V; urosomites coarsely serrate both dorsally and ventrally (Fig. 9B, C, E). Genital double-somite (Fig. 9B–D) symmetrical, 1.6 times as long as wide. Pair of sclerotized structures dorsolaterally, single copulatory pore midventrally. Urosomite 3–4 (Figure 9E) with body pits on dorsolateral surface. Anal somite (Fig. 9E–F) with strong spinules along entire posterior margin; pair of long sensilla above base of anal operculum. Anal operculum ovate, coarsely serrated and reaches over three-fourths of caudal ramus.

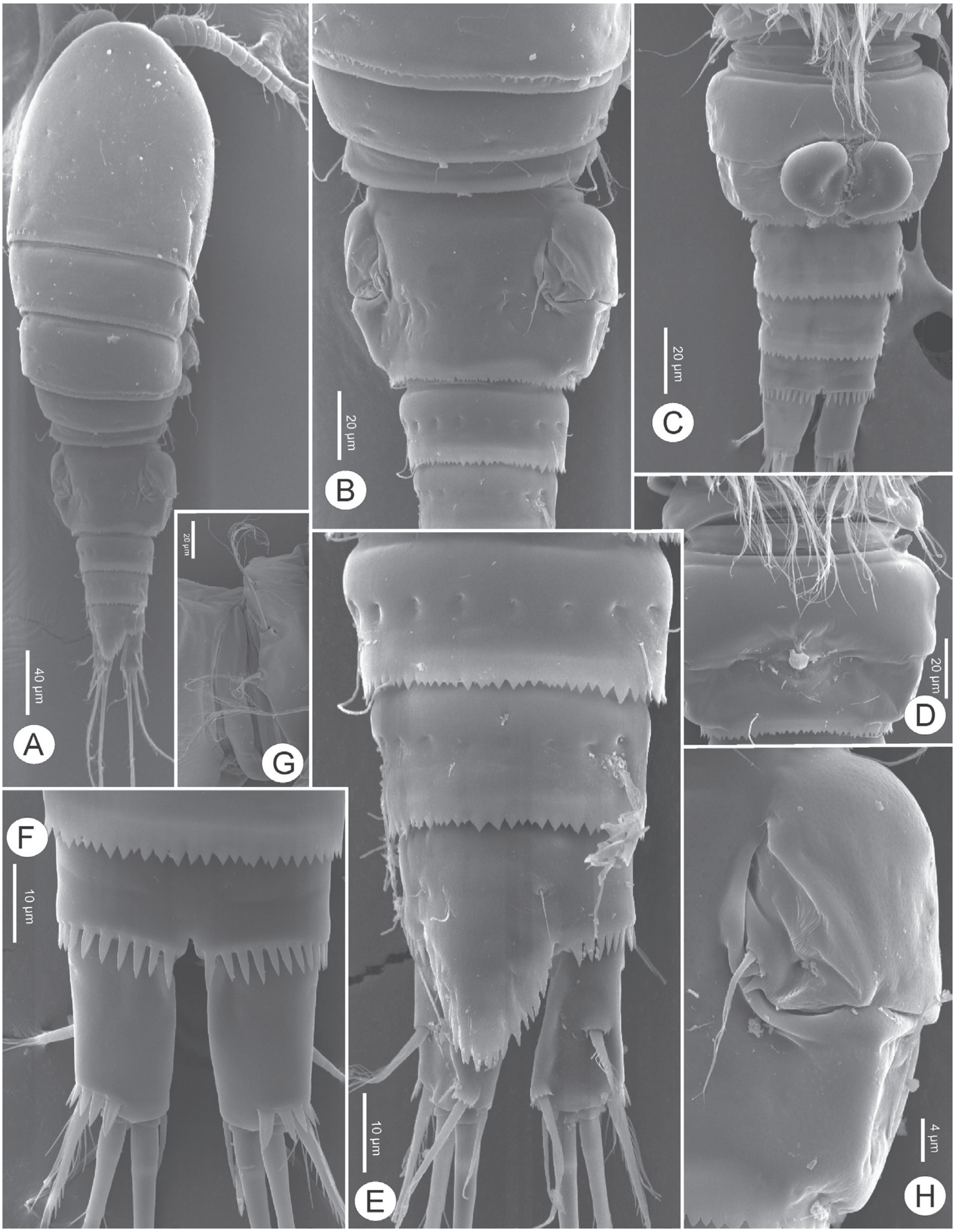

Figure 9. *Bryocyclops muscicola* (Menzel, 1926), SEM photographs of female: **A** habitus, dorsal view **B** pedigers III–V, genital double-somite, two later urosomites, dorsal view **C** urosome (genital double-somite with spermatophore), ventral view **D** genital double-somite, ventral view **E** urosome (without pediger V and genital double-somite), dorsal view **F** anal somite and caudal rami, ventral view **G** P5 **H** P6.

Caudal rami (Fig. 9E–F) parallel. Ramus 1.6 times as long as wide; with well-developed dorsal keel. Each ramus with four (seta II–V) pinnate setae and two (seta VI–VII) bare setae: posterolateral (III), outer terminal (IV) and dorsal (VII) setae with spinules above its insertion; setae IV and V (inner terminal seta) with breaking plane.

P1–P4 (Fig. 11B–E) biramous with two-segmented Exp and Enp but P4 with one-segmented Enp. Intercoxal sclerites with acute projections on distal margin. P2–P3 Exp-2 with two blunt-tipped setae (apical and inner seta) (Figure 11C). P1–P3 Enp-1 with spiniform process on outer distal corner. P4 Enp with spiniform process on mid-outer margin. Spine and setal formula of P1–P4 as follows (seta in Arabic numerals, spine in Roman numerals for outer-inner or outer-apical-inner seta/spine):

	Coxa	**Basis**	**Exp**		**Enp**	
			1	**2**	**1**	**2**
P1	0-1	1-I	I-0	III-2-3	0-1	1-I-2
P2	0-0	1-0	I-0	III-2-3	0-1	1-I+1-1
P3	0-0	1-0	I-0	III-2-3	0-1	1-I+1-3
P4	0-0	1-0	I-0	III-2-2	1-I+1-2	-

P5 (Figure 9G) completely fused to pediger V, represented by three pinnate setae: dorsal seta longest, on small prominence; two ventral setae completely fused with pediger, inner seta shortest.

P6 (Figure 9H) located on genital double-somite at 1/2 length, dorsolaterally; represented by one short pinnate seta and two tiny spinules on small plate.

Adult females with pair of egg sacs (Figure 12B), each with two eggs, with a mean diameter of 50 µm (n = 8).

Spermatophore (Figure 9C) bean-shaped, paired, visible on genital double-somite mid-posteroventrally.

Description of adult male. Body length (Figs 10, 11F–H) smaller than female with total body lengths of 432–440 µm (mean 436 µm), prosome/urosome length ratio 1.3 (n = 5). Body ornamentation, armature of P1–P2, P3–P4 Exp-2, and P5 similar to those of females. P3 (Figure 11I) with two-segmented Enp, Enp-1 with inner pinnate seta and spiniform process on outer distal margin. Enp-2 with three inner setae (distalmost seta bare, two others pinnate), transformed apical spine and outer pinnate seta. Transformed spine with medial-produced, semi-circular shape with spinules on swollen portion; with long distance between swollen portion and its tip; tip acute. P4 (Figure 11J) with two-segmented Enp; Enp-1 with inner pinnate seta and spiniform process on outer and inner distal margins; spiniform process strong and well-expressed on inner margin. Enp-2 with apical spine and three long pinnate setae, apical and inner seta subequal in length, 2.5 times as long as spine, outer seta shortest, 1.5 times longer than spine. P6 (Figure 11F, H) reduced to simple plate, represented by three unequal pinnate setae.

Geographical distribution. *Bryocyclops muscicola* is the most widely distributed species within the genus *Bryocyclops*, which is mainly found in Southeast Asia with one record finding from North America (Florida, Reid 1999). To date, the species has been found in Indonesia (Java, Sumatra) and Thailand, including the north eastern region (Loei and Chaiyaphum provinces), the eastern region (Sa Kaeo Province), the south-

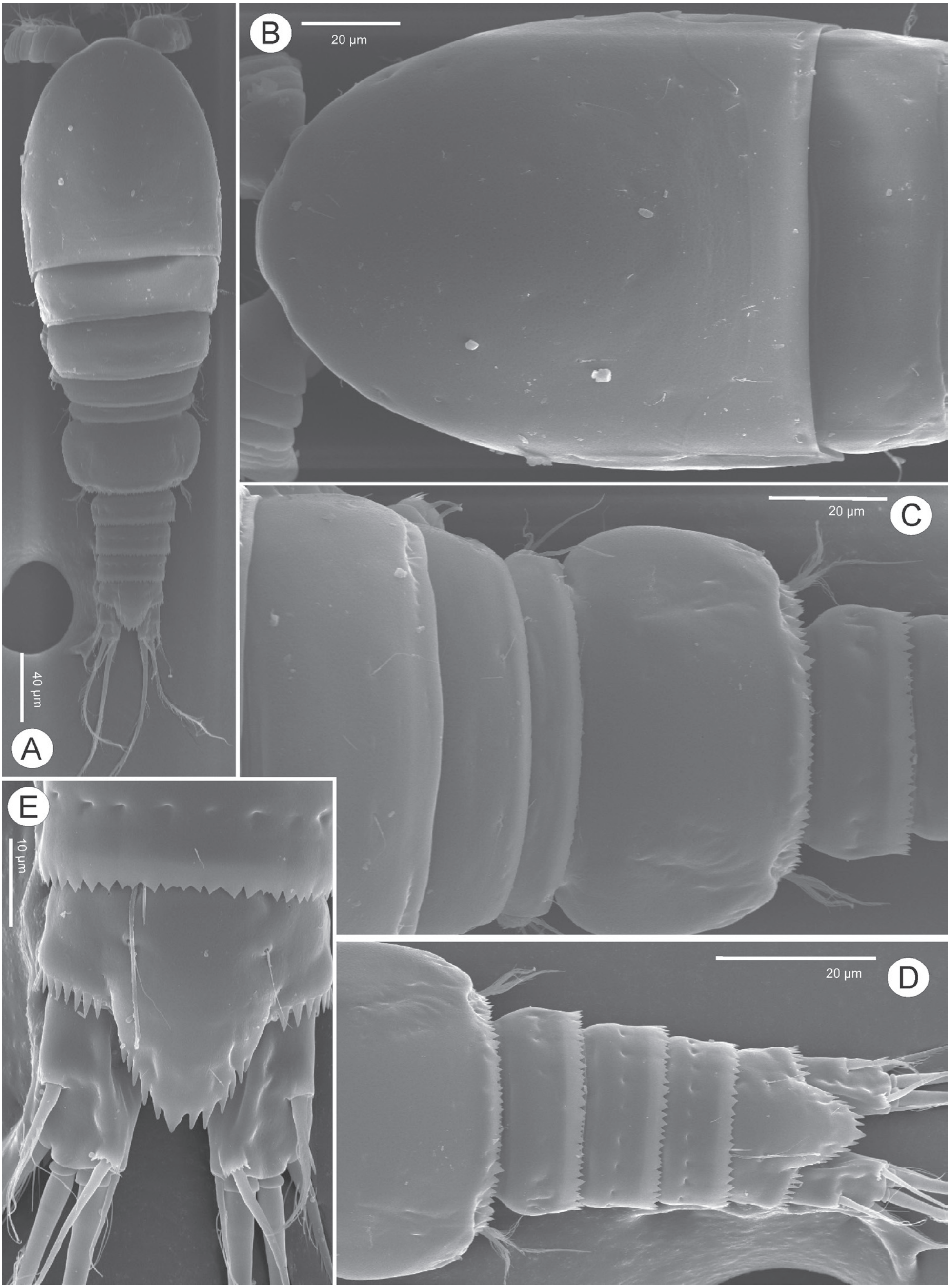

Figure 10. *Bryocyclops muscicola* (Menzel, 1926), SEM photographs of male in dorsal view **A** habitus **B** cephalothorax and pediger II **C** pedigers III–V, genital somite and later urosomites **D** genital somite and later urosomites **E** anal somite and caudal rami.

ern region (Chumphon, Nakhon Si Thammarat, and Satun provinces) (Menzel 1926; present study, see Figure 1).

Remarks. *Bryocyclops muscicola* belongs to *Bryocyclops* group II *sensu* Lindberg (1953) (Dussart and Defaye 2006)**.** All specimens of *B. muscicola* collected from caves in Thailand are consistent in terms of the details of their legs, anal operculum, and body ornamentation as observed by Menzel (1926) and Reid (1999). Some differences are noted on caudal rami and prosome: (1) the caudal ramus of Thailand's specimens have tiny spinules at the insertion of the dorsal seta (VII) instead of the lateral seta (III) in both sexes, and the males have an obviously longitudinal keel on their rami that is absent in the Florida's specimens; (2) the cephalothorax and pedigers II-IV of Thailand's specimens have serrated dorsal frills above their posterior margins, a frill only present on pedigers II-IV in the Florida specimens.

Discussion

Most members of the genus *Bryocyclops* have been previously found in semi-subterranean rather than subterranean habitats, such as moist moss, wet soils, leaf litter, and phytotelmata (Reid 1999, 2001). Some known species are only described from representatives of the male or the female and not described enough precisely (Dussart and Defaye 2006). After examining specimens from different regions of Thailand, *Bryocyclops* are among the most common cave-dwelling cyclopoids living in the epikarst zone. Currently, there are six species from Thailand and one species from Israel (*B. absalomi* Por, 1981) (see introduction). All species are presumed to have a restricted distribution and are also probably endemic to the areas (counties) in which they were first described. In this study, *B. muscicola* was for the first time found in subterranean environment in water containers filled directly with dripping water from stalactites or cliffs at the transition and the entrance zones (Fig. 12D, E, G). They have also been found in abundance in water tanks located in the dark zone of some caves (Figure 12F). Therefore, *B. muscicola* can be considered a stygophilous species as it successfully lives in the subterranean in both natural and artificial habitats.

Bryocyclops asetus sp. n. shares body ornamentation with members of group I (*B. anninae*; *B. maewaensis*; and *B. phyllopus*) and group II (*B. muscicola*; *B. caroli* Bjornberg, 1985; *B. campaneri* Rocha & Bjornberg, 1987; *B. muscicoloides* Watiroyram, 2018, and *B. trangensis* Watiroyram, 2018) according to the following characters: (1) the presence of dorsal serrated frills on the posterior margin of their prosomites (cephalothorax, pedigers II-IV of *B. asetus* sp. n., and *B. maewaensis*; pedigers II–IV of *B. campaneri*, *B. muscicola*, and *B. muscicoloides*; pediger III of *B. caroli*); (2) the presence of body groove on prosomites and urosomites (cephalothorax, pedigers II and IV, genital double-somite, and two subsequent urosomites of *B. asetus* sp. n., *B. campaneri*, *B. muscicola*, and *B. anninae*; cephalothorax, genital double-somite, and two subsequent urosomites of *B. muscicoloides*; genital double-somite of *B. trangensis*); and (3) the pres-

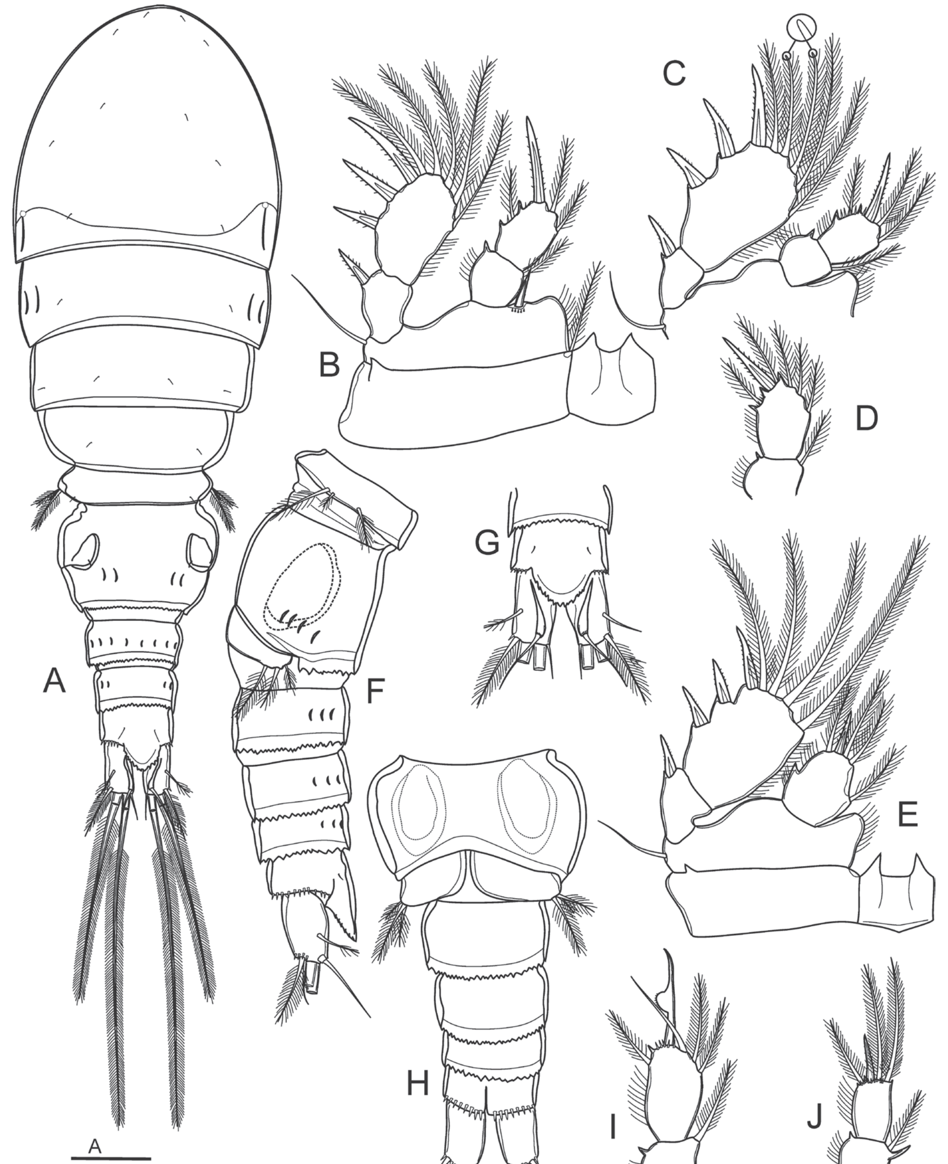

Figure 11. *Bryocyclops muscicola* (Menzel, 1926), female (**A–E**) and male (**F–J**) **A** habitus, dorsal view **B** P1 **C** P2 **D** P3 Enp **E** P4 **F** urosome, lateral view **G** anal somite and caudal rami, dorsal view **H** urosome (without pediger V), ventral view **I** P3 Enp **J** P4 Enp. Scale bar: 50 µm.

ence of cephalothorax scare (*B. asetus* sp. n., *B. maewaensis*, *B. phyllopus*, *B. muscicola*, *B. campaneri*, *B. muscicoloides*, and *B. trangensis*).

Bryocyclops absalomi Por, 1981 has sensory pits on cephalothorax, which were illustrated in SEM photographs (see Por 1981: fig. 23). This feature is observable

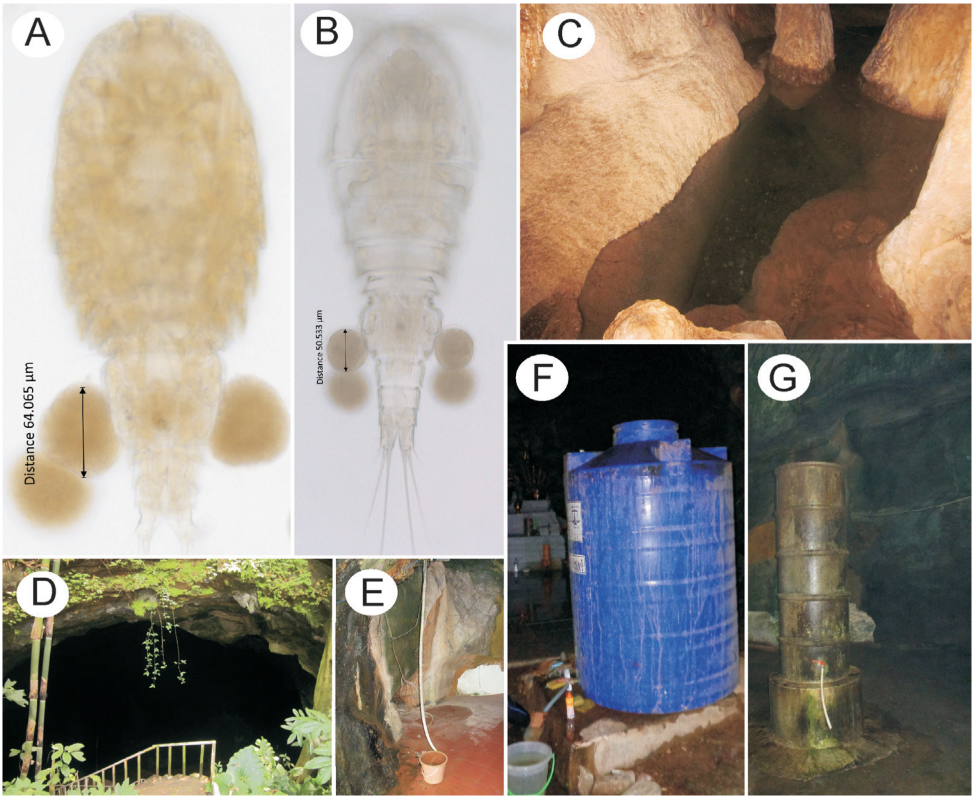

Figure 12. *Bryocyclops asetus* sp. n. (**A, C**) and *B. muscicola* (Menzel, 1926) (**B, D–G**) **A–B** photographs in light microscopy showing eggs **C–G** microcavernicolous habitats from different zones **C** pool **D–E** water container collecting drip water from cliff (water container not shown in **D**) and stalactite **F–G** water tank (**C, F** in dark zone **G** in transition zone **D, E** in entrance zone).

under both scanning electron and light microscopes (i.e., show dark spots or light spots in SEM or light photographs, respectively). These pits were described with different terminology by earlier authors, and are here called refractile points, another characteristic of body ornamentation in the genus *Bryocyclops*. The SEM photograph in Figure 9H confirms the possession of refractile points on genital double-somite of *B. muscicola*, which usually have more coarse points on the cephalothorax and later pedigers. These cuticular points have been known in all previously described species from Thailand (*B. maewaensis*, *B. maholarnensis*, *B. muscicoloides*, *B. trangensis*) but are not present in *B. asetus* sp. n., and seem to be reported in all its congeners, or even in other cyclopoids and harpacticoids such as in *Elaphoidella bromeliaecola* (Chappuis, 1928), in caves from Thailand (see Reid 1999 for review of this characteristic; Watiroyram et al. 2012, 2015; Watiroyram 2018; pers. obs.).

Fiers and van Damme (2017) noted that the presence of spurs on the caudal surface near the inner distal margin of P4 Enp in the genus *Bryocylops* indicated the degree of modified endopods. In this view, the new species and *B. anninae* probably have less unmodified P4 Enp by the absence of spurs on Enp-1. Compared to the original figures of members in group I *sensu* Lindberg (1953), they also showed less modified P4 Enp, except *B. maewaensis*, which has triangular spurs on the inner distal corner (see Watiroyram et al. 2012: figs 4D, 6D). Actually, only the females of group I have two-segmented P4 Enp (showing less modified P4 Enp) whereas other groups have more modified P4 Enp by representing only single segment. The female P4 Enp of other *Bryocyclops* species were modified or reduced into single segment, and the remnants of ancestral segments (i.e. outer spiniform processes on proximal segment) are represented by spurs or spiniform processes on outer margins such as *B. muscicola*, and *B. trangensis*. Two other Thai species, *B. muscicoloides* and *B. maholarnensis*, show more reduced P4 Enp by lacking processes on the outer margins. Generally, the female P4 Enp of its congeners has one spine and four setae, resulting in the fusion of Enp-1 (one seta) and Enp-2 (one spine and three setae), whereas *B. maholarnensis* has only two setae on the smaller segment. According to the above-mentioned morphology, *B. muscicoloides* and *B. maholarnensis* are apparently most adapted to subterranean habitats on the fourth leg, compared to its congeners, by shortening the segment and reducing the setae on their legs (Suárez-Morales 2015).

Bryocyclops asetus sp. n. has strongly divergent and robust caudal rami, which have never been observed in other members of the genus. *Bryocyclops maewaensis* has short and robust setae on the female P4 Enp, almost as long as the spine on the same segment, compared to those in other *Bryocyclops* species, which are slender and never shorter than spine. Brancelj (2009) remarked that divergent and robust caudal rami, and short and strong seta on the caudal rami and their legs, are presumed to be important morphological adaptations for efficient movement in narrow spaces and drifting prevention in epikarstic species. Peculiar adaptations on caudal rami seem to have diversified *B. asetus* sp. n. from its epigean lineage. In contrast to *Parastenocaris* Kessler, 1913, caudal adaptation of vertical drift prevention is not a result of epikarstic stress but is presented as an epigean ancestor and tends to be a preadaptation for epikarstic species (Cottarelli et al. 2012). The presence of pseudosomite anterior to the genital double-somite in interstitial species was considered to provide enhanced movement in a narrow space by increasing the flexibility of the urosome (Huys and Boxshall 1991): *B. muscicola* and *B. correctus* Kiefer, 1960 (synonym of *Haplocyclops pauliani* Kiefer, 1955 in the sense of Fiers 2002) also have pseudosomites, probably a preadaptation to living in both epigean and hypogean habitats. A reduction in the number of eggs and egg size also results in physiological adaptation to trophic stress, which is common in stygobiotic species (Cottarelli et al. 2012): the new species shares stygobiotic specialization with *B. muscicola*, a stygophilic species which was observed to have a reduced number of eggs per ovigerous females. However, *B. asetus* sp. n. has a larger egg size, which is an indication of stygobiotic adaptation for subterranean habitats (Fig. 12A–B).

Keys to species of group I *sensu* Lindberg (1953)

Females: *B. anninae* (Menzel, 1926); *B. chappuisi* Kiefer, 1928; *B. difficilis* Kiefer, 1935; *B. elachistus* Kiefer, 1935; *B. maewaensis* Watiroyram, Brancelj & Sanoamuang, 2012; *B. phyllopus* Kiefer; *B. asetus* sp. n.

1 Anal operculum triangular, with acute tip **2**
– Anal operculum ovate or semi-circular, with round tip **4**
2 Posterior margin of anal operculum serrate .... ***B. chappuisi***
– Posterior margin of anal operculum smooth **3**
3 Terminal accessory (VI) seta on caudal ramus short, not reaching beyond a fracture plane of inner terminal (V) seta .... ***B. anninae***
– Terminal accessory (VI) seta on caudal ramus long, reaching well beyond a fracture plane of inner terminal (V) seta .... ***B. phyllopus***
4 Posterior margin of anal operculum finely serrate .... ***B. elachistus***
– Posterior margin of anal operculum coarsely serrate **5**
5 P1 coxa without seta on inner distal corner .... ***B. asetus* sp. n.**
– P1 coxa with seta on inner distal corner **6**
6 P4 Enp-2 with three short and robust setae, as long as spine. ***B. maewaensis***
– P4 Enp-2 with three long and slender setae, relatively longer than spine .... ***B. difficilis***

Males: *B. ankaratranus* Kiefer, 1955; *B. apertus* Kiefer, 1935; *B. difficilis* Kiefer, 1935; *B. elachistus* Kiefer, 1935; *B. maewaensis* Watiroyram, Brancelj & Sanoamuang, 2012; *B. mandrakanus* Kiefer, 1955; *B. phyllopus* Kiefer, 1935; *B. asetus* sp. n.

1 Anal operculum triangular, with acute tip .... ***B. phyllopus***
– Anal operculum ovate or semi-circular, with round tip **2**
2 Posterior margin of anal operculum smooth .... ***B. apertus***
– Posterior margin of anal operculum serrate **3**
3 P1 coxa without seta on inner distal corner .... ***B. asetus* sp. n.**
– P1 coxa with seta on inner distal corner **4**
4 Posterior margin of anal operculum finely serrate .... ***B. elachistus***
– Posterior margin of anal operculum coarsely serrate **5**
5 Anal operculum less-produced, shorter than half of caudal ramus .... ***B. difficilis***
– Anal operculum well-produced, longer than half of caudal ramus **6**
6 P3 Enp-2 with one spine and four setae .... ***B. maewaensis***
– P3 Enp-2 with one spine and five setae 7
7 The expansion of transformed spine of P3 Enp-2 serrate .... ***B. ankaratranus***
– The expansion of transformed spine of P3 Enp-2 smooth .... ***B. mandrakanus***

Acknowledgements

This study was supported by the National Research Council of Thailand (Grant No. 256108A1340006).

References

Bjornberg MHGC (1985) *Bryocyclops caroli* sp. n. (Crustacea, Copepoda, Cyclopoida), the first representative of the genus in South America. Hydrobiologia 124: 237–241. https://doi.org/10.1007/BF00015240

Burmeister H (1834) Beiträge zur naturgeschichte der rankenfüsser (Cirripedia). G. Reimer, Berlin, 60 pp.

Brancelj A (2009) Fauna of an unsaturated karstic zone in central Slovenia: two new species of Harpacticoida (Crustacea: Copepoda), *Elaphoidella millennii* n. sp. and *E. tarmani* n. sp., their ecology and morphological adaptations. Hydrobiologia 621: 85–104. https://doi.org/10.1007/s10750-008-9634-3

Chappuis PA (1928) Neue Harpacticiden aus Java. Treubia 10: 271–283.

Cottarelli V, Bruno MC, Spena MT, Grasso R (2012) Studies on subterranean copepods from Italy, with descriptions of two new epikarstic species from a cave in Sicily. Zoological Studies 51(4): 556–582.

Dussart B, Defaye D (2006) World directory of Crustacea Copepoda of inland waters II-Cyclopiformes. Backhuys Publishers, Leiden, 354 pp.

Fiers F (2002) The genus *Haplocyclops* Kiefer, 1952 (Copepoda, Cyclopoida, Cyclopidae): redescription of the type-species, *H. gudrunae*, and its congeners. Hydrobiologia 474: 155–169. https://doi.org/10.1023/A:1016579619924

Fiers F, van Damme K (2017) *Thalamocyclops pachypes* gen. nov., sp. nov. (Copepoda: Cyclopoida: Cyclopidae), a crevicular cyclopine from Socotra Island (Yemen): tale of a remarkable survival drive. Journal of Natural History 51(41–42): 2463–2507. https://doi.org/10.1080/00222933.2017.1344328

Huys R, Boxshall GA (1991) Copepod evolution. The Ray Society, London, 468 pp.

Jocque M, Fiers F, Romero M, Martens K (2013) Crustacea in phytotelmata: a global overview. Journal of Crustacean Biology 33(4): 451–460. https://doi.org/10.1163/1937240X-00002161

Kessler E (1913) *Parastenocaris brevipes* nov. gen. et nov. spec., ein neuer Süsswasserharpacticide. Zoologischer Anzeiger 42(11): 514–520.

Kiefer F (1927) Versuch eines systems der Cyclopiden. Zoologischer Anzeiger 73: 302–308.

Kiefer F (1928) Beiträge zur copepodenkunde (IX). Zoologischer Anzeiger 76: 99–102.

Kiefer F (1935) Neue susswasser cyclopiden (Crustacea Copepoda) aus ostafrika. Bulletin de la Societe des Sciences de Cluj (Roumanie) 7: 237–242.

Kiefer F (1955) Neue Cyclopoida gnathostoma (Crustacea Copepoda) aus Madagaskar. II. Cyclopinae. Zoologischer Anzeiger 154: 222–232.

Kiefer F (1960) Zwei neue cyclopiden (Crust. Cop.) als bewöhner des sandlückensystems im niger (Französischer Sudan). Bulletin de l'Institut Français d'Afrique Noire 22: 395–401.

Lindberg K (1953) Les cyclopides (Crustacés Copépodes) très évolués en tant que habitants des eaux souterraines. Actes Premier Congrès International de Spéléologie 3: 71–83.

Menzel R (1926) Cyclopides muscicoles et bromélicoles de Java (Indes Néerlandaises). Annales de Biologie Lacustre 14: 209–216.

Por FD (1981) A new species of *Bryocyclops* (Copepoda: Cyclopoida) and of *Parastenocaris* (Copepoda: Harpacticoida) from a cave in Israel and some comments on the origin of the cavernicolous copepods. Israel Journal of Zoology 30: 35–46.

Rafinesque CS (1815) Analyse de la Nature ou Tableau de l'Univers et des Corps organises. Imp. Jean Barravecchia, Palermo, 224 pp.

Reid JW (1999) New records of *Bryocyclops* from the continental U.S.A., Puerto Rico, and Brazil (Copepoda: Cyclopoida: Cyclopidae). Journal of Crustacean Biology 19(1): 84–92. https://doi.org/10.2307/1549550

Reid JW (2001) A human challenge: discovering and understanding continental copepod habitats. Hydrobiologia 453/454: 201–226. https://doi.org/10.1023/A:1013148808110

Rocha CEF, Bjornberg MHGC (1987) Copepods of the Juréia Ecological Reserve, state of São Paulo, Brazil. II. The genera *Hesperocyclops*, *Muscocyclops*, and *Bryocyclops* (Cyclopoida, Cyclopidae). Hydrobiologia 153: 97–107. https://doi.org/10.1007/BF00006642

Suárez-Morales E (2015) Class Maxillopoda. In: James H, Thorp D, Rogers C (Eds) Thorp and Covich's freshwater invertebrates. Academic Press, Boston, 709–755. https://doi.org/10.1016/B978-0-12-385026-3.00029-2

Watiroyram S, Brancelj A, Sanoamuang L (2012) A new *Bryocyclops* Kiefer (Crustacea: Copepoda: Cyclopoida) from karstic caves in Thailand. The Raffles Bulletin of Zoology 60(1): 11–21.

Watiroyram S, Brancelj A, Sanoamuang L (2015) A new cave-dwelling copepod from northeastern Thailand (Cyclopoida: Cyclopidae). The Raffles Bulletin of Zoology 63: 426–437.

Watiroyram S (2018) Two new species of the genus *Bryocyclops* Kiefer, 1927 (Copepoda: Cyclopoida: Cyclopidae) from southern Thailand. The Raffles Bulletin of Zoology 66: 149–169.

ZooKeys 793: 53–62 (2018)
doi: 10.3897/zookeys.793.28342
http://zookeys.pensoft.net

RESEARCH ARTICLE

A peer-reviewed open-access journal
ZooKeys
Launched to accelerate biodiversity research

Anenteotermes cherubimi sp. n., a tiny dehiscent termite from Central Africa (Termitidae: Apicotermitinae)

Rudolf H. Scheffrahn[1], Yves Roisin[2]

1 *Fort Lauderdale Research and Education Center, Institute for Food and Agricultural Sciences, 3205 College Avenue, Davie, Florida 33314, USA* **2** *Evolutionary Biology and Ecology, CP 160/12, Université Libre de Bruxelles, Avenue F.D. Roosevelt 50, 1050 Brussels, Belgium*

Corresponding author: *Rudolf H. Scheffrahn* (rhsc@ufl.edu)

Academic editor: *D. Evangelista* | Received 12 July 2018 | Accepted 12 September 2018 | Published 29 October 2018

http://zoobank.org/5478DCB4-F1EE-45AB-BF6D-313309C0CEA1

Citation: Scheffrahn RH, Roisin Y (2018) *Anenteotermes cherubimi* sp. n., a tiny dehiscent termite from Central Africa (Termitidae: Apicotermitinae). ZooKeys 793: 53–62. https://doi.org/10.3897/zookeys.793.28342

Abstract

Anenteotermes cherubimi Scheffrahn, **sp. n.** is described from workers and male imagos collected in Cameroon and Republic of the Congo. This is the smallest soldierless termite known from Africa. As with many soldierless and soil-feeding termite species, the enteric valve morphology is a robust and essential diagnostic character for *An. cherubimi*. Preserved workers display pre-autothysis morphology and the effects of abdominal autothysis.

Keywords

abdominal autothysis, enteric valve armature, soldierless new species

Introduction

In his revision of the soldierless termites of Africa, Sands (1972) described 60 species (51 new) among 16 new genera, all beginning with the letter "A". All were previously placed in the genus *Anoplotermes* Müller. Sands (1972) described ten new species from his second-largest new genus, *Anenteotermes*. In his broader treatise on soil-inhabiting termite workers of Africa, Sands (1998) recapitulated his descriptions of *Anenteotermes* with one exception; he depicted the enteric valve armature (EVA) of "*Anenteotermes* new species" (plate 8, fig. 9). Sands (1998: 169) also noted "At least one new species awaits description from rain forest". We herein describe this remarkable new *Anenteotermes* as *A. cherubimi* sp. n., the smallest known soldierless termite in Africa.

Materials and methods

Preserved workers, stored in 85% ethanol, were positioned in a transparent petri dish filled with Purell® hand sanitizer (70% EtOH). Body sections and dissected guts were photographed as multi-layer montages using a Leica M205C stereomicroscope with a Leica DFC 425 module run with Leica Application Suite software version 3. Mandibles and EVA were mounted on slides with PVA mounting medium (Bioquip Products, Inc.) and photographed with a Leica CTR 5500 compound microscope using bright field lighting and the same montage software. Imagos were photographed in alcohol on sand. Terminology of the worker gut follows that of Sands (1972) and Noirot (2001). Measurements were obtained using an Olympus SZH stereomicroscope fitted with an ocular micrometer. All specimens described here are deposited in the authors' collections under the accession numbers AFR1508 and AFR1282 for RHS and CGO060 for YR.

Systematics

Anenteotermes cherubimi Scheffrahn, sp. n.

http://zoobank.org/12A5A940-6CDB-4B64-A710-C3B3B82CD832
Figures 1–5

Material. Holotype. Worker from colony UF no. AFR1508. University of Florida Termite Collection, Fort Lauderdale Research and Education Center, Davie, Florida. **Paratypes**. CAMEROON: Ebogo, slope above Nyong River (3.386, 11.466), 667 m elev., 23NOV2011, col. J. Křeček, AFR1282, two workers in capped plastic vial and approx. 25 workers desiccated in broken glass vial collected with *Orthotermes* sp. CAMEROON: Ebogo II (3.386, 11.682), 660 m elev., 10DEC2011, col. J. Šobotník, AFR1810, 4 workers, larvae. CONGO (Republic of): Mokabi SA (Groupe Rougier) logging concession (3.14658, 16.96377), 527 m elev., 8DEC2017, col. Y. Roisin, Accession no. CGO060, 7 male imagos and 11 workers in soil at base of tree in rainforest.

Type locality. CAMEROON: Korup National Park (5.0045, 8.8635), 109 m elev., 5DEC2011, col. J. Křeček, UF no. AFR1508, 53 workers collected under stone.

Description of worker (Figs 1–4, Table 1). Monomorphic, very small, approx. 2 mm. Head capsule yellowish, covered with approximately 100 setae of varying length (Figure 1A, B). Postclypeus moderately inflated, fontanelle indiscernible. Anterior margin of abdomen, in lateral view, raised vertically above metanotum and marked at apex by dehiscence line (Figure 2 A-C). Antennae with 13 articles; 2>3=4=5<6.

Table 1. Measurements (in mm) of *Anenteotermes cherubimi* workers (n = 18 from 4 colonies).

Measurement	mean	SD
Head length with postclypeus	0.482	0.019
Head width	0.493	0.015
Postclypeus length	0.120	0.007
Pronotum width	0.299	0.016
Hind tibia length	0.366	0.009
Fore-tibia length	0.333	0.015
Fore-tibia width	0.106	0.010
Fore-tibia width/length	0.320	0.033
Total length	2.17	0.23

Left mandible with apical and first marginal teeth well separated, long, and projecting well beyond line formed by third marginal tooth and molar prominence. A subsidiary (fourth) marginal tooth visible above molar prominence in dorsal (Figure 1C) views. Right mandible with apical tooth much longer than first marginal; third marginal nearly symmetrical. Fore-tibia moderately inflated; width:length ratio 0.32. Mesenteric tongue long and tubular forming long mixed segment (Figure 1D). P1 bridged to P3 through a broadly conical EV seating resembling a sunflower receptacle (Figure 3 A–C). Enteric valve cuticle consists of six cushions of unequal size (Figure 4). The largest two cushions comprise a soft basal part covered with fringed scales and 5–6 narrow spines, and bear sclerotized extensions that broaden into wing-like paddles; margins finely pectinate (40–70 compound spines per extension) and approx. a dozen more separated spines in interior of extension (Figure 4). Other cushions soft and scaly, without spines. Middle one, situated between the largest cushions, approx. half their size. Two cushions lateral to the major ones small, approx. half smaller than the middle one. Cushion opposite to the middle one approx. the same length as it, narrower. Soft cushions anchored in their seating and seating lumen filled with bacterial slime; extensions penetrate to middle of P3 lumen (Figure 3C).

Description of imago. (male) (Figure 5, Table 2). Tiny, 7 mm. Head with vertex and frons sepia brown, postclypeus slightly lighter. Genae and labrum light brown. Fontanelle ovoid, hyaline. Eyes dark sepia brown. Pronotum lighter than head capsule. Meso- and metanotum slightly lighter than pronotum, with hind margins tinged with yellow. Abdominal tergites and sternites light brown, sternites paler in middle. Wing membrane light brown, with darker veins. Legs light brown. Head capsule rounded posteriorly. Eyes of medium size, protruding. Ocelli elliptical, close to eyes. Antennae with 15 articles. Pronotum slightly broader than long, semi-octogonal, anterior corners deflected downward, hind margin nearly straight. Hind margins of meso- and metanotum narrow, sinuated. Wings long, approx. half their length beyond extremity of abdomen.

Diagnosis. *Anenteotermes cherubimi* is the smallest soldierless termite worker in Africa (head width, HW), followed by *Acidnotermes praus* (0.52 mm HW) and *An. nanus* (0.56 mm HW). The EVA of *A. cherubimi* is very diagnostic and unlike that of any other termite species in having two broad and symmetrical pectinate paddles as opposed

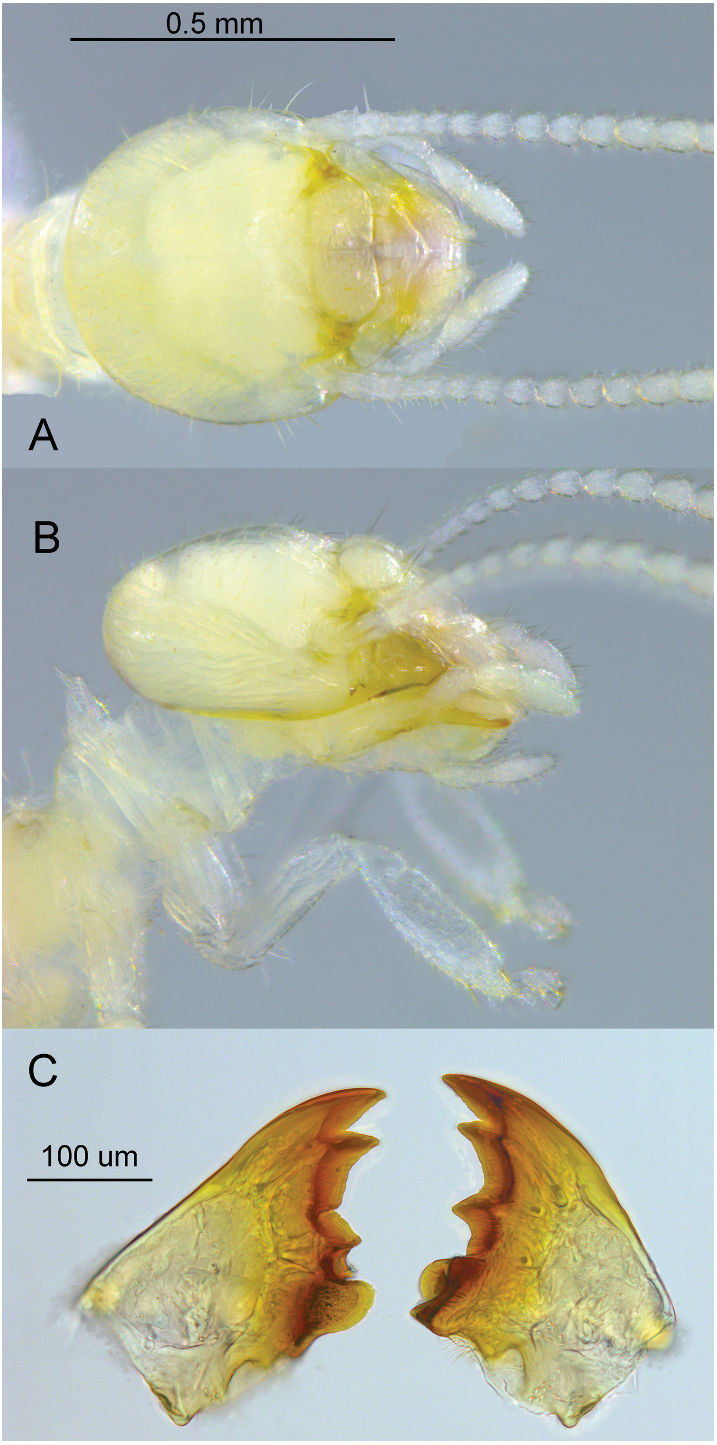

Figure 1. Worker of *Anenteotermes cherubimi* sp. n. **A** dorsal **B** lateral view of head and prothorax **C** mandibles.

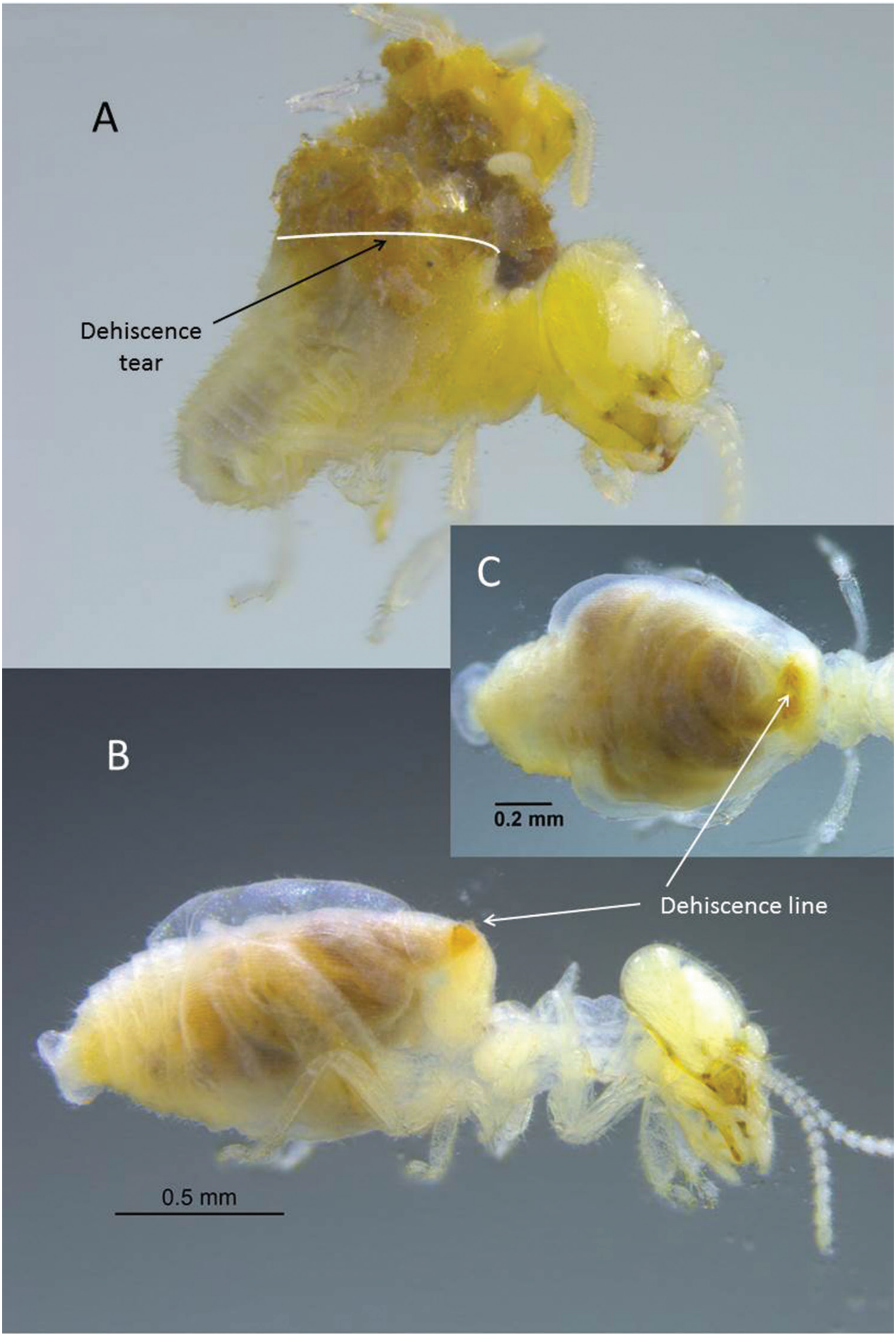

Figure 2. Worker of *Anenteotermes cherubimi* sp. n. **A** Gut contents expelled after tear of dehiscence line. Dehiscence line slightly open in lateral **B** and dorsal **C** views.

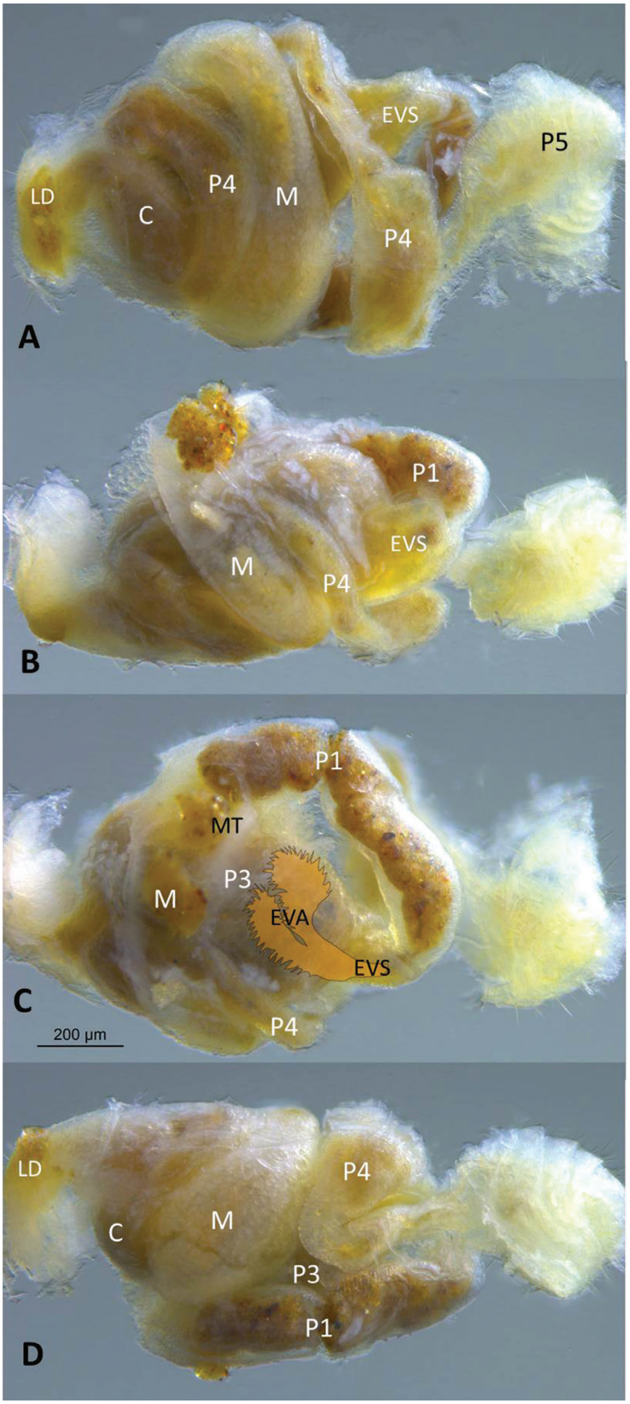

Figure 3. Gut of *Anenteotermes cherubimi* sp. n. worker. **A** dorsal **B** right with area near mixed segment and mesenteric tongue (MT) torn (see Figure **1D**) **C** ventral with position of enteric valve armature (EVA) and enteric valve seating (EVS) drawing superimposed to scale **D** left views. Abbreviations: C = crop, LD = dehiscence line; M = mesenteron; P1, P3, P4, and P5 = proctodeal segments.

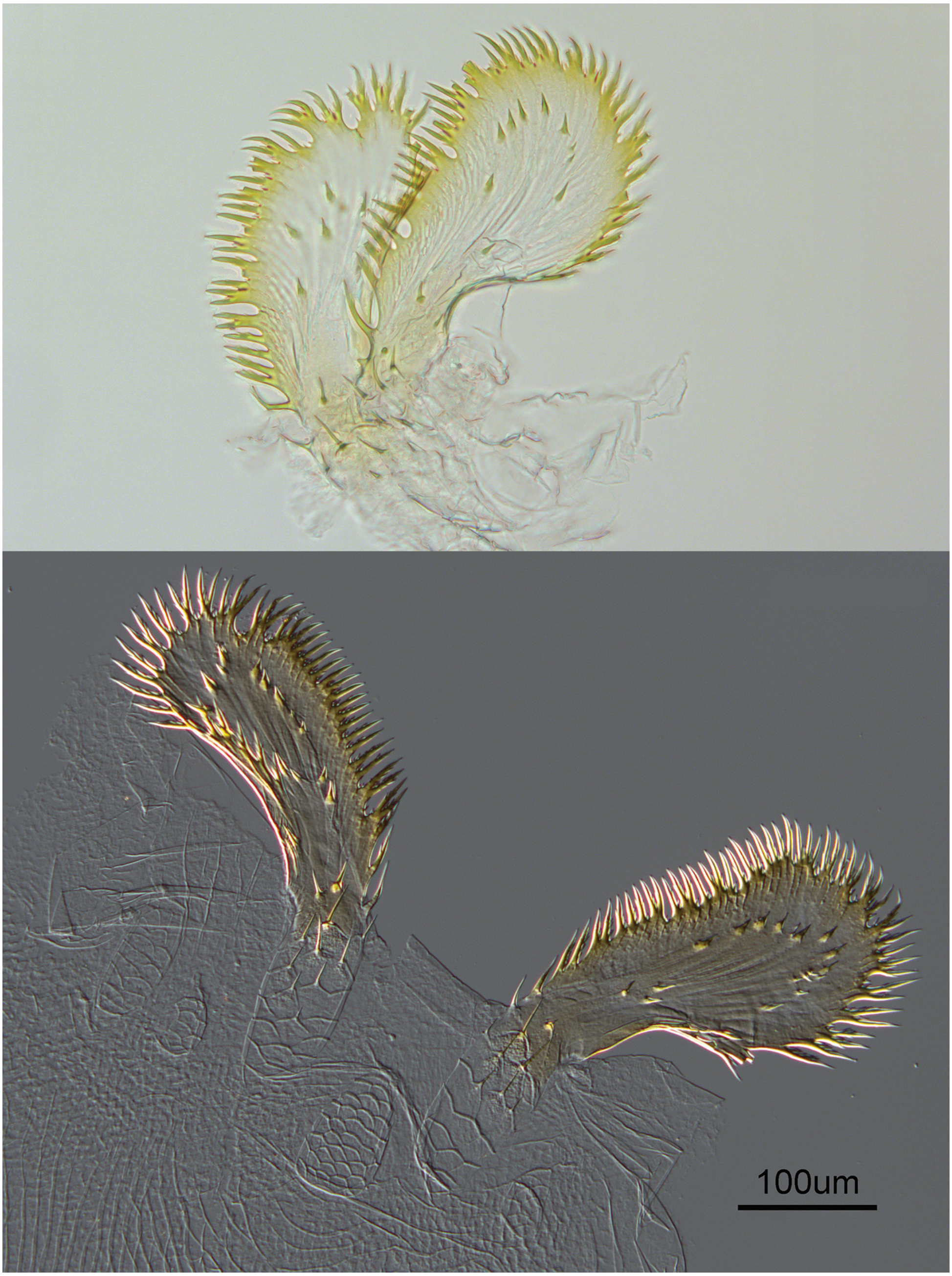

Figure 4. Enteric valve armature of *Anenteotermes cherubimi* sp. n. worker. Top: paddles folded (see Figure **3C**); bottom: paddles fully extended.

Table 2. Measurements (in mm) of *Anenteotermes cherubimi* male imagos (n = 6 from one colony).

Measurement	mean	SD
Head length to tip of labrum	0.685	0.023
Head length to anterior margin of postclypeus	0.513	0.008
Head width, maximum at eyes	0.591	0.013
Head, interocular width	0.447	0.011
Eye maximum diameter	0.183	0.005
Eye to head base distance	0.031	0.005
Ocellus maximum diameter	0.075	0.005
Ocellus to eye distance	0.017	0.003
Pronotum maximum length	0.407	0.007
Pronotum maximum width	0.515	0.018
Fore wing length from suture	5.89	0.08
Fore wing maximum width	1.51	0.06
Hind tibia length	0.523	0.009
Total length with wings	7.09	0.09
Total length without wings	3.92	0.16

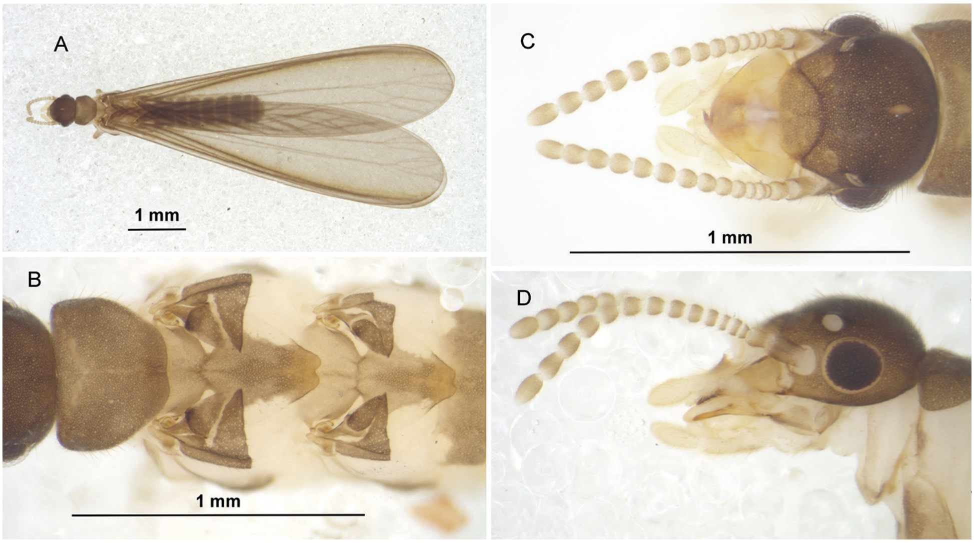

Figure 5. Male imago of *Anenteotermes cherubimi* sp. n. **A** dorsal view **B** dorsal nota **C** dorsal **D** lateral view of head.

to two narrow paddles in other *Aneneteotermes* spp. or tri- and hexa-radial, or asymmetrical armature as in other soldierless genera.

Comments. Sands (1998) placed "*Anenteotermes* new species" in this genus based on a well-developed mixed segment which is only shared in African soldierless workers by *Aderitotermes* and *Adaiphrotermes* (Sands 1972). Of these three genera, only *Anenteotermes* contain species with a single pair of sclerotized EV extensions penetrating into P3. The *Anenteotermes* worker key in Sands (1972, p. 194) can accommodate *An. cherubimi* by inserting a new couplet three as follows and renumbering the subsequent couplets:

3 Two enteric valve cushions (="extensions" as used above) wing-like and finely pectinate, W, 0.49–0.51 .... ***cherubimi***
– Two enteric valve cushions conical with 10–12 spines along their margins, W, 0.60–0.73 .... **4**

Biology and distribution. All records for *An. cherubimi* are from southern Cameroon and northern Congo. Deblauwe et al. (2008) collected "*Anenteotermes* sp. nov. (Sands, 1998)" from a subterranean habitat at all five vegetation types sampled in Cameroon (GPS location: 3.42, 13.15; east of above sites) including primary forest, secondary forests, and a riverine forest. Eggleton et al. (1995) collected three new *Anenteotermes* (possibly including *An. cherubimi*, as Sands was a coauthor) in Mbalmayo Forest Reserve from a young plantation, old secondary and near primary forest, but not from cleared or fallow land cover. Dibog et al. (1998) also collected *Anenteotermes* "sp. n. 1, 2" from Mbalmayo Forest Reserve (3.42, 11.48, altitude 701 m) from the Ebogo control plots. Sands (1998) suggests that some *Anenteotermes* spp., as with many other soil feeding termites, lives in nests built by other termites.

Etymology. Named after the cherubim, the biblical guardian angels. The EVA resembles a pair of angel wings.

Discussion

Sands (1982) described abdominal autothysis in two live soldierless species from Africa, *Alyscotermes kilimandjaricus* Sands and *Ateuchotermes muricatus* Sands. Upon grasping an ant with their mandibles, abdominal muscle convulsions were observed causing the integument to split along a line at the back of the metanotum and resulting in expulsion of their hind gut coils. Sands (1982) further noted that *Al. kilimandjaricus* workers secrete droplets of a clear fluid, stored in enlarged salivary glands and released from the dehiscence line before gut expulsion. In *At. muricatus*, the entire intestine of workers was expelled in "a few seconds". Sands (1982) did not mention a fluid exudate preceding the autothysis. In preserved workers of *An. cherubimi*, it was not possible to confirm a fluid reservoir, but the expulsion of guts from the abdomen was obvious (Figure 2A).

Acknowledgments

We thank the anonymous reviewers for their critical input. RHS offers appreciation to Jan Křeček and Jan Šobotník for collecting *An. cherubimi* workers. We are all grateful to the local Ebogo inhabitants for protecting their forest. These and many other valuable Cameroonian samples are deposited in the University of Florida Termite Collection. YR thanks V. Freycon, É. Forni and S. Gourlet-Fleury (CIRAD, Montpellier), for invitation and multifaceted assistance in the field. The trip to the Congo was supported by the DynAfFor project funded by the Fonds Français pour l'Environnement Mondial (FFEM) and the Agence Française de Développement (AFD). Thanks are due to Mokabi SA logging company for facilitating access to the field site. P. Martin and G. Josens helped with microscopic imagery. Financial support was provided by the Belgian F.R.S.-FNRS (PDR T.0065.15).

References

Deblauwe I, Dibog L, Missoup AD, Dupain J, Van Elsacker L, Dekoninck W, Bonte D, Hendrickx F (2008) Spatial scales affecting termite diversity in tropical lowland rainforest: a case study in southeast Cameroon. African Journal of Ecology 46: 5–18. https://doi.org/10.1111/j.1365-2028.2007.00790.x

Dibog L, Eggleton P, Forzi F (1998) Seasonality of soil termites in a humid tropical forest, Mbalmayo, southern Cameroon. Journal of Tropical Ecology 14: 841–850. https://doi.org/10.1017/S0266467498000601

Eggleton P, Bignell DE, Sands WA, Waite B, Wood TG, Lawton JH (1995) The species richness of termites (Isoptera) under differing levels of forest disturbance in the Mbalmayo Forest Reserve, southern Cameroon. Journal of Tropical Ecology 11: 85–98. https://doi.org/10.1017/S0266467400008439

Noirot C (2001) The gut of termites (Isoptera). Comparative anatomy, systematics, phylogeny. II. Higher termites. Annales de la Société Entomologique de France (NS) 37: 431–471. https://doi.org/10.1080/00379271.2009.10697634

Sands WA (1972) The soldierless termites of Africa (Isoptera: Termitidae). Bulletin of the British Museum (Natural History) Entomology (Suppl.) 18: 1–244.

Sands WA (1982) Agonistic behavior of African soldierless Apicotermitinae (lsoptera: Termitidae). Sociobiology 7: 61–72.

Sands WA (1998) The Identification of Worker Castes of Termite Genera from Soils of Africa and the Middle East. CAB International, Kent, 500 pp.

ZooKeys 793: 63–96 (2018)
doi: 10.3897/zookeys.793.28050
http://zookeys.pensoft.net

CHECKLIST

A peer-reviewed open-access journal
ZooKeys
Launched to accelerate biodiversity research

A synopsis of Estonian myriapod fauna (Myriapoda: Chilopoda, Diplopoda, Symphyla and Pauropoda)

Kaarel Sammet[1], Mari Ivask[2], Olavi Kurina[1]

1 *Institute of Agricultural and Environmental Sciences, Estonian University of Life Sciences, Kreutzwaldi st 5D, 51006 Tartu, Estonia* **2** *Tallinn University of Technology, Tartu College, Puiestee 78, 51008 Tartu, Estonia*

Corresponding author: *Kaarel Sammet* (kaarel.sammet@gmail.com)

Academic editor: *Nesrine Akkari* | Received 28 June 2018 | Accepted 17 September 2018 | Published 29 October 2018

http://zoobank.org/0D7B2412-5585-4AEA-81D4-1854A4415128

Citation: Sammet K, Ivask M, Kurina O (2018) A synopsis of Estonian myriapod fauna (Myriapoda: Chilopoda, Diplopoda, Symphyla and Pauropoda). ZooKeys 793: 63–96. https://doi.org/10.3897/zookeys.793.28050

Abstract

The data on Estonian Myriapoda are scattered in various publications and there has been no overview of the fauna up to the present. A critical summary of the previous information on Estonian Myriapoda is given, supplemented by new records and distribution maps. Altogether, 5784 specimens from 276 collecting sites were studied. To the hitherto recorded 14 centipede species are added *Lithobius melanops*, *L. microps*, *Geophilus carpophagus*, *G. flavus*, *Strigamia transsilvanica* and *Stenotaenia linearis*, a probably introduced species. Of the 27 published Estonian millipede species, the data on two species proved erroneous, and two new species were recorded (*Craspedosoma raulinsii* and *Cylindroiulus britannicus*). Two previously recorded millipede species – *Brachyiulus pusillus* and *Mastigophorophyllon saxonicum* – were not found in the recent samples, the latter may have become more rare or extinct. Pauropoda and Symphyla lack previous reliable records. Combined with published data, the number of myriapod species known from Estonia is now set at 52. Some changes in species distribution and frequencies were detected comparing the published data with new records. Some data about habitat preferences of the more common species are also given. The majority of species have a western Palaearctic distribution, while six species are at the northern limit of their ranges.

Keywords

check list, Chilopoda, Diplopoda, distribution, Estonia, Myriapoda, Pauropoda, soil invertebrates, Symphyla

Introduction

The research of Estonian Myriapoda has been quite unsystematic and sporadic. Very little has been published in English thus much of the information may be currently unavailable to the wider myriapodological community (e.g., Zapparoli 2003, Tuf et al. 2015). The first scant records of Myriapoda in Estonia date back to the second half of the XIX century. The first data are given by E. Haase (Haase 1886: 58), who mentions a "*Craspedosoma mutabile* v. *fasciatum* Latzel, 1884" specimen collected by A. E. Grube from Tartu. Subsequently, P. Schmidt reported the presence of *Pauropus Huxleyi* in the vicinity of Narva (Schmidt 1894) and O. Schubart published the data on two millipede species collected from Estonian bogs (Schubart 1924). W. Mierzeyewski collected in 1912 and 1926 some millipedes in the island Saaremaa, and in the years 1925 to 1929 W. Herold gathered a considerable millipede material from many places in Estonia. That material, containing 20 species, was also identified and published by O. Schubart (Schubart 1930), who repeated the data in his monograph on German Diplopoda (Schubart 1934). Part of the Herold material is currently preserved in the collection of Museum für Naturkunde, Berlin. In the 1930's, some ecological studies mention millipedes identified to genus level (e.g., Nõmmik 1939) and some species were listed in studies on plant pests (e.g., Zolk 1923, Kaarep et al. 1949). E. Palmén published one new record of Estonian diplopods in his overview of the Finnish fauna (Palmén 1949).

An unpublished collection of myriapods from 1937, preserved currently in the entomological collection of Estonian University of Life Sciences, Tartu (IZBE, identified by the Swedish zoologist H. Lohmander), has probably served as a basis to the list of ten centipede species in H. Riikoja's account of Estonian invertebrates (Riikoja 1955; referred to as pers. comm. with J. Vilbaste).

We owe thanks for much of what is known about Estonian Myriapoda to the works of the Estonian entomologist Juhan Vilbaste (1924–1985). His "Keys to Estonian Millipedes" lists 21 species as proven to occur in Estonia at that time (Vilbaste 1953). In addition, he published on Myriapoda in several local faunistic surveys, adding one centipede and five millipede species records and some ecological observations (Vilbaste 1970, Vilbaste 1979, Vilbaste et al. 1985, Vilbaste and Vilbaste 1993). Unfortunately, only two specimens of Vilbaste have subsisted (in the IZBE collection). The data provided by Schubart (1930) and Vilbaste (1953) have been reproduced by various subsequent authors (e.g., Lang 1954, Stojałowska 1961, Lokshina 1969). Thus, 14 centipede species and 27 millipede species were recorded from Estonia prior to the current study.

Material and methods

As complete as possible, bibliography of historical records of myriapods in Estonia was compiled, reviewing all the available faunistic studies and other records. The main Estonian zoological collections were searched for myriapod material (Estonian Museum of Natural History, Tallinn; Tartu University Museum of Natural history and the private insect collection of Allan Selin, Maardu). Some collections abroad known to house Estonian material were contacted for further information (Finnish Museum of Natural History and Zoologische Staatssammlung München, Germany).

New material was collected using: (1) pitfall traps, (2) Tullgren funnel and Kempson apparatus, (3) sifting moss, leaf litter and detritus with a standard entomological sieve, (4) manual searching in suitable habitats and daytime retreats, and (5) as by-catch of non-target species with window pane traps (attached to tree trunks) and Malaise traps (for particular description of the trapping projects, see Sammet et al. 2016 and Tomasson et al. 2014, respectively).

The material was collected from 276 localities covering all parts of Estonia (see Table 1 and Figure 1 for details). The distribution of Estonian species (Figures 2–5) is presented in 50×50 km UTM grid, also used in the „Atlas of European Millipedes" (Kime and Enghoff 2011, 2017) (compiled using Adobe Photoshop CS5 Extended). The relative abundances in different habitats of species with at least 25 findings were presented as diagrams (Figures 6–8). The habitats studied repeatedly with different methods were grouped into 14 types:

1. Coastal meadows and alvars;
2. Broad-leaved (nemoral) forests (dominated by *Quercus robur*, *Tilia cordata*, *Acer platanoides* and herbs in the understory);
3. Boreo-nemoral deciduous forests (dominated by *Alnus incana* or *Salix* species);
4. Dry heathland forests (dominated by *Pinus sylvestris*, with *Cladonia* sp. or *Calluna vulgaris* in understory);
5. Drier boreo-nemoral mixed forests (dominated by *Pinus sylvestris* with *Sorbus* and *Acer* and *Vaccinium myrtillus* in understory);
6. Mesophilic boreal forests (dominated by *Picea abies*, *Oxalis acetosella* in understory);
7. Hillock forests (dominated by *Corylus avellana*, herbs in the understory);
8. Carrs and paludifying forests (dominated by *Picea abies*, *Betula pendula* and *Pinus sylvestris*);
9. Bogs;
10. Fens and waterlogged meadows;
11. Inland mesophilic grasslands;
12. Rural gardens;
13. Urban parks and graveyards;
14. Arable fields.

The barplot diagrams were produced by dividing the number of findings in a habitat type by the proportion of sampling effort in that particular habitat (i.e. the number of "sampling events" consisting of one trapping period or one hand collecting trip with subsequent Tullgren extraction of soil and litter samples) (Figure 6). Other, more rare, habitats that were not studied with all the methods are not included. All studied material is preserved in 70% ethanol or a mix of ethanol and glycerol for Pauropoda.

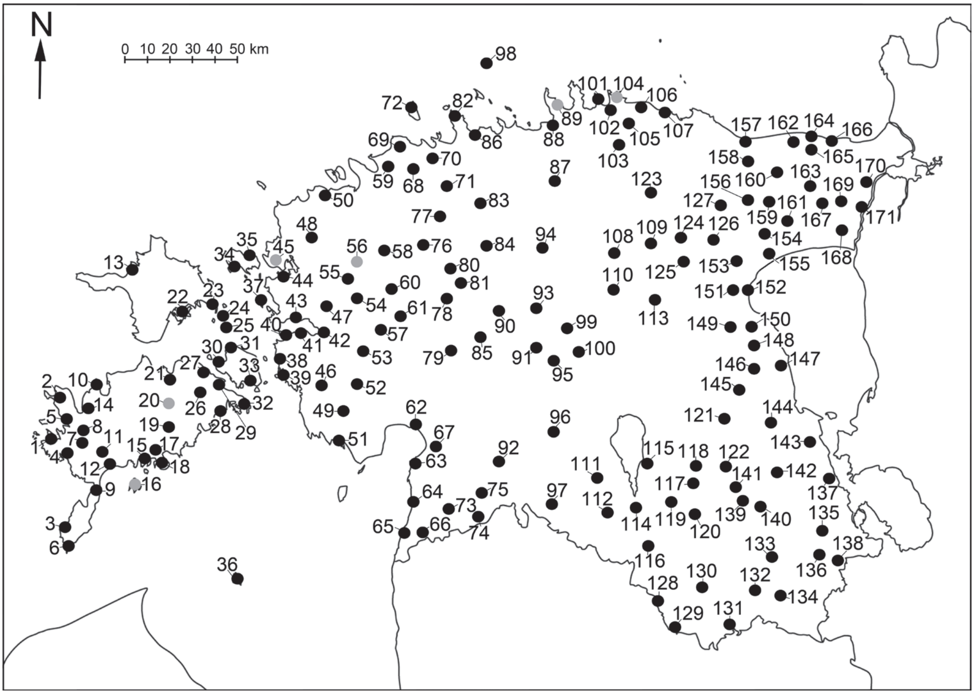

Figure 1. Collecting localities of Myriapoda in Estonia. Key: Dark circles = this study, light circles = literature data. For further details, see Table 1.

Some gonopods are preserved as microscope slides (using Euparal). The studied material is deposited in the entomological collection of Estonian University of Life Sciences (**IZBE**) and the soil biology collection of Tallinn University of Technology (**TTUSB**), both in Tartu, Estonia. Various keys for Central, Northern, and East, European myriapods were used for identification (Schubart 1934, Lokshina 1969, Zalesskaya 1978, Blower 1985, Andersson et al. 2005, Bonato et al. 2005, Barber 2009).

Results

All available material consisting of 1656 centipede, 4095 millipede, 29 symphylan, and six pauropod specimens were identified or re-identified and databased. The following list contains all the known published records of Estonian myriapods, followed by numbers of studied specimens and collecting localities. Full details for one finding from each locality are given in "Supplementary information". Only publications with original data are listed, subsequent ones citing these (e.g., Schubart 1934, Lang 1954, Stojałowska 1961, Lokshina 1969, Atlavinytė and Lokshina 1971, Blower 1985, Spuņģis 2010) are omitted. An asterisk (*) marks previously unpublished species. The full list of records with all details will be available through the Estonian eBiodiversity portal (http://elurikkus.ut.ee; Abarenkov et al. 2010) and Global Bi-

Table 1. Collecting localities of Estonian myriapods. The localities' numbers correspond to those on Figure 1. Localities within a range of less than 10 km are presented by one number, the different place names (sub-localities) under one number are designated consecutive letters (the coordinates apply only to the first of them).

No	Latitude, N	Longitude, E	Name
1	58.3300	21.9627	a Kuusnõmme, b Eeriksaare, c Atla
2	58.4467	21.9391	a Kõruse, b Undva, c Tagamõisa, d Neeme, e Tammese
3	57.9777	21.9971	Türju
4	58.2467	22.0311	Kipi
5	58.3909	22.0051	a Oju, b Vilsandi,
6	57.9095	22.0552	Sõrve peninsula
7	58.2833	22.1000	a Audaku, b Sutru, c Kivesselja, d Pätsumaa bog, e Pitkasoo, f Suurissoo hill, g Surnuaiamägi, h Nakimetsa, i Suurmägi, j Laasma, k Viidumägi, l Upsi
8	58.3163	22.0806	a Kanna, b Viidu
9	58.1234	22.1946	Lõu
10	58.5105	22.2330	Kugalepa
11	58.3188	22.3066	a Mõnnuste, b Paadla
12	58.2209	22.2752	Kaalupi
13	58.9414	22.4362	Paope
14	58.3986	22.1278	Viidumäe, Jürna liivad
15	58.2424	22.4246	Suurlaht
16	58.1453	22.0570	Abruka
17	58.3005	22.6459	a Ilpla, b Kudjape
18	58.2256	22.6885	Vanamõisa
19	58.3725	22.6697	a near Kaali lake, b Võrsna
20	58.4563	22.7076	Tika
21	58.5397	22.7307	Õeste
22	58.7962	22.7555	a Reigilaid, b Kassari
23	58.8289	22.9746	a Suur-Pihlakare, b Öakse, c Saarnaki, d Aruküla, e Heltermaa, f Sarve
24	58.7956	23.0063	a Saarnaki, b Hanikatsi, c Langekare
25	58.7421	23.1349	Ahelaid
26	58.4828	22.9800	a Koigi lake; b Koigi bog
27	58.5846	23.0246	Orinõmme
28	58.4394	23.0680	Asva
29	58.5506	23.1319	Orissaare
30	58.6114	23.0911	a Koguva, b Lepanina
31	58.6406	23.1588	a Paenase, b Nõmmküla, c Üügu, d Lõetsa
32	58.4568	23.2673	a Kahtla, b Kübassaare
33	58.5794	23.2709	a Mäla, b Võiküla
34	58.9697	23.2058	Vormsi: Kärret
35	59.0347	23.3047	Vormsi: Diby
36	57.8062	23.2396	Ruhnu
37	58.8377	23.3958	Liialaid
38	58.6421	23.5167	Hanila
39	58.5609	23.5522	a Puhtu, b Laelatu, c Pivarootsi
40	58.6918	23.5821	a Salevere Salumägi, b Saastna, c Metsküla
41	58.7440	23.6719	a Keemu, b Kirikuküla Tika, c Kirikuküla Allika, d Kirikuküla Ennu, e Viita, f Penijõe
42	58.7531	23.8465	a Kloostri, b Kelu, c Rõude, d Kasari, e Kirbla
43	58.8089	23.7011	Rannamõisa
44	58.9492	23.5681	a Haapsalu, b Linnamäe
45	59.2049	23.5988	Noarootsi
46	58.5336	23.8299	Paaderma
47	59.0356	23.6382	Ingiküla
48	59.0371	23.6609	Niibi
49	58.4319	24.0003	Tõhela
50	59.2594	23.8737	Vihterpalu
51	58.3144	23.9850	a Tõstamaa, b Suti
52	58.5380	24.0062	Nedrema
53	58.6455	24.1254	Kurese

No	Latitude, N	Longitude, E	Name
54	58.8075	24.0094	Patsu fen
55	58.9020	24.0284	a Marimetsa NR, b Kullamaa
56	58.9972	24.0562	Risti
57	58.7757	24.2498	Vana-Vigala
58	59.0723	24.2934	Turba bog
59	59.3315	24.3745	Tõmmiku
60	58.8958	24.3769	a Sõtke, b Valgu, c Raela
61	58.7805	24.5625	Inda
62	58.3884	24.5093	Pärnu
63	58.1369	24.5141	a Tolkuse bog, b Uulu,
64	58.0996	24.4737	a Pulgoja, b Pikla, c Häädemeeste
65	58.0067	24.4423	a Kabli b near Ikla
66	57.9947	24.5378	Laulaste NR
67	58.2709	24.6411	Laadi
68	59.3194	24.5581	a Saue, b Pääsküla
69	59.3816	24.4628	Vahi küla
70	59.3915	24.6434	Vana-Mustamäe
71	59.2661	24.6483	Kasemetsa-Kuresoo
72	59.5933	24.5025	Naissaar
73	58.0783	24.8338	Tali
74	58.0027	24.8769	Sookuninga NR
75	58.0711	24.8608	Kalita NR
76	58.9549	24.7641	a Raela, b Varbola
77	59.0725	24.8077	Hagudi
78	58.8879	24.6391	Loe
79	58.6328	24.7013	Lehu bog
80	58.9742	24.7021	Kuusiku; Keo
81	58.8983	24.7616	a Kõnnu, b Lellepere
82	59.5297	24.8577	Lubja
83	59.2377	24.9311	2km SE of Sõmeru
84	58.9459	25.1025	Loosalu
85	58.7080	24.8780	a Kõnnu bog, b Luuri bog
86	59.4630	24.9377	Maardu
87	59.2781	25.6212	Aegviidu
88	59.5084	25.5925	Uuri
89	59.5841	25.6263	Hara island
90	58.8165	25.1625	Käru
91	58.6396	25.3039	a Ramussaare, b Pikkmetsa, c Tõrvaaugu
92	58.2719	25.1798	Riimaru
93	58.8099	25.3394	Lokuta
94	59.0835	25.4052	a Mustla, b Mustla Pühajärv
95	58.6333	25.5500	a Võhma, b Koksvere
96	58.3593	25.5950	Viljandi
97	58.0818	25.5253	Viivre
98	59.6991	25.0211	Keri island
99	58.7259	25.6007	a Retla, b Kabala
100	58.6475	25.6717	a Arussaare, b Kirivere, c Järavere
101	59.6049	25.9229	Käsmu
102	59.5778	25.9556	Võsu
103	59.4481	26.0126	Viitna
104	59.4484	26.0118	Koljaku-Oandu NR
105	59.5166	25.9746	Palmse
106	59.5660	26.0880	a Oandu, b Vihula
107	59.5557	26.3533	Rutja; Varangu
108	58.9765	26.0454	Koeru
109	59.0232	26.2443	a Kamariku, b Rakke
110	58.8839	26.0433	Sopaalliku
111	58.1413	25.6803	Muti NR
112	58.0180	25.8794	Helme

No	Latitude, N	Longitude, E	Name
113	58.8457	26.2919	a Kärde hill, b Kaera, c Pedja
114	58.0063	26.0553	Soontaga NR
115	58.2388	26.1770	a Rannu, b 2 km SW of Rannu
116	57.9127	26.1883	Õru
117	58.1803	26.4205	Elva-Vitipalu NR
118	58.2386	26.4433	a Peedu, b Vapramäe
119	58.0399	26.2073	Prange
120	58.0533	26.4898	Otepää
121	58.3808	26.6222	a Rahinge, b Tiksoja, c Tähtvere bog, d Õssu, e Tartu Eerika, f Merimetsa, g Tartu Tähtvere, h Kõrveküla
122	58.2301	26.7010	Kambja
123	59.1857	26.1980	a Porkuni, b Lasila
124	59.0373	26.6758	between Venevere and Arukse
125	59.0115	26.4265	Karaski
126	58.9092	26.5046	a Pedjaääre, b Tudusoo NR
127	59.1527	26.8213	Suigu NR
128	57.6878	26.1854	Vaitka
129	57.6049	26.2749	Koiva wooded meadow, b Koivakonnu, c Taheva
130	57.7522	26.4926	a Karula Mähkli, b Küünimetsa
131	57.5727	26.6413	Mõisamõtsa NR
132	57.6938	26.8850	Saarlasõ küla
133	57.8386	27.0505	Võrusoo
134	57.7355	27.0627	Haanja NR
135	57.9422	27.4058	a Rebasemäe, b Ilumetsa
136	57.8433	27.4626	Piusa
137	58.1287	27.4990	Räpina
138	57.8168	27.5180	Obinitsa
139	58.0911	26.9050	Palojärv
140	58.0524	27.0286	Puuri
141	58.1514	26.8731	a Voorepalu, b Ihamaru NR
142	58.1777	27.1467	Mooste
143	58.2781	27.3210	Järvselja
144	58.3287	26.9892	Melliste
145	58.5170	26.9223	Konnamõisa
146	58.5633	26.8772	a Välgi NR, b Särgla, c Pataste
147	58.6032	27.1301	Alatskivi
148	58.6558	26.9469	a Pala, b Padakõrve NR
149	58.7296	26.8244	a Odivere, b Maarja-Magdaleena
150	58.7394	26.9452	Jõeääre
151	58.7430	26.8888	a Ruskavere. b Võtikvere NR
152	58.7841	26.9330	Nõmme
153	58.9636	26.8294	a Kõveriku, b Avinurme
154	59.0230	27.0591	Tudulinna
155	58.9656	27.0303	Lohusuu
156	59.1732	26.9438	Kaukvere
157	59.4443	26.9047	Aseri taga
158	59.3588	26.9238	Kiviõli
159	59.1644	27.0133	Muraka NR
160	59.3179	27.1235	Aidu
161	59.0894	27.1550	Muraka NR
162	59.3858	27.2218	Kohtla-Järve
163	59.2289	27.3247	Mäetaguse NR
164	59.4439	27.3350	a Valaste falls, b 5 km W of Toila
165	59.3948	27.3408	Kukruse
166	59.4302	27.3900	Toila
167	59.1523	27.3889	Jõuga
168	59.0711	27.6277	Agusalu LKA
169	59.0767	27.7033	Permisküla
170	59.2384	27.8377	Narva
171	59.1719	27.7961	a Poruni, b Gorodenka

odiversity Information Facility (http.//www.gbif.org). The nomenclature and synonymies follow the ChiloBase (Bonato et al. 2016), "Atlas of European millipedes" (Kime and Enghoff 2011, 2017) and McAlpine and Shear (2018) for centipedes and millipedes, respectively, and the "Catalogue of Myriapoda in the Nordic Countries" (Andersson et al. 2008, 2013) for Symphyla and Pauropoda. For each species, a brief overview of its distribution is given (with emphasis on North-Eastern Europe).

1. Chilopoda

1.1. Geophilomorpha

1.1.1. Geophilidae

****Geophilus carpophagus*** **Leach, 1814**
Fig. 2(1)

Studied material. 2 specimens from 2 localities.

General distribution. Western Palaearctic species (Andersson et al. 2005), present also in southern Sweden and south-western Finland (Andersson et al. 2008), Latvia (Bonato et al. 2005) and Lithuania (Tuf et al. 2015).

Comments. The species is rare in Estonia.

Geophilus electricus **(Linnaeus, 1758)**
Fig. 2(2)

Literature sources. Volkova 2016: 504.

Studied material. 5 specimens from 4 localities.

Distribution. Western Palaearctic species introduced also to North America (Andersson et al. 2005), present also in southern Sweden and south-western Finland (Andersson et al. 2008), Latvia (Bonato et al. 2005) and Lithuania (Tuf et al. 2015).

Comments. The species is rare in Estonia.

****Geophilus flavus*** **(De Geer, 1778)**
Figs 2(3), 6

Literature sources. Ivask et al. in press.

Studied material. 68 specimens from 24 localities.

General distribution. Western Palaearctic species introduced also to North America (Andersson et al. 2005), widespread in Scandinavia and Finland (Andersson et al. 2008), Latvia (Bonato et al. 2005) and Lithuania (Tuf et al. 2015).

Comments. A common species in different habitats, but absent in wet areas.

***Geophilus proximus* C.L. Koch, 1847**
Figs 2(4), 6

Literature sources. Riikoja 1955: 15, Ivask 2011: 2, Ivask et al. in press.

Studied material. 57 specimens from 26 localities.

General distribution. Central and North European species, (Andersson et al. 2005), widespread in Scandinavia and Finland (Andersson et al. 2008), Latvia (Bonato et al. 2005) and Lithuania (Tuf et al. 2015).

Comments. A common species in different habitats, but absent in wet areas.

***Geophilus truncorum* Bergsoe & Meinert, 1866**
Figs 2(5), 6

Literature sources. Vilbaste 1970: 174, Vilbaste et al. 1985: 152, Vilbaste and Vilbaste 1993: 319 [as: *Brachygeophilus truncorum* Mnr.], Ivask et al. in press.

Studied material. 66 specimens from 27 localities.

General distribution. Western Palaearctic species, present also in southern Sweden and south-western Finland (Andersson et al. 2008), Latvia (Bonato et al. 2005) and Lithuania (Tuf et al. 2015).

Comments. A common species in different habitats, especially in soil samples.

****Stenotaenia linearis* (C.L.Koch, 1835)**
Fig. 2(7)

Studied material. 5 specimens from 1 locality.

General distribution. Western Palaearctic species, exclusively synanthropic in northern Europe, present also in Latvia (Bonato et al. 2005) and Finland (Andersson et al. 2008).

Comments. The species was recently shown to comprise several cryptic lineages (Wesener et al. 2015). It is probably an introduced species in Estonia (only found in the Tartu Botanical Garden in Estonia and present also only synanthropically in the neighbouring countries).

***Pachymerium ferrugineum* (C. L. Koch, 1835)**
Figs 2(6), 6

Literature sources. Riikoja 1955: 15, Vilbaste 1970: 174, Vilbaste et al. 1985: 152, Ivask et al. in press.

Studied material. 31 specimens from 14 localities.

General distribution. Holarctic species (Andersson et al. 2005), widespread in Sweden and Finland (Andersson et al. 2008), Latvia (Bonato et al. 2005) and Lithuania (Tuf et al. 2015).

Comments. The species is more common in coastal areas and rare elsewhere. It seems to favour dry habitats.

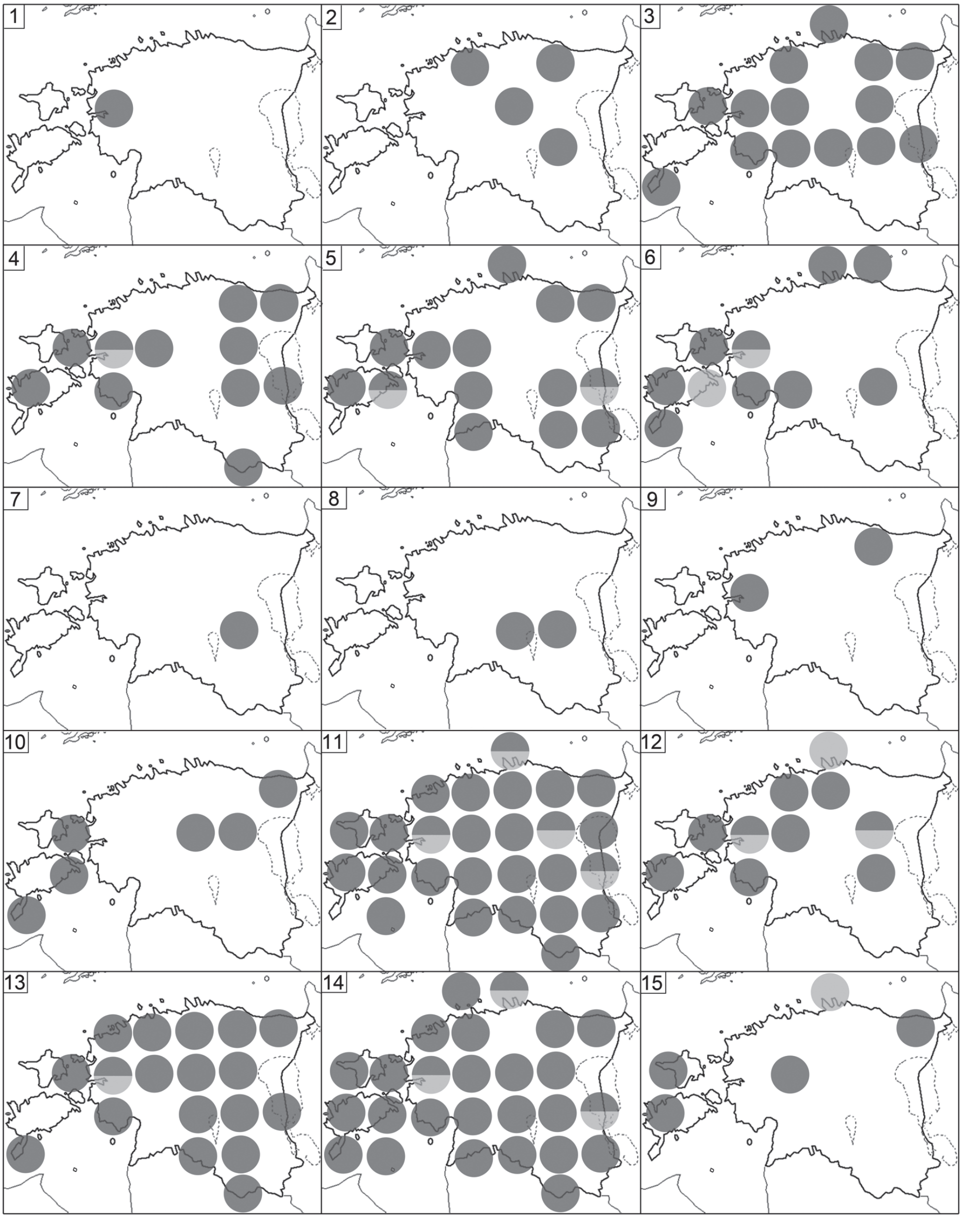

Figure 2. Distribution of Estonian Chilopoda. **1** *Geophilus carpophagus* **2** *G. electricus* **3** *G. flavus* **4** *G. proximus* **5** *G. truncorum* **6** *Pachymerium ferrugineum* **7** *Stenotaenia linearis* **8** *Strigamia transsilvanica* **9** *Lamyctes emarginatus* **10** *Lithobius borealis* **11** *L. curtipes* **12** *L. crassipes* **13** *L. erythrocephalus* **14** *L. forficatus* **15** *L. lucifugus*. Key: Dark circles = original data, light circles = literature data, divided circles = original and literature data.

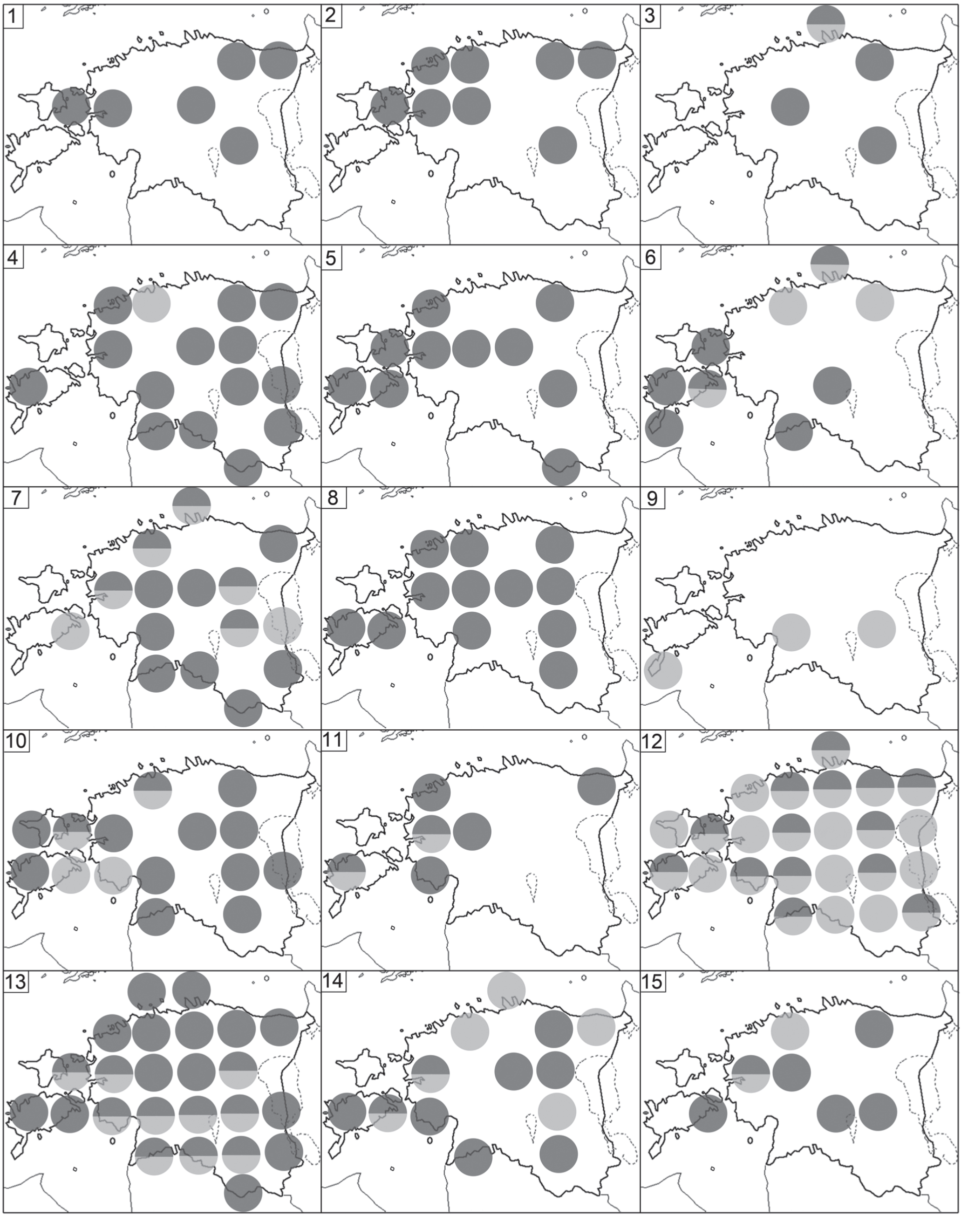

Figure 3. Distribution of Estonian Chilopoda (**1–5**) and Diplopoda (**6–15**). **1** *Lithobius melanops* **2** *L. microps* **3** *L. pelidnus* **4** *L. tenebrosus* **5** *Schendyla nemorensis* **6** *Polyxenus lagurus* **7** *Polyzonium germanicum* **8** *Craspedosoma raulinsii* **9** *Mastigophorophyllon saxonicum* **10** *Nemasoma varicorne* **11** *Brachydesmus superus* **12** *Polydesmus complanatus* **13** *P. denticulatus* **14** *P. inconstans* **15** *Blaniulus guttulatus*. For symbols see Fig. 2.

1.1.2 Linotaeniidae

******Strigamia transsilvanica* **(Verhoeff, 1928)**
Fig. 2(8)

Studied material. 3 specimens from 2 localities.

General distribution. Mainly a Central European species but recently found also in Latvia (Bonato et al. 2005). The species has no published records from north-western Russia (Volkova 2016), but there is a specimen collected from Izborsk (Pskov region, 10 km of Estonian border) in the IZBE collection.

Comments. The species is rare in Estonia. Both findings are from human settlements.

1.1.3. Schendylidae

Schendyla nemorensis **(C.L. Koch, 1837)**
Fig. 3(5)

Literature sources. Riikoja 1955: 15, Ivask et al. in press.

Studied material. 19 specimens from 12 localities.

General distribution. Western Palaearctic species (Barber 2009), introduced to North America, present also in southern Sweden and south-western Finland (Andersson et al. 2008), Latvia (Bonato et al. 2005), and Lithuania (Tuf et al. 2015).

Comments. More common in western Estonia, found mainly in soil samples.

1.2. Lithobiomorpha

1.2.1. Henicopidae

Lamyctes emarginatus **(Newport 1844)**
Fig. 2(9)

Literature sources. Riikoja 1955: 15 [as: *L. fulvicornis* Meinert], Ivask 2011: 1.

Studied material. 7 specimens from 4 localities.

General distribution. A semi-cosmopolitan species widespread also in Scandinavia and Finland (Andersson et al. 2008).

Comments. Locally common in western Estonia, not found elsewhere.

1.2.2. Lithobiidae

***Lithobius* (*Lithobius*) *borealis* Meinert, 1868**
Fig. 2(10)

Literature sources. Ivask 2011: 2.

Studied material. 11 specimens from 4 localities.

General distribution. Central and west-European species, present also in Sweden (Andersson et al. 2008), and Lithuania (Tuf et al. 2015).

Comments. More common in western Estonia, but nowhere abundant.

***Lithobius* (*Lithobius*) *erythrocephalus* C. L. Koch, 1847**
Figs 2(13), 6

Literature sources. Riikoja 1955: 15, Vilbaste 1979: 99, Vilbaste et al. 1985: 152, Ivask 2011: 2, Ivask et al. in press.

Studied material. 141 specimens from 48 localities.

General distribution. Western Palaearctic species, widespread in Scandinavia and Finland (Andersson et al. 2008), Latvia (Trautberg 1929) and Lithuania (Tuf et al. 2015).

Comments. A common species in different habitats.

***Lithobius* (*Lithobius*) *forficatus* (Linnaeus, 1758)**
Figs 2(14), 6

Literature sources. Riikoja 1955: 15, Vilbaste 1970: 173, Vilbaste et al. 1985: 152, Remm 1988: 128, Vilbaste and Vilbaste 1993: 319, Ivask 2011: 2, Kalda et al. 2015: 90, Ivask et al. in press.

Studied material. 352 specimens from 89 localities.

General distribution. Holarctic species, widespread in Scandinavia and Finland (Andersson et al. 2008), Latvia (Trautberg 1929) and Lithuania (Tuf et al. 2015), present also in Lenigrad region (north-western Russia) (Zalesskaya 1978).

Comments. One of the two most common centipede species in different habitats, but favours more xeric areas than *Lithobius curtipes*.

***Lithobius* (*Lithobius*) *lucifugus* L. Koch 1862**
Fig. 2(15)

Literature sources. Vilbaste 1979: 99, Vilbaste et al. 1985: 152, Vilbaste and Vilbaste 1993: 319.

Studied material. 5 specimens from 4 localities.

General distribution. Central- and south-east European species, present in Latvia (Trautberg 1929), Lithuania (Tuf et al. 2015) and on the Swedish islands Öland and Gotland (Andersson et al. 2008).

Comments. The species is widespread but rare in Estonia.

****Lithobius* (*Lithobius*) *melanops* Newport, 1845**

Fig. 3(1)

Studied material. 7 specimens from 7 localities.

General distribution. Western Palaearctic species introduced to North America, present also in and Sweden (Andersson et al. 2008), Latvia (Trautberg 1929) and Lithuania (Tuf et al. 2015), synanthropic in southern Finland (Palmen 1949).

Comments. The species is widespread but infrequent in Estonia.

***Lithobius* (*Lithobius*) *pelidnus* Haase, 1880**

Fig. 3(3)

Literature sources. Riikoja 1955: 15, Remm 1988: 128.

Studied material. 27 specimens from 4 localities.

General distribution. Central- and East-European species present also in southern Sweden (Andersson et al. 2008) and Lithuania (Tuf et al. 2015).

Comments. The species is widespread but infrequent in Estonia, found only in bogs and boreo-nemoral forests.

***Lithobius* (*Lithobius*) *tenebrosus* Meinert, 1872**

Figs 3(4), 6

Literature sources. Riikoja, 1955: 15 [as *Lithobius nigrifrons*], Ivask 2011: 1.

Studied material. 43 specimens from 25 localities.

General distribution. Western Palaearctic species common in Finland and Sweden (Andersson et al. 2005), Latvia (Trautberg 1929) and Lithuania (Tuf et al. 2015).

Comments. A common species in different habitats, but avoids human settlements. H. Lohmander (1948) described a subspecies *fennoscandicus* Lohmander 1948 from Scandinavia, the description of which Estonian specimens generally match, but as the main subspecific difference concern colouration, more fresh specimens need to be studied.

***Lithobius* (*Monotarsobius*) *crassipes* C.L. Koch, 1862**

Figs 2(12), 6

Literature sources. Riikoja 1955: 15, Vilbaste 1979: 99, Vilbaste et al. 1985: 152, Remm 1988: 128, Vilbaste and Vilbaste 1993: 319, Ivask et al. in press.

Studied material. 25 specimens from 18 localities.

General distribution. Palaearctic species, present also in southern Finland, Sweden (Andersson et al. 2008) and Lithuania (Tuf et al. 2015).

Comments. The species is widespread but infrequent in Estonia, avoids wet habitats.

Lithobius (*Monotarsobius*) *curtipes* C.L. Koch, 1847

Figs 2(11), 6

Literature sources. Riikoja 1955: 15; Vilbaste 1970: 173; Vilbaste 1979: 99; Vilbaste et al. 1985: 152, Remm 1988: 128, Vilbaste and Vilbaste 1993: 319, Ivask 2011: 1, Kalda et al. 2015: 90, Ivask et al. in press.

Studied material. 730 specimens from 106 localities.

General distribution. Mainly a central and East European species, common in Sweden and Finland (Andersson et al. 2005, Palmén 1948), Latvia (Trautberg 1929) and Lithuania (Tuf et al. 2015).

Comments. One of the two most common centipede species in different habitats, favours more fresh habitats than *L. forficatus*.

**Lithobius* (*Sigibius*) *microps* Meinert, 1868

Fig. 3(2)

Literature sources. Ivask et al. in press.

Studied material. 52 specimens from 17 localities.

General distribution. A western Palaearctic species, introduced to North America, also present in Finland, Sweden (Andersson et al. 2005), and Lithuania (Tuf et al. 2015).

Comments. The species is widespread but infrequent in Estonia, seems to avoid wet habitats.

2. Diplopoda

2.1. Polyxenida

2.1.1. Polyxenidae

Polyxenus lagurus Linnaeus, 1758

Fig. 3(6)

Literature sources. Palmén 1949: 4, Vilbaste 1953: 16, Vilbaste 1970: 174, Remm 1988: 128, Kime and Enghoff 2011: 21.

Studied material. 27 specimens from 8 localities.

General distribution. Holarctic species, present in Latvia (Spuņģis 2010), Lithuania (Atlavinytė and Lokshina 1971), Sweden, Finland (Andersson et al. 2008) and Leningrad region (north-western Russia) (Lokshina 1969).

Comments. The species is common in soil near seashore in Western Estonia, but rare and saproxylic inland. It may be more widespread, but underdetected due to its small size.

2.2. Polyzoniida
2.2.1. Polyzoniidae

***Polyzonium germanicum* Brandt, 1837**
Fig. 3(7)

Literature sources. Schubart 1930: 193, Vilbaste 1953: 45, Vilbaste 1970: 174, Vilbaste 1979: 99, Vilbaste et al. 1985: 152, Remm 1988: 128, Vilbaste and Vilbaste 1993: 319, Kime and Enghoff 2011: 42.

Studied material. 26 specimens from 16 localities.

General distribution. Western Palaearctic species, present in Latvia (Spuņģis 2010), Sweden, and Finland (Andersson et al. 2008).

Comments. The species is widespread but infrequent in different habitats, favours more fresh habitats and has not been found in human-disturbed areas.

2.3. Chordeumatida
2.3.1. Craspedosomatidae

******Craspedosoma raulinsii* Leach, 1814**
Figs 3(8), 7

Studied material. 277 specimens from 23 localities.

General distribution. Western Palaearctic species introduced also to North America, present in Latvia (Spuņģis 2010), Lithuania (Atlavinytė and Lokshina 1971), Sweden, and Finland (Andersson et al. 2008).

Comments. This represents the first formal record of the species in Estonia after its mention by Saar and Takkis (2010) in the popular journal GEO. The species is widespread but favours fresh habitats. It seems to have recently colonised Estonia (but see Discussion).

2.3.2 Mastigophorophyllidae

***Mastigophorophyllon saxonicum* Verhoeff, 1916**
Fig. 3(9)

Literature sources. Schubart 1930: 193, Vilbaste 1953: 18.

General distribution. Central European species absent from Scandinavia and Finland (Andersson et al. 2008, 2013), present in Lithuania (Atlavinytė and Lokshina 1971) formerly found from Latvia, but not recently recorded (Spuņģis 2010).

Comments. The species was described as frequent in southern Estonia (Schubart 1930) but there are no recent records since Vilbaste 1953. The species may have become more rare or extinct in Estonia. Schubart (1930) mentioned a few exact localities in his work, viz. Sõrve peninsula, Abruka Island, the vicinity of Pärnu and Vilbaste (1953) repeats these data and adds Tartu as the northern boundary of its range. All these localities were studied in the current research but the species was not found. It is possible that the record from Tartu refers instead to Haase's specimen of *Craspedosoma mutabile* var. *fasciatum*, interpreted as a misidentification of *M. saxonicum* by Schubart (1930). Vilbaste does not mention the species (nor any other Chordeumatids) in any of his later works.

2.4. Polydesmida

2.4.1. Polydesmidae

***Brachydesmus superus* Latzel, 1884**
Fig. 3(11)

Literature sources. Schubart 1930: 193, Vilbaste 1953: 19, Vilbaste 1970: 174, Ivask et al. in press.

Studied material. 14 specimens from 8 localities.

General distribution. Western Palaearctic species, introduced also to many other parts of the world, present in Latvia (Spuņģis 2010), Lithuania (Atlavinytė and Lokshina 1971), Sweden, and Finland (Andersson et al. 2008).

Comments. The species is widespread, but infrequent, in different habitats.

***Polydesmus complanatus* (Linnaeus, 1761)**
Figs 3(12), 7

Literature sources. Schubart 1930: 193, Vilbaste 1953: 20, Vilbaste et al. 1985: 152, Remm 1988: 128, Kime and Enghoff 2011: 62.

Studied material. 59 specimens from 24 localities.

General distribution. Western Palaearctic species, introduced also to North America, present in Latvia (Spuņģis 2010), Lithuania (Atlavinytė and Lokshina 1971), Sweden, Finland (Andersson et al. 2008), and Leningrad region (north-western Russia) (Lokshina 1969).

Comments. The species is widespread and common, in different habitats.

***Polydesmus denticulatus* C.L. Koch, 1847**
Figs 3(13), 7

Literature sources. Schubart 1930: 193, Vilbaste 1953: 21, Vilbaste 1970: 174, Vilbaste 1979: 99, Vilbaste et al. 1985: 152, Kime and Enghoff 2011: 63, Kalda et al. 2015: 90, Ivask et al. in press.

Studied material. 796 specimens from 82 localities.

General distribution. Western Palaearctic species, introduced also to North America, common in Latvia (Spuņģis 2010), Lithuania (Atlavinytė and Lokshina

1971), Sweden, Finland (Andersson et al. 2008), Leningrad, and Pskov regions (northwestern Russia) (Lokshina 1969).

Comments. The species is widespread and common, in different habitats.

Polydesmus inconstans Latzel, 1884

Figs 3(14), 7

Literature sources. Schubart 1930: 193 [as *Polydesmus coriaceus*], Vilbaste 1953: 22, Vilbaste 1970: 174, Remm 1988: 128, Kime and Enghoff 2011: 65, Ivask et al. in press.

Studied material. 29 specimens from 13 localities.

General distribution. Western Palaearctic species, introduced also to North America, present in Latvia (Spuņģis 2010), Lithuania (Atlavinytė and Lokshina 1971), Sweden, and Finland (Andersson et al. 2008).

Comments. The species is widespread but infrequent, in different habitats, but prefers woodlands. There has been a confusion of this species with Western European *P. coriaceus* Porat, 1871 (cf. Vilbaste 1953, Blower 1985, Spuņģis 2010). The record of *P. coriaceus* in a posthumously published work by J. Vilbaste (Vilbaste and Vilbaste 1993) is inexplicable and obviously erroneous. The Estonian specimens identified as *P. coriaceus* in Zoologische Staatssammlung München, Germany (Verhoeff collection, collected from Tallinn, no date) also belong to *P. inconstans* (J. Spelda, pers. comm.).

2.5. Julida

2.5.1. Blaniulidae

Blaniulus guttulatus (Fabricius, 1798)

Fig. 3(15)

Literature sources. Schubart 1930: 193, Kaarep et al. 1949: 176, Vilbaste 1953: 29, Kime and Enghoff 2017: 27, Ivask et al. in press.

Studied material. 35 specimens from 6 localities.

General distribution. Western Palaearctic species, introduced also to many other parts of the world, present in Latvia (Spuņģis 2010), Lithuania (Atlavinytė and Lokshina 1971), Sweden, Finland (Andersson et al. 2008) and Leningrad region (northwestern Russia) (Lokshina 1969).

Comments. The species is widespread but infrequent, mostly synanthropic.

Boreoiulus tenuis (Bigler, 1913)

Fig. 4(1)

Literature sources. Vilbaste 1953: 29, Ivask et al. in press.

Studied material. 7 specimens from 4 localities.

General distribution. Northern and central European species, present in Latvia (Spuņģis 2010), Finland (Andersson et al. 2008), and Leningrad region (north-western Russia) (Lokshina 1969).

Comments. The species is widespread but rare.

Nopoiulus kochii (Gervais, 1847)

Fig. 4(2)

Literature sources. Schubart 1930: 193 [as *Nopoiulus armatus*], Vilbaste 1953: 26, Vilbaste 1970: 174 [as *Nopoiulus venustus*], Kime and Enghoff 2017: 33.

Studied material. 7 specimens from 3 localities.

General distribution. Western Palaearctic species, introduced also to many other parts of the world, present in Latvia (Spuņģis 2010), Lithuania (Atlavinytė and Lokshina 1971), Sweden, Finland (Andersson et al. 2008), and Leningrad region (north-wWestern Russia) (Lokshina 1969).

Comments. The species is rare, found only in northern and western Estonia.

Proteroiulus fuscus (Am Stein, 1857)

Figs 4(3), 7

Literature sources. Schubart 1924: 57 [as *Nopoiulus palmatus caelebs*], Schubart 1930: 193, Vilbaste 1953: 27, Vilbaste 1970: 174, Vilbaste et al. 1985: 152, Remm 1988: 128, Vilbaste and Vilbaste 1993: 319, Kime and Enghoff 2017: 34, Ivask et al. in press.

Studied material. 239 specimens from 42 localities.

General distribution. Western Palaearctic species, introduced also to North America, present in Latvia (Spuņģis 2010), Lithuania (Atlavinytė and Lokshina 1971), Sweden, Finland (Andersson et al. 2008), Leningrad, and Novgorod regions (north-western Russia) (Lokshina 1969).

Comments. The species is widespread and common, especially in moist habitats, usually associated with decaying wood.

2.5.2. Nemasomatidae

Nemasoma varicorne C. L. Koch, 1847

Figs 3(10), 7

Literature sources. Vilbaste 1953: 25 [as *Isobates varicornis*], Kime and Enghoff 2017: 199, Ivask et al. in press.

Studied material. 126 specimens from 28 localities.

General distribution. Central and East-European species, present in Latvia (Spuņģis 2010), Lithuania (Atlavinytė and Lokshina 1971), Sweden and Finland (Andersson et al. 2008).

Comments. The species is widespread and common in different types of woodland. Climbs also in trees (as several individuals were found in trunk window traps).

2.5.3. Julidae

***Allajulus nitidus* (Verhoeff, 1891)**
Fig. 4(4)

Literature sources. Ivask 2011: 1, Ivask et al. in press.

Studied material. 38 specimens from 14 localities.

General distribution. Central and northern European species, not found in Latvia (Spuņģis 2010) and Finland, present in Sweden (Andersson et al. 2008, 2013).

Comments. The species is widespread but frequent only in western Estonia, mostly associated with open landscape.

***Brachyiulus pusillus* (Leach, 1814)**
Fig. 4(5)

Literature sources. Schubart 1930: 193 [as *Brachyiulus littoralis*], Vilbaste 1953: 42 [as *Brachyiulus littoralis*], Kime and Enghoff 2017: 47.

General distribution. Western Palaearctic species introduced to many parts of the world, rare in Latvia (Spuņģis 2010), present in Lithuania (Atlavinytė and Lokshina 1971) and southern Sweden, not found in Finland (Andersson et al. 2008, 2013).

Comments. No specimens were collected during our studies or are preserved in Estonian collections. The current status of the species in Estonia is unclear as it has been reported as rare also in the past. It seems that both Schubart (1930) and Vilbaste (1953) refer to the same single specimen (loc. 20). There appears to be another finding from Hiiumaa Island according to Kime and Enghoff (2017), but we failed to trace the origin of that record (H. Enghoff, pers. comm.). It is not impossible that the record from Hiiumaa is a misinterpretation of the historical place name Tickhof, which is present also on Hiiumaa (Kongo 2016), but Schubart states the locality as "*in einem Garten in Tickhof auf Ösel*" - "in a garden in Tickhof on Ösel (=Saaremaa island)", and Vilbaste (1953) repeats that almost literally.

******Cylindroiulus britannicus* (Verhoeff, 1891)**
Fig. 4(6)

Studied material. 10 specimens from 2 localities.

General distribution. Western Palaearctic species, introduced to many parts of the world, present in Latvia (Spuņģis 2010), Lithuania (Atlavinytė and Lokshina 1971), Sweden and Finland (Andersson et al. 2008).

Comments. The species is rare, found only on western Estonian islands.

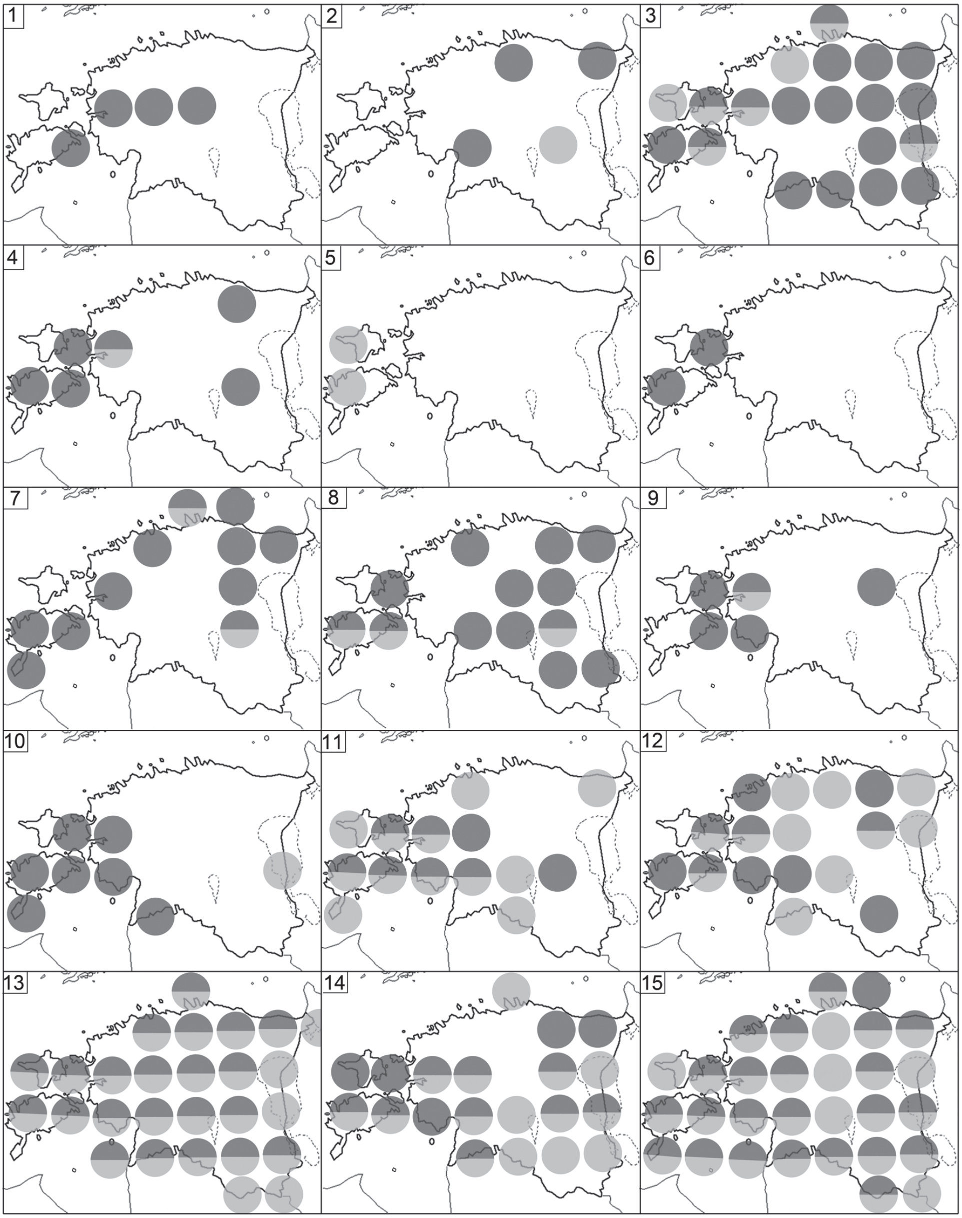

Figure 4. Distribution of Estonian Diplopoda. **1** *Boreoiulus tenuis* **2** *Nopoiulus kochii* **3** *Proteroiulus fuscus* **4** *Allajulus nitidus* **5** *Brachyiulus pusillus* **6** *Cylindroiulus britannicus* **7** *C. latestriatus* **8** *C. caeruleocinctus* **9** *Julus scandinavius* **10** *J. scanicus* **11** *J. terrestris* **12** *Leptoiulus cibdellus* **13** *L. proximus* **14** *Megaphyllum sjaelandicum* **15** *Ommatoiulus sabulosus*. For symbols see Fig. 2.

Cylindroiulus caeruleocinctus (Wood, 1864)

Figs 4(8), 7

Literature sources. Schubart 1930: 193 [as *Cylindroiulus teutonicus*], Kaarep et al. 1949: 176 [as *Cylindroiulus teutonicus*], Vilbaste 1953: 33 [as *Cylindroiulus teutonicus*], Kime and Enghoff 2017: 55.

Studied material. 237 specimens from 31 localities.

General distribution. Western Palaearctic species, introduced to North America, present in Latvia (Spuņģis 2010), Lithuania (Atlavinytė and Lokshina 1971), Sweden, Finland (Andersson et al. 2008), Leningrad, and Pskov regions (north-western Russia) (Lokshina 1969).

Comments. The species is widespread and common, especially in or close to human settlements. The records of *Ophyiulus pilosus* (Newport, 1842) as a pest of potatoes in Estonia (Zolk 1923) probably refer to this species instead (Vilbaste 1953).

Cylindroiulus latestriatus (Curtis, 1845)

Fig. 4(7)

Literature sources. Schubart 1930: 193 [as *Cylindroiulus frisius*], Vilbaste 1953: 35 [as *Cylindroiulus frisius*], Kime and Enghoff 2017: 63.

Studied material. 44 specimens from 14 localities.

General distribution. Western Palaearctic species, introduced to many parts of the world, present in Latvia (Spuņģis 2010), Lithuania (Atlavinytė and Lokshina 1971), Sweden, Finland (Andersson et al. 2008), and Leningrad region (north-western Russia) (Lokshina 1969).

Comments. The species is widespread but infrequent, more common in western Estonia. It seems to prefer drier habitats.

Julus scandinavius Latzel, 1884

Fig. 4(9)

Literature sources. Ivask 2011: 2, Ivask et al. in press.

Studied material. 17 specimens from 7 localities.

General distribution. Central and northern European species, not found in Latvia (Spuņģis 2010) and in Finland, present in southern Sweden (Andersson et al. 2008).

Comments. The species is widespread but infrequent, most findings are from Western Estonia.

Julus scanicus Lohmander, 1925

Figs 4(10), 7

Literature sources. Kaarep et al. 1949: 176, Vilbaste 1953: 38, Ivask 2011: 2, Ivask et al. in press.

Studied material. 252 specimens from 22 localities.

General distribution. Mainly a Central European species, present in Latvia (Spuņģis 2010), and southern Sweden, not found in Finland (Andersson et al. 2008, 2013).

Comments. The species is common in western Estonia, but not found elsewhere.

Julus terrestris Linnaeus, 1758

Figs 4(11), 7

Literature sources. Schubart 1930: 193, Vilbaste 1953: 39, Vilbaste 1970: 174, Vilbaste et al. 1985: 152, Kime and Enghoff 2017: 96, Ivask et al. in press.

Studied material. 304 specimens from 34 localities.

General distribution. Mainly a central European species, present in Latvia (Spuņģis 2010), Lithuania (Atlavinytė and Lokshina 1971), Sweden, and Finland (Andersson et al. 2008).

Comments. The species is frequent in western Estonia, but rare elsewhere. Clearly prefers open landscapes.

Leptoiulus cibdellus (Chamberlin 1921)

Figs 4(12), 7

Literature sources. Schubart 1930: 193 [as *Leptoiulus minutus*], Vilbaste 1953: 40 [as *Leptoiulus minutus*], Ivask 2011: 1, Kime and Enghoff 2017: 101, Ivask et al. in press.

Studied material. 274 specimens from 30 localities.

General distribution. Central European species, present in Latvia (Spuņģis 2010), Lithuania (Atlavinytė and Lokshina 1971), Sweden, and Finland (Andersson et al. 2008).

Comments. The species is widespread, but common only in western Estonia. Clearly prefers open landscapes.

Leptoiulus proximus (Němec, 1896)

Figs 4(13), 8

Literature sources. Schubart 1924: 57 [as *Leptoiulus buckkensis*], Schubart 1930: 193 [as *Leptoiulus buekkensis*], Vilbaste 1953: 39, Vilbaste 1970: 174, Vilbaste 1979: 99, Vilbaste et al. 1985: 152, Remm 1988: 128, Kime and Enghoff 2017: 250, Ivask et al. in press.

Studied material. 584 specimens from 81 localities.

General distribution. present in Latvia (Spuņģis 2010), Lithuania (Atlavinytė and Lokshina 1971), Sweden, Finland (Andersson et al. 2008), and Leningrad region (north-western Russia) (Lokshina 1969).

Comments. The species is widespread and very common in different habitats, with a slight preference to open landscape. The report of *Ophyiulus pilosus* in Estonia (Ivask 2011) has proved erroneous after re-examining the material, and belongs also to this species.

Megaphyllum sjaelandicum (Meinert, 1868)

Figs 4(14), 8

Literature sources. Schubart 1930: 193 [as *Chromatoiulus sjaelandicus*], Vilbaste 1953: 43 [as *Chromatoiulus sjaelandicus*], Vilbaste et al. 1985: 152, Remm 1988: 128, Lazányi and Vagalinski 2013: 86, Kime and Enghoff 2017: 128.

Studied material. 80 specimens from 25 localities.

General distribution. Central and eastern Palaearctic species, present in Latvia (Spuņģis 2010), southern Sweden, Finland (Andersson et al. 2008), Leningrad and Novgorod regions (north-western Russia) (Lokshina 1969).

Comments. The species is widespread and common in different habitats, with a slight preference to fresh forests.

Ommatoiulus sabulosus (Linnaeus, 1758)

Figs 4(15), 8

Literature sources. Schubart 1930: 193 [as *Archiulus sabulosus*], Vilbaste 1953: 45 [as *Schizophyllum sabulosum*], Vilbaste 1979: 99 [as *Schizophyllum sabulosum*], Remm 1988: 128 [as *Schizophyllum sabulosum*], Kalda et al. 2015: 90, Kime and Enghoff 2017: 276, Ivask et al. in press.

Studied material. 659 specimens from 84 localities.

General distribution. Western Palaearctic species, common in Latvia (Spuņģis 2010), Sweden, Finland (Andersson et al. 2008)m and Leningrad region (north-western Russia) (Lokshina 1969).

Comments. A very common species in different habitats. Climbs also in trees (as several individuals were found in trunk window traps). A mass outbreak of the species was observed near Ikla (south-western Estonia) in June 2018, where numerous specimens entered houses (see also Discussion).

Rossiulus vilnensis (Jawlowski, 1925)

Fig. 5(1)

Literature sources. Schubart 1930: 193 [as *Archiulus vilnense*], Vilbaste 1953: 44 [as *Schizophyllum (Sarmatiulus) vilnense*], Vilbaste and Vilbaste 1993: 319, Kime and Enghoff 2017: 155.

Studied material. 16 specimens from 8 localities.

General distribution. Central and east-European species (Lokshina 1969), present in Lithuania (Atlavinytė and Lokshina 1971) rare in Latvia (Spuņģis 2010), not found in Finland and Sweden (Andersson et al. 2008, 2013).

Comments. The species is widespread but infrequent, not found from northern Estonia.

Unciger foetidus C.L. Koch, 1838

Figs 5(2), 8

Literature sources. Schubart 1930: 193, Vilbaste 1953: 41, Vilbaste 1979: 99, Kime and Enghoff 2017: 168.

Studied material. 728 specimens from 18 localities.

General distribution. Western Palaearctic species, present in Latvia (Spuņģis 2010), Lithuania (Atlavinytė and Lokshina 1971), Sweden, southern Finland (Andersson et al. 2008).

Comments. The species is widespread and common, in different habitats, but avoids very wet ones and seems to be favoured by human influence.

Xestoiulus laeticollis (Porat, 1889)

Fig. 5(3)

Literature sources. Schubart 1930: 193 [as *Microiulus laeticollis mierzejewskii*], Vilbaste et al. 1985: 38 [as *Microiulus laeticollis mierzejewskii*], Remm 1988: 128, Vilbaste and Vilbaste 1993: 319, Kime and Enghoff 2017: 171, Ivask et al. in press.

Studied material. 19 specimens from 13 localities.

General distribution. Central and east European species, present in Lithuania (Atlavinytė and Lokshina 1971), Latvia (Spuņģis 2010) and southern Sweden, not found in Finland (Andersson et al. 2008, 2013).

Comments. The species is infrequent and found only from Western Estonia.

3. Symphyla

3.1 Scutigerellidae

**Scutigerella immaculata* (Newport, 1845)

Fig. 5(4)

Studied material. 14 specimens from 7 localities.

General distribution. Unclear, present in Finland and Sweden (Andersson et al. 2005, 2008, 2013) probably also in Latvia (Eglītis 1954).

3.2 Scolopendrellidae

**Symphylella vulgaris* (Hansen, 1903)

Fig. 5(5)

Studied material. 10 specimens from 6 localities.

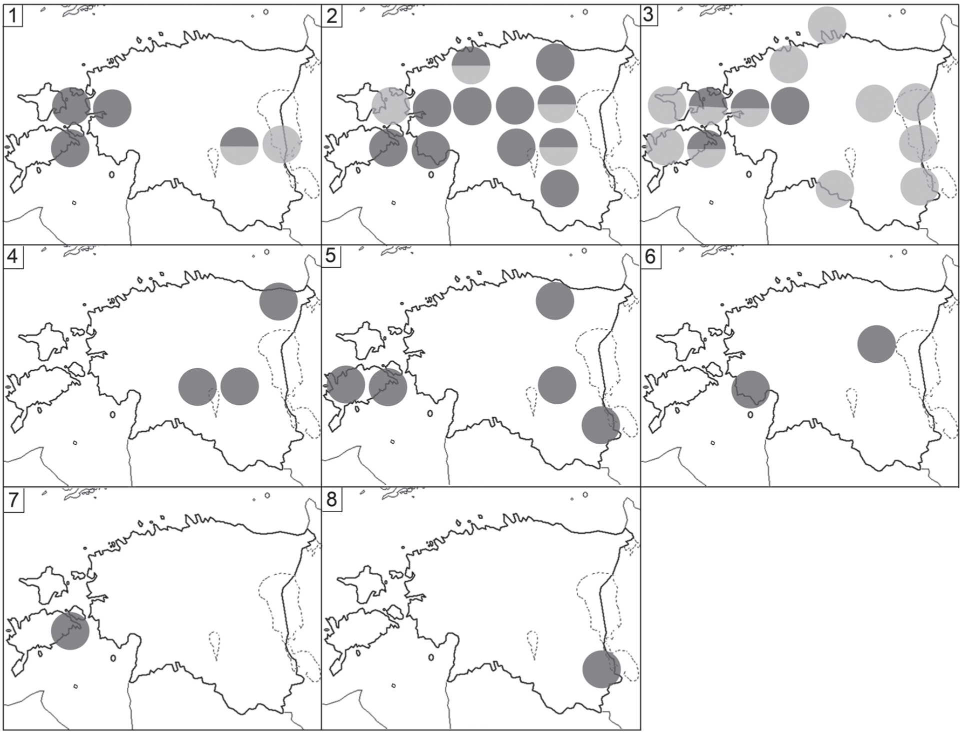

Figure 5. Distribution of Estonian Diplopoda (**1–3**), Symphyla (**4–6**) and Pauropoda (**7–8**). **1** *Rossiulus vilnensis* **2** *Unciger foetidus* **3** *Xestoiulus laeticollis* **4** *Scutigerella immaculata* **5** *Symphylella vulgaris* **6** *Scolopendrellopsis subnuda* **7** *Decapauropus cuenoti* **8** *D. gracilis*. For symbols see Fig. 2.

General distribution. A widespread Holarctic species, present in Finland and Sweden (Andersson et al. 2008), possibly also in Latvia (*Symphylella* sp. in Eglītis 1954).

****Scolopendrellopsis subnuda*** **(Hansen, 1903)**
Fig. 5(6)
Studied material. 5 specimens from 2 localities.

General distribution. Western Palaearctic species, present also in Sweden and Finland (Andersson et al. 2005).

4. Pauropoda

We regard the record of *Pauropus huxleyi* Lubbock, 1867 near Narva (Schmidt 1894, Andersson et al. 2005: 274) being dubious, as it is unclear from which side of the current Estonian-Russian border it was collected and since several related species were undescribed at the time.

Figure 6. Proportion of samples from different habitats and habitat preferences of common Estonian Chilopoda. Vertical axis: relative abundances (numbers of findings divided by proportion of sampling effort). Horizontal axis numbers represent habitat types as follows: **1** Coastal meadows and alvars **2** Broad-leaved (nemoral) forests **3** Boreo-nemoral deciduous forests **4** Dry heathland forests **5** Drier boreo-nemoral mixed forests **6** Mesophilic boreal forests **7** Hillock forests **8** Carrs and swamp forests **9** Bogs **10** Fens and waterlogged meadows **11** Inland mesophilic grasslands **12** Rural gardens **13** Urban parks and graveyards **14** Arable fields. For detailed description of habitats see Material and methods.

Figure 7. Habitat preferences of common Estonian Diplopoda. For explanation of the vertical axis and numbers denoting different habitats on the horizontal axis see Fig. 6.

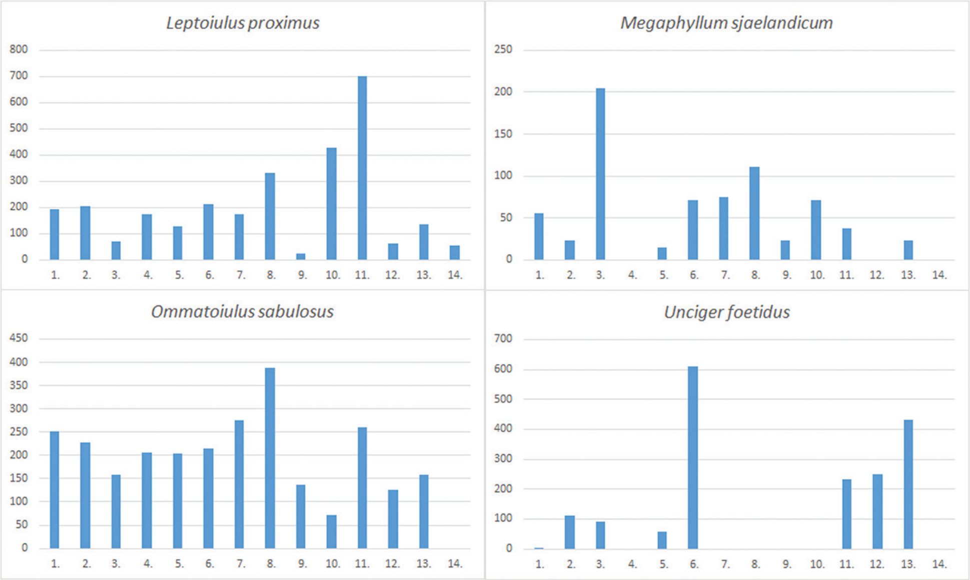

Figure 8. Habitat preferences of common Estonian Diplopoda. For explanation of the vertical axis and numbers denoting different habitats on the horizontal axis see Fig. 6.

4.1. Pauropodidae

****Decapauropus cuenoti*** **(Remy, 1931)**
Fig. 5(7)

Studied material. 5 specimens from 1 locality.

General distribution. Possibly a Holarctic species with predominantly a northern distribution, present also in Sweden and Finland (Andersson et al. 2005).

****Decapauropus gracilis*** **(Hansen, 1902)**
Fig. 5(8)

Studied material. 1 specimen from 1 locality.

General distribution. Possibly a Holarctic species with introductions to South Asia and South America, present also in Sweden and Finland (Andersson et al. 2005).

Discussion

The current study adds six centipede and two millipede new country records, while two millipedes, viz. *Polydesmus coriaceus* and *Ophyiulus pilosus* are presently removed from the Estonian checklist. All the Symphylan and Pauropod species represent new records.

It is unclear whether the new records are due to insufficient previous data (which may well be true for centipedes, except *Stenotaenia linearis*) or range shifts. The human or climate driven range shifts up to over hundred km northwards in recent decades have been also detected elsewhere (David 2009). The changes in occurrence frequencies of the species that have been observed also in the neighbouring countries, e.g., in Finland by Lehtinen and Terhivuo (1996), concern *Cylindroiulus caeruleocinctus* and *Unciger foetidus*. Both species were earlier reported as rare in Estonia (cf. Vilbaste 1953) but proved to be common and widespread after the present study. Mass outbreaks of some julid species have also spread northwards (Kania and Tracz 2005) and were recently seen in Lithuania e.g., *O. sabulosus* in 2015–2016 (J. Rimšaitė pers. comm.). This type of event is reported here for the first time in Estonia, with a localised outbreak of *O. sabulosus* in south-western Estonia, occurred in June 2018. The Estonian findings of *Lithobius pelidnus*, *Strigamia transsilvanica*, *Brachyiulus pusillus*, *Allajulus nitidus*, *Xestoiulus laeticollis*, and *Rossiulus vilnense* represent the northernmost records for those species.

The range of *Craspedosoma raulinsii* seems to expand north and eastwards. It was apparently first collected in Latvia between 2003 and 2008 (Andersson et al. 2005, Spuņģis 2010), 2010 in Estonia and 2006 in Moscow region of Russia (Golovatch and Matyukhin 2011). The first record(s) from Finland seem to be probably from 2001 to 2005 (reported as present in southern Finland by Andersson et al. 2005, but absent according to Kime 2001). However, we failed to find the original source of the Finnish records (V. Huhta, H. Enghoff, P. Djursvoll, P. Cardoso pers. comm.). The actual appearance of *C. raulinsii* in the Northern Baltic region can be decades earlier, as the myriapod fauna of Estonia and Latvia was not systematically monitored in the 1980-s and 1990-s. On the other hand, if the record of *Craspedosoma mutabile* var. *fasciatum* (if a synonym of *C. raulinsii*, as in Sierwald and Spelda 2018) from Tartu (Haase 1886) is correct, the species distribution range may have fluctuated also in the past. The name is a synonym of *Mastigona bosniense* according to Schubart (1934), and the identity with that species is also possible, as a specimen of *Mastigona* sp. (as *Heteroporatia* sp.) has been found in Latvia (Becker 1929, Spuņģis 2010).

Four species, viz. *Strongylosoma stigmatosum*, *Cylindroiulus punctatus*, *Archiboreiulus pallidus* and *Choneiulus palmatus*, occurring in neighbouring Latvia and/or Finland might be found also in Estonia, but more studies, especially in southern Estonia are needed. The species *Mastigophorophyllon saxonicum*, previously reported from many localities in southern Estonia was not re-found, and appears to have become more rare or extinct (which is also the case in Latvia, Spuņģis 2010). Spuņģis (2010) discusses the possibility that the northern Baltic records of *M. saxonicum* are misidentifications of *C. raulinsii*, which seems improbable to us as both species should have been well known for O. Schubart. Several species e.g., *Lamyctes emarginatus*, *Pachymerium ferrugineum*, *Julus terrestris*, *Julus scandinavius*, *Allajulus nitidus*, *Leptoiulus cibdellus*, and *Xestoiulus laeticollis* are more common in western Estonia or even restricted to this region characterised by milder maritime climate and calcareous soils e.g., *Geophilus carpophagus*, *Boreoiulus tenuis*, *Julus scanicus*, and *Cylindroiulus britannicus*.

The currently known fauna of Estonian Diplopoda and Chilopoda is quite similar to the neighbouring regions. 79% of the species are shared with Finland and 87.5 % are shared with Latvia. The similarity to Latvian fauna may be in fact even higher, as several species occurring both in Estonia and Lithuania might be present also in Latvia. Estonian Symphyla and Pauropoda deserve further attention. At present, they remain too poorly known to allow for any comparisons.

Acknowledgements

The study was partially funded by institutional research funding (IUT21-1) of the Estonian Ministry of Education and Research. We would like to thank Per Djursvoll, Henrik Enghoff, Lucio Bonato, Pedro Cardoso, Jolanta Rimšaitė and Jörg Spelda for various information. Our gratitude is also due to Mart Meriste, Ilmar Süda, Tõnu Talvi, Allan Selin, Urmas Jürivete, Tõnu Kesküla, Märt Kruus, Heli Kirik, Siiri Jürgenstein, Mati Martin, Erki Õunap, Jaan Viidalepp, Miina Oras and Hannes Järve who collected myriapods for the present study. Peter Decker and Ivan H. Tuf are thanked for their helpful comments and suggestions to the manuscript.

References

Abarenkov K, Tedersoo L, Nilsson RH, Vellak K, Saar I, Veldre V, Parmasto E, Prous M, Aan A, Ots M, Kurina O, Ostonen I, Jõgeva J, Halapuu S, Põldmaa K, Toots M, Truu J, Larsson K, Kõljalg U (2010) PlutoF – a Web Based Workbench for Ecological and Taxonomic Research, with an Online Implementation for Fungal ITS Sequences. Evolutionary Bioinformatics 6: 189–196. https://doi.org/10.4137/EBO.S6271

Atlavinytė O, Lokshina I (1971) [Millipedes of the Lithuanian SSR] Lietuvos TRS Mokslu akademijos darbai, C serja 2(55): 83–92. [in Russian]

Andersson G, Meidell B, Scheller U, Djursvoll P, Budd G, Gärdenfors U (2005) Nationalnyckeln till Sveriges flora och fauna. Mångfotingar Myriapoda. Uppsala, ArtDatabanken Sveriges Lantbruksuniversitet, 351 pp.

Andersson G, Djursvoll P, Scheller U (2008) Katalog över Nordens mångfotingar. Entomologisk Tidskrift 129: 173–190.

Andersson G, Djursvoll P, Scheller U (2013) En uppdatering av "Katalog över Nordens mångfotingar. Entomologisk Tidskrift 134(3): 149–152. [in Swedish]

Barber AD (2009) Centipedes. Keys and Notes for the Identification of the species. Synopses of the British fauna No.58 Field Studies Council, London, 215 pp.

Becker R (1929) Beiträge zur Diplopoden-Fauna Lettlands. Folia Zoologica et Hydrobiologica 1, 1: 10–52

Blower JG (1985) Millipedes: Keys and Notes for the Identification of the Species. Synopses of the British Fauna (New Series) vol 35, Brill/Backhuys, Leiden, 242 pp.

Bonato L, Minelli A, Spuņģis V (2005) Geophilomorph Centipedes of Latvia (Chilopoda, Geophilomorpha). Latvijas Entomologs 42: 5–17.

Bonato L, Chagas Junior A, Edgecombe GD, Lewis JGE, Minelli A, Pereira LA, Shelley RM, Stoev P, Zapparoli M (2016) ChiloBase 2.0 – A World Catalogue of Centipedes (Chilopoda). http://chilobase.biologia.unipd.it [accessed 30.03.2018]

David JF (2009) Ecology of millipedes (Diplopoda) in the context of global change. Soil Organisms 81(3): 719–733.

Eglītis V (1954) [Fauna of soils of the Latvian SSR]. Rīga, Zinātne, 262 pp. [in Russian]

Golovatch SI, Matyukhin AV (2011) New records of millipedes (Diplopoda), mainly from bird nests, in European Russia. Arthropoda Selecta 20(2): 115–116.

Haase E (1886) Schlesiens Diplopoden (Erste Hälfte). Zeitschrift für Entomologie, Neue Folge 11: 7–64.

Ivask M (2011) Myriapoda of Estonian seminatural grasslands. In: Book of abstracts. 13th Symposium of Nordic Soil Zoologists and PhD course, Lammi, Finland, August 25–29, 2011, 1–2.

Ivask M, Kuu A, Meriste M, Kutti S, Raamets J (in press) Chilopoda and Diplopoda of seminatural flooded meadows in Matsalu. Pedobiologia.

Kaarep E, Luhakooder A, Ratt A (1949) Tähtsamad taimehaigused ja kahjurid ning nende tõrje. RK Teaduslik Kirjandus, Tartu, 315 pp. [Major plant diseases and pests and their control; in Estonian]

Kalda K, Ivask M, Kutti S, Kuu A, Meriste M, Nei L, Peda J, Raukas A (2015) Soil Invertebrates in Semi-Coke Heaps of Estonian Oil Shale Industry. Oil Shale 32(1): 82–97. https://doi.org/10.3176/oil.2015.1.06

Kania G, Tracz H (2005) Mass occurrence and migration of *Ommatoiulus sabulosus* (Linnaeus, 1758) (Diplopoda, Julida: Julidae) in Poland. Peckiana 4: 57–66.

Kime RD (2001) The continental distribution of British and Irish millipedes, part 2. Bulletin of the British Myriapod and Isopod Group 17: 7–42.

Kime RD, Enghoff H (2011) Atlas of European Millipedes (Class Diplopoda), Vol.1 Orders Polyxenida, Glomerida, Platydesmida, Siphonocryptida, Polyzoniida, Callipodida, Polydesmida. Fauna Europaea Evertebrata No 3, Pensoft, Sofia-Moscow, 282 pp.

Kime RD, Enghoff H (2017) Atlas of European millipedes 2: Order Julida (Class Diplopoda). European Journal of Taxonomy 346: 1–299. https://doi.org/10.5852/ejt.2017.346

Kongo L (2016) Saksa-eesti kohanimed. “Abiks loodusevaatlejale” 100, Tartu, 304 pp. [German-Estonian place names; in Estonian]

Lang J (1954) Mnohonožky – Diplopoda. 1. vyd. Praha, Nakladatelství Československé akademie věd, 188 pp. (Fauna ČSR; sv. 2). [in Czech]

Lazányi E, Vagalinski B (2013) Redefinition of the millipede subgenus *Megaphyllum sensu stricto* Verhoeff, 1894 and neotype designation for *Megaphyllum austriacum* (Latzel, 1884) (Myriapoda: Diplopoda: Julida: Julidae). Zootaxa 3741(1): 55–100. https://doi.org/10.11646/zootaxa.3741.1.2

Lehtinen PT, Terhivuo J (1996) Notes and records of five garden millipedes (Diplopoda, Iulida) in Finland. Memorenda Societatis Pro Fauna et Flora Fennica 72: 6–12.

Lohmander H (1948) *Lithobius nigrifrons fennoscandicus* n. ssp. (Chilopoda, Lithobiidae). Annales Entomologici Fennici 14: 97–99.

Lokshina IE (1969) Key to millipedes Diplopoda of the plain part of the European USSR. Nauka Publishing, Moscow, 78 pp. [in Russian]

McAlpine DF, Shear W (2018) The millipede *Craspedosoma raulinsii* Leach, 1814 (Chordeumatida: Craspedosomatidae) in North America with comments on the derivation of its binomial name. Zootaxa 4455(2): 389–394. https://doi.org/10.11646/zootaxa.4455.2.8

Nõmmik A (1939) Lagunenud puulehtede ja osakeste lagunemise kiirusest ja neis sisalduvate mõningate elementide kaost. Eesti metsanduse aastaraamat 9: 197–222. [Leaf litter decomposition rate and loss of some elements; in Estonian]

Palmén E (1948) The Chilopoda of Eastern Fennoscandia. Annales Zoologici Societatis Zoologicae-Botanicae Fennicae Vanamo 13(4): 1–52.

Palmén E (1949) The Diplopoda of Eastern Fennoscandia. Annales Zoologici Societatis Zoo logicae-Botanicae Fennicae Vanamo 13(6): 1–45.

Remm K (1988) Koljaku-Oandu reservaadi samblarinde loomastik suve teisel poolel. In: Lahemaa Uurimused III Rahvuspargi looduse inventeerimine. Valgus, Tallinn, 120–141. [Fauna of moss-layer of Koljaku-Oandu nature reserve in the second half of summer; in Estonian]

Riikoja H (1955) Eesti NSV selgrootute fauna uurimise küsimusi. Eesti NSV Teaduste Akadeemia juures asuva Loodusuurijate Seltsi aastaraamat 48: 7–26. [Questions of Estonian invertebrate fauna research; in Estonian]

Saar L, Takkis K (2010) Teadlased ja õpilased elurikkuse jahil. GEO Estonia 6/10: 8–11. [Scientists and pupils in search of biodiversity; in Estonian]

Sammet K, Talvi T, Süda I, Kurina O (2016) Pseudoscorpions (Arachnida: Pseudoscorpiones) in Estonia: new records and an annotated checklist. Entomologica Fennica 27(4): 149–163.

Schmidt P (1894) Zur Kenntnis des inneren Baues des *Pauropus Huxleyi* Lubb. Zoologischer Anziger 17: 189–196.

Schubart O (1924) Myriapoda. In: Dampf A (Ed.) Zur Kenntnis der estländischen Moorfauna. II Beitrag. Sitzungsberichte der Naturforscher-Gesellschaft bei der Universität Dorpat 31(1–2): 57.

Schubart O (1930) Über die von Dr. Herold im Ost-Baltikum gesammelten Diplopoden, zugleich ein Beitrag zur Diplopodenfauna des Ost-Baltikums. Zoologischer Anzeiger 86(7/8): 189–208.

Schubart O (1934) Die Tierwelt Deutschlands. 28. Teil: Tausendfüßler oder Myriapoda: I. Diplopoda. Gustav Fischer Verlag, Jena, 318 pp.

Sierwald P, Spelda J (2018) MilliBase. http://www.millibase.org [accessed 29.03.2018]

Spuņģis V (2010) Fauna of Millipedes (Diplopoda) in Latvia with Notes on Occurrence, Habitat Preference and Abundance. Latvijas Entomologs 48: 107–115.

Stojałowska W (1961) Krocionogi (Diplopoda) Polski. Panstwowe Wydawnictwo Naukowe, Warzawa, 216 pp. [Millipedes of Poland; in Polish]

Tomasson K, Tammaru T, Kurina O (2014) Harvestmen (Arachnida: Opiliones) in Estonia: results of the Estonian Malaise Trap Project. Entomologica Fennica 25(3): 142–156.

Trautberg O (1929) Beitrag zur Kenntnis einiger in Lettland vorkommender Arten der Gattung *Lithobius* und *Geophilus*. Acta Universitatis Latviensis 20: 31–70.

Tuf IH, Ivinskis P, Rimšaitė J (2015) A checklist of the centipedes (Chilopoda) of Lithuania. Zootaxa 4052(3): 394–400. https://doi.org/10.11646/zootaxa.4052.3.9

Vilbaste J (1953) Eesti NSV tuhatjalgsete (Diplopoda) määraja. Abiks loodusevaatlejale nr.12. Loodusuurijate Selts Eesti NSV TA juures, Tartu, 49 pp. [Keys to Estonian Millipedes; in Estonian]

Vilbaste J (1970) Hulkjalgsed. In: Lääne-Eesti rannikualade loodus. Valgus, Tallinn, 165–175. [Myriapods; in Estonian]

Vilbaste J (1979) Molluscs and Myriapods of the Vooremaa hardwood-spruce forest. In: Spruce Forest Ecosystem Structure and Ecology. Estonian IBP Report 12, 95–100.

Vilbaste J, Haberman H, Krall E, Maavara V, Martin A, Remm E, Remm H, Siitan V, Viidalepp J, Vilbaste A (1985) Matsalu märgala maismaaselgrootud. In: Kumari E (Ed.) Matsalu – rahvusvahelise tähtsusega märgala. Valgus, Tallinn, 44–46. [Terrestrial invertebrates of Matsalu; in Estonian]

Vilbaste J, Vilbaste A (1993) Järvselja looduskaitsekvartali selgrootutest. Loodusuurijate Seltsi Aastaraamat 74: 318–319. [Invertebrates of Järvselja Nature Reserve; in Estonian]

Volkova JuS (2016) An Annotated Catalogue of Geophilomorph Centipedes (Myriapoda, Geophilomorpha) of European Russia. Entomological Review 96(4): 500–511. https://doi.org/10.1134/S0013873816040138

Wesener T, Voigtländer K, Decker P, Oeyen JP, Spelda J, Lindner N (2015) First results of the German Barcode of Life (GBOL) – Myriapoda project: Cryptic lineages in German *Stenotaenia linearis* (Koch, 1835) (Chilopoda, Geophilomorpha). ZooKeys 510: 15–29. https://doi.org/10.3897/zookeys.510.8852

Zalesskaya NT (1978) Key to the Lithobiomorph centipedes of USSR. Nauka, Moscow, 212 pp. [in Russian].

Zapparoli M (2003) The present knowledge on the European fauna of Lithobiomorpha (Chilopoda). Bulletin of the British Myriapod and Isopod Group 19: 20–41.

Zolk K (1923) Kodumaa kahjulikumad putukad. Riigi Statistika Keskbüroo, Tallinn, 70 pp. [Homeland's detrimental insects; in Estonian]

Supplementary material 1

Published records of Estonian myriapods

Authors: Kaarel Sammet, Mari Ivask, Olavi Kurina

Data type: occurrence

Explanation note: Full collecting details for one finding from each locality. The locality numbers correspond to those in Table 1 and Figure 1.

Link: https://doi.org/10.3897/zookeys.793.28050.suppl1

ZooKeys 793: 97–114 (2018)
doi: 10.3897/zookeys.793.26712
http://zookeys.pensoft.net

RESEARCH ARTICLE

A peer-reviewed open-access journal
ZooKeys
Launched to accelerate biodiversity research

New *Atanatolica* species from Ecuador (Trichoptera, Leptoceridae)

Ernesto Rázuri-Gonzales[1,3], Ralph W. Holzenthal[1], Blanca Ríos-Touma[2,4]

1 *Department of Entomology, University of Minnesota, 1980 Folwell Avenue, 219 Hodson Hall, St. Paul, Minnesota 55108, USA* **2** *Facultad de Ingenierías y Ciencias Aplicadas, Ingeniería Ambiental, Grupo de Investigación en Biodiversidad Medio Ambiente y Salud – BIOMAS – Universidad de Las Américas, Campus Queri, Quito, Ecuador* **3** *Departamento de Entomología, Museo de Historia Natural, Universidad Nacional Mayor de San Marcos, Lima, Perú* **4** *Instituto Nacional de Biodiversidad, Quito, Ecuador*

Corresponding author: *Blanca Ríos-Touma* (briostouma@gmail.com)

Academic editor: *Ana Previšić* | Received 16 May 2018 | Accepted 6 September 2018 | Published 29 October 2018

http://zoobank.org/33EE04F5-0C2C-4E63-B130-E0A508849BEA

Citation: Rázuri-Gonzales E, Holzenthal RW, Ríos-Touma B (2018) New *Atanatolica* species from Ecuador (Trichoptera, Leptoceridae). ZooKeys 793: 97–114. https://doi.org/10.3897/zookeys.793.26712

Abstract

Four new species of *Atanatolica* Mosely are described from Ecuador: *A. andina* **sp. n.**, *A. angulata* **sp. n.**, *A. curvata* **sp. n.**, and *A. decouxi* **sp. n.** These species belong to the *A. dominicana* group and constitute new records of the genus from Chimborazo, Imbabura, and Napo Provinces. Additionally, *A. andina* **sp. n.** represents the highest elevation recorded for any species in the genus at 3900 m. Size class data are also presented suggesting continuous larval growth for the probable larva of *A. decouxi* **sp. n.**, described and illustrated here. A new distribution record is provided for *A. manabi* from Carchi Province.

Keywords

Andes, aquatic insects, Grumichellinae, long-horned caddisflies, taxonomy

Introduction

Atanatolica Mosely, 1936 is a Neotropical genus in the long-horned caddisfly family Leptoceridae. Originally, the genus was established to include a single species, *Mystacides brasilianus* (Brauer, 1865), based on characters of the wing venation and male genitalia (Mosely 1936). Only *A. dominicana* Flint, 1968 and *A. botosaneanui* Flint, 1981 were described before Holzenthal's 1988 revision, which included descriptions of 14 new species and redescriptions of the previously described ones. More recently, four new species were described from Brazil and Peru (Costa and Calor 2014, Henriques-Oliveira and Santos 2014, Oláh 2016), bringing the current number of species in the genus to 21 (Holzenthal and Calor 2017). Holzenthal (1988) recognized two species groups, the *A. brasiliana* and the *A. dominicana* groups. The *A. brasiliana* group has a sessile fork I in the forewing while this fork is petiolate in *A. dominicana* group species.

Fourteen species of *Atanatolica* are known from the northern and central Andean countries (Venezuela, Colombia, Ecuador, Peru, and Bolivia); no species are known from the southern Andes (Chile, Argentina) (Holzenthal and Calor 2017, Oláh 2016). Four species are known from Brazil (two in the southeast, two in the northeast), two from Central America, and one from the Lesser Antilles. None of these species, except *A. dominicana*, are present in more than one country, and most are described from very few adults (Holzenthal 1988). Currently, there are three species known from Ecuador (Ríos-Touma et al. 2017): *A. acuminata* Holzenthal, 1988, *A. cotopaxi* Holzenthal, 1988, and *A. manabi* Holzenthal, 1988, all of them in the *dominicana* group.

Larvae are associated with small and medium-sized Neotropical mountain streams, waterfalls, their splash zones, and even outside the water in moist, semiterrestrial habitats (Flint 1968, Holzenthal 1988). Larvae and pupae are usually found in large numbers, often in groups, attached to the substrate by anterior silken pedicles or with silken strands attached to rocks to improve larval purchase and mobility on smooth surfaces (Holzenthal 1988). Ecologically, they are considered scrapers, probably feeding on periphyton and deposited organic matter (Holzenthal 1988, Holzenthal and Calor 2017). Adults are diurnal and form swarms above larval habitats, and therefore, they are not common at UV light traps commonly used to attract caddisflies (Holzenthal and Calor 2017). *Atanatolica bonita* Costa & Calor, 2014 is the only species in the genus for which there is any seasonal information available. Abundance of this species fluctuated through the year, with increasing abundance in the dry season, at least in the Brazilian region surveyed by Costa and Calor (2014).

Here we describe four new species of *Atanatolica* from Ecuador. These new species come from several localities along the Andes: *A. andina* sp. n. from the highlands of the Amazon drainage, *A. decouxi* sp. n. from the cloud forests of the Pacific drainage of the Andes, and *A. angulata* sp. n. and *A. curvata* sp. n. from the Amazon piedmont. For *A. decouxi* sp. n. we also describe the probable larva and provide size class information and some biological observations.

Material and methods

Localities and collecting methods

Atanatolica andina sp. n. was collected at high-altitude waterfalls surrounded by *páramo* vegetation in Parque Nacional Cayambe-Coca (Napo Province) and Parque Nacional Sangay (Chimborazo Province) using aerial nets. Additional specimens were collected by B. Gill, also at Parque Nacional Cayambe-Coca. Specimens of *Atanatolica decouxi* sp. n. were collected at Río de la Plata, a pristine stream in the Bosque Protector los Cedros (Imbabura Province) using UV lights and Malaise traps for adults and Surber nets and hand collecting for immatures. Bosque Protector los Cedros is part of the Choco-Darien floristic region, which is considered a biogeographic hotspot and priority conservation area due to its high species richness and endemism (Dodson and Gentry 1991, Myers et al. 2000). At the collection site the river has a small waterfall followed by two deep clear pools (Figure 1). The two other described species were borrowed from the Smithsonian Institution and were collected by O. S. Flint Jr. in the Amazon piedmont of Napo Province in 1990.

Locality data were formatted using the web application AUTOMATEX (Brown 2013) to increase consistency. The map was prepared in QGIS 3.2.2. Bonn (QGIS Development Team 2018). Vector and raster maps were made with Natural Earth (2018) and CIAT-CSI SRTM (Jarvis et al. 2008) data.

Specimen preparation

Adult specimens were prepared and examined following standard methods for pinned and alcohol preserved material (Blahnik and Holzenthal 2004, Blahnik et. al. 2007). Length of forewing was measured from base to apex with a microscale (BioQuip Products, Rancho Dominguez, California, USA). Body length, head width and length, and case length of all larvae collected (n = 89) were measured to establish size variation and stages across the collecting dates (as described by Resh 1976). Measurements were performed with the aid of a Zeiss V12 Discovery Stereoscope with an Axiocam ICc5 camera and the Axiovision SE64 software.

Male genitalia were soaked in 85% lactic acid and heated to 125 °C for 20 min to dissolve internal soft tissues. Olympus BX41 and SZX12 compound and stereomicroscopes outfitted with drawing tubes were used to examine specimens and to aid the rendering of detailed pencil drawings of genital structures and larvae, respectively. Pencil sketches were scanned and placed in Adobe Illustrator (Creative Cloud version) to serve as a template for vector illustrations. The plugin “Stipplism” (Astute Graphics) was used to apply stipple effects to illustrations. Morphological terminology follows that of Holzenthal (1988).

Types of the new species and other material examined are deposited in the University of Minnesota Insect Collection, St. Paul, Minnesota, USA (**UMSP**), the Museo Ecuatoriano de Ciencias Naturales, Instituto Nacional de Biodiversidad, Quito, Ecuador (**MECN**), and the National Museum of Natural History, Smithsonian Institution, Washington, DC (**NMNH**). Each specimen housed at UMSP or MECN was affixed with a barcode label (4-mil polyester, 8 × 14 mm, code 49) bearing a unique alphanumeric sequence beginning with the prefix UMSP to serve as a specimen identifier (UID) for upload of collection and specimen data to the UMSP database; UIDs for holotypes deposited in UMSP and NMNH are listed in the material examined.

Figure 1. A Río de la Plata, Reserva Los Cedros, type locality of *Atanatolica decouxi* sp. n. **B** Same, larvae of *A. decouxi* sp. n. on stream substrate.

Taxonomy

Atanatolica andina sp. n.

http://zoobank.org/A2D13672-1B8E-4D08-BA72-63A1BF05AE32
Figs 2, 8

Diagnosis. This new species is most similar to *A. acuminata* and *A. dominicana* from Ecuador and Dominica, respectively, based on the general structure of tergum X (i.e., subtriangular in shape, with digitate apicomesal processes). It differs from *A. acuminata* by the shorter, thicker apicomesal processes on tergum X, and the shorter and rounder apicolateral processes on tergum X; in lateral view, the apicolateral processes in *A. andina* sp. n. are much shorter than the apicomesal processes, whereas in *A. acuminata*, both processes are roughly equal in length and the apicolateral processes are accuminate. Additionally, the inferior appendages in *A. andina* sp. n. are inflated mesally in lateral view, but not in *A. acuminata*. From *A. dominicana*, it differs by having a much narrower and shallower mesal cleft on tergum X between the apicomesal processes. Additionally, the posteromesal margin of the inferior appendages in ventral view is rounder and more pronounced in *A. andina* sp. n., whereas in *A. dominicana*, this margin is straight.

Description. Adult male. Forewing length 9.8 ± 0.5 mm (n = 3). General color black, forewing membrane brown, covered in brown and white setae. Head with long, brown setae. Antennae with long, brown setae on scape and pedicel, flagellomeres with dark brown setae and ring of white setae basally. Maxillary palps brown, with long, brown hairs. Thorax black, with dark brown hairs. Forelegs brown, tarsomeres with white ring basally; mid legs dark brown with white setae; hind legs dark brown with white setae, interspersed with brown spines, increasing in thickness towards the tarsal segments. Tibial spur formula 0, 2, 2.

Genitalia. Segment IX annular, short, with anterior margin sinuous, posterior margin slightly produced mesally (Figure 2A). Preanal appendages shorter than tergum X,

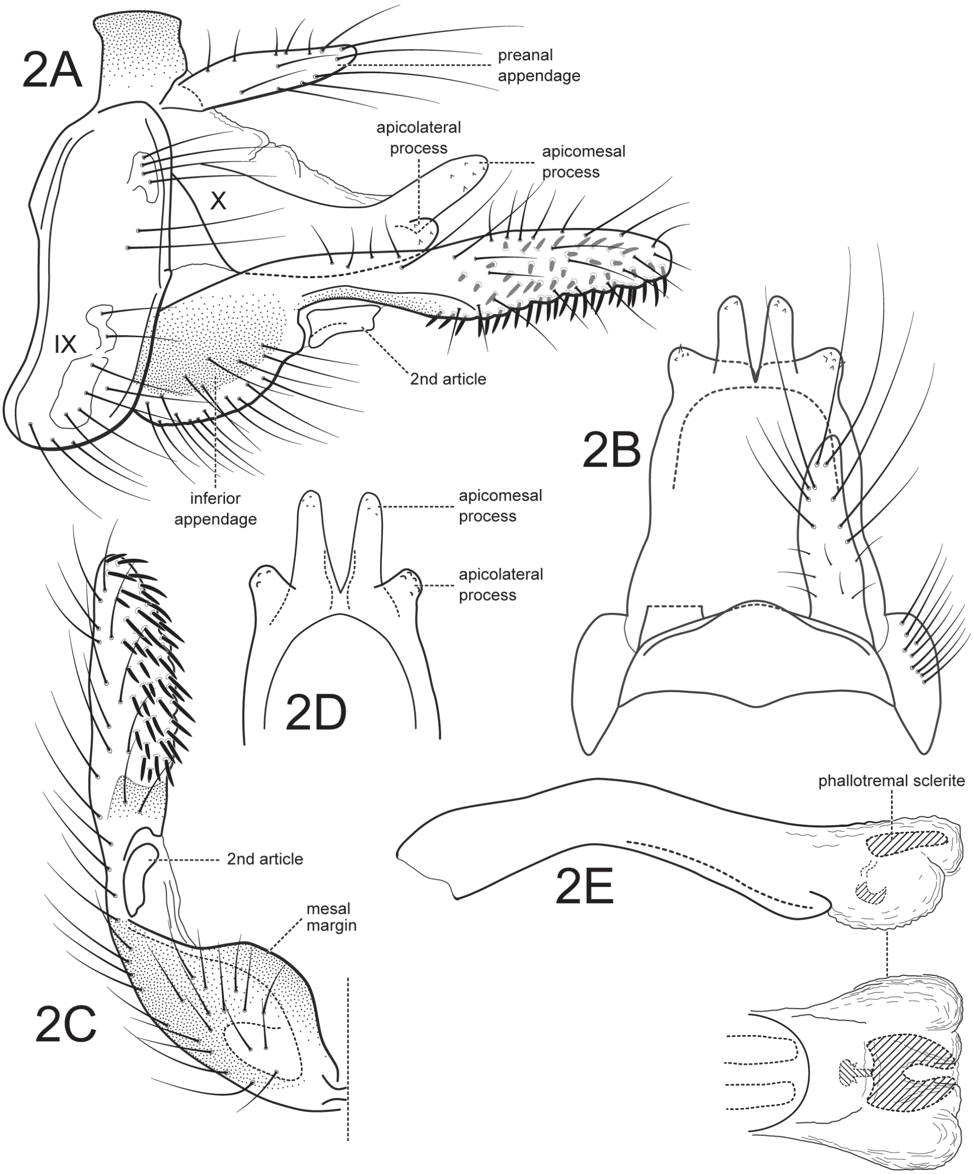

Figure 2. *Atanatolica andina* sp. n., male genitalia. **A** Lateral **B** Segments IX and X, dorsal **C** Inferior appendage, ventral **D** Tergum X, caudoventral **E** Phallic apparatus, lateral (inset: phallic apparatus apex, ventral). Abbreviations: IX abdominal segment IX, X abdominal tergum X.

slender, digitate, setose (Figure 2A, B). Tergum X slightly notched apicomesally, basal portion of tergum X membranous, with two pairs of sclerotized apical processes; apicomesal processes digitate and directed upwards in lateral view (Figure 2A); apicolateral processes much shorter than apicomesal processes, thumb-like, directed laterad in dorsal and caudoventral views (Figure 2B, D); apices with short spicules (Figure 2A, B, D). Inferior appendages with basal portion of first segment broad, setose, highly pigmented, mesal margin rounded, apical portion digitate, straight, slightly inflated subapically in ventral view (Figure 2C), covered with stout, spine-like setae on its mesal surface; second article short, rectangular (Fig 2A, C). Phallic apparatus simple, without any processes; phallobase tubular; phallotremal sclerites complex, consisting of pair of elongated sclerites basally (very faint in the specimens examined), hooked sclerite subapically, and U-shaped sclerite apically (rectangular in lateral view); endothecal membranes trilobed (Figure 2E).

Holotype male. ECUADOR: **Napo**: Reserva Ecológica Cayambe-Coca waterfall, rd. to Oyacachi, 0.32621°S, 78.1505°W, 3690 m, 26.ii.2012, B Ríos-Touma, L Pita (UMSP) [UMSP000098741].

Paratypes. ECUADOR: **Chimborazo**: small roadside waterfall on Highway E-46 (via Riobamba - Macas), 2.17572°S, 78.5047°W, 3527 m, 2♂, 25.i.2015, R Holzenthal, B Ríos-Touma (MECN); **Napo**: unnamed trib. to Oyacachi R., ca. 5.2 mi W of Oyacachi, 0.229504°S, 78.0059°W, 2823 m, 1♂, 24.ii.2012, B Gill (NMNH), unnamed tributary to Papallacta River, Hwy. E-28, ca. 1 km SW Papallacta, 0.38589°S, 78.1435°W, 3246 m, 8♂, 6♀, 25.i.2012, B Gill (NMNH), stream, 2.73 Km W Papallacta, Hwy. E-28, 0.534639°S, 78.2254°W, 3982 m, 8♂, 25.i.2012, B Kondratieff, B Gill (NMNH).

Etymology. Named after the Andean ranges where the specimens were collected.

Distribution. Napo and Chimborazo Provinces (Ecuador) (Figure 8). The species occurs at the highest elevation ever recorded for the genus.

Atanatolica angulata **sp. n.**

http://zoobank.org/4FFF866C-42EA-4014-BFFD-091D54B755A1
Figs 3, 8

Diagnosis. This species is related to *A. aurea* Holzenthal, 1988 from Colombia, and *A. penai* Holzenthal, 1988 from Bolivia, especially in the broad apicomesal processes of tergum X. The new species differs from *A. aurea* by the much shorter, acute, angulate apicomesal processes, and the rounded apicolateral processes on tergum X as well as the shape of the inferior appendages, especially the posteromesal margin of the first segment of this structure in ventral view. From *A. penai*, it differs by the shape of the apicomesal processes of tergum X, which in *A. angulata* sp. n. are strongly angulate. They also differ by the shape of the inferior appendages, which have a mesal bump on the inner surface in *A. penai*, but not in *A. angulata* sp. n.

Description. Adult male. Forewing length 9 mm (n = 1). General color light brown, forewing membrane brown, covered in golden and brown setae. Head with long, white setae. Antennae with long, white setae on scape and pedicel, flagellomeres with dark brown setae and ring of white setae basally. Maxillary palps light brown, with long, white and short brown hairs. Thorax light brown with brown hairs. Forelegs with coxae, trochanter, and femur light brown with long, white setae; tibia and tarsomeres with white and brown setae; mid and hind legs light brown with white and brown setae, tibia and tarsomeres with two rows of dark spines ventrally. Tibial spur formula 0, 2, 2.

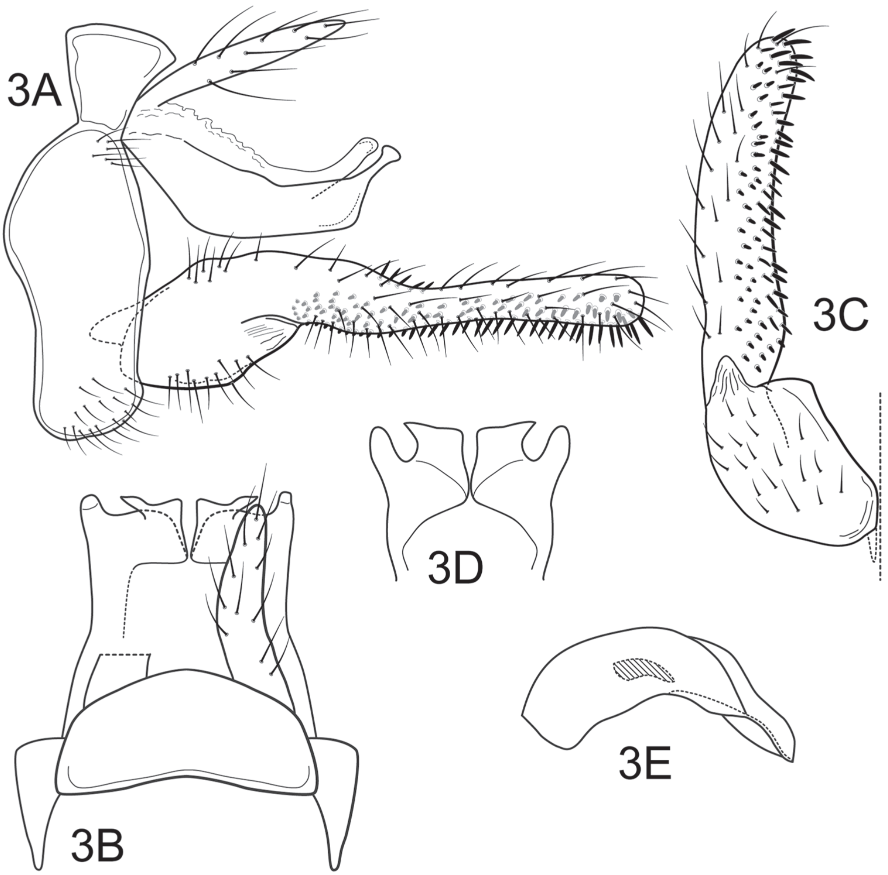

Figure 3. *Atanatolica angulata* sp. n., male genitalia. **A** Lateral **B** Segments IX and X, dorsal **C** Inferior appendage, ventral **D** Tergum X, caudoventral **E** Phallic apparatus, lateral.

Genitalia. Segment IX annular, short, with anterior and posterior margins sinuous, setae on ventral and lateral surfaces not associated with warts (Figure 3A). Preanal appendages slightly shorter than tergum X, slender, digitate, setose (Figure 3A, 3B). Tergum X notched apicomesally, basal portion of tergum X membranous, with two pairs of sclerotized apical processes; apicomesal processes flattened, directed dorsad in lateral view (Figure 3A), strongly angulate, posterolateral apex acute in dorsal and caudoventral views (Figure 3B,); apicolateral processes capitate, directed dorsad in lateral view, slightly longer than the apicomesal processes, but equally as long in dorsal and caudoventral views (Figs 3A, B, D), digitate in dorsal and caudoventral views (Figure 3B, D). Inferior appendages with basal portion of first segment broad, setose, mesal margin forming an angle, apical portion elongate, digitate, slightly curved, and slightly inflated basally in ventral view (Figure 3C), covered with stout, spine-like setae on mesal surface; second article apparently fused with the first segment, represented by triangular semimembranous process (Figure 3A, C). Phallic apparatus simple, without any processes; phallobase short, tubular, curved downwards; phallotremal sclerite simple, spine-like, curved; endothecal membranes not everted (Figure 3E).

Holotype male. ECUADOR: **Napo**: Río Jondachi, 30 km N Tena, 950 m, 10.ix.1990, OS Flint (NMNH) [USNMENT01295341].

Etymology. The specific name *angulata* is a Latin adjective referring to the angulate apicomesal processes on tergum X.

Distribution. Napo Province (Ecuador) (Figure 8).

Atanatolica curvata sp. n.

http://zoobank.org/2291EBFF-73FF-4F10-A776-C426797601AA
Figs 4, 8

Diagnosis. This new species resembles *A. homora* Oláh, 2016 from Peru in that both possess paired, basodorsal membranous lobes on tergum X, but in *A. homora* these lobes bear peg-like setae and are narrower than in *A. curvata* sp. n. Also, the apicomesal processes of tergum X are long and capitate in *A. homora* (Oláh 2016, fig 26), but short and digitate in *A. curvata* sp. n. (Figure 4B, D).

Description. Adult male. Forewing length 10.5 mm (n = 1). General color light brown, forewing membrane light brown, covered in golden setae throughout wing membrane and brown setae on costal margin. Head with long, yellow setae dorsally, brown setae ventrally. Antennae broken at second flagellomere, scape and pedicel with long, light brown setae. Maxillary palps light brown, with long, brown hairs. Thorax light brown with long, yellow setae. Forelegs light brown, tibia with brown setae, tarsomeres with white ring basally; mid and hind legs with yellow setae, and two rows of dark spines on tibia and tarsomeres. Tibial spur formula 0, 2, 2.

Genitalia. Segment IX annular, short, with anterior and posterior margins sinuous, with setae on ventral and lateral surfaces (ventral setae arising from a wart) (Fig. 4A). Preanal appendages shorter than tergum X, slender, digitate, setose (Figure 4A, 4B). Tergum X slightly notched apicomesally, basodorsal portion of tergum X membranous, produced into pair of membranous lobes; with two pairs of sclerotized apical processes; apicomesal processes digitate and directed dorsad in lateral view (Figure 4A); apicolateral processes shorter than apicomesal processes, apex subtriangular in dorsal view, directed laterad in dorsal and caudoventral views (Figure 4B, 4D). Inferior appendages with basal portion of first segment broad, setose, highly pigmented, mesal margin concave in ventral view (Figure 4C), apical portion digitate, curved mesad, inflated apically in ventral view, covered with stout, spine-like setae on its mesal surface; second article very small, short, triangular (Figures 4A, 4C). Phallic apparatus simple, without any processes; phallobase tubular; phallotremal sclerite simple, U-shaped in ventral view; endothecal membranes not everted (Figure 4D).

Holotype male. ECUADOR: **Napo**: 12 km W Baeza, 2380 m, 09.ix.1990, OS Flint (NMNH) [USNMENT01295342].

Etymology. The specific name *curvata* is a Latin adjective that means curved and refers to the strongly curved inferior appendages in ventral view.

Distribution. Napo Province (Ecuador) (Figure 8).

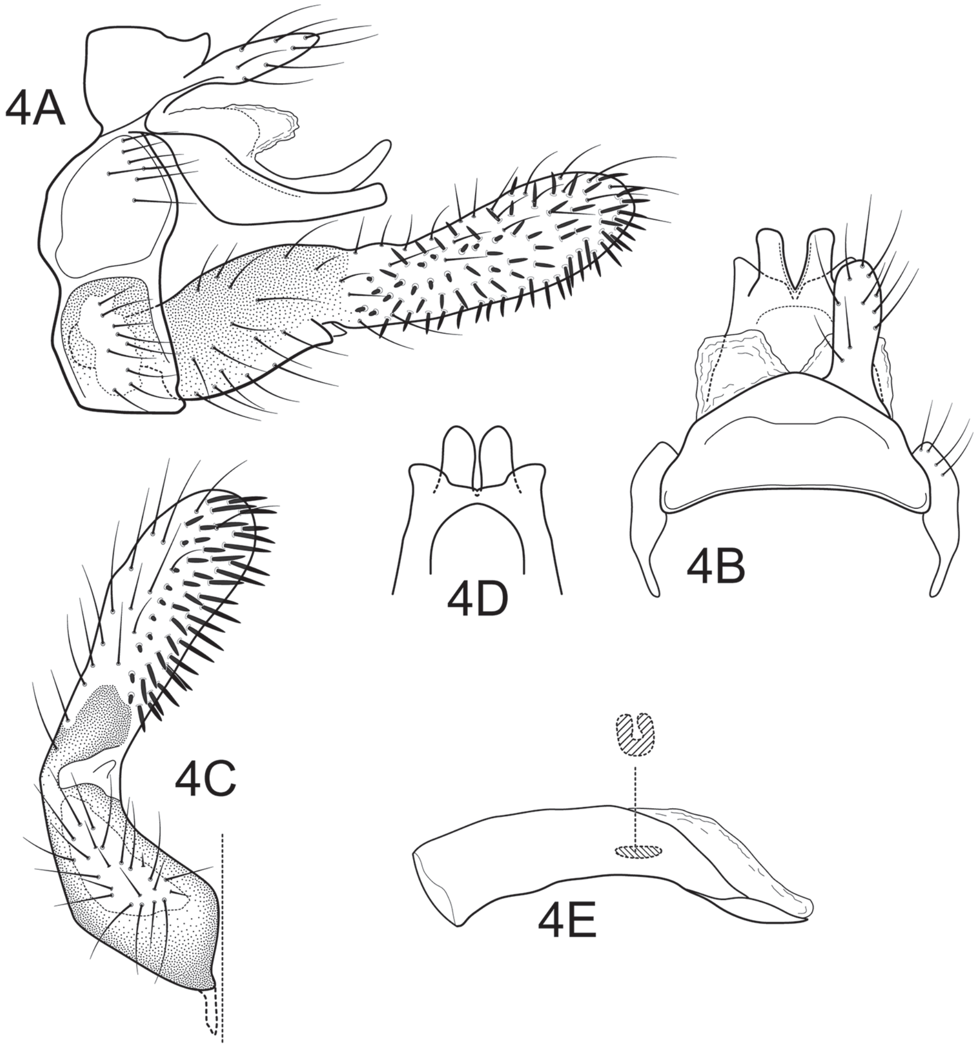

Figure 4. *Atanatolica curvata* sp. n., male genitalia. **A** Lateral **B** Segments IX and X, dorsal **C** Inferior appendage, ventral **D** Tergum X, caudoventral **E** Phallic apparatus, lateral (inset: phallotremal sclerite, ventral).

Atanatolica decouxi sp. n.

http://zoobank.org/BA4AF849-3B55-4347-B792-7EC60AF47C03
Figs 1B, 5, 6, 7, 8

Diagnosis. Morphology of the male genitalia of *A. decouxi* sp. n. is similar to *A. cotopaxi* Holzenthal, 1988 and *A. muyupampa* Holzenthal, 1988 from Ecuador and Bolivia, respectively. From *A. cotopaxi*, it differs by the slightly posteromesally produced segment IX, the longer preanal appendages reaching the apex of tergum X, and the shape and length of the apicolateral processes on tergum X, which are much shorter in *A. cotopaxi*. The putative larvae of *A. decouxi* sp. n. has spines on the anterior margin

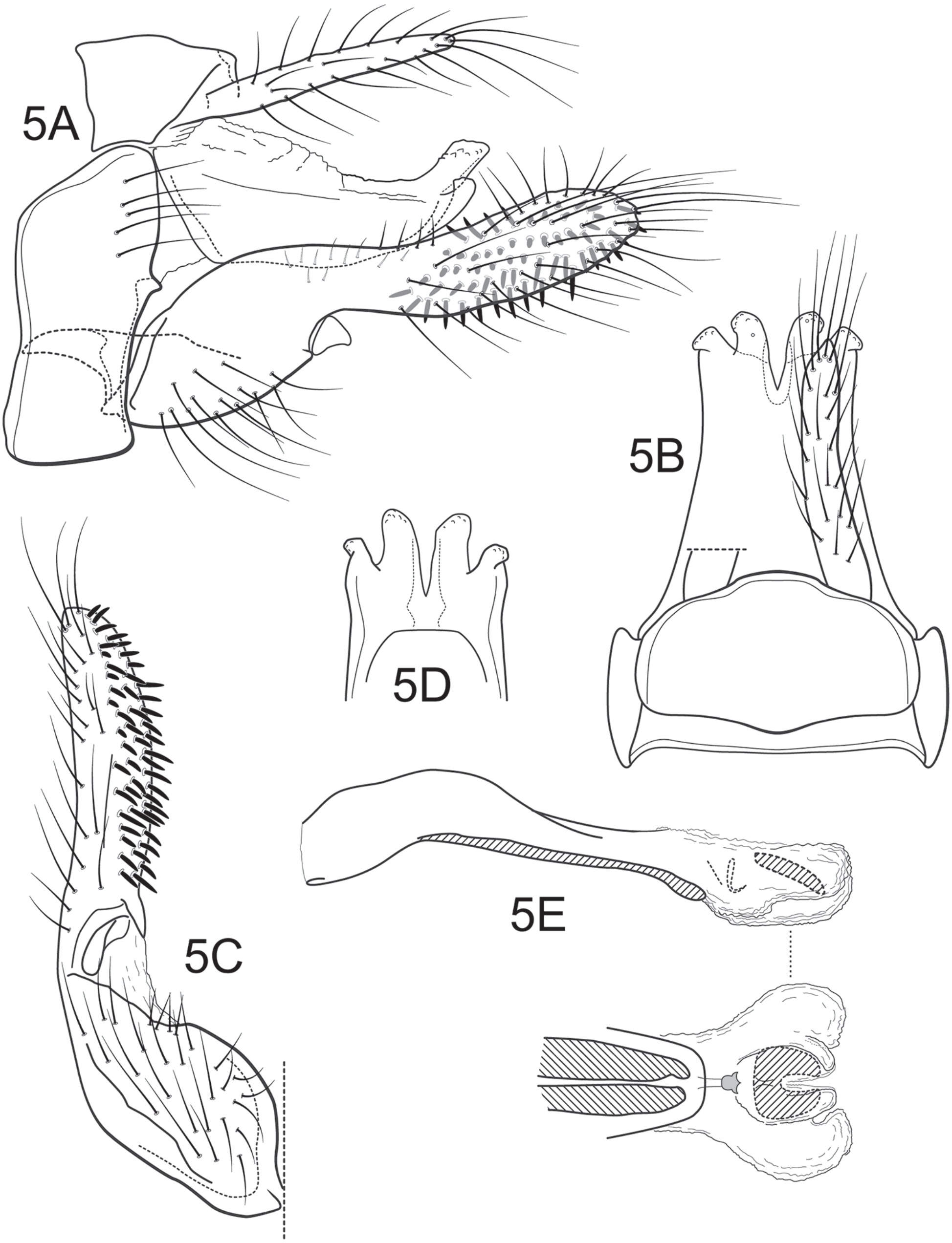

Figure 5. *Atanatolica decouxi* sp. n., male genitalia. **A** Lateral **B** Segments IX and X, dorsal **C** Inferior appendage, ventral **D** Tergum X, caudoventral **E** Phallic apparatus, lateral (inset: phallic apparatus apex, ventral).

of the legs, similar to those found in *A. cotopaxi*, as illustrated by Holzenthal (1988), but the adults are light brown, whereas in *A. cotopaxi*, they are dark brown. *Atanatolica muyupampa* differs from *A. decouxi* sp. n. by the shorter and laterally directed apicomesal processes on tergum X, and the deeper mesal cleft on tergum X between the apicomesal processes; in *A. decouxi* sp. n. both of these processes are apically rugose. Additionally, the inferior appendage in *A. decouxi* sp. n. is straight in ventral view, but curved mesad in *A. muyupampa*.

Description. Adult male. Forewing length 11 ± 0.5 mm (n = 3). General color light brown, forewing membrane light brown, covered in brown setae along the costal margin and yellow setae through the remainder of the forewing. Head with yellow and light brown hairs. Antennae with light brown hairs on the scape and pedicel, flagellomeres with dark brown setae and ring of white setae basally. Maxillary palps light brown, with long, brown hairs. Thorax brown with yellow and brown hairs. Fore and midlegs with coxae and trochanter with light brown hairs, remaining segments with dark brown setae and ring of yellow hairs basally. Hind legs with yellow hairs and interspersed brown spines, increasing in thickness towards the tarsal segments. Tibial spur formula 0, 2, 2.

Genitalia. Segment IX annular, short, with anterior margin sinuous, posterior margin slightly produced mesally (Figure 5A). Preanal appendages as long as tergum X, slender, digitate, setose (Figure 5A, B). Tergum X notched apicomesally, basal portion membranous, with two pairs of sclerotized apical processes; apicomesal processes digitate, slightly directed laterad in dorsal view (Figure 5B), apex rugose; apicolateral processes slightly shorter than apicomesal processes, thumb-like, directed laterad in dorsal and caudoventral views (Figure 5B, D), apex rugose. Inferior appendages with basal portion of first segment broad, setose, mesal margin rounded, apical portion digitate, almost straight in ventral view (Figure 5C), covered with stout, spine-like setae on its mesal surface; second article short, triangular, directed ventrad (Figure 5A, C). Phallic apparatus simple, without any processes; phallobase tubular; phallotremal sclerite complex, consisting of pair of elongated sclerites ventrally, hooked sclerite subapically, and U-shaped sclerite apically (subrectangular in lateral view); endothecal membranes trilobed (Figure 5E).

Larva. Largest instars, assumed to be the 5th, up to 13.8 mm in length (n = 89).

Head (Figure 6A) ovate, brown; eyes large; antennae very short; coronal suture very short, broad; ventral apotome a single sclerite, elongate rectangular, unpigmented; head with long, prominent primary setae in postgenal region and along anterior edge of frontoclypeal apotome; parietal region and frontoclypeus covered with short, closely appressed, clear setae; labrum quadrate, prominent, with row of many short to long primary setae along anterior third and many very short secondary setae along membranous apical edge; mandibles broadly triangular, without separate teeth, with smooth mesal scraping edge, patch of curved setae in mesal concavity (Figure 6A, B). Thorax (Figure 6A): pronotum slightly longer than wide, brown, except for unpigmented posterior edge; covered with two sclerites, with many long setae dorsally and laterally on anterior half, anterior edge with row of uniformly spaced short, spine-like setae. Mesonotal sclerites almost completely covering mesonotum, brown, with pair of small elongate-oval darkly pigmented anteromesal marks; with many long setae dorsally and laterally on anterior half, mesal setae forming W-shaped row. Metanotal *sa*1 (*setal area* 1) and *sa*2 sclerites completely fused, forming large single median plate with posterolateral corners extended and directed medially, with brown pigmentation mesally and small patches

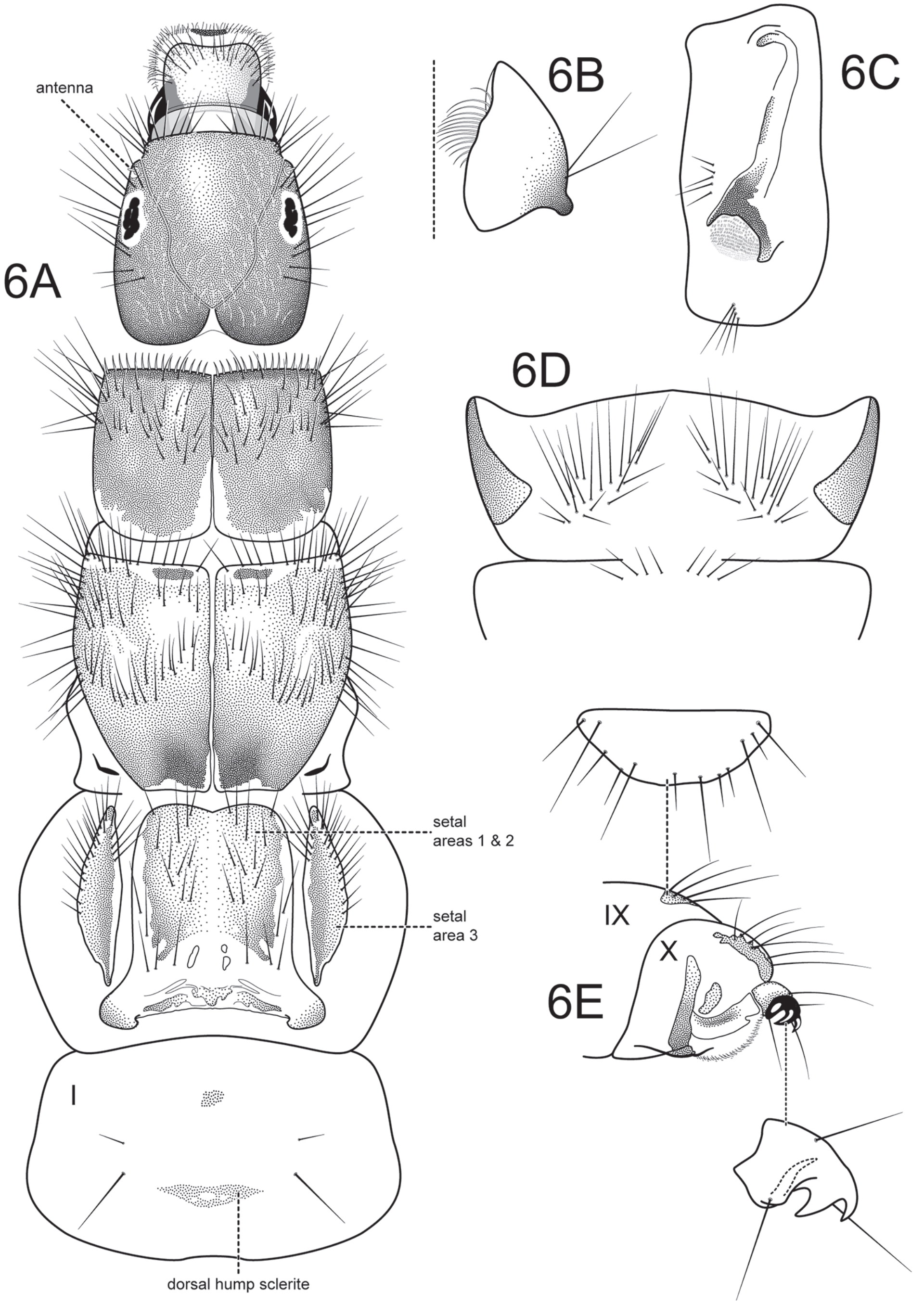

Figure 6. *Atanatolica decouxi* sp. n., larva (tentative association). **A** Head, thorax, and abdominal; segment I, dorsal **B** Right mandible (enlarged), dorsal **C** Abdominal segment I, left lateral **D** Metasternum and abdominal segment I (partial), ventral **E** Abdominal segments IX and X, left lateral; upper inset: segment IX dorsal sclerite (enlarged), lower inset: anal claw (enlarged).

of pigmentation along posterior edge; covered with long setae; *sa*3 sclerites long, oval, brown, except for narrow unpigmented mesal edge, with long marginal setae. Meso- and metapleural sclerites large, brown; metasternum (Figure 6D) with pair of ventrolateral patches of ca. 20 long setae. Foretrochantin horn-shaped (Figure 7A). Legs elongate, cylindrical, robust, brown, setose; foreleg the shortest, hind leg the longest; short, spine-like setae present on anterior (mesal) surface of tibia and tarsus of foreleg (Figure 7A and inset) and tarsi of midleg and hind leg, hind tibia with incomplete suture at basal third (Figure 7B, C, and insets); tarsal claws short, thick. Abdomen: long and slender, abdominal gills not apparent; segment I with small, elongate-oval dorsal sclerite and dorsolateral setae, one long, one short (Figure 6A); lateral hump sclerite (Figure 6C) of segment I prominent, elongate, ventral portion heavily sclerotized and encompassing membranous, raised area covered with minute setae, dorsal portion very lightly sclerotized and extending almost to dorsum of segment; with anteromesal and ventrolateral rows of ca. 4–5 setae; abdominal fringe sinuous, very narrow, composed of minute spicules; with small lateral tubercles on segment VIII (identical as those illustrated by Henriques-Oliveira and Santos 2012: fig 2H); dorsal sclerite of segment IX semicircular in dorsal view (Figure 6E upper inset), with ca. 12 alternating short and long setae along posterior edge; anal prolegs (Figure 6E) each with narrow ventral plate in addition to small lateral sclerite and ventral sole plate, dorsolaterally with darkly pigmented secondary lateral sclerite; band of uniform small spines adjacent to anal opening; anal claw with robust primary hook and single dorsal accessory hook (Figure 6E lower inset).

Larval case. Elongate, narrow, gently curved and tapering, up to 20 mm long (Figure 7D); composed of small sand grains; posterior opening restricted to small opening by silken ring (Figure 7D inset); prior to pupation case fixed to substrate by short silken peduncle (Figure 7E), and anterior opening closed by silken cap with single opening (Figure 7F).

Remarks. Larvae described here are tentatively assigned to *A. decouxi* sp. n. Unfortunately, no adult male metamorphotype pupae were collected to confirm the association. Larvae and adults were collected at the same site, but on different dates, and adults of only the single species were collected. In our previous collections of species in the genus and from museum material, it appears that species of *Atanotolica* do not co-occur at a site, lending support to this tentative association. The probable larva of *A. decouxi* is very similar to those described previously by Holzenthal (1988) and Henriques-Oliveira and Santos (2014). The larva of *A. decouxi* sp. n. described here is very similar to *A. nordestina* Henriques-Oliveira & Santos, 2014 in overall color and structure, but the morphology of the small spine-like setae on the anterior surfaces of the tibiae and tarsi may be distinctive; at least they are different from several species illustrated by Holzenthal (1988: figs 34–41) and most similar to those of *A. cotopaxi*. The lateral hump sclerite is also very similar to that described for *A. cotopaxi* by Holzenthal (1988: fig. 50) and *A. nordestina* (Henriques-Oliveira and Santos 2014: fig 2G). The case of *A. cotopaxi* is made of transparent silk with a few rock inclusions (Holzenthal 1988: fig 71), while those of *A. decouxi* sp. n. and *A. nordestina* are made entirely of rocks.

Holotype male. ECUADOR: **Imbabura**: Reserva Los Cedros, Río de la Plata, 0.32495°N, 78.7808°W, 1587 m, 15.iii.2012, B Ríos-Touma, G Bragado, T Policha (UMSP) [UMSP000158717].

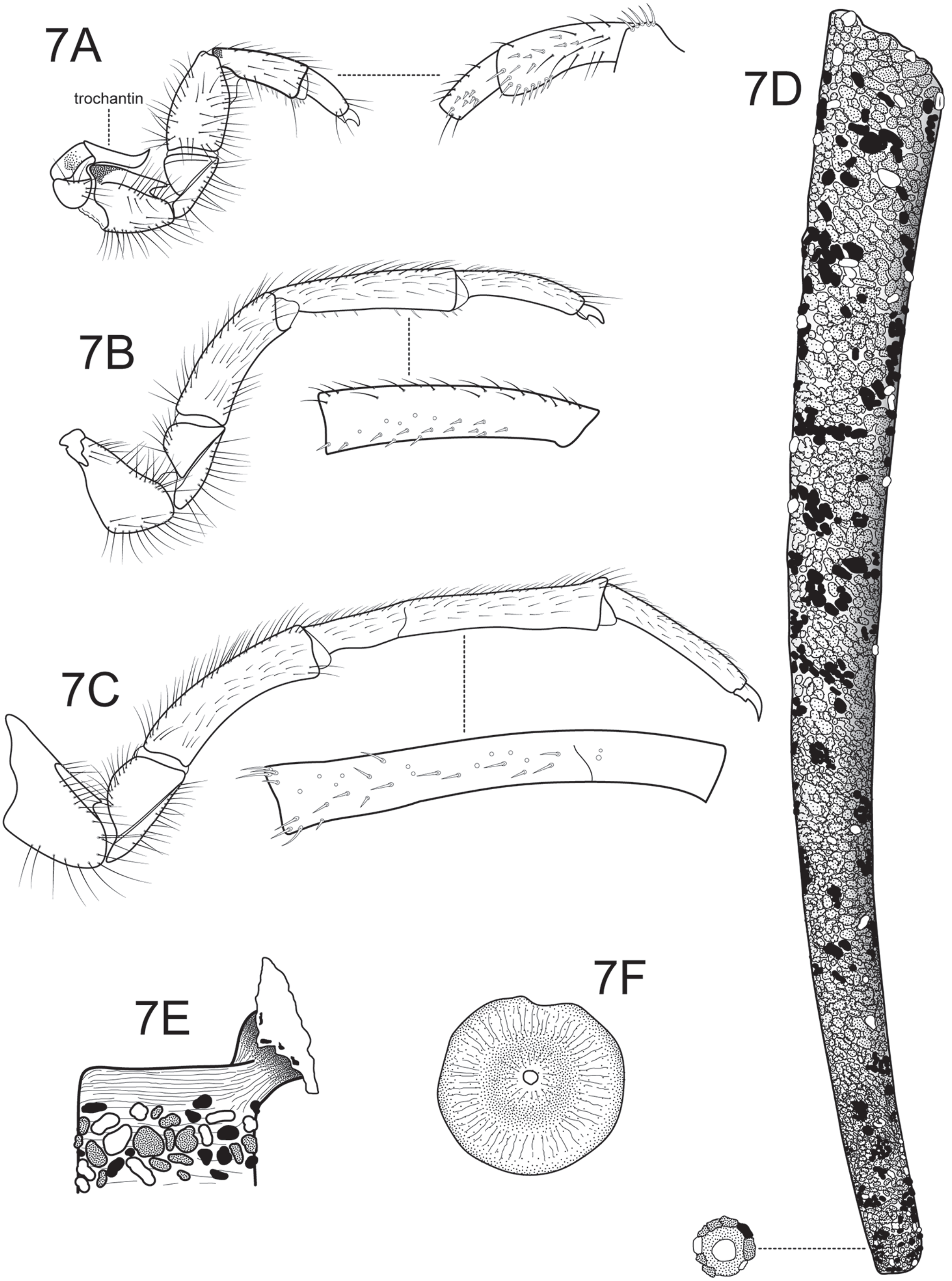

Figure 7. *Atanatolica decouxi* sp. n., larva (tentative association). **A** Right foreleg (inset: fore tibia and tarsus, anterior surface) **B** Right midleg (inset: tibia, anterior surface) **C** Right hind leg (inset: tibia, anterior surface) **D** Larval case, lateral (inset: posterior opening) **E** Pupal peduncle **F** Pupal anterior silken cap.

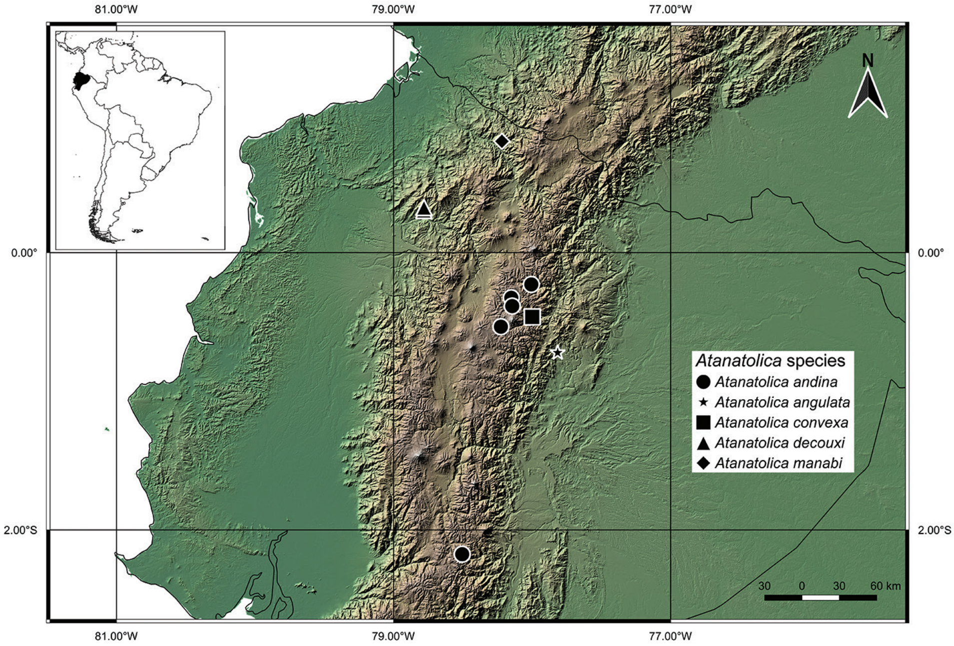

Figure 8. Distribution map of the new *Atanatolica* species described from Ecuador.

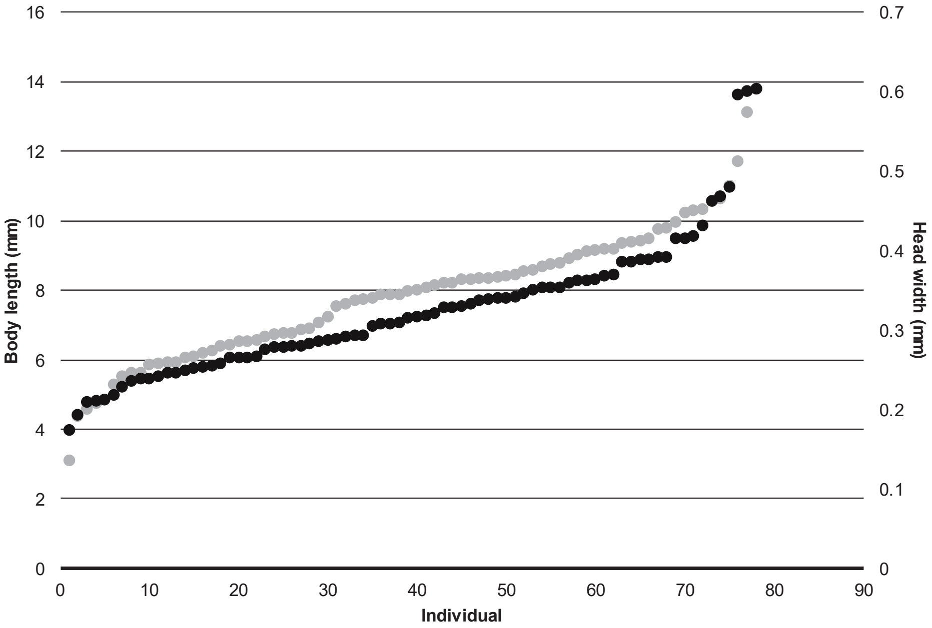

Figure 9. Body length (mm) (gray) and head width (mm) (black) of *A. decouxi* sp. n. larvae (n = 89) from Río de la Plata, Reserva Los Cedros, Imbabura Province, Ecuador.

Paratypes. ECUADOR: **Imbabura**: Reserva Los Cedros, Río de la Plata, 0.32495°N, 78.7808°W, 1587 m, 1♂, 1♀, 15.iii.2012, B Ríos-Touma, G Bragado, T Policha (UMSP), Reserva Los Cedros, tributary to Río Los Cedros, 0.30374°N, 78.782°W, 1312 m, 1♂, 2♀, 18-19.x.2011, R Holzenthal, B Ríos-Touma, A Encalada (MECN).

Additional material examined. ECUADOR: **Imbabura**: Reserva Los Cedros, Río de la Plata, 0.32495°N, 78.7808°W, 1587 m, 84 larvae, 18.x.2011, R Holzenthal, B Ríos-Touma, A Encalada (MECN), 5 larvae (UMSP).

Etymology. We dedicate this species to José DeCoux, an exceptional person who has been protecting Bosque Protector Los Cedros for more than three decades.

Distribution. Imbabura Province (Ecuador) (Figure 8).

Natural history. Larvae were found in high densities in the Río de la Plata on rocks adjacent to a large pool and in the riffle below the pool, forming groups of individuals (Figure 1B). All larvae were submerged. Larvae were observed feeding by scrapping periphytic algae growing on rocks. We were not able to differentiate separate stages of larvae collected, but the size distribution suggests continuous growth in this tropical region (Figure 9).

New distribution record

Atanatolica manabi Holzenthal, 1988:83 [Type locality: Ecuador, Manabi, Santo Domingo de los Colorados (79 km W); NMNH; ♂].

ECUADOR: Carchi: Río Hualchancito near Hacienda Primavera, 0.80279°N, 78.21816°W, 1200 m, 1♂, 1♀, 11.ix.2017, B Ríos-Touma (UMSP) (Figure 8).

The species was previously recorded from three males and several series of larvae collected from "Santo Domingo de los Colorados" and vicinity by workers from the Smithsonian Institution in the mid-1970s. The specimens from Carchi represent the only additonal records of the species since those collections. The male genitalia are identical to those illustrated for the holotype by Holzenthal (1988: fig. 21). In the Carchi specimens, the wings of the strikingly colored adults are in perfect condition. The forewings are brown with a large patch of golden hairs on the apical half extending as a band along the posterior (anal) margin to near its base (dorsal on specimen when wings folded at rest). The apical edge of the forewing bears a fringe of bright, white hairs. The legs and antennae are banded with white and brown hairs.

Discussion

The four species described here belong to the *Atanatolica dominicana* species group established by Holzenthal (1988) based on wing venation characters (fork I in the forewing distinctly petiolate). All but one of the species described here are known from only one locality, which suggests that members of the genus are diverse in the Andes. The only exception is *A. andina* sp. n., which is more widespread and occurs at the highest elevations recorded for the genus (3980 m). It likely occurs at other, high elevation sites along the Andes. This species, and the others described here, represent the first members of the genus described from Ecuador since Holzenthal's (1988) study, indicating the lack of collecting and taxonomic research in a region undergoing environmental changes due to climate change, agriculture, and mining.

Acknowledgements

This research was supported by Universidad de Las Americas project AMB.BRT.17.005 "Diversidad y Distribución de Trichoptera de Ecuador" in collaboration with INABIO (Instituto Nacional de Biodiversidad, ECUADOR) and University of Minnesota Agricultural Experiment Station projects MIN17-017 and 17-094. We are grateful to José DeCoux (Los Cedros) for the facilities during our field trips. Andrea C. Encalada, Raúl Acosta, Gisella Bragado, Tobias Policha, Lina Pita, Jolanda Huisman, and Xavier Amigo (*Nature Experience*) kindly provided field assistance. We are grateful to Rafael Souza for his very useful suggestions to improve the manuscript and to Ana Previšić for her editorial assistance. ERG was funded by a FONDECYT-CONCYTEC doctoral fellowship (contract number 277-2015- FONDECYT). This support is gratefully acknowledged.

References

Blahnik RJ, Holzenthal RW (2004) Collection and curation of Trichoptera, with an emphasis on pinned material. Nectopsyche, Neotropical Trichoptera Newsletter 1: 8–20. http://hdl.handle.net/11299/190744

Blahnik RJ, Holzenthal RW, Prather AL (2007) The lactic acid method for clearing Trichoptera genitalia. In: Bueno-Soria J, Barba-Álvarez R, Armitage BJ (Eds) Proceedings of the 12th International Symposium on Trichoptera. The Caddis Press, Columbus, Ohio, 9–14.

Brauer F (1865) Zweiter bericht uber die auf der Weltfahrt der kais. Fregatte Novara gesammelten Neuroptera. Verhandlungen der Kaiserlich-Königlichen Zoologischen-Botanischen Gesellschaft in Wien 15: 415–422.

Brown BV (2013) Automating the "Material examined" section of taxonomic papers to speed up species descriptions. Zootaxa 3683: 297–299 [web version; accessed on 08/05/2018]. https://doi.org/10.11646/zootaxa.3683.3.8

Costa AM, Calor AR (2014) A new species of *Atanatolica* Mosely 1936 (Trichoptera: Leptoceridae) from Serra Bonita, Bahia, Brazil. Zootaxa 3790: 194–200. https://doi.org/10.11646/zootaxa.3790.1.10

Dodson CH, Gentry AH (1991) Biological extinction in Western Ecuador. Annals of the Missouri Botanical Garden 78: 273–295. https://doi.org/10.2307/2399563

Flint OS Jr (1968) Bredin-Archbold-Smithsonian Biological Survey of Dominica, 9. The Trichoptera (Caddisflies) of the Lesser Antilles. Proceedings of the United States National Museum 125: 1–86. https://doi.org/10.5479/si.00963801.125-3665.1

Henriques-Oliveira AL, Santos APM (2014) Two new species of *Atanatolica* Mosely 1936 (Trichoptera: Leptoceridae) from Peru and Northeastern Brazil. Zootaxa 3869: 537–547. https://doi.org/10.11646/zootaxa.3869.5.3

Holzenthal RW (1988) Studies in Neotropical Leptoceridae (Trichoptera), VIII: the genera *Atanatolica* Mosely and *Grumichella* Müller (Triplectidinae: Grumichellini). Transactions of the American Entomological Society 114: 71–128.

Holzenthal RW, Calor AR (2017) Catalog of the Neotropical Trichoptera (Caddisflies). ZooKeys 654: 1–566. https://doi.org/10.3897/zookeys.654.9516

Jarvis A, Reuter HI, Nelson A, Guevara E (2008) Hole-filled seamless SRTM data V4, International Centre for Tropical Agriculture (CIAT). http://srtm.csi.cgiar.org

Mosely ME (1936) A revision of the Triplectidinae, a subfamily of the Leptoceridae (Trichoptera). Transactions of the Royal Entomological Society of London 85: 91–130. https://doi.org/10.1111/j.1365-2311.1936.tb00241.x

Myers N, Mittermeier RA, Mittermeier CG, de Fonseca GAB, Kent J (2000) Biodiversity hotspots for conservation priorities. Nature 403: 853–858. https://doi.org/10.1038/35002501

Natural Earth (2018) Free vector and raster map data. http://naturalearthdata.com

Oláh J (2016) New species and records of Trichoptera collected by Mr. A. G. Duff. More phenomics and less genomics! Opuscula Zoologica (Budapest) 47: 155–171.

QGIS Development Team (2018) QGIS Geographic Information System. Open Source Geospatial Foundation Project. https://qgis.osgeo.org

Resh VH (1976) Life histories of coexisting species of *Ceraclea* caddisflies (Trichoptera: Leptoceridae): the operation of independent functional units in a stream ecosystem. Canadian Entomologist 108: 1303–1318. https://doi.org/10.4039/Ent1081303-12

ZooKeys 793: 115–133 (2018)
doi: 10.3897/zookeys.793.27661
http://zookeys.pensoft.net

RESEARCH ARTICLE

A peer-reviewed open-access journal
ZooKeys
Launched to accelerate biodiversity research

Six new species and a new record of *Linan* Hlaváč in China, with a key to species (Coleoptera, Staphylinidae, Pselaphinae)

Yu-Qing Zhang[1], Li-Zhen Li[1], Zi-Wei Yin[1]

[1] *Department of Biology, Shanghai Normal University, 100 Guilin Road, Shanghai, 200234, P. R. China*

Corresponding author: *Zi-Wei Yin* (pselaphinae@gmail.com)

Academic editor: *J. Klimaszewski* | Received 26 June 2018 | Accepted 6 September 2018 | Published 29 October 2018

http://zoobank.org/43BE1555-34DC-4D94-A051-C90E12C65F34

Citation: Zhang Y-Q, Li L-Z, Yin Z-W (2018) Six new species and a new record of *Linan* Hlaváč in China, with a key to species (Coleoptera, Staphylinidae, Pselaphinae). ZooKeys 793: 115–133. https://doi.org/10.3897/zookeys.793.27661

Abstract

Six new species of the genus *Linan* Hlaváč are described from central to southern China: *L. arcitibialis* **sp. n.** (Hubei), *L. denticulatus* **sp. n.** (Guizhou), *L. divaricatus* **sp. n.** (Jiangxi), *L. geneolatus* **sp. n.** (Guizhou), *L. mangshanus* **sp. n.** (Hunan), and *L. mulunensis* **sp. n.** (Guangxi), with illustrations of habitus and major diagnostic characters. *Linan megalobus* Yin & Li, originally described from Guizhou, is newly recorded in Hubei. An updated key to and a distributional map of all 16 known species are provided.

Keywords

China, distribution, identification key, *Linan*, new record, new species, Tyrini

Introduction

The pselaphine genus *Linan* Hlaváč belongs to the tribe Tyrini that is comprised of ten species predominantly distributed in China (with one species extending southwards to northern Thailand; Figure 11) (Hlaváč 2003; Yin et al. 2011, 2013; Yin and Li 2012, 2013). Members are characterized by the head lacking or with indistinct vertexal and frontal foveae, laterally expanded or protuberant maxillary palpomeres II–IV, roughly punctate head and pronotum, lack of a transverse antebasal sulcus on the pronotum, and presence of a median metaventral fovea. Based on presence or absence of modification on male antennomeres IX–X, two species groups were defined (Yin and Li 2013). The current diversity of *Linan* remains underexplored. Here we report the discovery of six new species based on the material from various areas in China collected after 2012. The species number of *Linan* now rises to 16, we accordingly provide an updated identification key and distributional maps for the genus.

Material and methods

All material treated in this study is housed in the Insect Collection of Shanghai Normal University, Shanghai, China (**SNUC**).

The label data of the material are quoted verbatim, additional information is included in parentheses. Dissected parts were preserved in Euparal on plastic slides that were placed on the same pin with the specimen. The habitus image was taken using a Canon 5D Mark III camera in conjunction with a Canon MP-E 65mm f/2.8 1–5× Macro Lens, and a Canon MT-24EX Macro Twin Lite Flash was used as light source. Images of the morphological details were produced using a Canon G9 camera mounted to an Olympus CX31 microscope under transmitted light. Zerene Stacker (version 1.04) was used for image stacking. The base map was produced from http://www.simplemappr.net/ (Shorthouse 2010). All images were optimized and grouped into plates in Adobe Photoshop CS5 Extended.

The following acronyms are used in the text: BL–length of the body (= HL + PL + EL + AL); HL–length of the head from the anterior clypeal margin to the occipital constriction; HW–width of the head across eyes; PL–length of the pronotum along the midline; PW–maximum width of the pronotum; EL–length of the elytra along the suture; EW–maximum width of the elytra; AL–length of the dorsally visible part of abdomen along the midline; AW–maximum width of the abdomen. Paired structures are treated as singular, except for eyes, metaventral processes, and parameres which are treated as plural.

Taxonomy

Linan arcitibialis sp. n.

http://zoobank.org/2C08CE31-68A0-4BEE-BAF3-BD9B3A1B6009
Figs 1A, 2, 11A

Type material. (36 ♂♂, 40 ♀♀). **Holotype: CHINA:** ♂: 'China: Hubei, Enshi Tujia and Miao Autonomous Prefecture, Xingdoushan N. R. (星斗山自然保护区), San-xian-chang (三县场), 30°2'20.48"N, 109°8'33.89"E, 1114 m, 20.v.2017, sift, Zhou GC, Tian T, & Huang ZG leg.' (SNUC). **Paratype: CHINA:** 4 ♂♂, 8 ♀♀, same label data as holotype; 15 ♂♂, 16 ♀♀, same label data, except '19.v.2017'; 11 ♂♂, 15 ♀♀, same label data, except '30°2'46.03"N, 109°7'49.39"E, 1205 m, 18.v.2017'; 1 ♂, same

Figure 1. Dorsal habitus of *Linan* species. **A** *L. arcitibialis* sp. n. **B** *L. denticulatus* sp. n. Scale bars: 1 mm.

label data, except ‘30°2'29.98"N, 109°8'1.60"E, 1253 m, 18.v.2017’; 1 ♂, ‘China: Hubei, Enshi Tujia and Miao Autonomous Prefecture, Changtanhe (长潭河), Lianghekou Village (两河口村), 30°0'6.00"N, 109°44'27.36"E, 1234 m, 14.v.2017, sift, Zhou GC, Tian T, & Huang ZG leg.’; 1 ♂, ‘China: Hubei, Enshi Tujia and Miao Autonomous Prefecture, Xianfeng Hsien (咸丰县), Huangjindong Country (黄金洞乡), Maliuxi Village (麻柳溪村), 29°57'34.15"N, 109°1'15.82"E, 752 m, 24.viii.2017, sift, Zhou GC & Irfan M leg.’; 2 ♂♂, 1 ♀, ‘China: Chongqing City, Pengshui Hsien(彭水县), Moweishan Scenic Spot (摩围山风景区), 29°11'11.15"N, 108°2'59.32"E, 1234 m, 1568 m, 25.vii.2017, sift, Zhou GC & Irfan M leg.’ (all in SNUC).

Diagnosis of male. Length 2.71–2.77 mm; antennomere IX expanded laterally, with small process near apex; long metaventral processes narrowing toward apex; protibia with distinct apical spine; mesotibia strongly arched; metatrochanter with short, blunt ventral projection.

Description. Male (Figure 1A). Length 2.71–2.77 mm. Head slightly longer than wide, HL 0.62–0.63 mm, HW 0.55–0.56 mm; eyes small, each composed of about 24 facets. Antennal scape elongate, about 3.3 times as long as wide, antennomeres II–VIII similar, each about as long as wide, antennomere IX (2A) much longer than wide, an-

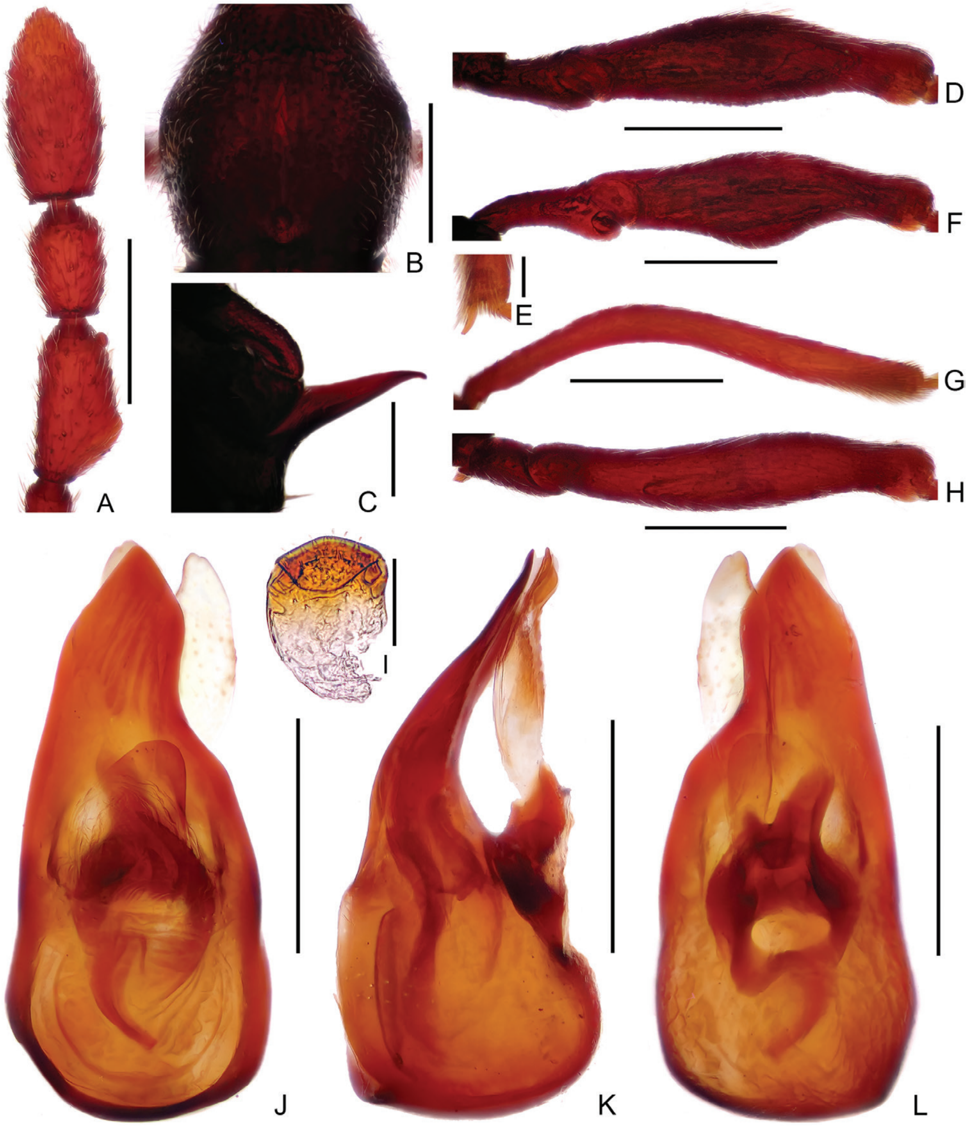

Figure 2. Diagnostic features of male *Linan arcitibialis* sp. n. **A** Antennal club **B** Pronotum **C** Metaventral process, in lateral view **D** Protrochanter and profemur **E** Apex of protibia **F** Mesotrochanter and mesofemur **G** Mesotibia **H** Metatrochanter and metafemur **I** Sternite IX **J–L** Aedeagus, in dorsal view (**J**), lateral (**K**), and ventral (**L**) view. Scale bars: 0.3 mm (**A, B, D, F, G, H**); 0.2 mm (**C, J, K, L**); 0.05 mm (**E**); 0.1 mm (**I**).

gularly expanded laterally at basal third, with small rounded process near apex, antennomeres X–XI simple. Pronotum (Figure 2B) about as long as wide, PL 0.57–0.58 mm, PW 0.55–0.57 mm. Elytra much wider than long, EL 0.60–0.63 mm, EW 0.93–0.95 mm. Metaventral processes (Figure 2C) long, narrowing apically. Protrochanter and profemur simple (Figure 2D), protibia with small but distinct spine (Figure 2E) at apex; mesotrochanter simple, mesofemur expanded ventrally at middle (Figure 2F), mesotibia (Figure 2G) strongly arched at basal 2/5; metatrochanter (Figure 2H) with short, blunt ventral projection. Abdomen slightly wider than elytra, AL 0.92–0.93 mm, AW 0.95–0.98 mm; tergite IV about twice as long as tergite V; sternite IX as in Figure 2I. Length of aedeagus (Figure 2J–L) 0.49 mm; median lobe asymmetric, narrowing apically; elongate parameres moderately broadened dorso-ventrally, narrowed at apex.

Female. Similar to male in general morphology; eyes each composed of about 24 facets; antennae and legs simple; lacking metaventral processes. Measurements: BL 2.47–2.69 mm, HL 0.57–0.60 mm, HW 0.50–0.51 mm, PL 0.53–0.55 mm, PW 0.52–0.55 mm, EL 0.48–0.59 mm, EW 0.92–0.99 mm, AL 0.89–0.95 mm, AW 0.95–0.99 mm.

Distribution. China: Hubei (Figure 11A).

Etymology. The new specific epithet refers to the strongly arched mesotibiae.

Comparative notes. The new species is placed as a member of the *L. cardialis*-group based on the modified male antennomere IX. *Linan arcitibialis* is the only member of the group that exhibits a simple antennomere X. Combined with the unique form of antennomere IX and strongly arched mesotibia, males of this species can be readily separated from all other congeners at a quick glance.

Linan denticulatus **sp. n.**

http://zoobank.org/CC051B42-2913-471B-8F88-FFE9E6963CD8
Figs. 1B, 3, 11B

Type material. (1 ♂, 1 ♀). **Holotype: CHINA:** ♂: 'China: N. Guizhou, Daozhen County (道真县), Dashahe N. R. (大沙河自然保护区), 29°10'12"N, 107°33'36"E, mixed leaf litter, sifted, 1730 m, 07.VII.2015, Jiang, Peng, Tu, & Zhou leg.'(SNUC). **Paratype: CHINA:** 1 ♀, same label data as the holotype, (SNUC).

Diagnosis of male. Length 2.61mm; antennomeres IX–XI enlarged, lacking obvious modification; short metaventral processes narrowing toward apex, area above metacoxae projecting; protibia with distinct apical spine; metatrochanter with blunt, apically curved ventral projection.

Description. Male (Figure 1B). Length 2.61mm. Head longer than wide, HL 0.57 mm, HW 0.51 mm; eyes each composed of about 18 facets. Antenna with scape about 2.8 times as long as wide, antennomeres II–VIII similar, each about as long as wide, antennomeres IX–XI enlarged, simple (Figure 3A). Pronotum (Figure 3B) about as long as wide, PL 0.53 mm, PW 0.52 mm. Elytra much wider than long, EL 0.64 mm, EW 0.90 mm. Metaventral processes (Figure 3C) short, pointed apically. Protrochanter and profemur (Figure 3D) simple, protibia with large, triangular spine at apex (Figure 3E); mesotrochanter and mesofemur simple (Figure 3F); metatrochanter (Figure 3G) with blunt, apically curved ventral projection. Abdomen slightly wider than elytra, AL 0.93 mm, AW 1.00 mm; tergite IV about twice as long as tergite V; sternite IX as in Figure 3H. Length of aedeagus (Figure 3I–J) 0.48 mm; median lobe asymmetric, narrowing apically; elongate parameres expanded dorso-ventrally, slightly curved ventrally at basal 2/5 in lateral view.

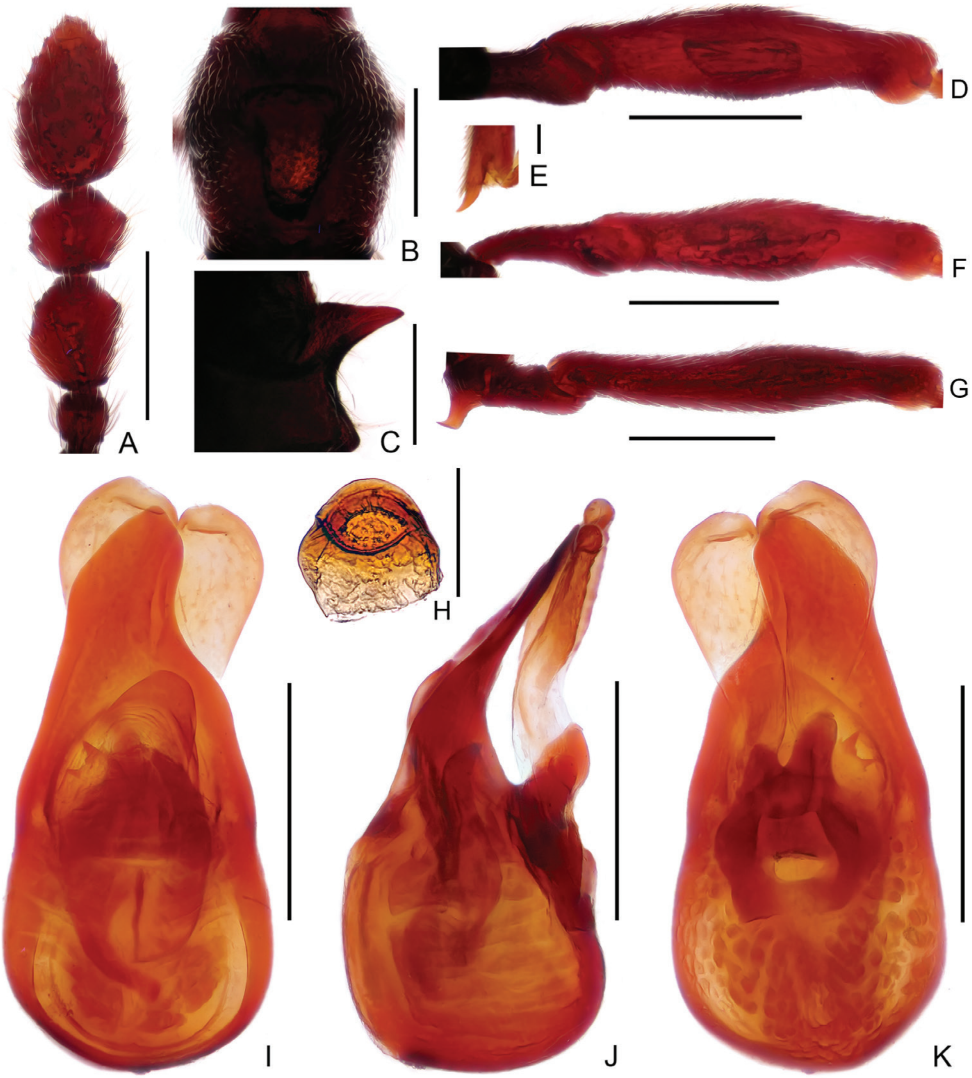

Figure 3. Diagnostic features of male *Linan denticulatus* sp. n. **A** Antennal club **B** Pronotum **C** Metaventral process, lateral view **D** Protrochanter and profemur **E** Apex of protibia **F** Mesotrochanter and mesofemur **G** Metatrochanter and metafemur **H** Sternite IX **I–K** Aedeagus, in dorsal view (**I**), lateral (**J**), and ventral (**K**) view. Scale bars: 0.3 mm (**A, B, D, F, G**); 0.2 mm (**C, I, J, K**); 0.05 mm (**E**); 0.1 mm (**H**).

Female. Similar to male in general morphology; eyes each composed of about 18 facets; antennae and legs simple; lacking metaventral processes. Measurements: HL 0.57 mm, HW 0.51 mm, PL 0.52 mm, PW 0.51 mm, EL 0.58 mm, EW 0.94 mm, AL 0.93 mm, AW 1.00 mm.

Distribution. China: Guizhou (Figure 11B).

Etymology. The specific epithet refers to the large apical spine of the protibia.

Comparative notes. *Linan denticulatus* is placed as a member of the *L. chinensis*-group based on the unmodified male antennomeres IX–X, and externally resembles

L. hujiayaoi Yin & Li from Guangxi. These two species share a similar form of the antennal club, short metaventral processes, and the blunt, apically curved ventral projection of the metatrochanter. They can be best separated by the much more distinct apical projection of the protibia, and median lobe of the aedeagus with a strongly narrowed apical part and much broader parameres in the new species.

Linan divaricatus **sp. n.**
http://zoobank.org/8D5A2E97-1E58-4A47-AFEC-268427873AC
Figs. 4A, 5, 11A

Type material. (7 ♂♂). **Holotype: CHINA:** ♂: 'China: W. Jiangxi Province, Luxi County (芦溪县), Wugong Shan (武功山), 27°27'53"N, 114°10'47"E, mixed forest, leaf litter, wood sifted & beating, ca. 1570 m, 27.x.2013, Peng, Shen & Yan leg.'(SNUC). **Paratype: CHINA:** 3 ♂♂, same label data as holotype; 1 ♂, Jiangxi, Pingxiang City, Wugong Shan National Park, 27°27'55"N, 114°09'58"E, cableway station to Baoshui Waterfall, broad leaf, sifted, 1000–1350 m, 20.vii.2013, Song, Yin, Yu leg.'; 2 ♂♂, 'China: W. Jiangxi Province, Luxi County, Yangshimu(羊狮幕), 27°33'38"N, 114°14'35"E, mixed forest, leaf litter, wood sifted & beating, ca. 1580m, 25.x.2013, Peng, Shen & Yan leg.' (all in SNUC).

Diagnosis of male. Length 2.74–2.82 mm; antennomeres IX–X strongly modified, antennomere IX angulate at anterolateral corner, obliquely connecting with strongly transverse antennomere X; broad metaventral processes bifurcate at apex; protibia with small apical spine; mesotrochanter with tiny ventral spine.

Description. Male (Figure 4A). Length 2.74–2.82 mm. Head longer than wide, HL 0.60–0.64 mm, HW 0.55–0.56 mm; eyes each composed of about 30 facets. Antenna with scape about 4.2 times as long as wide, antennomeres II–III and VIII similar, each about as long as wide, IV–VII each longer than wide, antennomere IX (Figure 5A) strongly expanded, angulate at anterolateral corner, antennomere X strongly transverse, obliquely connecting with IX. Pronotum (Figure 5B) slightly longer than wide, PL 0.56–0.57 mm, PW 0.49–0.51 mm. Elytra much wider than long, EL 0.62–0.64 mm, EW 0.87–0.90 mm. Metaventral processes (Figure 5C) broad, bifurcate at apex in lateral view. Protrochanter and profemur simple (Figure 5D), protibia with indistinct spine (Figure 5E) at apex; mesotrochanter (Figure 5F) with tiny ventral spine, mesofemur simple; metatrochanter and metafemur simple (Figure 5G). Abdomen slightly wider than elytra, AL 0.96–0.97mm, AW 0.89–0.93 mm; tergite IV about twice as long as tergite V; sternite IX as in Figure 5H. Length of aedeagus (Figure 5I–K) 0.45 mm; median lobe symmetric, pointed apically at middle; parameres strongly curved ventrally and constricted at apices in lateral view.

Female. Unknown.

Distribution. China: Jiangxi (Figure 11A).

Etymology. The new specific epithet refers to the long and bifurcate metaventral processes.

Figure 4. Dorsal habitus of *Linan* species **A** *L. divaricatus* sp. n. **B** *L. geneolatus* sp. n. Scale bars: 1 mm.

Comparative notes. The new species belongs to the *L. cardialis*-group based on the strongly modified male antennomere IX. *Linan divaricatus* is most similar to *L. huapingensis* and *L. geneolatus* sp. n. (described below) in sharing both the angulate anterolateral corner of male antennomere IX, and median lobe of aedeagus strongly constricted at middle of the apex. From both latter species the new species differs by the relatively much broader antennomere IX, much broader metaventral processes bifurcate at the apex, and simple metatrochanter. In *L. geneolatus* sp. n., the male antennomere X is also strongly excavate at basal half.

Linan geneolatus sp. n.

http://zoobank.org/1BC5BDEC-1AAB-4B39-94C6-0F973EE70C5A
Figs. 4B, 6, 11A

Type material. (1 ♂). **Holotype: CHINA:** ♂: ‘China: N. Guizhou, Daozhen County, Dashahe N. R., 29°10'12"N, 107°33'36"E, mixed leaf litter, sifted, 1730 m, 07.VII.2015, Jiang, Peng, Tu, & Zhou leg.’ (SNUC).

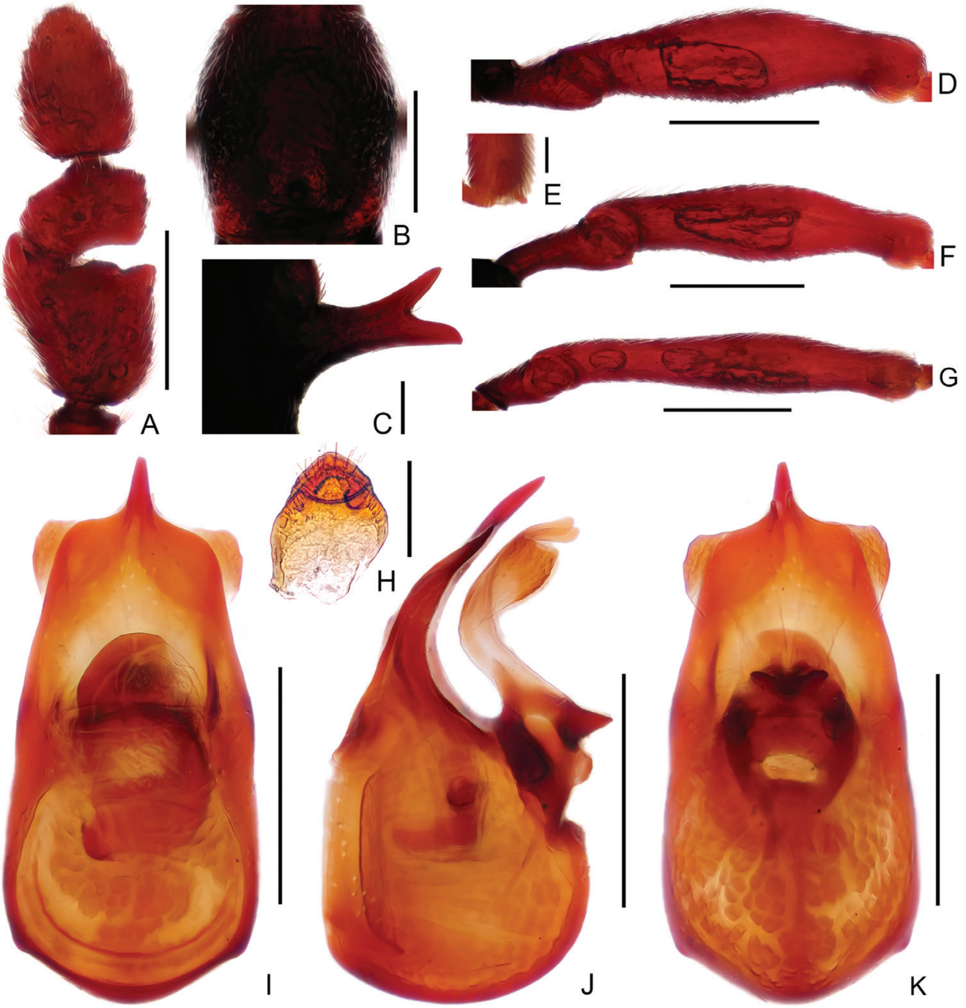

Figure 5. Diagnostic features of male *Linan divaricatus* sp. n. **A** Antennal club **B** Pronotum **C** Metaventral process, lateral view **D** Protrochanter and profemur **E** Apex of protibia **F** Mesotrochanter and mesofemur **G** Metatrochanter and metafemur **H** Sternite IX **I–K** Aedeagus, in dorsal view (**I**), lateral (**J**), and ventral (**K**) view. Scale bars: 0.3 mm (**A, B, D, F, G**); 0.1 mm (**C, H**); 0.05 mm (**E**); 0.2 mm (**I, J, K**).

Diagnosis of male. Length 3.06 mm; postgenae broadly expanded laterally; antennomeres IX–X strongly modified, IX strongly projecting at anterolateral corner, X broadly concave at basal half; metaventral processes short; metatrochanter with short, blunt ventral projection.

Description. Male (Figure 4B). Length 3.06 mm. Head slightly longer than wide, HL 0.69 mm, HW 0.66 mm; postgenae expanded laterally; eyes prominent, each composed of about 22 facets. Antenna with scape about 3.8 times as long as wide, antennomeres II–IV and VIII similar, each about as long as wide, V–VII each slightly longer than wide, antennomere IX (Figure 6A) broad, strongly projecting at anterolateral corner, antennomere X transverse, broadly concave at basal half. Pronotum (Figure 6B)

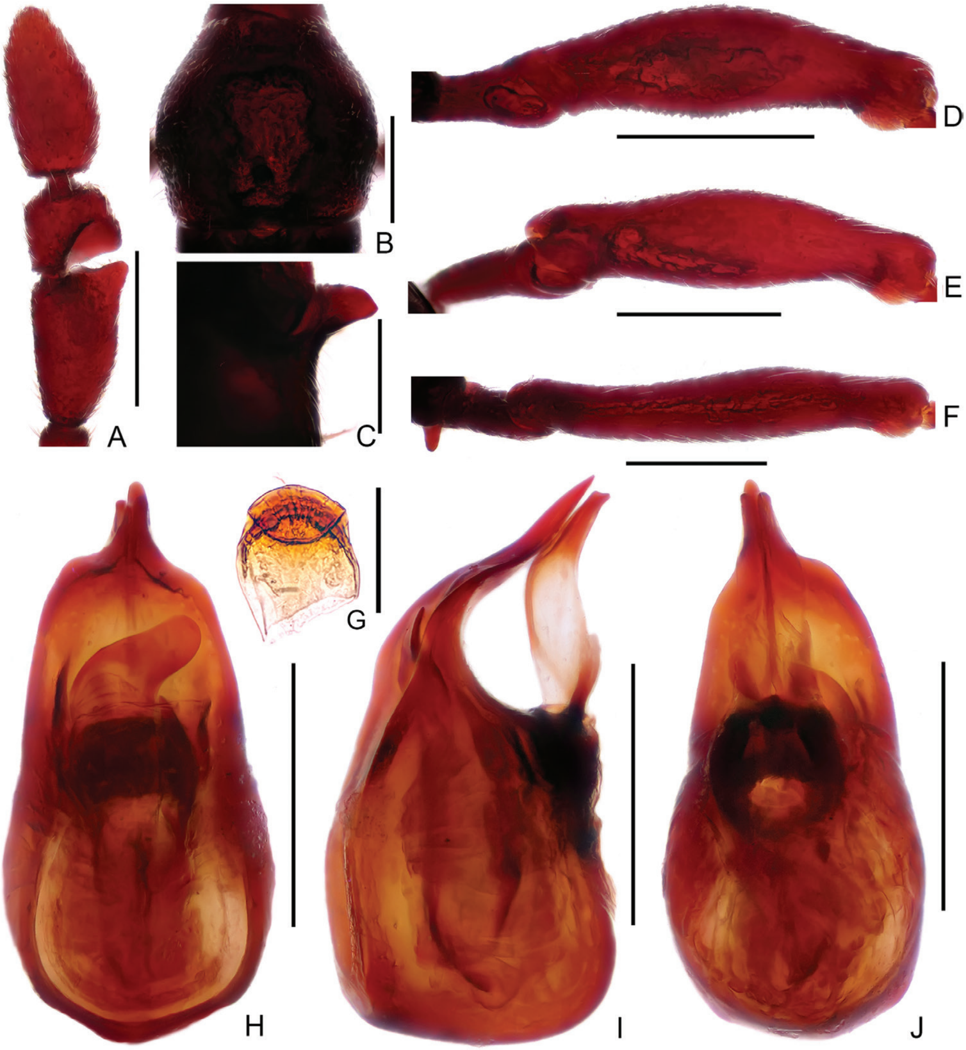

Figure 6. Diagnostic features of male *Linan geneolatus* sp. n. **A** Antennal club **B** Pronotum **C** Metaventral process, lateral view **D** Protrochanter and profemur **E** Mesotrochanter and mesofemur **F** Metatrochanter and metafemur **G** Sternite IX **H–J** Aedeagus, in dorsal view (**H**), lateral (**I**), ventral (**J**) view. Scale bars: 0.3 mm (**A, B, D, E, F**); 0.2 mm (**C, H, I, J**); 0.1 mm (**G**).

about as long as wide, PL 0.60 mm, PW 0.59 mm. Elytra much wider than long, EL 0.69 mm, EW 0.98 mm. Metaventral processes (Figure 6C) short, narrowing at apex in lateral view. Protrochanter and profemur (Figure 6D), and mesotrochanter and mesofemur (Figure 6E) simple; metatrochanter (Figure 6F) with short, blunt ventral projection. Abdomen slightly wider than elytra, AL 0.99 mm, AW 1.06 mm; tergite IV about twice as long as tergite V; sternite IX as in Figure 6G. Length of aedeagus (Figure 6H–J) 0.44 mm; median lobe nearly symmetric, strongly constricted at middle of apex.

Female. Unknown.

Distribution. China: Guizhou (Figure 11A).

Etymology. The new specific epithet refers to the strongly expanded postocular margins.

Comparative notes. The new species is placed as a member of the *L. cardialis*-group based on the strongly modified antennomere IX in the male, and is most similar to *L. huapingensis* in the shape of antennomere IX and spinose metatrochanter in the male. These two species can be separated by antennomere X being strongly excavate at the basal half, and the short metaventral processes in males of the new species, while in *L. huapingensis* the antennomere X lacks an excavation, and the metaventral processes are much longer and thinner. Otherwise, *Linan geneolatus* is the only member of the genus that exhibits broadened postgenae, which makes it readily separable from all other congeners.

Linan mangshanus sp. n.

http://zoobank.org/05B40319-57BA-4391-8A67-17E88B068130

Figs 7A, 8, 11B

Type material. (2 ♂♂). **Holotype: CHINA:** ♂: 'China: Hunan, Chenzhou, Yizhang Hsien (宜章县), Mangshan N. R. (莽山自然保护区), 24°56'26"N, 112°59'18"E, mixed forest, leaf litter, wood sifted & beating, 1400 m, 26.iv.2015, Peng, Tu, Zhou leg.' (SNUC). **Paratype: CHINA:** 1 ♂, same label data as the holotype, (SNUC).

Diagnosis of male. Length 3.25–3.35 mm; antennomere IX–X strongly modified, IX strongly expanded and bent at lateral margin, with distinct process at anteromesal corner; broad metaventral processes expanded at apex in lateral view; metacoxa with roundly triangular ventral projection.

Redescription. Male (Figure 7A). Length 3.25–3.35 mm. Head longer than wide, HL 0.69–0.75 mm, HW 0.60–0.64 mm; eyes prominent, each composed of about 33 facets. Antenna with scape about 3.8 times as long as wide, antennomeres II–III and VIII similar, each about as long as wide, IV slightly longer than wide, V–VII each much longer than wide, antennomere IX (Figure 8A) much longer than wide, strongly expanded and bent at lateral margin, with distinct process at anteromesal corner, antennomere X strongly transverse. Pronotum (Figure 8B) slightly longer than wide, PL 0.65–0.66 mm, PW 0.60–0.63 mm. Elytra much wider than long, EL 0.71–0.73 mm, EW 1.07–1.08 mm. Metaventral processes (Figure 8C) broad, expanded at apex in lateral view. Protrochanter, profemur simple (Figure 8D), mesotrochanter, and mesofemur (Figure 8E) simple; metacoxa (Figure 8F) with short and triangular ventral projection. Abdomen slightly wider than elytra, AL 1.20–1.21mm, AW 1.12–1.13 mm; tergite IV about twice as long as tergite V; sternite IX as in Figure 8G. Length of aedeagus (Figure 8H–J) 0.56 mm; median lobe symmetric; elongate parameres slightly curved ventrally at middle in lateral view.

Female. Unknown.

Distribution. China: Hunan (Figure 11B).

Etymology. The new species is named after the type locality, i.e., Mangshan Nature Reserve.

Comparative notes. The new species is placed as a member of the *L. cardialis*-group based on the modified male antennomere IX, and most similar to *L. hain-*

Figure 7. Dorsal habitus of *Linan* species. **A** *L. mangshanus* sp. n. **B** *L. mulunensis* sp. n. Scale bars: 1 mm.

anicus Hlaváč in shape of male antennomere IX. They can be readily separated by the much broader metaventral processes, lack of a large apical projection of the protibia, complete symmetric aedeagal median lobe, and different structures of the endophallus of the new species. The broad metaventral processes, projecting metacoxae, and high symmetry of the aedeagal median lobe are shared by *L. uenoi* Yin & Nomura from Guangxi. They differ mainly by the modified antennomeres VII–VIII of *L. uenoi*, a quite distinct feature for a member of *Linan*.

Linan mulunensis **sp. n.**

http://zoobank.org/2129E81A-E3FD-479E-82D8-E9313AEF52D3
Figs 7B, 9, 11B

Type material. (2 ♂♂). **Holotype: CHINA:** ♂: 'China: Guangxi, Hechi City, Mulun N. R. (木论自然保护区), 25°12'14"N, 108°5'46"E, mixed leaf litter, sifted, 460 m, 27.VII.2015, Chen, He, & Hu leg.' (SNUC). **Paratype: CHINA:** 1 ♂, same label data as holotype, (SNUC).

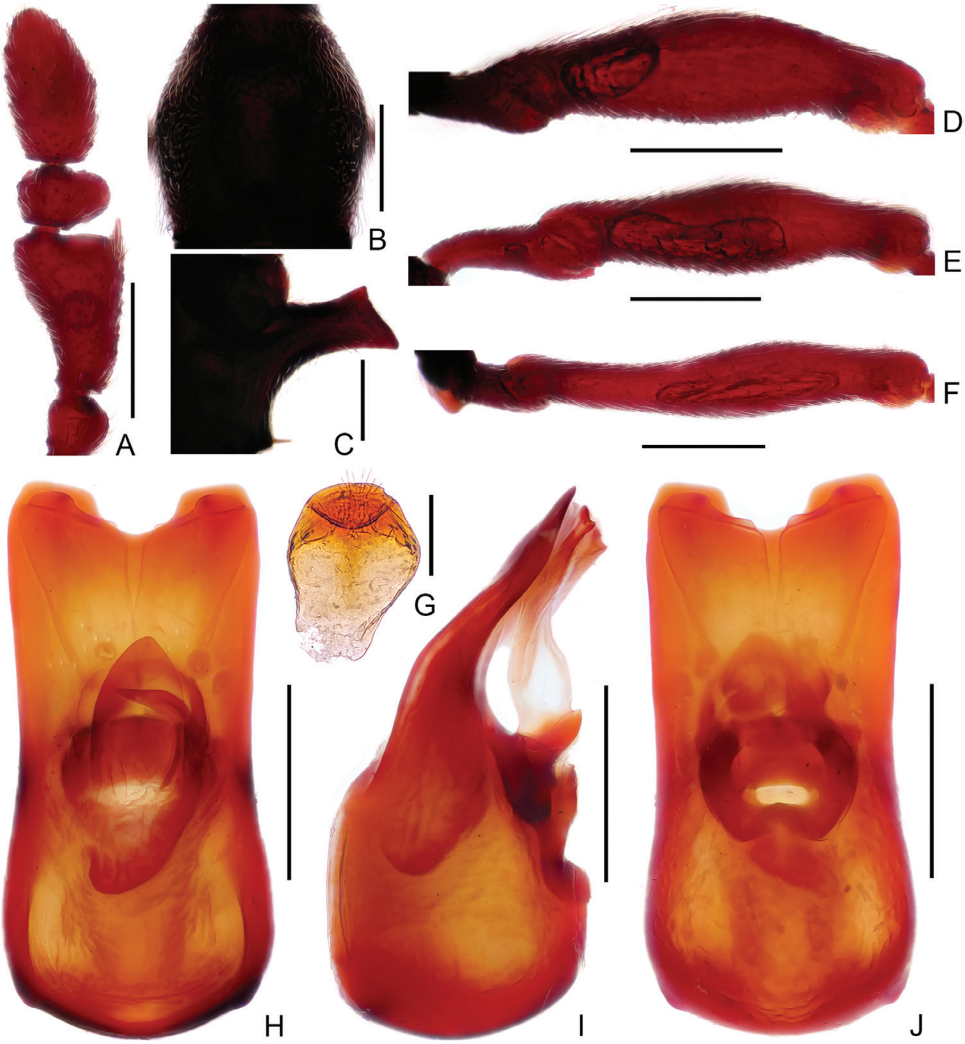

Figure 8. Diagnostic features of male *Linan mangshanus* sp. n. **A** Antennal club **B** Pronotum **C** Metaventral process, lateral view **D** Protrochanter and profemur **E** Mesotrochanter and mesofemur **F** Metatrochanter and metafemur **G** Sternite IX **H–J.** Aedeagus, in dorsal view (**H**), lateral (**I**), ventral (**J**) view. Scale bars: 0.3 mm (**A, B, D, E, F**); 0.2 mm (**C, H, I, J**); 0.1 mm (**G**).

Diagnosis of male. Length 2.75–2.77 mm; antennomeres IX–XI elongate, lacking modification; long metaventral processes narrowed apically; protibia with acute apical spine; metacoxa with large, apically narrowing and blunt ventral projection.

Description. Male (Figure 7B). Length 2.75–2.78 mm. Head slightly longer than wide, HL 0.59–0.60 mm, HW 0.52–0.53 mm; eyes small, each composed of about 18 facets. Antennal scape about 4.0 times as long as wide, antennomeres V–VII slightly longer than II–IV and VIII, antennomeres IX–XI simple (Figure 9A). Pronotum (Figure 9B) about as long as wide, PL 0.55–0.56 mm, PW 0.55–0.56 mm. Elytra much

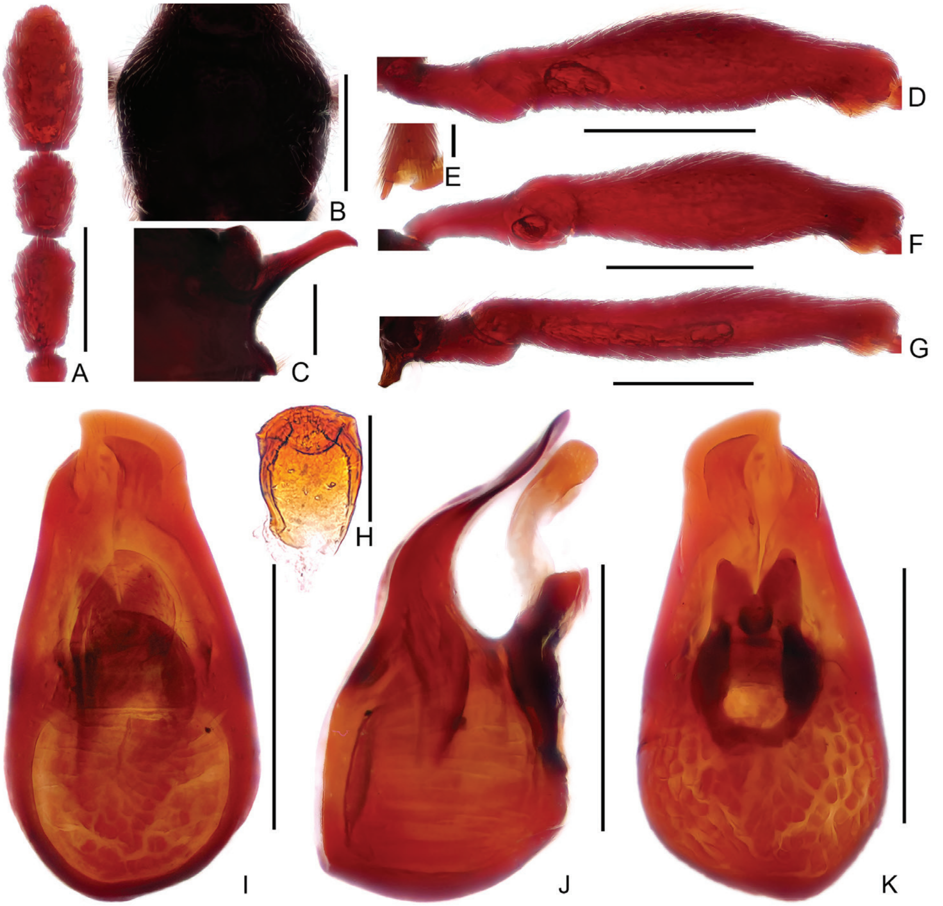

Figure 9. Diagnostic features of male *Linan mulunensis* sp. n. **A** Antennal club **B** Pronotum **C** Metaventral process, lateral view **D** Protrochanter and profemur **E** Apical spur of protibia **F** Mesotrochanter and mesofemur **G** Metatrochanter and metafemur **H** Sternite IX **I–K** Aedeagus, in dorsal view (**I**), lateral (**J**), ventral (**K**) view. Scale bars: 0.3 mm (**A, B, D, F, G**); 0.2 mm (**C, I, J, K**); 0.05 mm (**E**); 0.1 mm (**H**).

wider than long, EL 0.66–0.70 mm, EW 0.93–0.95 mm. Metaventral processes (Figure 9C) long, narrowed apically, with short, distinct protuberance above metacoxae. Protrochanter and profemur simple (Figure 9D); protibia with small but distinct spine (Figure 9E) at apex; mesotrochanter and mesofemur simple (Figure 9F); metacoxa (Figure 9G) with blunt, apically narrowed ventral projection. Abdomen slightly wider than elytra, AL 0.93–0.94 mm, AW 0.97–0.98 mm; tergite IV about twice as long as tergite V; sternite IX as in Figure 9H. Length of aedeagus (Figure 9I–K) 0.37 mm; median lobe asymmetric at apex, narrowing apically; parameres strongly curved in lateral view.

Female. Unknown.

Distribution. China: Guangxi Province (Figure 11B).

Etymology. The new species is named after the type locality, i.e., Mulun Nature Reserve.

Figure 10. Diagnostic features of male *Linan megalobus*. **A** Dorsal habitus **B** Antennal club **C** Pronotum **D** Metaventral process, lateral view **E** Protrochanter and profemur **F** Protibia **G** Apical spur of protibia **H** Mesotrochanter and mesofemur **I** Metatrochanter and metafemur **J** Sternite IX **K–M** Aedeagus, in dorsal view (**K**), lateral (**L**), ventral (**M**) view. Scale bars: 1 mm (**A**); 0.3 mm (**B, C, E, F, H, I**); 0.2 mm (**D, K, L, M**); 0.05 mm (**G**); 0.1 mm (**J**).

Comparative notes. The new species is placed as a member of the *L. chinensis*-group based on the simple male antennomeres IX–X. The form and proportions of antennomeres IX–XI are similar to *L. chinensis* (Löbl) and *L. inornatus* Yin & Li. However, both known species lack a projection on the ventral margin of metacoxa in the males, where there is a large, apically narrowed projection for the new species.

Linan megalobus Yin & Li, 2011 in Yin et al. 2011

Figs. 10, 11B

Linan megalobus Yin & Li, 2011 in Yin et al. 2011: 132.

Additional material examined. 1 ♂, 1 ♀, 'China: Hubei, Enshi Tujia and Miao Autonomous Prefecture, Xingdoushan N. R., San-xian-chang, 30°2'20.48"N, 109°8'33.89"E, 1114 m, 20.v.2017, sift, Zhou GC, Tian T, & Huang ZG leg.' (SNUC).

Distribution. China: Guizhou, Hubei (**new provincial record**) (Figure 11B).

Discussion. *Linan megalobus* was originally described from Kuankuoshui Nature Reserve (宽阔水自然保护区) in Guizhou, and placed as a member of the *L. cardialis*-

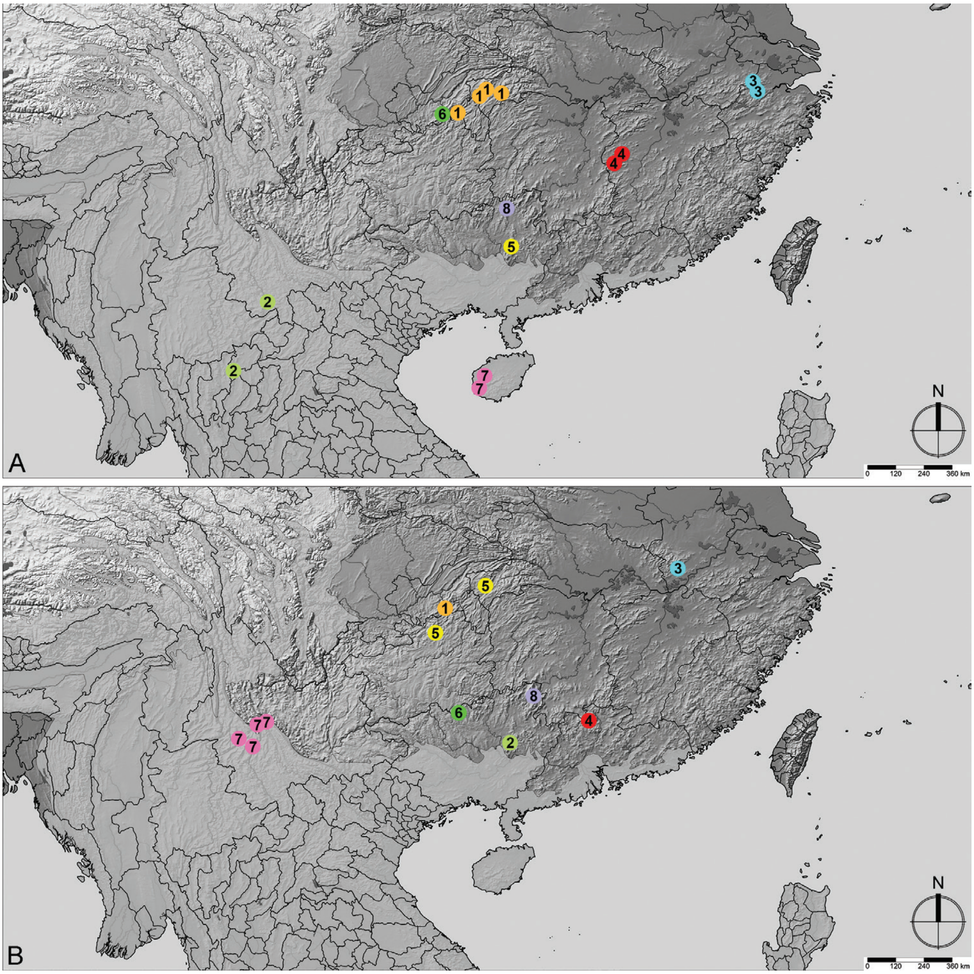

Figure 11. Distribution of *Linan* species. **A** *L. arcitibialis* (1), *L. cardialis* (2), *L. chinensis* (3), *L. divaricatus* (4), *L. fortunatus* (5), *L. geneolatus* (6), *L. hainanicus* (7), *L. huapingensis* (8) **B** *L. denticulatus* (1), *L. hujiayaoi* (2), *L. inornatus* (3), *L. mangshanus* (4), *L. megalobus* (5), *L. mulunensis* (6), *L. tendothorax* (7), *L. uenoi* (8).

group (Yin et al. 2011). The population from Hubei shows little variation in external morphology (Figure 10A–J) compared to that from the type locality, but possesses distinctly broader parameres of the aedeagus (Figure 10K–M). The present new record extends the range of this species some 280 km to the southwest.

Key to males

1 Antennae with antennomeres IX or X strongly modified .... **2 (*L. cardialis*-group)**
– Antennae with antennomeres IX–X simple, not modified .... **12 (*L. chinensis*-group)**

2 Antennomere IX angularly expanded laterally at basal third, with small rounded process near apex (Fig. 2A); mesotibiae strongly arched (Fig. 2G). (China: Hubei, Chongqing; Fig. 11A) .... ***L. arcitibialis*** **sp. n.**

– Antennomere IX strongly broadened apically, never expanded at basal third, often angularly projecting at apex; mesotibiae only slightly arched............. **3**

3 Median lobe of aedeagus strongly and abruptly constricted at middle of apex **4**

– Median lobe of aedeagus laterally bent, or emarginate at middle of apex..... **6**

4 Antennomere X broadly concave at basal half (Fig. 6A); postgenae broadly expanded laterally (Fig. 4B). (China: Guizhou; Fig. 11A)......***L. geneolatus*** **sp. n.**

– Antennomere X lacking excavation; postgenae roundly constricted posteriorly **5**

5 Antennomere VIII slightly transverse (Fig. 4A), IX about as long as wide (Fig. 5A); metaventral processes thick, bifurcate at apex in lateral view (Fig. 5C); protibia with indistinct apical spine (Fig. 5E); metatrochanter simple (Fig. 5G). (China: Jiangxi; Fig. 11A) .... ***L. divaricatus*** **sp. n.**

– Antennomere VIII about as long as wide, IX much longer than wide (Yin and Li 2013: 149, fig. 6A); metaventral processes thin, rounded at apex in lateral view (Yin and Li 2013: 149, fig. 6C); protibia simple; metatrochanter with short triangular ventral spine (Yin and Li 2013: 149, fig. 6F). (China: Guangxi; Fig. 11A) .... ***L. huapingensis*** **Yin & Li**

6 Median lobe of aedeagus nearly symmetric, broadly emarginate at middle of apex **7**

– Median lobe of aedeagus asymmetric, usually narrowing and bent to right (morphological position) at apex, never emarginate at middle.................... **8**

7 Antennomeres VII–VIII strongly modified, IX about 1.45 times as long as wide, slightly angulate at anterolateral corner (Yin et al. 2013: 351, fig. 29); protibia with small apical spine (Yin et al. 2013: 351, fig. 33); aedeagus (Yin et al. 2013: 351, figs 37–39) relatively stouter, length / width about 1.75. (China: Guangxi; Fig. 11B) ....***L. uenoi*** **Yin & Nomura**

– Antennomeres VII–VIII simple, IX about 1.20 times as long as wide, with long acute projection at anterolateral corner (Fig. 8A); protibia simple; aedeagus (Fig. 8H–J) relatively more slender, length / width about 2.25. (China: Hunan; Fig. 11B)..***L. mangshanus*** **sp. n.**

8 Pronotal lateral margins roundly expanded basolaterally (Yin and Li 2012: 94, fig. 6D). (China: Yunnan; Fig. 11B) ....***L. tendothorax*** **Yin & Li**

– Pronotal lateral margins evenly rounded laterally, not expanded basolaterally **9**

9 Pronotal and elytral basolateral margins densely setose (Yin and Li 2013: 146, fig. 4A). (China: Guangxi; Fig. 11A)....................... ***L. fortunatus*** **Yin & Li**

– Pronotal and elytral basolateral margins lacking dense setae **10**

10 Antennomere IX strongly bent at lateral margin (Yin et al. 2011: 128, fig. 9). (China: Hainan; Fig. 11A)...................................... ***L. hainanicus*** **Hlaváč**

– Antennomere IX straight or slightly broadened at lateral margin **11**

11 Pro- and mesotrochanter with distinct, pointed ventral spine (Yin et al. 2011: 130, figs 22, 23); protibia with short, bluntly rounded protuberance at apex; aedeagus with short and narrow parameres (Yin et al. 2011: 131, figs 27, 28). (China: Yunnan; Thailand: Wiang Pa Pao; Fig. 11A) ..... ***L. cardialis* Hlaváč**

– Pro- and mesotrochanter simple; protibia with elongate, rounded protuberance at apex (Yin et al. 2011: 131, fig. 26); aedeagus with long, apically strongly broadened parameres (Fig. 10K–M, Yin et al. 2011: 131, figs 35–36). (China: Hubei; Guizhou, Fig. 11B) .... ***L. megalobus* Yin & Li**

12 Antennomere IX slightly to moderately transverse **13**

– Antennomere IX slightly to distinctly elongate **14**

13 Antennomere VIII about as long as wide (Fig. 3A); protibia with distinct apical spine (Fig. 3E); median lobe of aedeagus asymmetric, strongly narrowed at apical fourth (Fig. 3I–K). (China: Guizhou; Fig. 11B) .... ***L. denticulatus* sp. n.**

– Antennomere VIII moderately transverse (Yin and Li 2013: 150, fig. 7A); protibia simple, lacking spine at apex; median lobe of aedeagus nearly symmetric, uniformly narrowing from middle toward apex (Yin and Li 2013: 150, fig. 7H–J). (China: Guangxi; Fig. 11B) .... ***L. hujiayaoi* Yin & Li**

14 Metaventrite with short, distinct protuberances above metacoxae (Fig. 9C); protibia with small, acute apical spine (Fig. 9E); metacoxa with large, apically narrowing and blunt ventral projection (Fig. 9G). (China: Guangxi; Fig. 11B) .... ***L. mulunensis* sp. n.**

– Metaventrite lacking protuberances above metacoxae; protibia lacking apical spine; metacoxa simple **15**

15 Metaventral processes relatively shorter, narrowing at apex (Yin et al. 2011: 128, fig. 18); elytra and abdomen relatively broader in contrast to pronotum (PW : EW : AW = 1.00 : 1.88–1.90 : 2.02–2.03) (Yin et al. 2011: 128, fig. 2). (China: Zhejiang; Fig. 11A) .... ***L. chinensis* (Löbl)**

– Metaventral processes relatively much longer, broad at apex (Yin et al. 2011: 128, fig. 20); elytra and abdomen relatively narrower in contrast to pronotum (PW : EW : AW = 1.00 : 1.62–1.64 : 1.75–1.78) (Yin et al. 2011: 128, fig. 4). (China: Anhui; Fig. 11B) .... ***L. inornatus* Yin & Li**

Acknowledgments

We thank Donald S. Chandler (Durham, USA), Michael Caterino (Clemson, USA), and Peter Hlaváč (Praha, Czech Republic) for critically reviewing the manuscript. This study was supported by the National Natural Science Foundation of China (No. 31501874, 31872965).

References

Hlaváč P (2003) A taxonomic revision of the Tyrini of the Oriental region. II. Systematic study on the genus *Pselaphodes* and its allied genera (Coleoptera: Staphylinidae: Pselaphinae). Annales de la Société Entomologique de France 38: 283–297.

Shorthouse DP (2010) SimpleMappr, an online tool to produce publication-quality point maps. http://www.simplemappr.net [Accessed June 19, 2018]

Yin Z-W, Li L-Z (2012) Notes on Michael Schülke's pselaphine collections from China. – Tyrini. I. genera *Labomimus* Sharp, *Linan* Hlaváč and *Pselaphodes* Westwood (Coleoptera, Staphylinidae, Pselaphinae). ZooKeys 251: 83–118. https://doi.org/10.3897/zookeys.251.4099

Yin Z-W, Li L-Z (2013) Five new species of the genera *Labomimus* and *Linan* from Guangxi, South China (Coleoptera: Staphylinidae: Pselaphinae). Acta Entomologica Musei Nationalis Pragae 53: 141–153.

Yin Z-W, Li L-Z, Zhao M-J (2011) A review of the genus *Linan* (Coleoptera: Staphylinidae: Pselaphinae). Acta Entomologica Musei Nationalis Pragae 51: 123–135.

Yin Z-W, Nomura S, Li L-Z (2013) New species and new records of the *Pselaphodes* complex of genera (Staphylinidae: Pselaphinae: Tyrini) from China. Annales Zoologici 63: 343–356. https://doi.org/10.3161/000345413X669595

ZooKeys 793: 135–142 (2018)
doi: 10.3897/zookeys.793.24790
http://zookeys.pensoft.net

RESEARCH ARTICLE

A peer-reviewed open-access journal
ZooKeys
Launched to accelerate biodiversity research

Contribution to the genus *Filipinolotis* Miyatake, 1994 (Coleoptera, Coccinellidae, Sticholotidini)

Yanqing Lv[1,2], Xiaoning Zhang[1], Adam Ślipiński[3], Yurong He[1], Xingmin Wang[1]

1 *Key Laboratory of Bio-Pesticide Innovation and Application, Engineering Technology Research Center of Agricultural Pest Biocontrol, Guangdong Province; Department of Entomology, South China Agricultural University, Guangzhou 510640, China* **2** *Zengcheng Entry-exit Inspection and Quarantine Bureau, Guangzhou 511340, China* **3** *CSIRO Ecosystem Sciences, Australian National Insect Collection, GPO Box 1700, Canberra, ACT 2601, Australia*

Corresponding authors: *Yurong He* (yrhe@scau.edu.cn); *Xingmin Wang* (wangxmcn@scau.edu.cn)

Academic editor: *M. Thomas* | Received 4 March 2018 | Accepted 22 August 2018 | Published 29 October 2018

http://zoobank.org/FDD1CD38-187F-438E-B549-8125C2DF4C63

Citation: Lv Y, Zhang X, Ślipiński A, He Y, Wang X (2018) Contribution to the genus *Filipinolotis* Miyatake, 1994 (Coleoptera, Coccinellidae, Sticholotidini). ZooKeys 793: 135–142. https://doi.org/10.3897/zookeys.793.24790

Abstract

The genus *Filipinolotis* Miyatake has been reviewed in this study. Descriptions and illustrations of two species (*F. latefasciata* Miyatake and *F. purpuratorotunda* Wang, Zhang & Ślipiński, **sp. n.**) in the Luzon island of the Philippines, are given. The male genitalia of *F. latefasciata* are described for the first time. A key to known species is also provided.

Keywords

Coccinelloidea, Coleoptera, *Filipinolotis*, Luzon, new species, Philippines, Sticholotidini

Introduction

The family Coccnellidae is an abundant species group of beetles. Ślipiński (2007) proposed a two subfamily system with Microweiseinae and Coccinellinae, merging Sticholotidini into an expanded concept of Coccinellinae (Escalona and Ślipiński

2012). The tribe Sticholotidini was defined by Gordon (1977) and Miyatake (1994). The final composition of Sticholotidini and the taxonomic status of many genera are not fully resolved (Ślipiński 2004). Coccinellid evolutionary history is borne out in previous molecular studies (Giorgi et al. 2009; Seago et al. 2011; Robertson et al. 2015).

Miyatake (1994) revised the Asian genera of the tribe Sticholotidini and proposed six new genera: *Synonychimorpha*, *Chilocorellus*, *Sulcolotis*, *Filipinolotis*, *Mimoserangium,* and *Coelolotis* for the species described from China, Philippines, and Vietnam. The genus *Filipinolotis* was erected with *F. latefasciata* Miyatake, 1994 as the type species from Luzon Island, Philippines. *Filipinolotis* is similar to *Sticholotis* except for some differences in characters of the hind wings (atrophied), antennae (shorter with distinct club), prosternal process (raised), and epipleura (broad). To date, *F. latefasciata* has been the only species in the genus *Filipinolotis*. In this paper, *F. purpuratorotunda*, sp. n. from Luzon Island in the Philippines is described and added to this genus.

Materials and methods

The specimens examined were collected from Luzon, Philippines. All materials were deposited at Australian National Insect Collection, CSIRO, Canberra, Australia (**ANIC**), South China Agricultural University, Guangzhou, China (**SCAU**), and Museum für Naturkunde in Berlin, Germany (**MNB**). External morphology was observed with a dissecting stereoscope (Zeiss Stemi 2000-cs). The following measurements were made with an ocular micrometer:

TL	total length, length from apical margin of clypeus to apex of elytra;
TW=EW	total width, width across both elytra at widest part;
TH	height, from the highest part of the beetle to elytral outer margins;
HW	head width in a frontal view, widest part including eyes;
PL	pronotal length, from the middle of anterior margin to the base of pronotum;
PW	pronotal width at widest part;
EL	elytral length, along the suture, from the apex to the base including the scutellum.

Images were taken with digital cameras (AxioCam HRc and Coolsnap-Procf & CRI Micro*Color) connected to a dissecting microscope in the Key Laboratory of Bio-Pesticide Innovation and Application, Engineering Technology Research Center of Agricultural Pest Biocontrol, Guangdong Province of South China. The software AxioVision Rel. 4.8 and Image-Pro Plus 5.1 were used to capture images from the cameras. Software Adobe Photoshop CC 2015 was used for cleaning up images.

Terminology follows Ślipiński (2007) and Ślipiński and Tomaszewska (2010). Type specimens designated in the present paper are deposited at ANIC and SCAU.

Taxonomy

Filipinolotis Miyatake, 1994

Filipinolotis Miyatake, 1994: 254. Type species: *Filipinolotis latefasciata* Miyatake, 1994.

Diagnosis. The genus *Filipinolotis* can be distinguished from other genera of the tribe Sticholotidini by the following characters: body rounded, glabrous, dorsum strongly convex (Figs 1a–c, 2a–c); antennae with 11 antennomeres (Figs 1e, 2e); hind wings atrophied; elytral epipleuron unevenly broadened; abdomen with five ventrites, abdominal postcoxal lines incomplete (Figs 1n, s, 2m).

Description. *Body* rounded, dorsum strongly convex and glabrous (Figs 1a–c, 2a–c). Head smooth, with sparse short hairs (Figs 1c, 2c). Antennae with 11 antennomeres, scape and pedicel robust, pedicel shorter than scape; flagellum 9-segmented, gradually broadening towards apex, last-three antennomeres forming a fusiform club (Figs 1d–e, 2d–e).

Clypeus protruded with anterior margin slightly emarginate at middle (Figs 1c, 2c). Labrum transverse, narrowly rounded and covered with dense, long setae (Figs 1h, 2h). Mandible with two apical teeth, sharp and smooth without additional denticles (Figs 1d, f, 2d, f). Maxillary palp 4-segmented with terminal segment cut obliquely at apex (Figs 1d, g, 2d, g). Labial palpomere 3-segmented, with robust 2ndsegment and slender terminal segment, ligula membranous and plump, insertion of labial palps is anterior on the prementum (Figs 1i, 2i).

Pronotum transverse, strongly convex, emarginate at anterior margin, hind margin bent into a curved shape; lateral margin slightly oblique, with fine groove continuing towards basal corner from anterior corner, anterior angles rounded and smooth, hind angles obtuse and smooth (Figs 1a–c, 2 a–c). Scutellum minute, triangular (Figs 1a, c; 2a, c). Elytra without humeral angles, strongly convex, almost as wide at anterior margin as hind margin of pronotum, lateral margins extremely narrow; lateral margins with narrow rim, invisible from above (Figs 1a–c, 2a–c). Hind wings atrophied.

Prosternum T-shaped. Prosternal process narrowed, less than 0.6 times width of coxal diameter and not prominent anteriorly between coxae, prosternal carinae present and fan-shaped (Figs 1l, 2k). Mesoventrite trapezoid-shaped, coarsely keeled on the anterior edge, metaventrite as long as mesoventrite (Figs 1m, 2l). Elytral epipleuron wide and uneven, gradually narrowed to apex. Legs with pubescence rather dense, coxae square-shaped, obvious robust; trochanter triangular, robust; femora thick, deeply grooved beneath for tibiae when retracted; length of tibia subequal to femur, slender, and widening but not angulate outwardly; tarsi 4-segmented; claws simple and slender, without teeth (Figs 1j, k, 2j). Abdomen with five ventrites in both sexes, ventrite 1 length measured below coxal cavity, almost as long as ventrites 2nd to 4th combined, abdominal postcoxal lines incomplete, not recurved but meeting hind margin of ventrite 1 (Figs 1n, s, 2m).

Male genitalia: tegmen stout, basal piece with distinct strut and additional, dorsal strut-like projection, parameres well developed and setose apically. Penis uniformly tubular, curved (Figs 1o–r, 2n–q).

Female genitalia: coxites long triangular with interior margin slightly emarginate, setose apically; styli conspicuous (Figure 1t).

Distribution. Philippines.

Key to the species of *Filipinolotis*

1 Pronotum reddish yellow, elytra blackish and shiny, with a broad transverse reddish yellow band in middle (Figure 1a–c); apex of penis gradually narrowing down (Figure 1o, p); penis guide of tegmen in ventral view broad and flat, rounded with uniform setae apically (Figure 1q, r) ....***F. latefasciata*** **Miyatake**

– Pronotum and elytra purplish to black, shiny, without any spots (Figure 2a–c); apex of penis tubular with membranous gonopore at apex (Figure 2n, o); penis guide of tegmen in ventral view narrow and symmetrical, horn-shaped apically (Figure 2p, q) .... ***F. purpuratorotunda*** **Wang, Zhang & Ślipiński, sp. n.**

Filipinolotis latefasciata Miyatake, 1994

Figure 1

Filipinolotis latefasciata Miyatake, 1994: 255

Diagnosis. This species can be recognized by the following combination of characters: pronotum reddish yellow, elytra blackish shiny with a broad transverse reddish yellow band in the middle (Figure 1a–c); penis guide of tegmen in ventral view broad and flat, with a rounded apex, parameres narrow and almost straight with dense setae at apices (Figure 1q–r); penis uniformly tubular, curved, gradually narrowing to apex (Figure 1o–r).

Description. TL: 1.92–2.3 mm, TW: 1.86 mm, TH: 1.35–1.38 mm, TL/TW: 1.03–1.24; PL/PW: 0.38–0.42; EL/EW: 0.89–1.08; HW/TW: 0.39; PW/TW:0.67–0.74.

Head reddish yellow (Figure 1c, d). Pronotum reddish yellow (Figure 1a–c). Scutellum blackish shiny (Figure 1a, c). Elytra blackish and shiny, with a broad transverse reddish yellow band at middle, covering almost half of elytra (Figure 1a–c). Underside blackish brown, except claws yellowish.

Body rounded, dorsum strongly convex and glabrous (Figure 1a–c). Head large, with sparse short golden pubescence (Figure 1d). Pronotum glabrous with uniformly minute and dense punctures (Figure 1a–c). Elytra convex, entire surface uniformly punctate (Figure 1a–c). Elytral epipleuron with sparse golden pubescence. Prosternum with sparse golden pubescence and inconspicuous punctures (Figure 1l). Mesoventrite

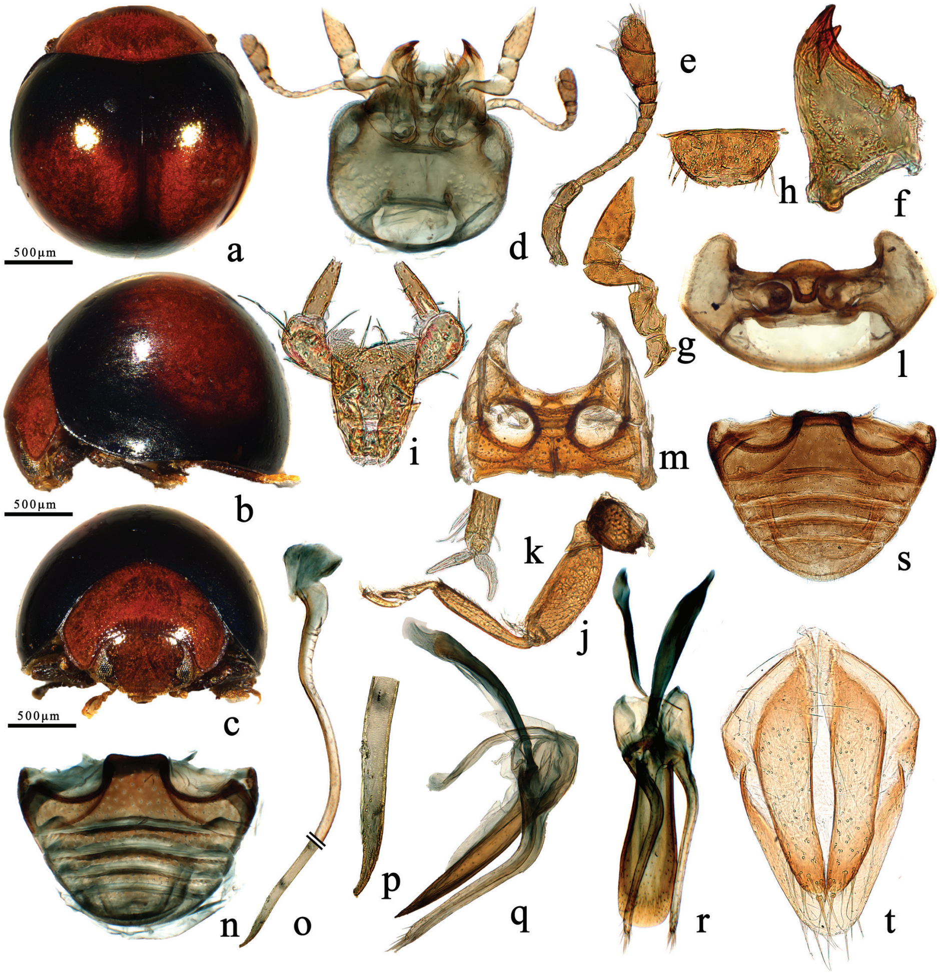

Figure 1. Morphological characters of the genus *Filipinolotis*. **a–t** *F. latefasciata* Miyatake. **a** dorsal habitus **b** lateral habitus **c** frontal habitus **d** head, ventral **e** antenna **f** mandible **g** maxilla **h** labrum **i** labium **j** front leg **k** tarsal claws **l** prothorax, ventral **m** mesoventrite and metaventrite **n** male abdomen **o** penis **p** apex of penis **q** tegmen, lateral view **r** tegmen, ventral view **s** female abdomen **t** ovipositor.

and metaventrite with sparse golden pubescence and inconspicuous punctures, mesoventrite with narrow intercoxal process, chin piece formed on the anterior margin of mesoventrite; metaventrite short, as wide as mesoventrite (Figure 1m). Legs with dense golden pubescence (Figure 1j, k). Abdomen with sparse golden hairs and uniform punctures (Figure 1n, s).

Male genitalia (Figure 1o–r). Tegmen stout and symmetrical, penis guide in lateral view wide at base and gradually narrowing to pointed apex, the basal 2/3 with membranous prominence; in ventral view broad and flat, rounded apically; parameres narrow and almost straight with dense setae at apices (Figure 1q–r), phallobase membranous. Penis simple tubular, curved, gradually narrowing along apical third to pointed apex, penis capsule membranous, without inner arm (Figure 1o–p).

Material examined. Philippines: 1 male, Mt. Polis, Lepanto, Luzon Prov., Böttcherleg (MNB); 1 female, Mt. Data, Mountain, Luzon Prov., 7500 ft, 23.iv.1946; 1 male Philippines, Luzon (ANIC).

Distribution. Philippines (Luzon).

Filipinolotis purpuratorotunda Wang, Zhang & Ślipiński, sp. n.

http://zoobank.org/D188809E-F91D-44D4-853E-BB53986EBCA6
Figure 2

Diagnosis. This species is similar to *F. latefasciata* Miyatake but it can be distinguished from the latter as follows: body uniformly black with purple shine, without spots (Figure 2a–c); penis guide of tegmen in ventral view narrow with a nipple-shaped apex (Figure 2p, q); apex of the penis truncate, membranous (Figure 2o). In *F. latefasciata*, pronotum reddish yellow, elytra blackish and shiny, with a broad transverse reddish yellow band in the middle (Figure 1a–c); penis guide of tegmen in ventral view broad and flat, with rounded apex (Figure 1r); apex of the penis pointed (Figure 1o, p).

Description. TL: 1.99–2.63 mm, TW: 1.84–2.55 mm, TH: 1.28–1.8 mm, TL/TW: 1.03–1.08; PL/PW: 0.40–0.49; EL/EW: 0.93; HW/TW: 0.34–0.39; PW/TW: 0.59–0.60.

Color: Head, pronotum, scutellum, elytra purplish shiny black, without spots (Figure 2a–c). Underside blackish brown, except yellowish claws.

Body rounded, dorsum strongly convex and glabrous (Figure 2a–c). Head large with scattered short golden pubescence (Figure 2c, d). Pronotum glabrous, with uniformly distributed punctures (Figure 2a–c). Scutellum of isosceles triangle shape (Figure 2a, c). Elytral surface uniformly punctate (Figure 2a–c). Prosternum, mesoventrite, and metaventrite with scattered golden pubescence and inconspicuous punctures (Figure 2k, l). Elytral epipleuron with uniform golden pubescence. Legs with dense golden pubescence (Figure 2j, l). Abdomen with sparse golden pubescence and uniformly distributed punctures (Figure 2m).

Male genitalia. Tegemen stout and symmetrical, tegminal strut stout and straight; penis guide in lateral view almost straight and gradually narrowing along apical third to pointed apex, with membranous prominence at basal half; in ventral view narrowest at base and gradually broadening to apex, then strongly narrowed to form a nipple-shaped apex; parameres with dense long setae apically, longer than penis guide; phallobase membranous (Figure 2p, q). Penis uniformly tubular, curved, basal capsule membranous, without distinct arms; apex of penis subtruncate with membranous appendage (Figure 2n, o).

Types. Holotype: Philippines: 1 male, La Trinidad, Luzon Prov., 1300m, 4–5. IV.1968, Benqae (ANIC); Paratypes: Philippines: 1 male, Island of Basilan, Baker (ANIC); 1 male, Disimungal, Madela, Quirino, Eastern Luzon, XII.2014 (SCAU).

Disribution. Philippines (Luzon).

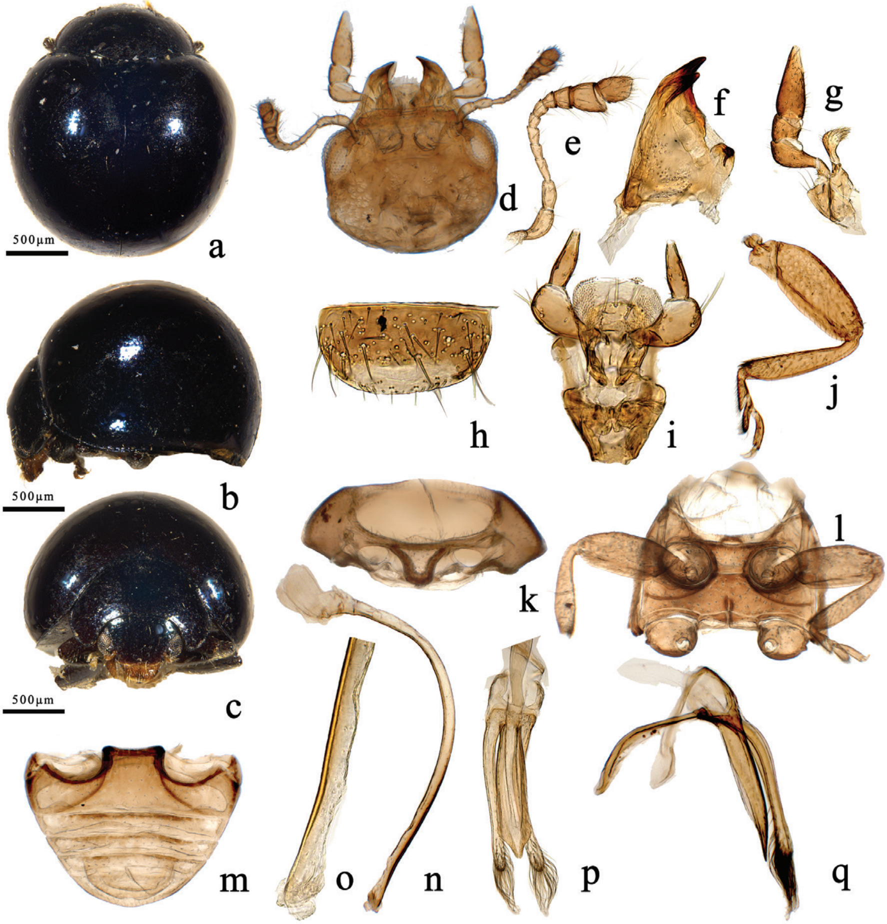

Figure 2. *Filipinolotis purpuratorotunda* sp. n. **a** dorsal habitus **b** lateral habitus **c** frontal habitus **d** head, ventral **e** antenna **f** mandible **g** maxilla **h** labrum **i** labium **j** front leg **k** prothorax, ventral **l** mesoventrite and metaventrite **m** abdomen **n** penis **o** apex of penis **p** tegmen, ventral view **q** tegmen, lateral view.

Etymology. The name *purpuratorotunda* is composed of the word *purpuratus*, which refers to the purplish color of the body and *rotundus*, referring to the rounded body shape.

Acknowledgements

We are grateful to Prof. Shaukat Ali (SCAU) who revised the English. The research was supported by National Natural Science Foundation of China (31501884), Science and Technology Planning Project of Guangdong Province (2017A020208060), the Science and Technology Program of Guangzhou (201804020070, 151800033).

References

Escalona HE, Ślipiński SA (2012) Generic revision and phylogency of Microweiseinae (Coleoptera: Coccinellidae). Systematic Entomology 37: 125–171. https://doi.org/10.1111/j.1365-3113.2011.00601.x

Miyatake M (1994) Revisional studies on Asian genera of the subfamily Sticholotidinae (Coleoptera: Coccinellidae). Memoirs of the College of Agriculture, Ehime University 38: 254–256.

Gordon RD (1977) Classification and phylogeny of the New World Sticholotidinae (Coccinellidae). Coleopterists Bulletin 31: 185–228.

Giorgi JA, Vandenberg NJ, Mchugh JV, Forrester JA, Ślipiński SA, Miller KB, Shapiro LR, Whiting MF (2009) The evolution of food preferences in Coccinellidae. Biological Control 51: 215–231. https://doi.org/10.1016/j.biocontrol.2009.05.019

Robertson JA, Ślipiński SA, Moulton M, Shockley FW, Giorgi A, Lord NP, Mckenna DD, Towaszewska W, Forrester J, Miller KB, Whiting MF, Mchugh JV (2015) Phylogeny and classification of Cucujoidea and the recognition of a new superfamily Coccinelloidea (Coleoptera: Cucujiformia). Systematic Entomology: 1–34. https://doi.org/10.1111/syen.12138

Seago AE, Giorgi JA, Li J, Ślipiński SA (2011) Phylogeny, classification and evolution of ladybird beetles (Coleoptera: Coccinellidae) based on simultaneous analysis of molecular and morphological data. Molecular Phylogenetics and Evolution 60: 137–151. https://doi.org/10.1016/j.ympev.2011.03.015

Ślipiński SA (2004) Revision of the Australian Coccinellidae (Coleoptera). Part 2. Tribe Sticholotidini. Annales Zoologici (Warszawa) 54: 389–402.

Ślipiński SA (2007) Australian ladybird beetles (Coleoptera: Coccinellidae) their biology and classification. ABRS, Canberra, 56 pp.

Ślipiński SA, Tomaszewska W (2010) Coccinellidae Latreille, 1802. In: Leschen RAB, Beutel RG, Lawrence JF (Eds) Handbook of Zoology, Vol. 2, Coleoptera. Walter de Gruyter GmbH & Co. KG, Berlin/New York, 454–472.

ZooKeys 793: 143–155 (2018)
doi: 10.3897/zookeys.793.29313
http://zookeys.pensoft.net

RESEARCH ARTICLE

A peer-reviewed open-access journal
ZooKeys
Launched to accelerate biodiversity research

A review of the genus *Apronopa* van Achterberg (Hymenoptera, Braconidae, Alysiinae) with a key to species

Francisco Javier Peris-Felipo[1], Sergey A. Belokobylskij[2]

1 *Bleichestrasse 15, Basel CH-4058, Switzerland* **2** *Zoological Institute, Russian Academy of Sciences, St Petersburg, 199034, Russia; Museum and Institute of Zoology, Polish Academy of Sciences, Wilcza 64, Warszawa 00-679, Poland*

Corresponding author: *Francisco Javier Peris-Felipo* (peris.felipo@gmail.com)

Academic editor: *J. Fernandez-Triana* | Received 26 August 2018 | Accepted 11 October 2018 | Published 29 October 2018

http://zoobank.org/FA6EFB73-5490-45C8-B259-94C7E66F97AC

Citation: Peris-Felipo FJ, Belokobylskij SA (2018) A review of the genus *Apronopa* van Achterberg (Hymenoptera, Braconidae, Alysiinae) with a key to species. ZooKeys 793: 143–155. https://doi.org/10.3897/zookeys.793.29313

Abstract

A review of the genus *Apronopa* van Achterberg, 1980 with illustrated re-descriptions of the known species and a key for their identification is provided.

Keywords

Braconidae, Alysiinae, *Apronopa*, parasitoid wasp, Palaearctic, redescription, illustration, key

Introduction

The genus *Apronopa* van Achterberg, 1980 is small, with only three known species, and rarely collected taxon with a Palaearctic distribution (Yu et al. 2016). This genus is a distinct member of the *Aspilota* generic-group. The main characters for diagnosis of *Apronopa* are *Aspilota*-like wing venation (with very narrow and long pterostigma), absence of dorsope on the first metasomal tergite and usually a sculptured basal part of second metasomal tergite (van Achterberg 1980, Belokobylskij 1998).

The main aim of this study is the preparation of a complete and richly illustrated redescription of all known *Apronopa* species (some of which have non-English original descriptions), estimation of their diagnostic species characters and preparation of the first comprehensive key for determination of all described species.

Materials and methods

For the terminology of morphological features, sculpture and measurements see Peris-Felipo et al. (2014); for wing venation nomenclature see van Achterberg (1993); for measurements of the marginal cell see Peris-Felipo and Belokobylskij (2017). Material was imaged using a Digital Microscope Keyence VHX-2000 and Adobe Photoshop® imaging system. The types of described species are deposited in the collection of the Hungarian Natural History Museum (Budapest, Hungary; HNHM), the Naturalis Biodiversity Center (Leiden, the Netherlands; RMNH), the Zoological Institute of the Russian Academy of Sciences (St Petersburg, Russia; ZISP) and the Zoologische Staatssammlung München (München, Germany; ZSSM).

Taxonomic results

Class Hexapoda Blainville, 1816
Order Hymenoptera Linnaeus, 1758
Family Braconidae Nees, 1811
Subfamily Alysiinae Leach, 1815
Tribe Alysiini Leach, 1815

Genus *Apronopa* van Achterberg, 1980

Apronopa van Achterberg, 1980: 75; Tobias 1986: 195; Fischer 1991: 8; Wharton 1994: 640; Belokobylskij 1998: 169, 217; Belokobylskij and Tobias 2007: 10; Yu et al. 2016.

Diagnosis. Paraclypeal fovea small, far from inner border of eye. Mandibles small, tridentate, without transverse carina. Upper tooth small; median tooth rather wide and short; lower tooth wide, lobe shaped. Antenna thickened; first flagellar segment longer than second segment. Mesoscutum without postero-medial mesoscutal pit; notauli present on horizontal surface of mesoscutum reaching half or two thirds of mesoscutum; precoxal sulcus present, wide or narrow, oblique, crenulate-rugose, rarely almost smooth; propodeum with different types of sculpture, without areas delineated by carinae. Marginal cell of forewing always long; vein r longer than pterostigma width; vein 2-SR present and rather distinctly sclerotized; veins m-cu and cu-a always strongly postfurcal; subvertical vein 2-SR+M long; first subdiscal cell closed postero-apically by vein CU1b; vein CU1a arising from vein 3-CU1 distinctly behind its middle. Metasoma more or less distinctly depressed dorso-ventrally; first metasomal tergite without dorsope; second tergite usually striate-rugulose in basal one-third or two thirds.

Hosts. Unknown.

Apronopa haeselbarthi **van Achterberg, 1980**

Figs 1, 2

Apronopa haeselbarthi van Achterberg, 1980: 75; Tobias 1986: 195; Fischer 1991: 9; Yu et al. 2016.

Type material. Holotype: female, Germany, Dransfeld, B/L 2.vi.1966 (Haeselbarth leg.) (ZSSM). Paratypes: 1 female, 1 male, Germany, Schotten, Hessen, Fi., Streu, v.1967 (Haeselbarth leg.) (♀ in RMNH, ♂ in ZSSM).

Description. Female (holotype).

Head. In dorsal view, 1.6 times as wide as long, 1.2 times as wide as mesoscutum, smooth, with temple rounded behind eyes. Eye in lateral view 1.3 times as high as wide and 1.5 times as wide as temple medially. POL equal to OD; OOL 2.5 times OD. Face 1.9 times as wide as high; inner margins of eyes subparallel. Clypeus 2.5 times as wide as high, slightly concave ventrally. Paraclypeal fovea almost reaching half distance between clypeus and inner border of eye. Mandible almost parallel-sided, about as long as its maximum width. Upper tooth small; middle tooth rather wide and short, weakly directed upwards; lower tooth wide, curved and obtuse. Antenna more than 9-segmented (apical segments missing). Scape 1.8 times as long as pedicel. First flagellar segment 2.2 times as long as its apical width, 1.3 times as long as second segment. Second flagellar segment 1.6 times, third to seventh segments 1.3–1.5 times as long as their maximum width.

Mesosoma. In lateral view about as long as high. Mesoscutum (dorsal view) about as long as its maximum width, smooth, sparsely setose. Notauli present on horizontal surface of mesoscutum reaching anterior two-third of mesoscutum. Prescutellar depression smooth, with median and lateral carinae, 2.8 times as long as its maximum width. Precoxal sulcus wide, smooth, not reaching anterior and posterior margins of mesopleuron. Posterior mesopleural furrow weakly crenulate. Propodeum sculptured, with several small smooth areas. Propodeal spiracles very small, its diameter 0.2 times as large as distance from spiracle to anterior margin of propodeum.

Wings. Length of forewing 2.4 times its maximum width. Marginal cell 4.2 times as long as its maximum width, ending almost on apex of wing. Vein 3-SR 1.5 times as long as vein 2-SR. Vein SR1 2.8 times as long as vein 3-SR. First subdiscal cell 3.0 times as long as its maximum width. Hindwing 4.3 times as long as its maximum width.

Legs. Hind femur 4.0 times as long as its maximum width. Hind tibia weakly widening towards apex, 8.5 times as long as its maximum subapical width, about as long as hind tarsus. First segment of hind tarsus 1.8 times as long as second segment.

Metasoma. First tergite weakly and curvedly widening towards apex, 1.1 times as long as its apical width, rugose-reticulate. Second tergite distinctly striate with reticulation in two-thirds baso-medially. Ovipositor 3.6 times as long as first tergite, almost as long as metasoma, 2.2 times as long as hind femur.

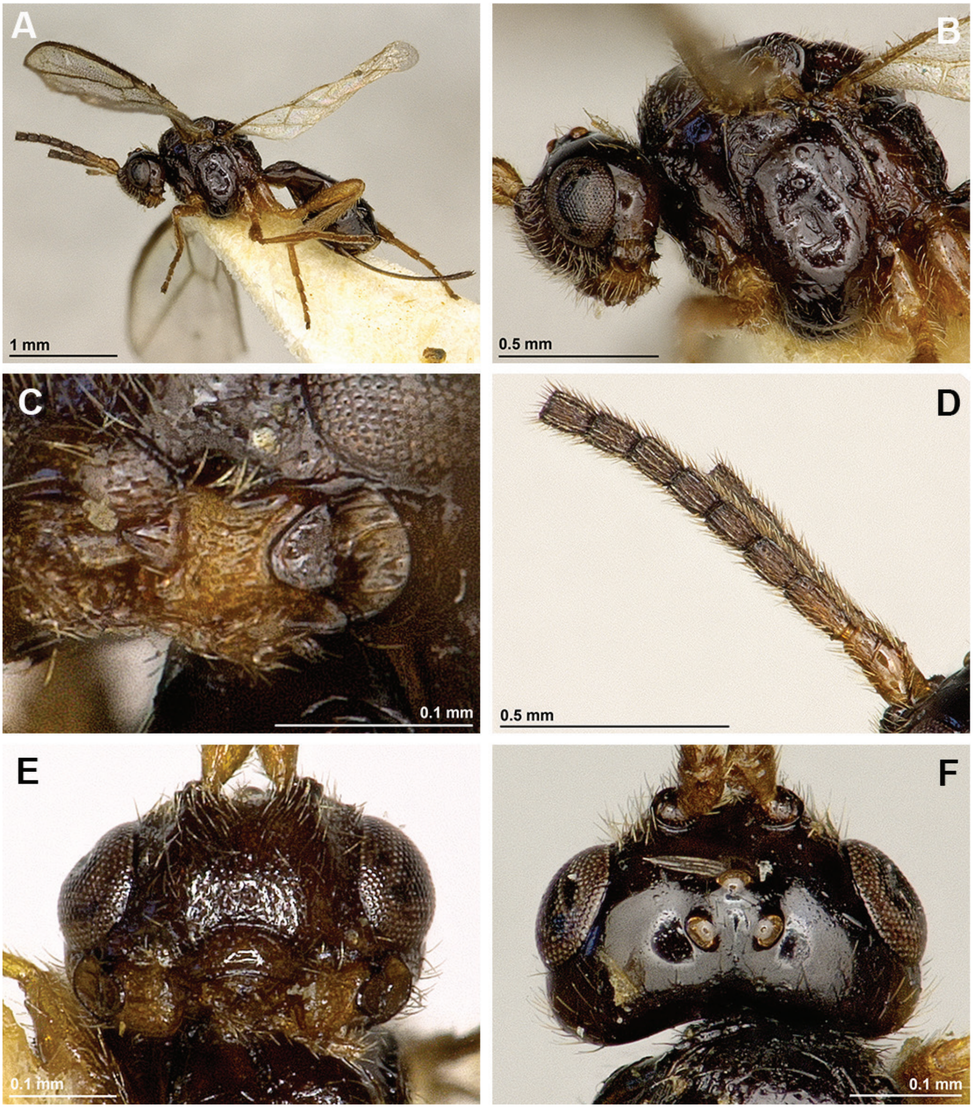

Figure 1. *Apronopa haeselbarthi* van Achterberg, 1980 (female, holotype) **A** Habitus, lateral view **B** Head and mesosoma, lateral view **C** Mandible **D** Antenna **E** Face, frontal view **F** Head, dorsal view.

Colour. Body, flagellar segments of antenna and pterostigma dark brown to black. Mandible and legs brown. First metasomal tergite similar in colour to second and third tergites. Wings almost hyaline.

Length. Body 2.5 mm, forewing 3.0 mm, hindwing 2.2 mm.

Variation. Length of body 2.0–2.5 mm, forewing 2.0–3.0 mm. Antennae with 23 segments.

Male. Body length 1.9 mm. Forewing length 2.4 mm. Otherwise similar to female.

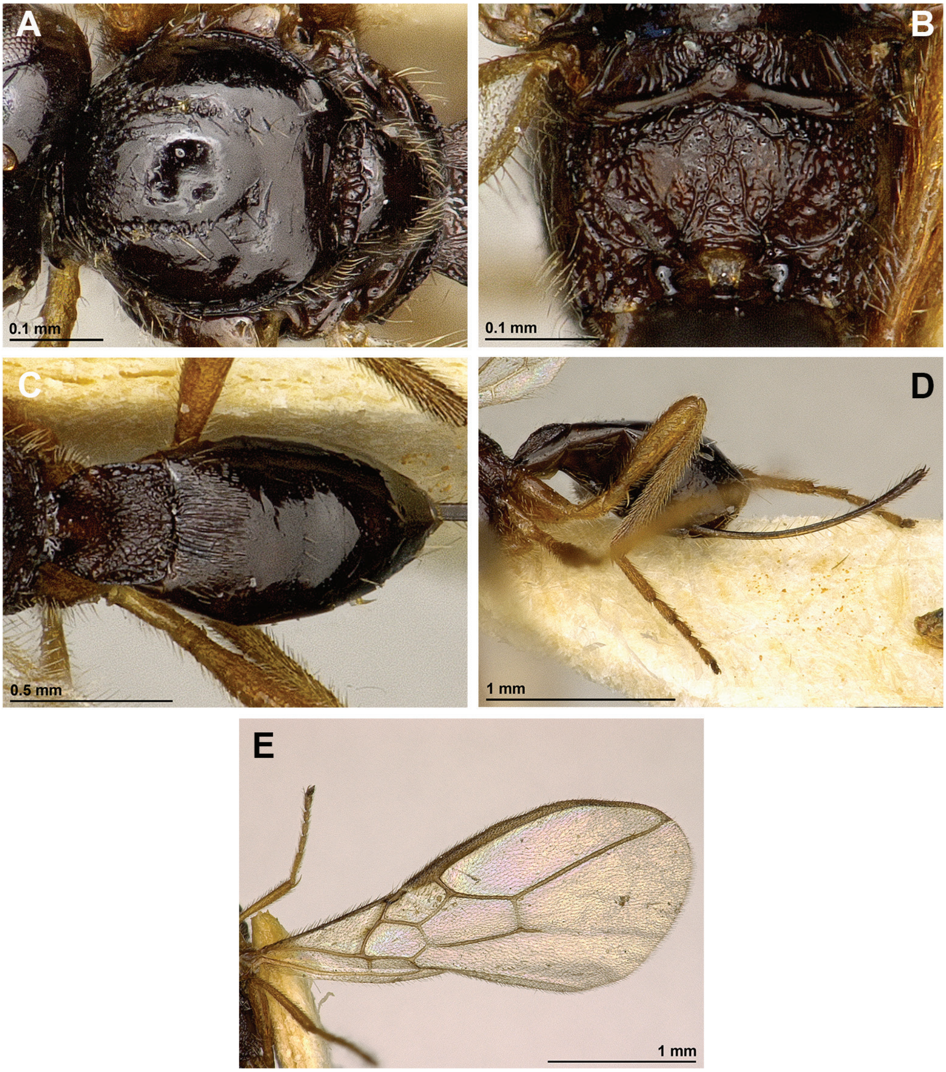

Figure 2. *Apronopa haeselbarthi* van Achterberg, 1980 (female, holotype) **A** Mesonotum, dorsal view **B** Propodeum, dorsal view **C** Metasoma, dorsal view **D** Hind leg, metasoma and ovipositor, lateral view **E** Forewing.

Comparative diagnosis. This species is similar to *A. ussuricola* Belokobylskij, 1998 (Russia), but differs from it in having the eye in lateral view 1.5 times as wide as temple medially (1.2 times in *A. ussuricola*), face 1.9 times as wide as high, distinctly and densely punctate-rugulose (1.6 times and weakly and sparsely punctate-rugulose in *A. ussuricola*), clypeus 2.5 times as wide as high (3.0 times in *A. ussuricola*), vein 3-SR 1.5 times as long as vein 2-SR (2.0 times in *A. ussuricola*), and ovipositor 3.6 times as long as first metasomal tergite (2.1 times in *A. ussuricola*).

Distribution. Germany, Slovakia.

Apronopa levis Papp, 2007

Figs 3, 4

Apronopa levis Papp, 2007: 15; Yu et al. 2016.

Type material. Holotype: female, North Korea, Prov. Kangwon Kumgang-san, 24.ix.1978, in the woods around Oe-Kungang resthouse, No. 396 (A. Vojnits & L. Zombori leg.), Type No. 10970 (HNHM).

Description. Female (holotype).

Head. In dorsal view, 1.8 times as wide as long, 1.4 times as wide as mesoscutum, smooth, with temple rounded behind eyes. Eye in lateral view 1.3 times as high as wide and 1.1 times as wide as temple medially. POL 0.8 times OD; OOL 3.1 times OD. Face 1.8 times as wide as high; inner margins of eyes subparallel. Clypeus 2.5 times as wide as high, slightly concave ventrally. Paraclypeal fovea not reaching middle of distance between clypeus and inner border of eye. Mandible almost parallel-sided, about as long as its maximum width. Upper tooth small, wide and obtuse; middle tooth rather wide and short, directed forward; lower tooth wide, curved and obtuse. Antenna more than 20-segmented (apical segments missing). Scape 1.5 times as long as pedicel. First flagellar segment 2.5 times as long as its apical width, 1.4 times as long as second segment. Second flagellar segment 1.5 times, third to 18th segments 1.3–1.4 times as long as their maximum width.

Mesosoma. In lateral view 1.1 times as long as high. Mesoscutum (dorsal view) 0.9 times as long as its maximum width. Notauli present, on horizontal surface of mesoscutum reaching almost half of mesoscutum. Prescutellar depression smooth, with median and lateral carinae, 2.5 times as long as its maximum width. Precoxal sulcus narrow, crenulate, reaching anterior margin of mesopleuron but not reaching posterior margins of mesopleuron. Posterior mesopleural furrow crenulate. Propodeum anteriorly densely rugose, posteriorly (on its long declivous part) almost smooth, with several wrinkles. Propodeal spiracles small, its diameter 0.2 times as large as distance from spiracle to anterior margin of propodeum.

Wings. Length of forewing 2.6 times its maximum width. Marginal cell 4.4 times as long as its maximum width, ending on apex of wing. Vein 3-SR 1.8 times as long as vein 2-SR. Vein SR1 2.4 times as long as vein 3-SR. First subdiscal cell 2.5 times as long as its maximum width. Hind wing 5.3 times as long as its maximum width.

Legs. Hind femur 4.0 times as long as its maximum width. Hind tibia weakly widened at apex, 9.0 times as long as its maximum subapical width, about as long as hind tarsus. First segment of hind tarsus 1.9 times as long as second segment.

Metasoma. First tergite weakly curvedly, widened at apex, about as long as its apical width, reticulate-rugose. Second tergite entirely smooth. Ovipositor 1.8 times as long as first tergite, 0.7 times as long as metasoma, 3.0 times as long as hind femur.

Colour. Body, flagellar segments of antenna and pterostigma brown to dark brown. Mandible, scape, pedicel and legs light brown. First metasomal tergite similar in colour to second and third tergites. Wings almost hyaline.

Length. Body 3.0 mm, forewing 3.1 mm, hindwing 2.1 mm.

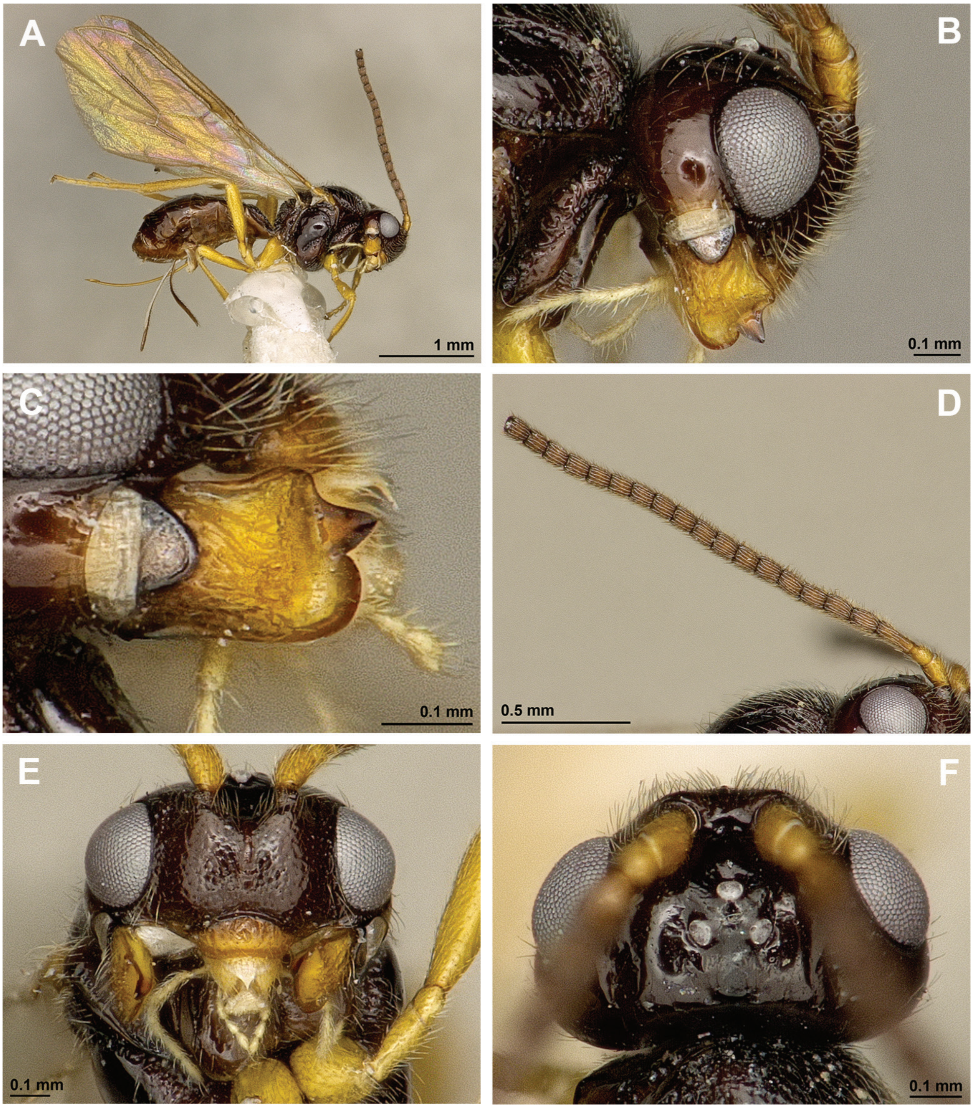

Figure 3. *Apronopa levis* Papp, 2007 (female, holotype) **A** Habitus, lateral view **B** Head, lateral view **C** Mandible **D** Antenna **E** Face, frontal view **F** Head, dorsal view.

Male. Unknown.

Comparative diagnosis. This species is very similar to *Apronopa ussuricola* Belokoblyskij, 1998 (Russian Far East) but differs from them in having an entirely smooth second tergite (tergite striate with rugosity baso-medially in *A. ussuricola*), clypeus 2.5 times as wide as high (3.0 times in *A. ussuricola*), first flagellar segment 2.5 times as long as its maximum width (2.0 times in *A. ussuricola*), and ovipositor 1.8 times as long as first metasomal tergite (2.1 times in *A. ussuricola*).

Distribution. North Korea

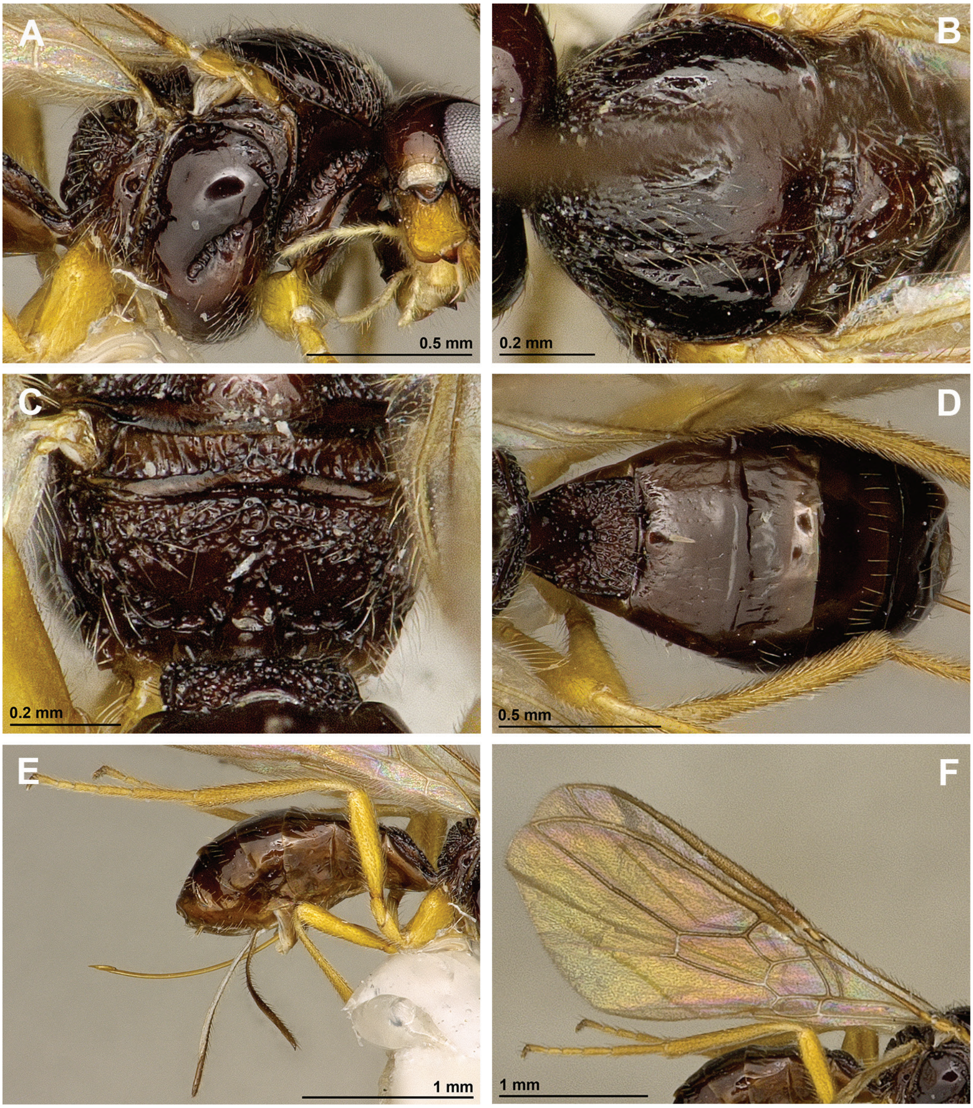

Figure 4. *Apronopa levis* Papp, 2007 (female, holotype) **A** Mesosoma, lateral view **B** Mesonotum, dorsal view **C** Propodeum, dorsal view **D** Metasoma, dorsal view **E** Hind leg, metasoma and ovipositor, lateral view **F** Forewing.

Apronopa ussuricola Belokobylskij, 1998
Figs 5, 6

Apronopa ussuricola Belokobylskij, 1998: 217; Yu et al. 2016.

Type material. Holotype: female, Primorskiy kray, env. Ussuriysk, dry meadow, 15.vi.1993 (S. Belokobylskij leg.) (ZISP).

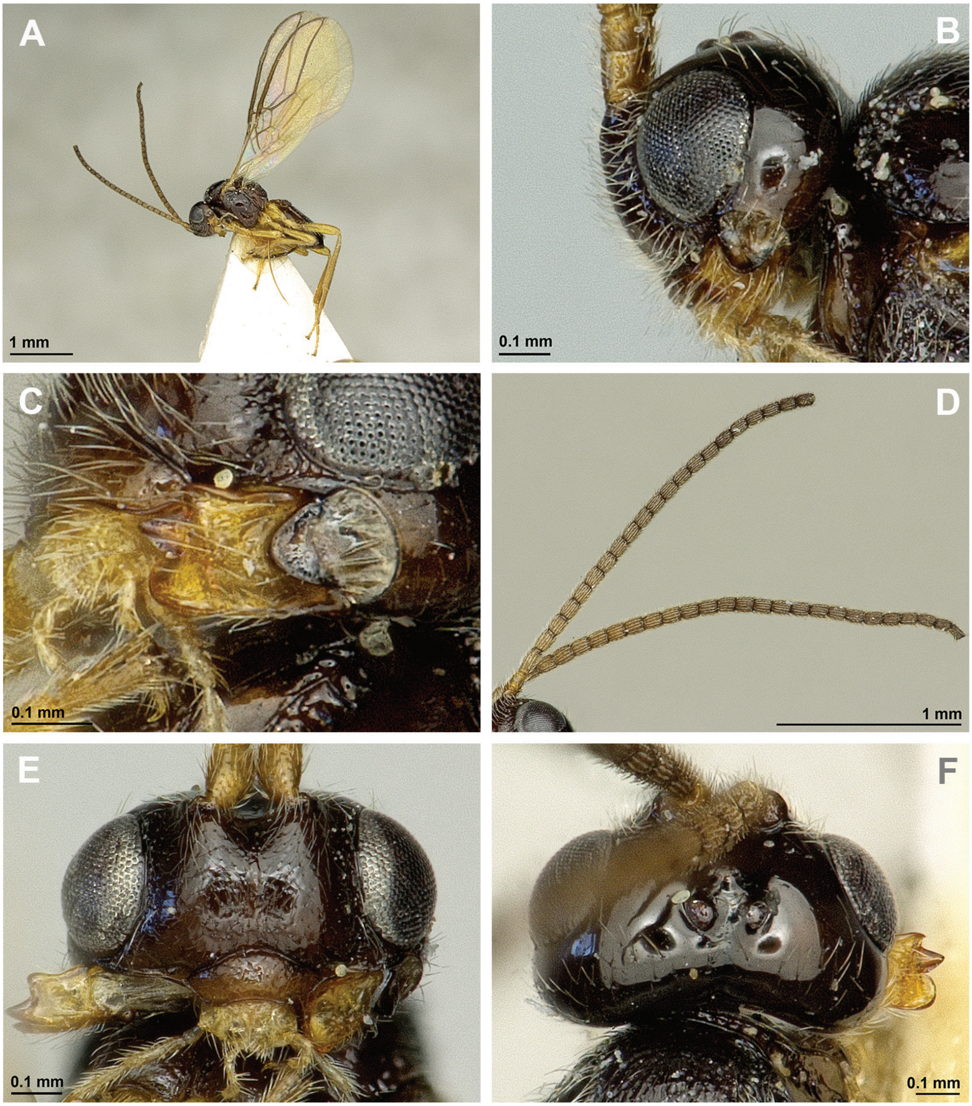

Figure 5. *Apronopa ussuricola* Belokobylskij, 1998 (female, holotype) **A** Habitus, lateral view **B** Head, lateral view **C** Mandible **D** Antenna **E** Face, frontal view **F** Head, dorsal view.

Description. Female (holotype).

Head. In dorsal view, 1.8 times as wide as long, 1.4 times as wide as mesoscutum, smooth, with temple rounded behind eyes. Eye in lateral view 1.4 times as high as wide and 1.2 times as wide as temple medially. POL equal to OD; OOL 3.0 times OD. Face 1.6 times as wide as high; inner margins of eyes subparallel. Clypeus 3.0 times as wide as high, slightly concave ventrally. Paraclypeal fovea not reaching middle distance between clypeus and inner border of eye. Mandible almost parallel-sided, as long as its maximum width. Upper tooth very small; middle tooth rather wider and short, directed forwards; lower

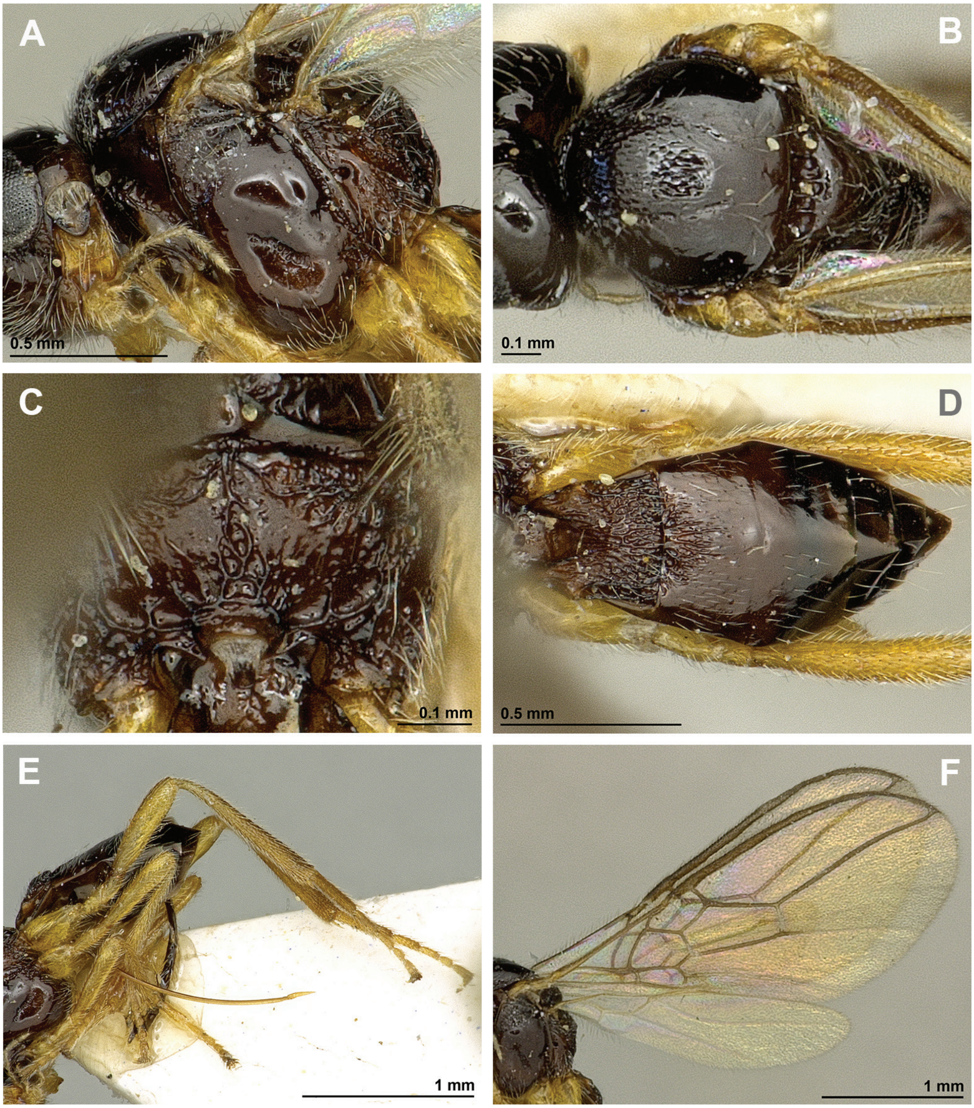

Figure 6. *Apronopa ussuricola* Belokobylskij, 1998 (female, holotype) **A** Mesosoma, lateral view **B** Mesonotum, dorsal view **C** Propodeum, dorsal view **D** Metasoma, dorsal view **E** Hind leg, metasoma and ovipositor, lateral view **F** Fore- and hindwings.

tooth wide, curved and obtuse. Antenna more than 27-segmented (apical segments missing). Scape 1.1 times as long as pedicel. First flagellar segment 2.0 times as long as its apical width, 1.3 times as long as second segment. Second flagellar segment 1.3 times as long as its maximum width, third to 25th segments 1.2–1.4 times as long as their maximum width.

Mesosoma. In lateral view 1.1 times as long as high. Mesoscutum (dorsal view) 0.9 times as long as its maximum width. Notauli present on horizontal surface of mesoscutum reaching two-thirds of mesoscutum. Prescutellar depression smooth, with median and lateral carinae, about 2.0 times as long as its maximum width. Precoxal sulcus rather wide, crenulate, not reaching anterior and posterior margins of mesopleuron. Posterior mesopleural furrow shortly crenulate. Propodeum rugose-reticulate, with smooth latero-medial areas. Propodeal spiracles rather small, its diameter 0.4 times as large as distance from spiracle to anterior margin of propodeum.

Wings. Length of forewing 2.2 times its maximum width. Marginal cell 4.5 times as long as its maximum width, ending on apex of wing. Vein 3-SR 2.0 times as long as vein 2-SR. Vein SR1 2.6 times as long as vein 3-SR. First subdiscal cell 2.5 times as long as its maximum width. Hindwing 5.0 times as long as its maximum width.

Legs. Hind femur 4.0 times as long as its maximum width. Hind tibia weakly widened at apex, 7.8 times as long as its maximum subapical width, about as long as hind tarsus. First segment of hind tarsus 1.7 times as long as second segment.

Metasoma. First tergite weakly widening towards apex, about as long as its apical width, rugose-reticulate. Second tergite in baso-medial half striate with reticulation. Ovipositor 2.1 times as long as first tergite, 1.1 times as long as metasoma, 3.4 times as long as hind femur.

Colour. Body, flagellar segments of antenna and pterostigma brown to dark brown. Mandible, scape, pedicel and legs light brown. First metasomal tergite similar in colour to second and third tergites. Wings almost hyaline.

Length. Body 2.0 mm, forewing 2.4 mm, hindwing 1.5 mm.

Male. Unknown.

Comparative diagnosis. This species is similar to *Apronopa haeselbarthi* van Achterberg, 1980 (Slovakia and Germany); differences between both species are showed under the description of the latter species.

Distribution. Russia (south of Far East).

Key to *Apronopa* species

1 Second metasomal tergite entirely smooth (Fig. 4D). Body length 3.0 mm. North Korea .... ***A. levis* Papp (♀)**

– Second metasomal tergite striate with rugosity in baso-medial one- or two-thirds (Figs 2C, 6D). Body length 1.9–2.5 mm **2**

2 Eye in lateral view 1.5 times as wide as temple medially (Fig. 1B). Face 1.9 times as wide as high, distinctly and densely punctate-rugulose (Fig. 1E).Vein 3-SR 1.5 times as long as vein 2-SR (Fig. 2E). Ovipositor 3.6 times as long as first metasomal tergite (Fig. 2D). Body length 1.9–2.5 mm. Germany, Slovakia .... ***A. haeselbarthi* van Achterberg (♀♂)**

– Eye in lateral view 1.2 times as wide as temple medially (Fig. 5B). Face 1.6 times as wide as high, weakly and sparsely punctate-rugulose (Fig. 5E). Vein 3-SR 2.0 times as long as vein 2-SR (Fig. 6F). Ovipositor about 2.0 times as long as first metasomal tergite (Fig. 6E). Body length 2.0 mm. Russia (Far East) .... ***A. ussuricola* Belokobylskij (♀)**

Discussion

Most of the genera belonging to the *Aspilota* group (Peris-Felipo et al. 2014) are rather monomorphic in the structures of metasoma, which are usually laterally compressed, entirely smooth behind the first tergite, and the first tergite always with a distinct dorsope. The only exception is the genus *Apronopa* van Achterberg, 1980, which was recently described from Europe and placed within the *Aspilota* generic-group - and compared with the very large genus *Aspilota* Foerster, 1863 (van Achterberg 1980). However, this genus is characterized by the combination of unique and previously unknown characters (in this generic group) such as the presence of dorso-ventrally depressed metasoma, the absence of dorsope on the first metasomal tergite, and usually the presence of sculpturing on the base of the second metasomal tergite. Only three species have been described so far in this rare genus, *A. haeselbarthi* known only from Germany and Slovakia (van Achterberg 1980, Capek and Lukas 1989) and two species from the Eastern Palaearctic, *A. ussuricola* from the south of the Russian Far East (Belokobylskij 1998) and *A. levis* from North Korea (Papp 2007). The first two species have distinct sculpturing on the second tergite (one of the main features of *Apronopa*), but the North Korean species is characterized by an entirely smooth second tergite; however, other characters indicate that it belongs to the genus *Apronopa*. The lack of sculpturing on the second tergite in *A. levis* additionally underlines its position in the *Aspilota* generic-group. Furthermore, Wharton (1994) mentioned that several specimens from undescribed species were seen in the Colorado Museum and that this material would be described by T. Munk; however, that material has not been described yet.

An additional aspect to highlight is the rarity of specimens in collections, which hinders a better understanding (including molecular characters) of this peculiar genus. Any new samples and study of their phylogenetic position would allow us to better understand its position within the *Aspilota* group.

Acknowledgements

We are very thankful to Frederique Bakker from the Naturalis Biodiversity Center (Leiden, Netherlands; RMNH), Zoltán Vas from the Hungarian Natural History Museum (Budapest, Hungary; HNHM), Stefan Schmidt and Lukas Kirschey from the Zoologische Staatssammlung München (München, Germany; ZSSM) for the loan of material. Also, we want to thank Isabelle Zuecker, Mirjam Luzzi and Matthias Borer, Naturhistorisches Museum Basel, Switzerland, for their kindness and help during our work with the photosystem. This work was partly supported for the second author by the Russian Foundation for Basic Research (project No. 16–04–00197).

References

Achterberg C van (1980) Three new Palaearctic genera of Braconidae (Hymenoptera). Entomologische Berichten 40: 72–80.

Achterberg C van (1993) Illustrated key to the subfamilies of the Braconidae (Hymenoptera: Ichneumonoidea). Zoologische Verhandelingen 283: 1–189.

Belokobylskij SA (1998) 9. Alysiinae (Alysiini). In: Lehr PA (Ed.) Key to insects of the Russian Far East. Vol. 4. Neuropteroidea, Mecoptera, Hymenoptera. Pt 3. Dal'nauka, Vladivostok, 162–298. [In Russian]

Belokobylskij SA, Tobias VI (2007) Subfamily Alysiinae. Group of genera close to *Aspilota*. In: Lelej AS (Ed.) Key to insects of the Russian Far East. Vol. 4. Neuropteroidea, Mecoptera, Hymenoptera. Pt 5. Dal'nauka, Vladivostok, 9–133. [In Russian]

Capek M, Lukas J (1989) Apocrita Parasitica, Ichneumoidea, Braconidae. Acta Faunistica Entomologica Musei Nationalis Pragae 19: 27–44.

Fischer M (1991) Integration einiger Gattungen der Alysiini in ein diagnostisches System (Hymenoptera, Braconidae, Alysiinae). Linzer Biologische Beiträge 23(1): 3–35.

Papp J (2007) Braconidae (Hymenoptera) from Korea, XXII. Subfamily Alysiinae. Acta Zoologica Academiae Scientiarum Hungaricae 53(1): 1–38. https://doi.org/10.17109/AZH.62.1.1.2016

Peris-Felipo FJ, Belokobylskij SA (2017) Revision of the New World species of the genus *Dinotrema* (Hymenoptera: Braconidae: Alysiinae). Zootaxa 4382 (1): 1–55. https://doi.org/10.11646/zootaxa.4382.1.1

Peris-Felipo FJ, Belokobylskij SA, Jiménez-Peydró R (2014) Revision of the Western Palaearctic species of the genus *Dinotrema* Foerster, 1862 (Hymenoptera, Braconidae, Alysiinae). Zootaxa 3885 (1): 1–483. https://doi.org/10.11646/zootaxa.3885.1.1

Peris-Felipo FJ, Broad G, Belokobylskij SA, Jiménez-Peydró R (2014) Three new *Adelphenaldis* species (Hymenoptera: Braconidae: Alysiinae) from Africa, with first descriptions of the female of *A. subsurrectionis* (Fischer) and the male of *A. claricornis* (Fischer). African Entomology 22(3): 561–576. https://doi.org/10.4001/003.022.0318

Tobias VI (1986) Subfamily Alysiinae. In: Medvedev GS (Ed.) Opredelitel' nasekomykh Evropeyskoy chasti SSSR [Key to insects of the USSR European part], Vol. 3, Part 5, Nauka, Leningrad, 100–231. https://doi.org/10.5962/bhl.title.46334 [In Russian]

Wharton RA (1994) New genera, species, and records of New World Alysiinae (Hymenoptera, Braconidae). Proceedings of the Entomological Society of Washington 96: 630–664.

Yu DS, Achterberg C van, Horstmann K (2016) Taxapad 2016, Ichneumonoidea 2015. Database on flash-drive. Ottawa, Ontario.